Zachodniopomorski Uniwersytet Technologiczny w Szczecinie

Wydział Biotechnologii i Hodowli Zwierząt

ZACHODNIOPOMORSKI UNIWERSYTET TECHNOLOGICZNY W SZCZECINIE
WYDZIAŁ BIOTECHNOLOGII I HODOWLI ZWIERZĄT
KATEDRA MIKROBIOLOGII I BIOTECHNOLOGII

Daria Ciecholewska-Juśko

Rozprawa doktorska

OPRACOWANIE I CHARAKTERYSTYKA MATERIAŁÓW BIONANOCELULOZOWYCH DO ZAPOBIEGANIA KOLONIZACJI PRZEZ DROBNOUSTROJE PATOGENNE ORAZ DO ERADYKACJI BIOFILMÓW BAKTERYJNYCH

Rozprawa doktorska wykonana w Katedrze Mikrobiologii i Biotechnologii pod kierunkiem dr hab. inż. Karola Fijałkowskiego, prof. ZUT

Szczecin 2022

Publikacje naukowe wchodzące w skład cyklu stanowiącego rozprawę doktorską zatytułowaną:

„Opracowanie i charakterystyka materiałów bionanocelulozowych do zapobiegania kolonizacji przez drobnoustroje patogenne oraz do eradykacji biofilmów bakteryjnych”

[D-1] Ciecholewska-Juśko, D., Żywicka, A., Junka, A., Drozd, R., Sobolewski, P., Migdał, P., Kowalska, U., Toporkiewicz, M., Fijałkowski, K. (2021). Superabsorbent crosslinked bacterial cellulose biomaterials for chronic wound dressings. *Carbohydrate Polymers*, *253*, 117247.

IF_{2021} – 9,381; 140 pkt. MEiN

Mój wkład w powstanie tej pracy polegał na udziale w opracowywaniu koncepcji i metodologii badań oraz udziale we wszystkich etapach eksperymentu, które obejmowały: przygotowanie mikroorganizmów, przygotowanie pożywek i reagentów testowych, zorganizowanie stanowiska badawczego, wytwarzanie i oczyszczanie celulozy bakteryjnej, przeprowadzenie i optymalizację procesu modyfikacji celulozy bakteryjnej, ocenę efektywności procesu modyfikacji, analizę właściwości fizykochemicznych zmodyfikowanej celulozy bakteryjnej tj. analizę makro i mikrostruktury (przygotowanie prób do analizy z wykorzystaniem skaningowego mikroskopu elektronowego), analizę struktury chemicznej za pomocą spektroskopii w podczerwieni, analizę parametrów wodnych i gęstości, przygotowanie prób do analizy cytotoksyczności z wykorzystaniem mikroskopu konfokalnego, a także na udziale w opracowaniu uzyskanych wyników, przeprowadzeniu analiz statystycznych oraz napisaniu manuskryptu.
Mój udział procentowy szacuję na 60%.

[D-2] Ciecholewska-Juśko, D., Broda, M., Żywicka, A., Styburski, D., Sobolewski, P., Gorący, K., Migdał, P., Junka, A., Fijałkowski, K. (2021). Potato juice, a starch industry waste, as a cost-effective medium for the biosynthesis of bacterial cellulose. *International Journal of Molecular Sciences, 22*(19), 10807.

IF_{2021} – 5,923; 140 pkt. MEiN

Mój wkład w powstanie tej pracy polegał na udziale w opracowywaniu koncepcji i metodologii badań oraz udziale we wszystkich etapach eksperymentu, które obejmowały: zorganizowanie stanowiska badawczego, przygotowanie, charakterystykę i ocenę składu pożywki, przygotowanie mikroorganizmów, wytwarzanie i oczyszczanie celulozy bakteryjnej, ocenę żywotności komórek bakteryjnych podczas hodowli, analizę zmian składu pożywki podczas hodowli, analizę właściwości fizykochemicznych otrzymanej celulozy bakteryjnej, tj. analizę mikrostruktury, struktury chemicznej (za pomocą spektroskopii w podczerwieni), parametrów wodnych, gęstości, przygotowanie prób do analizy wytrzymałości mechanicznej, przygotowanie prób do analizy cytotoksyczności z wykorzystaniem mikroskopu konfokalnego,

a także ocenę aktywności przeciwdrobnoustrojowej celulozy bakteryjnej zaimpregnowanej antyseptykiem. Dodatkowo, mój wkład w powstanie tej pracy polegał na przeprowadzeniu analiz statystycznych oraz napisaniu manuskryptu.
Mój udział procentowy szacuję na 60%.

[D-3] Ciecholewska-Juśko, D., Junka, A., Fijałkowski, K. (2022). The crosslinked bacterial cellulose impregnated with octenidine dihydrochloride-based antiseptic as an antibacterial dressing material for highly-exuding, infected wounds. *Microbiological Research, 263,* 127125.

IF_{2022} – 5,415; 100 pkt. MEiN

Mój wkład w powstanie tej pracy polegał na udziale w opracowywaniu koncepcji i metodologii badań oraz udziale we wszystkich etapach eksperymentu, które obejmowały: przygotowanie mikroorganizmów, przygotowanie pożywek i reagentów testowych, zorganizowanie stanowiska badawczego, wytwarzanie i oczyszczanie celulozy bakteryjnej, przeprowadzenie procesu modyfikacji celulozy bakteryjnej, impregnację materiałów celulozowych antyseptykiem, przeprowadzanie analiz: pochłaniania i utrzymania antyseptyku, pochłaniania sztucznego wysięku, uwalniania antyseptyku w sztucznym łożysku rany (za pomocą spektroskopii UV-VIS), ocenę aktywności przeciwdrobnoustrojowej i przeciwbiofilmowej (metoda dyfuzyjno-krążkowa, testy żywotności komórek), przygotowanie prób do analizy cytotoksyczności z wykorzystaniem mikroskopu konfokalnego, a także na udziale w opracowaniu uzyskanych wyników, przeprowadzeniu analiz statystycznych oraz napisaniu manuskryptu.
Mój udział procentowy szacuję na 85%.

[D-4] Ciecholewska-Juśko, D., Żywicka, A., Junka, A., Woroszyło, M., Wardach, M., Chodaczek, G., Szymczyk-Ziółkowska, P., Migdał, P., Fijałkowski, K. (2022). The effects of rotating magnetic field and antiseptic on in vitro pathogenic biofilm and its milieu. *Scientific reports*, *12*(1), 1-19.

IF_{2022} – 4,380; 140 pkt. MEiN

Mój wkład w powstanie tej pracy polegał na udziale w opracowywaniu koncepcji i metodologii badań oraz udziale we wszystkich etapach eksperymentu, które obejmowały: przygotowanie mikroorganizmów, przygotowanie pożywek i reagentów testowych, zorganizowanie stanowiska badawczego, wytwarzanie i oczyszczanie celulozy bakteryjnej, impregnację celulozy bakteryjnej antyseptykiem, hodowlę biofilmów bakteryjnych, konstrukcję układów doświadczalnych, ich ekspozycję na wirujące pole magnetyczne, analizę uwalniania antyseptyku z nośnika celulozowego, ocenę efektywności przeciwbiofilmowej przygotowanych nośników z celulozy bakteryjnej, przygotowanie prób do analiz z użyciem chromatografu cieczowego z tandemową spektrometrią mas, chromatografu gazowego, mikroskopu konfokalnego, skaningowego mikroskopu elektronowego, a także na udziale w opracowaniu uzyskanych wyników, przeprowadzeniu analiz statystycznych oraz napisaniu manuskryptu.
Mój udział procentowy szacuję na 60%.

3 z 4 prac wchodzących w skład cyklu stanowiącego niniejszą rozprawę doktorską (**publikacje D-2, D-3, D-4**) zostały opublikowane w otwartym dostępie (Open Access). Dodatkowo, w celu transparentności i łatwego dostępu do publikowanych treści, jedyna praca nieopublikowana w otwartym dostępie (**publikacja D-1**) została udostępniona jako preprint w bazie bioRxiv: https://www.biorxiv.org/content/10.1101/2020.03.04.975003v2.

Ogólna liczba punktów za cykl prac stanowiących rozprawę doktorską według wykazu czasopism naukowych MEiN z dnia 1 grudnia 2021 r., zgodny z rokiem ukazania się pracy wynosi 520 punktów.

Sumaryczny Impact Factor (IF) za cykl prac stanowiących rozprawę doktorską zgodny z rokiem ukazania się prac wynosi 25,099.

W przypadku wyżej wymienionych prac eksperymentalnych miałam wiodący udział w badaniach, od udziału w opracowaniu koncepcji i metodologii, po opracowanie, interpretację i opublikowanie wyników. Prowadzone przeze mnie badania miały charakter interdyscyplinarny, dlatego były wykonywane we współpracy z ekspertami z różnych obszarów nauk inżynieryjnych, przyrodniczych i medycznych. Część prowadzonych badań była wykonywana w ramach grantu OPUS 14 finansowanego ze źródeł Narodowego Centrum Nauki pn. „Analiza mechanizmów zwiększonej efektywności substancji przeciwdrobnoustrojowych względem biofilmów w obecności wirującego pola magnetycznego".

Podczas prowadzenia badań, których wyniki umożliwiły mi przygotowanie publikacji składających się na niniejszą rozprawę doktorską, współpracowałam z naukowcami z Katedry Mikrobiologii i Biotechnologii ZUT na Wydziale Biotechnologii i Hodowli Zwierząt - dr inż. Radosławem Drozdem, dr inż. Anną Żywicką i mgr inż. Martą Woroszyło. Nawiązałam również współpracę z dr inż. Piotrem Sobolewskim i dr inż. Krzysztofem Gorącym z Katedry Inżynierii Polimerów i Biomateriałów na Wydziale Technologii i Inżynierii Chemicznej ZUT, dr Danielem Styburskim z Laboratorium Chromatografii i Spektrometrii Mas na Wydziale Biotechnologii i Hodowli Zwierząt ZUT, dr inż. Urszulą Kowalską z Centrum Bioimmobilizacji i Innowacyjnych Materiałów Opakowaniowych na Wydziale Nauk o Żywności i Rybactwa ZUT, dr hab. inż. Marcinem Wardachem, prof. ZUT z Katedry Maszyn i Napędów Elektrycznych na Wydziale Mechanicznym ZUT, dr hab.n.med. Adamem Junką, profesorem Uczelni z Katedry i Zakładu Mikrobiologii Farmaceutycznej i Parazytologii na Wydziale Farmaceutycznym Uniwersytetu Medycznego im. Piastów Śląskich we Wrocławiu, dr inż. Pawłem Migdałem z Katedry Higieny Środowiska i Dobrostanu Zwierząt na Wydziale Biologii i Hodowli Zwierząt Uniwersytetu Przyrodniczego we Wrocławiu oraz dr inż. Patrycją Szymczyk-Ziółkowską z Centrum Zaawansowanych Systemów Produkcyjnych na Wydziale Mechanicznym Politechniki Wrocławskiej. Współpracowałam także z dr hab. Grzegorzem Chodaczkiem i dr Moniką Toporkiewicz z Laboratorium Bioobrazowania Polskiego Ośrodka Rozwoju Technologii PORT we Wrocławiu oraz z mgr inż. Michałem Brodą z Pomorsko-Mazurskiej Hodowli Ziemniaka w Strzekęcinie, który realizuje doktorat wdrożeniowy. Współpraca obejmowała wspólne wykonywanie badań i analiz, wykorzystanie sprzętu oraz pomoc w interpretacji otrzymanych wyników, a także przygotowanie publikacji naukowych i zgłoszeń patentowych.

Załącznik 1. Kopie publikacji naukowych wchodzących w skład cyklu stanowiącego rozprawę doktorską.

Załącznik 2. Kopie suplementów publikacji naukowych wchodzących w skład cyklu stanowiącego rozprawę doktorską.

Załącznik 3. Oświadczenia współautorów publikacji naukowych wchodzących w skład cyklu stanowiącego rozprawę doktorską wraz z określeniem ich indywidualnego udziału.

Załącznik 4. Sumaryczne zestawienie dorobku naukowego.

Zachodniopomorski Uniwersytet Technologiczny w Szczecinie

Wydział Biotechnologii i Hodowli Zwierząt

Autoreferat

Daria Ciecholewska-Juśko

Rozprawa doktorska

OPRACOWANIE I CHARAKTERYSTYKA MATERIAŁÓW BIONANOCELULOZOWYCH DO ZAPOBIEGANIA KOLONIZACJI PRZEZ DROBNOUSTROJE PATOGENNE ORAZ DO ERADYKACJI BIOFILMÓW BAKTERYJNYCH

Szczecin 2022

Spis treści

Wykaz skrótów ... 9
Streszczenie ... 10
1. Wprowadzenie ... 12
2. Hipotezy ... 16
3. Cel badawczy ... 17
4. Materiały i metody badawcze ... 18
4.1. Mikroorganizmy ... 18
4.2. Bioreaktory wspomagane wirującym polem magnetycznym ... 18
4.3. Wytwarzanie celulozy bakteryjnej ... 19
4.5. Określenie ilości i żywotności komórek K. xylinus podczas wytwarzania celulozy bakteryjnej ... 19
4.6. Oczyszczanie i wstępna charakterystyka celulozy bakteryjnej ... 19
4.7. Modyfikacja celulozy bakteryjnej ... 20
4.8. Analiza właściwości fizykochemicznych celulozy bakteryjnej ... 20
4.8.1. Ocena makro- i mikrostruktury ... 20
4.8.2. Skład pierwiastkowy powierzchni ... 20
4.8.3. Skład chemiczny ... 20
4.8.4. Parametry związane z absorpcją i utrzymaniem cieczy ... 21
4.8.5. Gęstość ... 21
4.8.6. Właściwości mechaniczne ... 21
4.8.7. Cytotoksyczność ... 21
4.9. Impregnacja celulozy bakteryjnej antyseptykiem oraz analiza jej podstawowych właściwości ... 22
4.9.1. Zdolność do pochłaniania wysięku ... 22
4.9.2. Kinetyka uwalniania antyseptyku w sztucznym łożysku rany ... 22
4.10. Analiza aktywności przeciwdrobnoustrojowej celulozy bakteryjnej zaimpregnowanej antyseptykiem ... 23
4.10.1. Hodowle bakteryjne na podłożu stałym ... 23
4.10.2. Hodowle bakteryjne w podłożu płynnym ... 23
4.10.3. Hodowle bakteryjne w formie biofilmu ... 23
4.11. Wpływ wirującego pola magnetycznego na wybrane parametry związane uwalnianiem antyseptyku z celulozy bakteryjnej ... 23
4.11.1. Analiza ilości uwolnionego antyseptyku i szybkości jego penetracji przez warstwy biofilmu ... 23
4.11.2. Analiza efektu przeciwdrobnoustrojowego ... 23
4.11.3. Analiza morfologiczna bakterii tworzących biofilm ... 24
4.11.4. Analiza zawartości cukrów w macierzy biofilmu ... 24
4.12. Analiza statystyczna ... 24

5. Wyniki 24
6. Wnioski 34
7. Cytowana literatura 35
8. Omówienie pozostałych osiągnięć naukowo-badawczych 39
8.1. Osiągnięcia naukowe związane z produkcją i wykorzystywaniem celulozy bakteryjnej 39
8.2. Osiągnięcia naukowe związane z zastosowaniem celulozy bakteryjnej jako nośnika dla substancji przeciwdrobnoustrojowych w celu eradykacji biofilmów bakteryjnych. ... 40
8.3. Osiągnięcia naukowe związane z wytwarzaniem przeciwdrobnoustrojowych filtrów na bazie celulozy bakteryjnej 42
8.4. Osiągnięcia naukowe związane z wpływem wirującego pola magnetycznego na efektywność działania substancji przeciwdrobnoustrojowych względem biofilmów 43

Wykaz skrótów

Skróty użyte w niniejszym autoreferacie pochodzą z publikacji wchodzących w skład cyklu stanowiącego rozprawę doktorską.

ATR-FTIR - spektroskopia fourierowska osłabionego całkowitego odbicia w podczerwieni, ang. *Attenuated Total Reflectance Fourier Transform Infrared Spectroscopy*

BC – celuloza bakteryjna, ang. *bacterial cellulose*

ECM – macierz zewnątrzkomórkowa, ang. *extracellular matrix*

OCT – antyseptyk na bazie dichlorowodorku oktenidyny

PJ – sok komórkowy z bulw ziemniaków, ang. *potato juice*

RMF – wirujące pole magnetyczne, ang. *rotating magnetic field*

SEM – skaningowa mikroskopia elektronowa, ang. *scanning electron microscopy*

SR – współczynnik pęcznienia, ang. *swelling ratio*

WHC – zdolność do utrzymania wody, ang. *water holding capacity*

BC_d/BC_w – sucha/mokra niemodyfikowana celuloza bakteryjna, ang. *dry/wet bacterial cellulose*

MBC_d/MBC_w – sucha/mokra modyfikowana celuloza bakteryjna, ang. *dry/wet modified bacterial cellulose*

OCT-BC_d/OCT-BC_w – sucha/mokra niemodyfikowana celuloza bakteryjna zaimpregnowana antyseptykiem na bazie dichlorowodorku oktenidyny, ang. *OCT-impregnated dry/wet bacterial cellulose*

OCT-MBC_d/OCT-MBC_w – sucha/mokra modyfikowana celuloza bakteryjna zaimpregnowana antyseptykiem na bazie dichlorowodorku oktenidyny, ang. *OCT-impregnated dry/wet modified bacterial cellulose*

Streszczenie

Głównym celem niniejszej rozprawy doktorskiej było opracowanie i charakterystyka materiałów bionanocelulozowych do zapobiegania kolonizacji przez drobnoustroje patogenne oraz do eradykacji biofilmów bakteryjnych.

Celuloza bakteryjna (BC, ang. *bacterial cellulose*), zwana też bionanocelulozą, to polimer o unikalnych właściwościach, dzięki którym znajduje on zastosowanie w wielu gałęziach przemysłu i dziedzinach nauki. Podczas prowadzenia badań w ramach niniejszej rozprawy doktorskiej, do biosyntezy BC wykorzystano szczep referencyjny *Komagataeibacter xylinus* (ATCC 53524), a proces wytwarzania BC prowadzono w warunkach stacjonarnych. W celu uzyskania materiału o polepszonych właściwościach fizykochemicznych, opracowano metodę modyfikacji polegającą na przeprowadzeniu reakcji krzyżowego sieciowania BC w obecności kwasu cytrynowego jako czynnika sieciującego oraz katalizatorów – wodorofosforanu disodu, wodorowęglanu sodu, wodorowęglanu amonu i ich mieszanin. Ustalono, że w wyniku przeprowadzonej reakcji, włókna BC nie zapadały się podczas dehydratacji, dzięki czemu otrzymywano bionanomateriały o trójwymiarowej, warstwowej strukturze z licznymi przestrzeniami powietrznymi, która odróżniała je od suchej, niemodyfikowanej BC występującej w postaci cienkiej folii. Analizy parametrów fizykochemicznych modyfikowanej BC wykazały, że charakteryzuje się ona znaczną poprawą właściwości związanych z chłonnością i utrzymaniem wody w porównaniu do niemodyfikowanej, suchej BC, ale również do specjalistycznych, wysokochłonnych opatrunków komercyjnych. Dodatkowo, modyfikowana BC nie wykazywała cytotoksyczności względem komórek fibroblastów, co sugeruje, że może być ona z powodzeniem stosowana w aplikacjach biomedycznych.

Udowodniono, że materiały na bazie modyfikowanej BC, funkcjonalizowane poprzez impregnację antyseptykiem na bazie dichlorowodorku oktenidyny (OCT), stanowią doskonałe materiały opatrunkowe o wysokiej aktywności przeciwdrobnoustrojowej i przeciwbiofilmowej. Materiały te, dzięki swojej strukturze charakteryzowały się wydłużonym uwalnianiem OCT, wysoką zdolnością pochłaniania wysięku, dobrym przyleganiem do zakrzywionych powierzchni oraz możliwością długiego przechowywania w stanie suchym, łącząc w sobie zalety suchej i mokrej BC.

Ponadto wykazano, że aktywność OCT uwalnianego z nośnika na bazie BC może być wzmacniana przez działanie wirującego pola magnetycznego (RMF, ang. *rotating magnetic field*), dzięki wpływowi RMF na proces uwalniania i penetracji OCT przez warstwy biofilmu. W tym kontekście wykazano również, że RMF zaburza morfologię komórek tworzących biofilm oraz powoduje zmiany w macierzy biofilmowej, w tym w jej porowatości i składzie chemicznym. Ustalono także, że RMF przy niskim stężeniu OCT i krótkim czasie kontaktu nośnika z biofilmem, umożliwia uzyskanie istotnego obniżenia żywotności komórek bakteryjnych. Z tego względu, połączenie BC impregnowanej substancjami o działaniu przeciwdrobnoustrojowym z czynnikami fizycznymi umożliwiającymi ich kontrolowane uwalnianie może być szczególnie obiecujące w eradykacji biofilmów zwłaszcza w trudnodostępnych miejscach rany.

Biorąc pod uwagę, że możliwości szerokiego stosowania BC są ciągle istotnie ograniczone ze względu na wysokie koszty pożywki wykorzystywanej do jej produkcji, w ramach prowadzonych badań opracowano i przeanalizowano możliwości wykorzystania pożywki produkcyjnej na bazie soku komórkowego z bulw ziemniaków, odpadu przemysłu skrobiowego. Jak ustalono, ze względu na wartość odżywczą soku ziemniaczanego, pożywka ta nie wymagała dodatkowej obróbki wstępnej ani suplementacji. Wydajność biosyntezy BC w pożywce na bazie soku z bulw ziemniaków była porównywalna do procesu, w którym

zastosowano standardową pożywkę Hestrin-Schramm (H-S). Wykazano także, że BC wytwarzana z użyciem pożywki na bazie soku ziemniaczanego, nie różniła się pod względem struktury, parametrów fizykochemicznych oraz składu chemicznego od BC wytworzonej z wykorzystaniem pożywki H-S.

Abstract

The main objective of the doctoral dissertation was to develop and analyze the effectiveness of bacterial cellulose (BC) bionanomaterials in preventing microbial colonization and eradicating biofilms of pathogenic microorganisms.

Bacterial cellulose (BC), also known as bionanocellulose, is a polymer with unique properties, used in many industries and fields of science. During the research, the reference strain of *Komagataeibacter xylinus* (ATCC 53524) was used for the biosynthesis of BC. The production process was carried out under stationary conditions. In order to obtain a modified BC with improved physicochemical properties, a cross-linking reaction method was developed, with the use of citric acid as a cross-linking agent and disodium phosphate, sodium bicarbonate, ammonium bicarbonate, and their mixtures as catalysts. As a result of the reaction, BC fibers did not collapse during dehydration, which allowed for obtaining bionanomaterials with a three-dimensional layered structure and numerous air spaces distinguishing them from dry, unmodified BC. Furthermore, analyses of the physicochemical parameters of the modified BC showed that this material was characterized by a significant improvement in the properties related to water absorption and retention compared to unmodified, dry BC, but also to specialized, highly-absorbing commercial dressings. In addition, the modified BC showed no cytotoxicity to fibroblast cells, which suggests that it can be successfully used in biomedical applications.

It was proven that modified BC materials functionalized by impregnation with an antiseptic based on octenidine dihydrochloride (OCT) are excellent dressing materials with high antimicrobial and anti-biofilm activity. Thanks to their structure, these materials were characterized by the prolonged release of OCT, increased ability to absorb exudate, good adhesion to the curved surfaces, and the possibility of long-term dry storage, combining the advantages of dry and wet BC.

Moreover, it was shown that the antimicrobial effect of OCT released from the BC-based carrier could be enhanced by the action of a rotating magnetic field (RMF), which influences the process of OCT release and penetration through subsequent biofilm layers. In addition, it was demonstrated that RMF affects the biofilm-forming cells by disturbing their morphology and changing the porosity and composition of the extracellular matrix. It was found that the RMF, at a low concentration of OCT and a short contact time of the OCT-impregnated carrier with biofilm, allows for a significant reduction in the viability of biofilm-forming cells. Therefore, combining BCs impregnated with antimicrobial substances with physical agents enabling their controlled release may be particularly promising in biofilm eradication, especially in hard-to-reach wound sites.

The widespread use of the BC is limited because of the high cost of ingredients used for the production medium. Therefore, the research also included the development of a new culture medium based on potato tuber juice, a significant waste of the starch industry. Due to the nutritional value of the potato juice, the obtained medium did not require any pre-treatment or supplementation. The BC synthesis efficiency using the potato juice medium was comparable to the process with a standard Hestrin-Schramm (H-S) medium. It was also shown that there were no differences in the structure, physicochemical parameters, and chemical composition between the BC synthesized with the potato juice and conventional H-S media.

1. Wprowadzenie

Problem naukowy, który został podjęty w ramach rozprawy doktorskiej dotyczy przede wszystkim opracowania i charakterystyki materiałów bionanocelulozowych do zapobiegania kolonizacji przez drobnoustroje patogenne oraz do eradykacji biofilmów bakteryjnych.

Przewlekłe, trudno gojące się rany stanowią istotny problem dla współczesnej medycyny, zarówno ze względu na zagrożenie zdrowia i życia pacjentów jak i obciążenie ekonomiczne, z którym wiąże się przedłużone leczenie (Omar i wsp., 2017; Moormeier i Bayles, 2017). Wilgotne i bogate w substancje odżywcze środowisko ran przewlekłych zapewnia warunki korzystne dla rozwoju drobnoustrojów, których obecność w ranie znacznie utrudnia stworzenie skutecznego schematu terapeutycznego. Jednymi z najczęściej izolowanych drobnoustrojów będących czynnikami etiologicznymi infekcji ran są *Staphylococcus aureus* i *Pseudomonas aeruginosa* (Wolcott i wsp., 2016; Bassetti i wsp., 2018). Bakterie te charakteryzują się wysokim potencjałem wirulencji, który pozwala im uniknąć nie tylko odpowiedzi układu odpornościowego gospodarza, ale również skutków antybiotykoterapii (Shettigar i wsp., 2016). Wspólnym i jednocześnie jednym z najważniejszych czynników wirulencji umożliwiającym adaptację do środowiska zakażenia obu tych gatunków bakterii jest ich zdolność do tworzenia biofilmu (Moormeier i Bayles, 2017).

Biofilm, zwany również błoną biologiczną, to forma występowania drobnoustrojów w ustrukturyzowanej społeczności otoczonej macierzą zewnątrzkomórkową (ECM, ang. *extracellular matrix*), złożoną z białek, polisacharydów i zewnątrzkomórkowego DNA. Macierz biofilmu tworzy rusztowanie zapewniające bakteriom ochronę przed czynnikami zewnętrznymi, zwłaszcza w niesprzyjającym środowisku (Bjarnsholt, 2013). Biofilm powstaje zarówno na powierzchniach biologicznych jak i abiotycznych. Tworzenie się biofilmów jest procesem cyklicznym, składającym się z kilku następujących po sobie etapów (**Ryc. 1**). Pierwszy z nich to adhezja komórek do powierzchni, która początkowo jest procesem odwracalnym. Przejście do etapu nieodwracalnego przytwierdzenia do powierzchni wiąże się ze zmniejszeniem ekspresji genów wici oraz rozpoczęciem wytwarzania składników ECM i adhezyn (Sauer i wsp., 2022). W dalszej kolejności następuje kolonizacja powierzchni, czyli wzrost i proliferacja komórek bakteryjnych osłoniętych ECM (Moormeier i Bayles, 2017). Po osiągnięciu określonej gęstości komórek, uruchamiany jest mechanizm inicjujący degradację ECM, dzięki któremu bakterie osadzone w zewnętrznych warstwach biofilmu mogą się z niego uwolnić i zapoczątkować cykl tworzenia biofilmu w kolejnych miejscach. Rozproszenie komórek bakteryjnych może nastąpić również w wyniku mechanicznego uszkodzenia biofilmu (Omar i wsp., 2017).

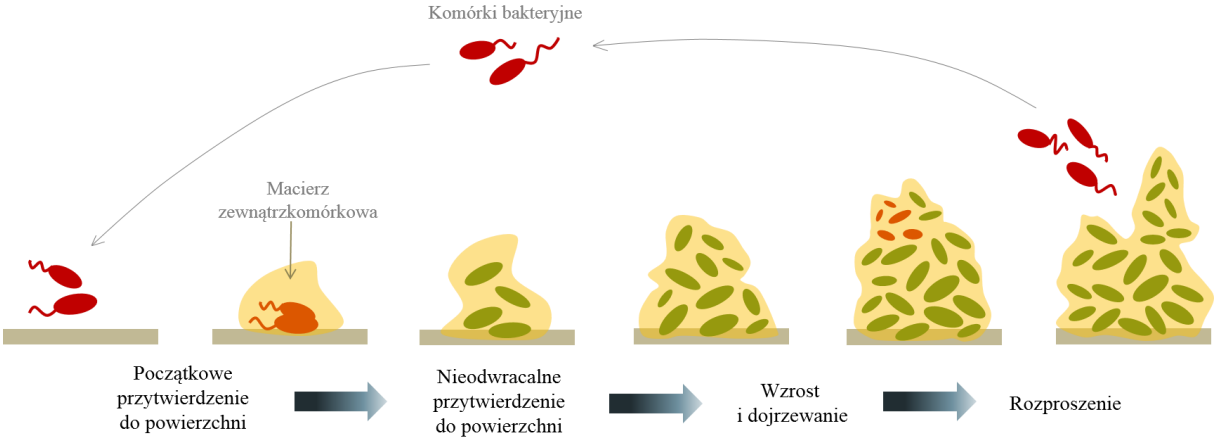

Rycina 1. Etapy powstawania biofilmu bakteryjnego

Komórki w formie biofilmu wykazują znacznie zwiększoną tolerancję na środki przeciwdrobnoustrojowe oraz na działanie układu odpornościowego w porównaniu do komórek planktonicznych (nie związanych z podłożem) (Wu i wsp., 2015). Jest to istotne z medycznego i weterynaryjnego punktu widzenia, ponieważ biofilm stanowi jeden z głównych problemów terapeutycznych będąc przyczyną bardzo wielu, często przewlekłych infekcji ran u ludzi i zwierząt (Clutterbuck i wsp., 2007). Obecność biofilmu w ranie prowadzi do hamowania procesów zapalnych oraz uszkadzania otaczającej tkanki (w wyniku produkcji przez drobnoustroje enzymów proteo- i lipolitycznych), w efekcie czego proces gojenia jest znacznie wydłużony (Percival i wsp., 2015; Omar i wsp., 2017).

Zagadnienia związane z opracowywaniem terapii przeciwbiofilmowych należą do jednych z najbardziej dynamicznie rozwijających się gałęzi nauki. Obecny standard w leczeniu ran zakażonych drobnoustrojami tworzącymi biofilm obejmuje oczyszczanie rany, stosowanie miejscowych i ogólnoustrojowych środków przeciwdrobnoustrojowych oraz opatrunków. Zastosowanie opatrunków o działaniu przeciwdrobnoustrojowym, czyli nośników połączonych z substancjami aktywnymi, przyspiesza zamykanie ran, co sprawia, że stan pacjenta ulega znacznej poprawie, a koszty związane z opieką medyczną maleją (Shahriari-Khalaji i wsp., 2020). W związku z pojawianiem się coraz większej liczby szczepów opornych na antybiotyki, w proces leczenia ran zainfekowanych najczęściej wdrażane są inne środki przeciwdrobnoustrojowe, zarówno syntetyczne (antyseptyki, chemioterapeutyki, nanocząsteczki) jak i naturalne (ekstrakty roślinne, olejki eteryczne, alkaloidy pochodzenia roślinnego) (Zheng i wsp., 2020; Swingler i wsp., 2021; Darvishi i wsp., 2021).

Do wytwarzania materiałów opatrunkowych można zastosować polimery syntetyczne (poli(alkohol winylowy), poli(N-winylopirolidon, poli(kwas akrylowy), poli(glikol etylenowy)) lub naturalne (chitozan, chityna, alginian, celuloza, kolagen, pektyna) (Massarelli i wsp., 2020; Zheng i wsp., 2020). Możliwe jest również wytwarzanie opatrunków o różnej postaci, włączając bandaże, folie, hydrożele, gąbki, pianki oraz maty (Teixeira i wsp., 2020; Zheng i wsp., 2020). Opatrunek na rany powinien być nietoksyczny, nie wykazywać działania alergizującego, zapobiegać zanieczyszczeniu rany z zewnątrz (zwłaszcza wnikaniu drobnoustrojów), charakteryzować się zdolnością do utrzymania wysokiej wilgotności w miejscu rany przy jednoczesnym efektywnym pochłanianiu płynów (krwi, wysięku), umożliwiać wymianę gazową między raną a otoczeniem oraz wykazywać aktywność przeciwdrobnoustrojową (Gámez-Herrera i wsp., 2020; Zheng i wsp., 2020). W kontekście aktywności przeciwdrobnoustrojowej, korzystne jest, aby opatrunek charakteryzował się przedłużonym uwalnianiem substancji czynnej, co zapewnia utrzymanie efektywnego stężenia leku w miejscu infekcji **(**Gámez-Herrera i wsp., 2020). Obecnie, przemysł farmaceutyczny koncentruje się na wykorzystywaniu biopolimerów, ze względu na ich biokompatybilność, trwałość, zdolność do wspomagania regeneracji tkanek, biodegradowalność oraz korzystne właściwości fizykochemiczne (Zheng i wsp., 2020).

Jednym z biopolimerów stosowanych jako materiał opatrunkowy jest celuloza bakteryjna (BC, ang. *bacterial cellulose*), ze względu na rozmiar włókien zwana także bionanocelulozą. Zdolnością do biosyntezy BC charakteryzują się bakterie m.in. z rodzajów *Komagataeibacter, Acetobacter, Rhizobium, Agrobacterium, Azotobacter, Enterobacter, Sarcina*. Za jednego z najwydajniejszych producentów BC uważa się Gram ujemną, tlenową bakterię należącą do gatunku *Komagataeibacter xylinus* (wcześniej *Gluconacetobacter xylinus*) (Lahiri i wsp., 2021). Celuloza bakteryjna jest syntetyzowana na powierzchni pożywki produkcyjnej (**Ryc. 2A**) w postaci wielowarstwowej, elastycznej membrany uformowanej z gęsto usieciowanych nanofibryli (**Ryc. 2B**). Membrana ta chroni komórki bakteryjne przed szkodliwymi czynnikami środowiska zewnętrznego (promieniowanie UV, zmiany temperatury, niska wilgotność) oraz pozwala im utrzymać się na powierzchni pożywki, gdzie

mają dostęp do tlenu (Czaja i wsp., 2006). Po oczyszczeniu BC z pozostałości pożywki i komórek bakteryjnych, otrzymuje się czysty, silnie uwodniony materiał (około 99% masy BC stanowi woda) (**Ryc. 2C**).

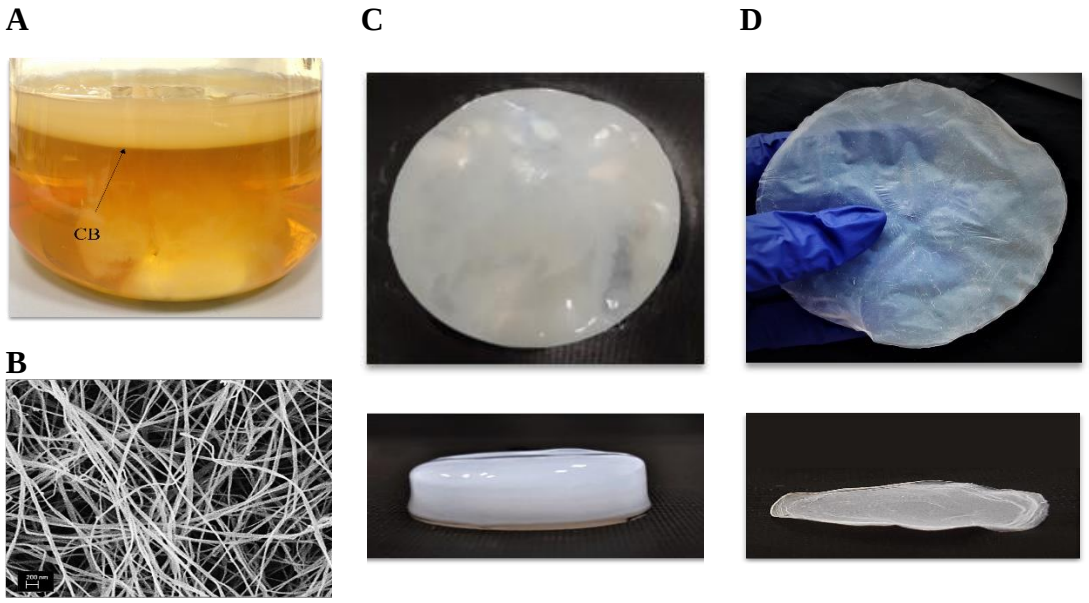

Rycina 2. A – celuloza bakteryjna (BC) w naczyniu hodowlanym; B – nanowłókna BC wizualizowane za pomocą skaningowego mikroskopu elektronowego (VEGA3, Tescan, Czechy; powiększenie 20.000x); C – oczyszczona, nigdy nie suszona BC; D – sucha BC.

Właściwości BC, takie jak wysoka czystość chemiczna, wytrzymałość mechaniczna, duża porowatość, wysoki stopień krystaliczności, nietoksyczność, biozgodność, brak działania alergizującego oraz biodegradowalność, umożliwiają zastosowanie tego biomateriału w medycynie, weterynarii, przemyśle kosmetycznym, farmaceutycznym, tekstylnym, elektronicznym oraz spożywczym, (Czaja i wsp., 2006; Sulaeva i wsp., 2015; Lahiri i wsp., 2021). Dodatkową zaletą wynikającą ze stosowania BC jest łatwy proces jej produkcji i oczyszczania oraz możliwość wytwarzania tego polimeru w dowolnym kształcie i rozmiarze. BC cieszy się szczególnie dużym zainteresowaniem pod względem wykorzystania w aplikacjach biomedycznych, np. jako integralna część systemów dostarczania leków, materiał do wytwarzania implantów, stentów, sztucznych naczyń krwionośnych oraz systemów do regeneracji kości i nerwów (Saska i wsp., 2010; Zaborowska i wsp., 2011; Swingler i wsp., 2021).

Jak wykazano w pracach Czaja i wsp. (2006), Bielecki i wsp. (2012), Portela i wsp. (2019), BC, zwłaszcza w postaci silnie uwodnionej membrany, która nigdy nie była suszona, jest z powodzeniem stosowana jako materiał opatrunkowy na przewlekłe rany i oparzenia. Wynika to z właściwości BC takich jak plastyczność, duża porowatość zapewniająca wymianę gazową między raną a otoczeniem, a także hydrożelowa struktura i silne uwodnienie, które zwiększa komfort pacjenta w trakcie użytkowania opatrunku, jednocześnie zapewniając wilgotne środowisko, uznawane za kluczowy wymóg w terapii ran (Portela i wsp., 2019). Dodatkowo, BC można z łatwością łączyć z substancjami o działaniu przeciwdrobnoustrojowym, zarówno w postaci roztworów jak i nanocząsteczek. Obecnie na rynku dostępne są materiały opatrunkowe na bazie mokrej BC, w tym o działaniu przeciwdrobnoustrojowym, m.in. Dermafill™, Bionext®, PrimaCell™, Bioprocess®, Xcell® (de Amorim i wsp., 2022).

W przeciwieństwie do BC uwodnionej, znacznie mniejszą uwagę pod kątem potencjalnego wykorzystania jako materiał opatrunkowy poświęca się BC suchej. Istnieje tylko kilka publikacji naukowych opisujących wykorzystanie częściowo lub całkowicie wysuszonej BC jako materiał opatrunkowy (Wei i wsp., 2011; Portela i wsp., 2019). Zastosowanie suchej BC wiąże się z ograniczeniami spowodowanymi zmianą jej morfologii i parametrów fizykochemicznych następujących podczas suszenia. W wyniku odwodnienia, trójwymiarowa sieć nanofibryli BC, utrzymywana wcześniej przez zawarte w niej cząsteczki wody, nieodwracalnie spłaszcza się, tworząc cienką, przezroczystą folię (**Ryc. 2D**, Zheng i wsp., 2021; Swingler i wsp., 2021). Z punktu widzenia zastosowania jako materiał opatrunkowy, zdolność do wchłaniania cieczy przez suchą BC jest niewielka, co jest niekorzystne zwłaszcza w przypadku ran z dużym wysiękiem wymagających ciągłego odbierania znacznych ilości płynu z łożyska rany. Co więcej, możliwość pochłaniania niewielkich ilości wysięku powoduje szybkie wysychanie opatrunku, a to z kolei stwarza ryzyko przywierania do rany (Ul-Islam i wsp., 2012; Zheng i wsp., 2021; Swingler i wsp., 2021). Dodatkowo, w przypadku próby otrzymania opatrunku o właściwościach przeciwdrobnoustrojowych, niska chłonność suchej BC nie pozwala na zaabsorbowanie takich ilości substancji aktywnych, które pozwoliłyby na utrzymanie stabilnego efektu przeciwdrobnoustrojowego (Swingler i wsp., 2021). Niemniej jednak, stosowanie BC, która nie była wcześniej suszona komplikuje proces pakowania oraz zmniejsza czas przydatności takiego materiału.

Warto również zwrócić uwagę, że zarówno mokra jak i sucha BC, podobnie jak wiele innych biopolimerów, nie są w stanie zapewnić przedłużonego uwalniania zaabsorbowanych substancji o działaniu przeciwdrobnoustrojowym. Materiały te charakteryzują się profilem uwalniania, w którym w ciągu krótkiego czasu następuje gwałtowny „wyrzut" substancji, co jest niekorzystne zwłaszcza w przypadku mokrej BC mogącej zawierać znaczne ilości leku, ponieważ nagromadzenie niektórych substancji czynnych w ranie może doprowadzić do efektu toksycznego (Hanna i wsp., 2020).

Aby zwiększyć możliwości zastosowania mokrej i suchej BC jako materiał opatrunkowy, wprowadza się różnego rodzaju modyfikacje zarówno *in situ*, zachodzące na poziomie hodowli, jak i *ex situ,* w oczyszczonej BC (Stumpf i wsp., 2018). Efektem modyfikacji BC może być na przykład poprawa jej właściwości chłonnych oraz wydłużenie czasu uwalniania pochłanianych przez nią substancji aktywnych. Wśród najczęściej stosowanych modyfikacji wyróżnia się modyfikacje chemiczne, tworzenie kompozytów z innymi materiałami/substancjami, obniżanie krystaliczności czy liofilizację (Rajwade i wsp., 2015; Torres i wsp., 2019; He i wsp., 2021).

Możliwość kontrolowanego uwalniania substancji przeciwdrobnoustrojowych z materiałów opatrunkowych jest szczególnie ważna w przypadku ran zainfekowanych o skomplikowanej strukturze z występującymi w nich zagłębieniami i „kieszeniami", gdzie biofilm może przetrwać leczenie prowadzone w konwencjonalny sposób i odbudować się w stosunkowo krótkim czasie (Zhao i wsp., 2013). Z tego względu, oprócz opracowywania materiałów opatrunkowych, które mogłyby dostarczać substancje aktywne w miejsce infekcji, poszukuje się również metod, które pozwolą na ich kontrolowane uwalnianie. Dotyczy to utrzymywania efektywnych stężeń substancji przeciwdrobnoustrojowych w ranie przez możliwie długi czas (co pozwoli na uniknięcie konieczności częstych zmian opatrunków) oraz zwiększenia penetracji tych substancji przez warstwy biofilmu, zapewniając ich docieranie nawet w trudno dostępne miejsca w ranie. Wśród badanych metod wyróżnia się zastosowanie ultradźwięków, terapii podciśnieniowej, zimnej plazmy, pola elektrycznego oraz różnych rodzajów pola magnetycznego (Kim i Steinberg, 2012; Lázaro-Martínez i wsp., 2018; Junka i wsp., 2018; Gupta i Ayan, 2019; Darvishi i wsp., 2021). Dodatkowo, wiele proponowanych metod zakłada wykorzystanie czynników fizycznych, które oprócz wpływu na procesy związane z uwalnianiem substancji aktywnych z nośników, wykazują bezpośrednie działanie

na komórki znajdujące się w biofilmach bakteryjnych, promując ich eradykację. Przykładowo, wykazano, że w wyniku ekspozycji drobnoustrojów na pole magnetyczne, może dochodzić do zmian kształtu komórek bakteryjnych, przepuszczalności błony komórkowej a nawet utraty jej integralności, co prowadzi do ich zniszczenia (Luo i wsp., 2005; Konopacki i wsp., 2019). Jednym z rodzajów pola magnetycznego jest wirujące pole magnetyczne (RMF, ang. *rotating magnetic field*), którego oś wiruje względem układu odniesienia, a zwrot pozostaje stały wzdłuż osi. Wykazano, że RMF może mieć wpływ zarówno na zmiany w fizjologii i morfologii komórek bakteryjnych, jak i na ruch naładowanych cząsteczek, a w konsekwencji również na procesy mieszania i dyfuzji (Rakoczy i wsp., 2017, Konopacki i wsp., 2019, **publikacja A-10**).

Dzięki prostemu procesowi biosyntezy i oczyszczania, jak również możliwości wprowadzania różnego rodzaju modyfikacji (w tym, w celu nadawania właściwości przeciwdrobnoustrojowych), BC jest bardzo obiecującym biopolimerem w kontekście zastosowania jako materiał opatrunkowy. Niemniej jednak, poważnym i największym ograniczeniem szerokiego stosowania BC są wysokie koszty jej produkcji, związane głównie ze składnikami pożywki produkcyjnej. Z tego względu, poszukuje się alternatywnych źródeł składników odżywczych dla bakterii syntetyzujących celulozę (Revin i wsp., 2018; Abol-Fotouh i wsp., 2020). Znane są metody wytwarzania BC z użyciem pożywek produkcyjnych na bazie surowców naturalnych bądź odpadowych, w tym soków i skórek owocowych, serwatki, łusek ryżu czy kukurydzy (Kongruang, 2007; Revin i wsp., 2018). Jednakże, aby możliwa była wydajna biosynteza BC, pożywki te muszą być dodatkowo suplementowane lub poddawane energo- i kosztochłonnym etapom obróbki wstępnej (Goelzer i wsp., 2009; Kurosumi i wsp., 2009; Revin i wsp., 2018).

Połączenie prostych, ekonomicznie korzystnych procesów modyfikacji BC, zapewniających spełnienie wszystkich wymogów stawianych nowoczesnym opatrunkom z doborem odpowiedniego środka przeciwdrobnoustrojowego i ewentualnych czynników wspomagających, może przyczynić się do opracowania strategii terapeutycznej wymierzonej w przewlekłe rany zainfekowane przez drobnoustroje tworzące biofilm.

2. Hipotezy

1. Materiały na bazie BC modyfikowanej za pomocą reakcji krzyżowego sieciowania z wykorzystaniem kwasu cytrynowego oraz katalizatorów, które podczas rozkładu termicznego i w reakcjach z kwasami wydzielają duże ilości gazów, charakteryzują się zestawem parametrów fizykochemicznych korzystnych w kontekście ich zastosowania jako materiały opatrunkowe na przewlekłe rany z dużym wysiękiem u ludzi i zwierząt (**publikacja D-1**).

2. Sok komórkowy z bulw ziemniaków może stanowić źródło składników odżywczych dla bakterii syntetyzujących celulozę, zapewniając wydajną produkcję tego materiału, nie wpływając przy tym negatywnie na jej parametry fizykochemiczne (**publikacja D-2**).

3. Materiały na bazie BC wytworzonej w pożywce z soku komórkowego z bulw ziemniaków, modyfikowanej za pomocą reakcji krzyżowego sieciowania z wykorzystaniem kwasu cytrynowego oraz mieszaniny wodorofosforanu disodu i wodorowęglanu sodu jako katalizatorów oraz zaimpregnowanej antyseptykiem (dichlorowodorkiem oktenidyny), charakteryzują się zwiększoną zdolnością do pochłaniania wysięku w porównaniu do niemodyfikowanej BC (**publikacja D-3**).

4. Materiały na bazie BC wytworzonej w pożywce z soku komórkowego z bulw ziemniaków, modyfikowanej za pomocą reakcji krzyżowego sieciowania z wykorzystaniem kwasu cytrynowego oraz mieszaniny wodorofosforanu disodu i wodorowęglanu sodu jako katalizatorów, charakteryzują się wydłużonym czasem uwalniania antyseptyku (dichlorowodorku oktenidyny), w porównaniu do niemodyfikowanej BC (**publikacja D-3**).

5. Materiały na bazie BC wytworzonej w pożywce z soku komórkowego z bulw ziemniaków, modyfikowanej za pomocą reakcji krzyżowego sieciowania z wykorzystaniem kwasu cytrynowego oraz mieszaniny wodorofosforanu disodu i wodorowęglanu sodu jako katalizatorów oraz zaimpregnowanej antyseptykiem (dichlorowodorkiem oktenidyny), charakteryzują się wysoką aktywnością przeciwdrobnoustrojową wobec *S. aureus* i *P. aeruginosa* w hodowlach płynnych oraz w postaci biofilmu *in vitro* (**publikacja D-3**).

6. RMF zwiększa stopień uwalniania antyseptyku (dichlorowodorku oktenidyny) z nośnika na bazie BC oraz jego penetrację przez kolejne warstwy biofilmu wytwarzanego przez *S. aureus* i *P. aeruginosa in vitro* (**publikacja D-4**).

7. RMF zwiększa efektywność działania antyseptyku (dichlorowodorku oktenidyny) uwolnionego z nośnika na bazie BC, wobec biofilmów bakteryjnych wytwarzanych przez *S. aureus* i *P. aeruginosa in vitro* (**publikacja D-4**).

3. Cel badawczy

Podstawowym celem publikacji wchodzących w skład osiągnięcia naukowego i stanowiących podstawę ubiegania się o stopień naukowy doktora było opracowanie materiałów bionanocelulozowych do zapobiegania kolonizacji przez drobnoustroje patogenne oraz eradykacji biofilmów bakteryjnych.

Cele szczegółowe

1. Dobranie katalizatorów reakcji krzyżowego sieciowania (spośród bezpiecznych, łatwo dostępnych i niedrogich substancji), które podczas rozkładu termicznego i w reakcjach z kwasami wydzielają duże ilości nieszkodliwych gazów (**publikacja D-1**).

2. Optymalizacja metody modyfikacji BC za pomocą reakcji krzyżowego sieciowania z uwzględnieniem wybranych katalizatorów, w celu uzyskania materiałów charakteryzujących się zwiększoną zdolnością do pochłaniania i utrzymywania cieczy (względem BC niemodyfikowanej), przy jednoczesnym zachowaniu nietoksyczności (**publikacja D-1**).

3. Ocena możliwości zastosowania soku komórkowego z bulw ziemniaków jako pełnowartościowej pożywki produkcyjnej do wytwarzania BC przez szczepy *K. xylinus* (**publikacja D-2**).

4. Ocena zdolności do pochłaniania sztucznego wysięku przez materiały na bazie BC wytworzonej w pożywce z soku komórkowego z bulw ziemniaków, modyfikowanej za

pomocą reakcji krzyżowego sieciowania z wykorzystaniem kwasu cytrynowego oraz mieszaniny wodorofosforanu disodu i wodorowęglanu sodu jako katalizatorów oraz zaimpregnowanej antyseptykiem (dichlorowodorkiem oktenidyny) (**publikacja D-3**).

5. Ocena kinetyki uwalniania antyseptyku (dichlorowodorku oktenidyny) z materiałów na bazie BC wytworzonej w pożywce z soku komórkowego z bulw ziemniaków i modyfikowanej za pomocą reakcji krzyżowego sieciowania z wykorzystaniem kwasu cytrynowego oraz mieszaniny wodorofosforanu disodu i wodorowęglanu sodu jako katalizatorów (**publikacja D-3**).

6. Ocena właściwości przeciwdrobnoustrojowych materiałów na bazie BC wytworzonej w pożywce z soku komórkowego z bulw ziemniaków, modyfikowanej za pomocą reakcji krzyżowego sieciowania z wykorzystaniem kwasu cytrynowego oraz mieszaniny wodorofosforanu disodu i wodorowęglanu sodu jako katalizatorów oraz zaimpregnowanej antyseptykiem (dichlorowodorkiem oktenidyny), względem bakterii w hodowlach na pożywkach stałych i płynnych oraz w postaci biofilmu (**publikacja D-3**).

7. Ocena wpływu RMF na stopień uwalniania antyseptyku (dichlorowodorku oktenidyny) z nośnika na bazie BC, a następnie jego penetracji przez warstwy biofilmu bakteryjnego *in vitro* (**publikacja D-4**).

8. Ocena wpływu RMF na efektywność działania antyseptyku (dichlorowodorku oktenidyny) uwolnionego z nośnika na bazie BC wobec biofilmów bakteryjnych wytwarzanych przez *S. aureus* i *P. aeruginosa in vitro* (**publikacja D-4**).

4. Materiały i metody badawcze

4.1. Mikroorganizmy

W celu wytwarzania celulozy bakteryjnej (BC) wykorzystano referencyjny szczep mikroorganizmów należący do gatunku *K. xylinus* ATCC 53524 (American Type Culture Collection) (**publikacje D-1, D-2, D-3, D-4**) oraz szczepy *K. xylinus* ATCC: 53582, 23770, 700178, 23768, 23769, 35959, 14851 (**publikacja D-2**).

Aktywność przeciwdrobnoustrojową i przeciwbiofilmową BC impregnowanej antyseptykiem na bazie dichlorowodorku oktenidyny (OCT) analizowano względem bakterii *S. aureus* (ATCC 6538) i *P. aeruginosa* (ATCC 15542) (**publikacje D-2**, **D-3**, **D-4**) oraz klinicznych izolatów gronkowców należących do gatunków *S. aureus*, *S. equorum*, *S. warneri*, *S. xylosus*, a także 4 klinicznych izolatów *P. aeruginosa* (kolekcja mikroorganizmów Katedry Mikrobiologii i Biotechnologii, ZUT).

4.2. Bioreaktory wspomagane wirującym polem magnetycznym

Badania z wykorzystaniem wirującego pola magnetycznego (RMF) przeprowadzono przy użyciu prototypowych bioreaktorów (opisanych i zaprezentowanych w **publikacjach A-9, A-10 i A-11**), wyposażonych w aparaturę kontrolno-pomiarową (urządzenia zaprojektowane

i zbudowane samodzielnie, na potrzeby badań prowadzonych w Katedrze Mikrobiologii i Biotechnologii).

Analizy i wizualizacje związane z charakterystyką wirującego pola magnetycznego (RMF) wykonano we współpracy z dr hab. inż. Marcinem Wardachem, prof. ZUT z Katedry Maszyn i Napędów Elektrycznych ZUT w Szczecinie.

4.3. Wytwarzanie celulozy bakteryjnej

W celu otrzymania BC, prowadzono hodowlę stacjonarną *K. xylinus* w 28°C przez 7 dni z wykorzystaniem pożywki produkcyjnej H-S (**publikacje D-1, D-2, D-3, D-4**). W zależności od rodzaju eksperymentu, biosyntezę BC prowadzono w naczyniach hodowlanych o różnym kształcie (np. falkony, szalki Petriego) oraz przy użyciu różnych objętości pożywki produkcyjnej.

4.4. Przygotowanie i charakterystyka pożywki produkcyjnej na bazie soku komórkowego z bulw ziemniaków

Umyte i obrane ziemniaki rozdrobniono z użyciem wysokoobrotowej sokowirówki (Bosch, MES3500, Niemcy), następnie odstawiono w celu osadzenia się skrobi, dekantowano, rozcieńczono wodą destylowaną w proporcji 1:1 i autoklawowano. W ostatnim etapie pożywkę wirowano w celu usunięcia części stałych. Pożywkę na bazie soku komórkowego z bulw ziemniaków opracowano we współpracy z mgr inż. Michałem Brodą z Pomorsko-Mazurskiej Hodowli Ziemniaka w Strzekęcinie, z której pochodziły bulwy ziemniaków użyte do produkcji pożywki (**publikacje D-2, D-3**).

Stężenie cukrów, w tym glukozy, fruktozy i sacharozy oraz kwasu glukonowego w pożywce na bazie soku komórkowego z bulw ziemniaków oznaczano przy użyciu chromatografu cieczowego z tandemową spektrometrią mas (LC-MS/MS, 1260 Infinity II Series LC, Agilent, USA) we współpracy z dr Danielem Styburskim z Laboratorium Chromatografii i Spektroskopii Mas ZUT w Szczecinie (**publikacja D-2**). Stężenie białka całkowitego oznaczano metodą Bradforda (**publikacja D-2**). Stężenie skrobi oznaczano metodą jodometryczną (**publikacja D-2**).

4.5. Określenie ilości i żywotności komórek K. xylinus podczas wytwarzania celulozy bakteryjnej

Ilość i żywotność komórek *K. xylinus* w pożywce produkcyjnej oraz w membranach BC oznaczano z wykorzystaniem testu alamarBlue (Thermo Fisher Scientific, USA). Odczyty fluorescencji wykonywano przy długościach fali wzbudzenia 540 nm i fali emisji 590 nm z wykorzystaniem czytnika mikropłytek (Synergy HTX, Biotek, USA) (**publikacja D-2**).

4.6. Oczyszczanie i wstępna charakterystyka celulozy bakteryjnej

Próby BC inkubowano przez 90 min w 0,1 M roztworze wodorotlenku sodu w temperaturze 80°C (**publikacje D-1, D-2, D-3, D-4**). Po oczyszczaniu, próby BC ważono w celu ustalenia efektywności procesu biosyntezy (**publikacja D-2**), lub w celu dobrania materiałów o jednakowej wadze do dalszych eksperymentów (**publikacja D-3**).

4.7. Modyfikacja celulozy bakteryjnej

Próby BC modyfikowano z wykorzystaniem metody polegającej na przeprowadzeniu reakcji krzyżowego sieciowania. Reakcję prowadzono w temperaturze 160°C z użyciem kwasu cytrynowego jako czynnika sieciującego, a także wodorofosforanu disodu, wodorowęglanu sodu, wodorowęglanu amonu i ich mieszanin oraz podfosforynu sodu jako katalizatorów (**publikacje D-1, D-3**). Opracowaną metodę modyfikacji BC zoptymalizowano w celu ustalenia dokładnych warunków reakcji, a wyniki tej optymalizacji przedstawiono w **Suplemencie publikacji D-1**.

Efektywność sieciowania BC w optymalnych warunkach reakcji obliczano jako procentowy przyrost masy (WPG, ang. *weight percent gain*) według ze wzoru:

$$WPG\ [\%] = \frac{W_m - W_u}{W_u} * 100\%$$

Gdzie: W_m – waga suchej, modyfikowanej BC, and W_u – waga suchej, niemodyfikowanej BC.

4.8. Analiza właściwości fizykochemicznych celulozy bakteryjnej

Wszystkie poniżej opisane analizy wykonywano z użyciem BC modyfikowanej za pomocą reakcji krzyżowego sieciowania oraz BC niemodyfikowanej jako próby kontrolnej.

4.8.1. Ocena makro- i mikrostruktury

Analizę makrostruktury BC przeprowadzono z wykorzystaniem mikroskopu stereoskopowego (Leica S9i, Leica Microsystems, Niemcy; **publikacja D-1**), natomiast analizę mikrostruktury z wykorzystaniem skaningowego mikroskopu elektronowego (SEM, ang. *scanning electron microscope*, VEGA3, Tescan, Czechy oraz Auriga 60, Zeiss, Niemcy). Powyższe badania przeprowadzono we współpracy z dr inż. Urszulą Kowalską z Centrum Bioimmobilizacji i Innowacyjnych Materiałów Opakowaniowych ZUT w Szczecinie oraz dr inż. Pawłem Migdałem z Katedry Higieny Środowiska i Dobrostanu Zwierząt Uniwersytetu Przyrodniczego we Wrocławiu (**publikacje D-1, D-2**).

4.8.2. Skład pierwiastkowy powierzchni

Analizę elementarną powierzchni BC przeprowadzono z wykorzystaniem SEM (Auriga 60, Zeiss, Niemcy) i detektora EDX (Oxford Instruments, Wielka Brytania) (**publikacja D-1**). Analizę tą wykonano we współpracy z dr inż. Pawłem Migdałem z Katedry Higieny Środowiska i Dobrostanu Zwierząt Uniwersytetu Przyrodniczego we Wrocławiu.

4.8.3. Skład chemiczny

Do oznaczenia składu chemicznego BC wykorzystano metodę Spektroskopii Fourierowskiej Osłabionego Całkowitego Odbicia w Podczerwieni (ATR-FTIR, ang. *Attenuated Total Reflectance Fourier Transform Infrared Spectroscopy*) z zastosowaniem spektroskopu Bruker Co. (USA) (**publikacje D-1, D-2**). Otrzymane widma analizowano przy użyciu oprogramowania Spectragryph 1.2. Dodatkowo, wykonano analizę korelacji 2D z wykorzystaniem programu 2DShige© v1.3 oraz OriginPro 8 (Origin Software Solutions, Wielka Brytania) (**publikacja D-1**). Analizę chemometryczną głównych składowych wykonano przy użyciu pakietów FactoMineR i Factorextra oprogramowania RStudio z pomocą dr inż. Radosława Drozda z Katedry Mikrobiologii i Biotechnologii ZUT w Szczecinie. Na

podstawie uzyskanych widm absorbancji obliczono również stopień krystaliczności (**publikacja D-2**) korzystając ze wzoru:

$$f_\alpha = A750 / (A750 + A710)$$

A710, A750 – intensywność absorbancji przy określonej długości fali

4.8.4. Parametry związane z absorpcją i utrzymaniem cieczy

Zdolność BC do pochłaniania cieczy (współczynnik pęcznienia, SR, ang. *swelling ratio*) ustalono na podstawie pomiarów wagi BC wysuszonej oraz wagi BC po ponownym uwodnieniu (**publikacje D-1, D-2**), korzystając ze wzoru:

$$SR\ [\%] = \frac{(W_w - W_d)}{W_d} * 100\%$$

W_w – mokra masa BC, W_d – sucha masa BC.

Zdolność BC do utrzymywania cieczy (współczynnik utrzymywania wody, WHC, ang. *water holding capacity*) ustalono na podstawie pomiarów wagi BC suchej oraz wagi BC po ponownym uwodnieniu w trakcie wirowania (200 *g*) lub suszenia (37°C) (**publikacje D-1, D-2**), korzystając ze wzoru:

$$WHC[\%] = \frac{W_w - W_{dw}}{W_d} * 100\%$$

W_w mokra masa BC, W_{dw} - masa BC podczas suszenia/wirowania, W_d – sucha masa BC.

Powyższe metody zastosowano również do oceny pochłaniania i utrzymywania OCT przez BC modyfikowaną za pomocą reakcji krzyżowego sieciowania (**publikacja D-3**).

4.8.5. Gęstość

Gęstość BC ustalano na podstawie pomiarów masy suchej BC w powietrzu oraz w metanolu wykonanych z wykorzystaniem wagi hydrostatycznej (XA 52/Y, Radwag, Polska) (**publikacje D-1, D-2**), korzystając ze wzoru:

$$g = \frac{W_d}{W_d - W_m} * g_{methanol}$$

W_d – masa suchej BC w powietrzu, and W_m – masa suchej BC w metanolu.

4.8.6. Właściwości mechaniczne

Właściwości mechaniczne oceniano zgodnie z normą PN-EN ISO 527-1, przy użyciu uniwersalnej maszyny wytrzymałościowej Instron (USA) (**publikacja D-2**). Badano wytrzymałość na rozciąganie i wydłużenie przy zerwaniu w temperaturze pokojowej. Analizy wykonano we współpracy z dr inż. Krzysztofem Gorącym z Katedry Inżynierii Polimerów i Biomateriałów ZUT w Szczecinie.

4.8.7. Cytotoksyczność

Analizę stopnia cytotoksyczności BC przeprowadzono za pomocą oceny żywotności fibroblastów linii L929 zgodnie z normą ISO 10993-5:2009. Wykonywano test bezpośredniego

kontaktu z BC oraz analizy z użyciem ekstraktów przygotowanych z prób BC (**publikacje D-1, D-2, D-3**). Żywotność komórek fibroblastów oceniano za pomocą testu opartego o pomiar fluorescencji resazuryny. Pomiary wykonywano przy długości fali wzbudzenia 540 nm i fali emisji 590 nm z wykorzystaniem czytnika mikropłytek (Synergy HTX, Biotek, USA). Procent żywych komórek obliczono z wykorzystaniem wzoru:

$$\%\ żywotności\ komórek = \left(\frac{FLs-FLb}{FLc-FLb}\right)\ x\ 100$$

FL – intensywność fluorescencji, indeksy *s, b, c* – próba, blank, kontrola

Ponadto, zastosowano barwienie z wykorzystaniem barwników SYTO-9 i jodku propidyny (Thermo Fisher Scientific, USA). Wizualizacji żywych i martwych fibroblastów dokonano za pomocą mikroskopu konfokalnego (Leica SP8, Leica Microsystems, Niemcy) (**publikacje D-1, D-2, D-3**). Powyższe analizy wykonano we współpracy z dr inż. Piotrem Sobolewskim z Katedry Inżynierii Polimerów i Biomateriałów ZUT w Szczecinie, dr hab. n. med. Adamem Junką, prof. Uczelni z Katedry i Zakładu Mikrobiologii Farmaceutycznej i Parazytologii Uniwersytetu Medycznego im. Piastów Śląskich we Wrocławiu oraz dr Moniką Toporkiewicz i dr hab. Grzegorzem Chodaczkiem z Laboratorium Bioobrazowania Sieci Badawczej ŁUKASIEWICZ – PORT we Wrocławiu.

4.9. Impregnacja celulozy bakteryjnej antyseptykiem oraz analiza jej podstawowych właściwości

Suchą BC impregnowano poprzez zanurzenie w roztworze OCT na 24 h w 4°C (**publikacje D-2, D-3, D-4**). W przypadku mokrych prób BC, roztwór OCT wymieniano co 2 h.

4.9.1. Zdolność do pochłaniania wysięku

Próby BC zaimpregnowanej OCT zanurzano w roztworze symulowanego płynu z rany (sztucznego wysięku, skład: surowica bydlęca, NaCl, $NaHCO_3$, KCl, K_2HPO_4 x $3H_2O$, $MgCl_2$ x $6H_2O$, $CaCl_2$, Na_2SO_4, bufor TRIS), z dodatkiem czerwieni Congo jako indykatora absorpcji i inkubowano z mieszaniem przez 7 dni, dokonując interwałowych pomiarów spektrofotometrycznych przy długości fali 300 nm (Synergy HTX, Biotek, USA) (**publikacja D-3**).

4.9.2. Kinetyka uwalniania antyseptyku w sztucznym łożysku rany

Sztuczne łożyska rany utworzono z wykorzystaniem szalek Petriego o średnicy 9 cm zawierających podłoże TSA (ang. *tryptic soy agar*) o 4% zawartości agaru, z uprzednio przygotowanym okrągłym zagłębieniem o średnicy 2,8 cm wypełnionym 3 mL sztucznego wysięku. Tak przygotowane podłoża przykrywano matą teflonową z wyciętym otworem (**publikacja D-3**).

Próby BC zaimpregnowane OCT układano na szalkach ze sztucznym łożyskiem rany. Ilość uwolnionego antyseptyku oceniano na podstawie pomiarów spektrofotometrycznych (270 nm) sztucznego wysięku pobieranego w różnych modelach czasowych - 8 h (model krótki) oraz 7 dni (model długi) (**publikacja D-3**).

4.10. Analiza aktywności przeciwdrobnoustrojowej celulozy bakteryjnej zaimpregnowanej antyseptykiem

4.10.1. Hodowle bakteryjne na podłożu stałym

Wykorzystano standardową metodę dyfuzyjno-krążkową, zgodnie z rekomendacją Europejskiego Komitetu ds. Badania Wrażliwości Drobnoustrojów (EUCAST, ang. *European Committee on Antimicrobial Susceptibility Testing*) (**publikacja D-2, D-3**). Dodatkowo, w celu określenia aktywności przeciwdrobnoustrojowej w zależności od czasu kontaktowego, metoda ta została zmodyfikowana poprzez przekładanie prób BC co 1 h na świeże podłoże z uprzednio wysianymi drobnoustrojami testowymi (**publikacja D-3**).

4.10.2. Hodowle bakteryjne w podłożu płynnym

Próby BC zaimpregnowane OCT inkubowano w zawiesinach *S. aureus* i *P. aeruginosa* przez 7 dni w 37°C. Żywotność bakterii oceniano w różnych odstępach czasowych przy użyciu testu redukcji soli tetrazolowej (MTT, MilliporeSigma, USA), dokonując odczytów absorbancji przy długościach fali 540 nm i 690 nm (Synergy HTX, Biotek, USA) (**publikacje D-3**).

4.10.3. Hodowle bakteryjne w formie biofilmu

Wykorzystano model łożyska rany opisany w punkcie *4.9.2.*, w którego zagłębieniu umieszczano gazy pokryte biofilmem bakteryjnym *S. aureus* i *P. aeruginosa*. Na powierzchni umieszczano natomiast materiały na bazie BC zaimpregnowanej OCT. Układy te inkubowano przez 7 dni w 37°C. Żywotność bakterii oceniano w różnych odstępach czasowych z wykorzystaniem testu redukcji MTT (MilliporeSigma, USA) (**publikacja D-3**).

4.11. Wpływ wirującego pola magnetycznego na wybrane parametry związane uwalnianiem antyseptyku z celulozy bakteryjnej

4.11.1. Analiza ilości uwolnionego antyseptyku i szybkości jego penetracji przez warstwy biofilmu

Do badań wykorzystano bioreaktory wyposażone w generatory RMF i specjalnie skonstruowane układy doświadczalne zawierające dyski agarowe pokryte biofilmem ułożone bezpośrednio na sobie (dysk kontaktowy, środkowy, dolny). BC zaimpregnowaną OCT umieszczano na dysku kontaktowym (**publikacja D-4**). Tak przygotowane układy doświadczalne poddawano ekspozycji na RMF (w czasie 1, 2 i 3 h, przy częstotliwości pola (5 i 50 Hz). Następnie, w celu ekstrakcji OCT, krążki agarowe inkubowano w metanolu. Pomiarów stężenia wyekstrahowanego OCT dokonywano przy użyciu chromatografii cieczowej z tandemową spektrometrią mas (LC-MS/MS, 1260 Infinity II Series LC, Agilent, USA). Na podstawie uzyskanych wyników określono szybkość penetracji i ilość OCT w kolejnych krążkach agarowych reprezentujących warstwy biofilmu (**publikacja D-4**).

4.11.2. Analiza efektu przeciwdrobnoustrojowego

Aktywność przeciwdrobnoustrojową BC zaimpregnowanej OCT i eksponowanej na RMF o częstotliwości 5 i 50 Hz określano wobec biofilmów *S. aureus* i *P. aeruginosa* z wykorzystaniem metody A.D.A.M. (ang. *Antibiofilm Dressing's Activity Measurement*, Junka i wsp., 2017), z użyciem układu opisanego w rozdziale *4.11.1.* (**publikacja D-4**). Żywotność

komórek w biofilmie na kolejnych dyskach oznaczano za pomocą testu redukcji MTT (MilliporeSigma, USA) (**publikacje D-3, D-4**).

4.11.3. Analiza morfologiczna bakterii tworzących biofilm

Wizualizacji wpływu RMF i OCT uwalnianego z nośnika na bazie BC na żywotność komórek w biofilmie dokonano za pomocą barwienia z użyciem barwników SYTO-9 i jodku propidyny (Thermo Fisher Scientific, USA) oraz oceny wybarwionych prób za pomocą mikroskopu konfokalnego (Leica SP8, Leica Microsystems, Niemcy). Do wizualizacji biofilmów wykorzystywano także analizę SEM (Zeiss, EVO MA25, Niemcy). Analizy obrazów mikroskopowych dokonano z użyciem oprogramowania Imaris 9 oraz ImageJ (**publikacja D-4**). Badania mikroskopowe prowadzono we współpracy z dr inż. Patrycją Szymczyk-Ziółkowską z Katedry Technologii Laserowych, Automatyzacji i Organizacji Produkcji Politechniki Wrocławskiej oraz dr hab. Grzegorzem Chodaczkiem z Laboratorium Bioobrazowania Polskiego Ośrodka Rozwoju Technologii PORT we Wrocławiu.

4.11.4. Analiza zawartości cukrów w macierzy biofilmu

Próby biofilmu eksponowanego na RMF oczyszczano z komórek bakteryjnych, dializowano i analizowano za pomocą chromatografii gazowej sprzężonej z pojedynczym kwadrupolem spektrometru masowego (GC-MS/MS, Shimadzu, QP2010, Japonia). Uzyskane wyniki porównywano do nieeksponowanych na RMF biofilmów kontrolnych (**publikacja D-4**).

4.12. Analiza statystyczna

Wszystkie dane przedstawiano jako średnie ± odchylenia standardowe średnich (SEM) uzyskanych z co najmniej trzech różnych pomiarów (**publikacje D-1, D-2, D-3, D-4**). W celu wykazania prawidłowości między zmiennymi wykorzystano analizę głównych składowych (PCA, ang. *principal component analysis*), a korelację między zmiennymi przedstawiono na wykresie punktowym 3D (**publikacja D-1**). Różnice statystyczne między próbami określano za pomocą jednoczynnikowej analizy wariancji (ANOVA) oraz testu post hoc Tukey'a (**publikacje D-1, D-2, D-3, D-4**).

5. Wyniki

Wszystkie etapy badań stanowią powiązany ze sobą cykl eksperymentalny, opisujący w pierwszej kolejności charakterystykę materiałów bionanocelulozowych otrzymanych za pomocą modyfikacji w procesie krzyżowego sieciowania. W dalszym etapie, cykl ten opisuje analizy związane z możliwością wykorzystania otrzymanych biomateriałów jako nośników dla substancji wykazujących aktywność przeciwdrobnoustrojową wobec bakterii w formie planktonicznej oraz w formie biofilmu. Oprócz materiałów o właściwościach przeciwdrobnoustrojowych, prowadzone badania związane były także z oceną możliwości zastosowania RMF w celu intensyfikacji efektu przeciwdrobnoustrojowego poprzez kontrolowanie uwalniania antyseptyku z materiału celulozowego i zwiększenie jego penetracji przez warstwy biofilmu. Dodatkowo, w celu wykazania możliwości obniżenia kosztów związanych z produkcją BC, w badaniach podjęto również próbę opracowania pożywki na bazie soku komórkowego z bulw ziemniaków – głównego odpadu przemysłu skrobiowego.

Etap 1. Opracowanie i optymalizacja metody modyfikacji BC oraz charakterystyka otrzymanego materiału.
Etap ten obejmował:

- Opracowanie i optymalizację procesu modyfikacji BC poprzez zastosowanie reakcji krzyżowego sieciowania z użyciem czynnika sieciującego i katalizatorów;
- Analizę właściwości fizykochemicznych i cytotoksyczności otrzymanych materiałów oraz porównanie ich do niemodyfikowanej BC;

Etap 2. Opracowanie i charakterystyka pożywki produkcyjnej do wytwarzania BC na bazie soku komórkowego z bulw ziemniaków.
Etap ten obejmował:

- Opracowanie i optymalizację procesu przygotowania pożywki na bazie soku komórkowego z bulw ziemniaków;
- Analizę składu opracowanej pożywki;
- Analizę parametrów dotyczących biosyntezy BC (ilość komórek *K. xylinus* w trakcie biosyntezy BC i określenie efektywności tego procesu);
- Analizę właściwości fizykochemicznych oraz cytotoksyczności BC otrzymanej z zastosowaniem pożywki na bazie soku komórkowego z bulw ziemniaków i porównanie ich z właściwościami BC otrzymanej z zastosowaniem standardowej pożywki H-S.

Etap 3. Wykorzystanie BC wytwarzanej z użyciem pożywki produkcyjnej na bazie soku komórkowego z bulw ziemniaków i modyfikowanej w procesie krzyżowego sieciowania jako materiału opatrunkowego na zainfekowane rany z dużym wysiękiem.
Etap ten obejmował:

- Impregnację modyfikowanej BC substancją przeciwdrobnoustrojową (OCT);
- Analizę profilu uwalniania OCT z modyfikowanej BC;
- Analizę pochłaniania wysięku z modyfikowanej BC zaimpregnowanej OCT;
- Analizę właściwości przeciwdrobnoustrojowych i przeciwbiofilmowych modyfikowanej BC zaimpregnowanej OCT;
- Analizę przylegania modyfikowanej BC zaimpregnowanej OCT do zakrzywionych powierzchni;

Etap 4. Badanie wpływu RMF na uwalnianie OCT z nośnika na bazie BC oraz na eradykację biofilmu bakteryjnego.
Etap ten obejmował:

- Ocenę wpływu RMF na proces uwalniania OCT z nośnika na bazie BC i jego penetracji przez kolejne warstwy biofilmu;
- Ocenę wpływu RMF na efektywność przeciwbiofilmową OCT uwolnionego z nośnika na bazie BC;
- Ocenę wpływu RMF na morfologię komórek bakteryjnych w biofilmie i skład macierzy zewnątrzkomórkowej;

Etap 1

Mimo wysokiego potencjału aplikacyjnego BC wynikającego z jej unikalnych właściwości, istnieją pewne ograniczenia w kontekście jej zastosowania jako materiału opatrunkowego. Idealnym rozwiązaniem tego problemu wydaje się opracowanie metody modyfikacji, pozwalającej na połączenie korzyści płynących ze stosowania mokrej i suchej BC. Z tego powodu, celem mojej pierwszej pracy było opracowanie i optymalizacja modyfikacji pozwalającej na stworzenie bezpiecznego bionanomateriału, który nawet w stanie suchym zachowuje wysoką zdolność absorbcji i utrzymania cieczy, wykorzystując proste reakcje oraz bezpieczne, ogólnodostępne i niedrogie odczynniki chemiczne (**publikacja D-1**).

Reakcje krzyżowego sieciowania w wysokiej temperaturze były wykorzystywane do modyfikacji wielu biopolimerów, jednak do roku 2020 włącznie, odnalazłam tylko 2 prace opisujące zastosowanie tego procesu w odniesieniu do BC (Meftahi i wsp., 2018; Frone i wsp., 2020). Meftahi i wsp. (2018) przeprowadzili modyfikację z zastosowaniem kwasu cytrynowego jako czynnika sieciującego oraz podfosforynu sodu jako katalizatora, otrzymując materiał o 3-krotnie wyższej zdolności do ponownego uwodnienia w porównaniu z niemodyfikowaną BC. Zastosowane odczynniki były już wcześniej szeroko opisywane jako reagenty w reakcjach sieciowania innych polimerów (Gyawali i wsp., 2010; Ye i wsp., 2015; El-Fawal i wsp., 2018). Kwas cytrynowy jest szczególnie obiecującym czynnikiem sieciującym nie tylko ze względu na jego nietoksyczność i bezpieczeństwo stosowania, ale także na wysoką stabilność wiązań sieciujących, które tworzy z celulozą (Sotolářová i wsp., 2021). Co ważne, kwas cytrynowy jest łatwo dostępny i niedrogi, co umożliwia jego zastosowanie na dużą skalę. Pierwszym celem prowadzonych badań było dobranie katalizatorów reakcji krzyżowego sieciowania, które w połączeniu z kwasem cytrynowym pozwoliłyby na otrzymanie biomateriału o wysokiej wodochłonności. Skupiając się na potencjalnym zastosowaniu opracowywanych przeze mnie materiałów w medycynie i weterynarii, oraz mając na uwadze aspekt proekologiczny, wybrałam odczynniki znajdujące się na liście substancji ogólnie uznanych za bezpieczne (GRAS, ang. *Generally Recognized As Safe*) według Agencji ds. Żywności i Leków (FDA, ang. *Food and Drug Administration*). Substancjami tymi były wodorofosforan disodu, wodorowęglan sodu, wodorowęglan amonu oraz ich mieszaniny. Wykluczyłam natomiast potencjalnie szkodliwe substancje, m.in. opisywany wcześniej podfosforyn sodu, którego rozkład termiczny powoduje powstawanie wysoce toksycznego gazu – fosfiny. Wiedząc, że reakcja krzyżowego sieciowania celulozy prowadzona w wysokiej temperaturze polega na łączeniu grup hydroksylowych jej cząsteczek (Qi i wsp., 2016), jako katalizatory dobrałam substancje wydzielające duże ilości gazów w reakcji z kwasami i podczas rozkładu termicznego (m.in. substancje używane w piekarnictwie), zakładając, że uwolniony gaz wypełni przestrzenie między włókami i warstwami BC i zapobiegnie zapadaniu się jej trójwymiarowej struktury podczas wysychania, w pewien sposób zastępując ubywające cząsteczki wody.

Następnie przeprowadziłam kompleksową optymalizację procesu modyfikacji BC z uwzględnieniem zastosowania 7 różnych wariantów katalizatorów, dobierając odpowiednie warunki takie jak profil czasowo-temperaturowy reakcji, stężenia odczynników oraz ich ilość w mieszaninie reakcyjnej. Jako, że głównym celem mojej pracy była poprawa zdolności sorpcyjnych BC w stanie suchym, na tym parametrze oparłam proces optymalizacji, poszukując jak najwyższych wartości współczynnika pęcznienia (SR, ang. *swelling ratio*). Wyniki optymalizacji przedstawiłam w **Suplemencie publikacji D-1**.

Po otrzymaniu modyfikowanej BC, przeprowadziłam szczegółową analizę jej parametrów fizykochemicznych. Analiza makro i mikromorfologiczna pozwoliła na zaobserwowanie przestrzeni powietrznych i bąbelków powietrza w strukturze modyfikowanej BC. Natężenie tych zmian zależało od rodzaju zastosowanego katalizatora. Analiza przekroju BC wykazała natomiast wyraźną strukturę warstwową modyfikowanego materiału.

Wielowarstwowy układ przestrzenny jest charakterystyczny dla BC, ponieważ wiąże się z biologicznymi i fizycznymi procesami jej syntezy – włókna celulozy są wydzielane przez komórki bakteryjne do przestrzeni pozakomórkowej tworząc cienką warstwę na powierzchni pożywki hodowlanej (Keshk, 2014; Shao i wsp., 2017). Z biegiem czasu na powierzchni pojawia się kolejna warstwa celulozy (komórki migrują ku górze), spychając poprzednią ku dołowi – proces ten powtarza się do wyczerpania składników odżywczych. Fakt zaobserwowania wielowarstwowej struktury w przypadku modyfikowanej BC potwierdza, że proces modyfikacji skutecznie zapobiega zapadaniu się warstw BC podczas suszenia. Porównanie składu chemicznego modyfikowanej i niemodyfikowanej BC z wykorzystaniem analizy ATR-FTIR pozwoliło mi stwierdzić, że wszystkie zastosowane katalizatory miały znaczący wpływ na strukturę chemiczną BC. Odzwierciedlało się to głównie w pojawieniu się pasma charakterystycznego dla grupy karbonylowej (Crépy i wsp., 2011) oraz pasma estrowego (Schilling i wsp., 2010).

Zastosowania biomedyczne BC zależą w dużej mierze od jej parametrów związanych z chłonnością i utrzymaniem cieczy. Właściwości te zależą z kolei od rozmiaru i objętości porów oraz od powierzchni właściwej materiału (Gatenholm i Klemm, 2010; Zaborowska i wsp., 2010). W przypadku materiałów opatrunkowych, wysoka chłonność zapewnia ciągłe odbieranie wysięku, jednocześnie sprawiając, że opatrunek nie przylega do rany, co ułatwia jego zmianę oraz zapobiega niszczeniu nowo tworzącej się tkanki (Portela i wsp., 2019; Ul-Islam i wsp., 2012). Ponadto, wysoka zdolność absorpcyjna BC względem cieczy i małych cząstek sprawia, że jest ona również doskonałym nośnikiem dla substancji przeciwdrobnoustrojowych stosowanych wspomagająco w gojeniu ran (de Oliveira Barud i wsp., 2016). Wyniki moich badań wykazały, że w przypadku każdego z zastosowanych wariantów modyfikacji otrzymywane były materiały charakteryzujące się znacznie wyższym współczynnikiem pęcznienia w porównaniu z suchą, niemodyfikowaną BC (w przypadku zastosowania mieszaniny wodorosforanu disodu i wodorowęglanu sodu jako katalizatorów była to wartość 5-krotnie wyższa). Również współczynnik utrzymania wody (WHC, ang. *water holding capacity*) był znacznie wyższy w przypadku modyfikowanej BC. W przypadku tego parametru, oznacza to, że modyfikowane próbki znacznie wolniej traciły wilgoć w porównaniu z BC niemodyfikowaną. Aby określić rzeczywisty potencjał aplikacyjny otrzymanych przeze mnie materiałów, porównałam ich chłonność z nowoczesnymi, komercyjnymi opatrunkami dedykowanymi do stosowania na rany z dużym wysiękiem. W tym wypadku wykazałam, że modyfikowana BC charakteryzowała się ponad 1,5-krotnie wyższą pojemnością wodną w porównaniu z opatrunkami komercyjnymi (**Suplement publikacji D-1**). Podczas dalszych badań wykazałam również, że wydajność sieciowania nie koreluje bezpośrednio z wartościami parametrów wodnych. Potwierdza to jednak hipotezę, że podstawową rolą środka sieciującego jest usztywnienie struktury BC (Qi i wsp., 2016; Widsten i wsp., 2014), podczas gdy dopiero jednoczesne działanie środka sieciującego i katalizatorów zapewnia odpowiednie właściwości sorpcyjne suchych materiałów. Dopełnieniem prowadzonych przeze mnie analiz były badania cytotoksyczności względem komórek fibroblastów linii L929, które potwierdziły, że ekstrakty modyfikowanych próbek BC nie wykazywały toksyczności niezależnie od badanego wariantu modyfikacji. Natomiast w przypadku metody kontaktowej jedynie materiały modyfikowane z wykorzystaniem wodorowęglanu amonu powodowały istotne zmniejszenie żywotności fibroblastów. Otrzymane wyniki sugerują, że opracowana metoda modyfikacji może znaleźć zastosowanie w produkcji innowacyjnych, wysokochłonnych materiałów opatrunkowych dedykowanych do leczenia ran przewlekłych.

Poza publikacją, wymiernym efektem przeprowadzonych prac badawczych jest również patent:

Ciecholewska, D., Fijałkowski, K. *Sposób wytwarzania modyfikowanej celulozy bakteryjnej o znacznych właściwościach sorpcyjnych*, nr zgłoszenia: P. 430888, nr prawa wyłącznego: Pat.240308, 2019.

Etap 2

Jednym z głównych czynników ograniczających stosowanie BC na szeroką skalę jest jej wysoka cena, wynikająca przede wszystkim z wysokich kosztów pożywki produkcyjnej. Z tego powodu, od wielu lat prowadzone są intensywne badania, których podstawowym celem jest zwiększenie efektywności i/lub zmniejszenie kosztów produkcji BC. Również w przypadku badań prowadzonych przeze mnie w ramach pracy doktorskiej podjęłam się próby opracowania nowej pożywki produkcyjnej umożliwiającej poprawienie ekonomicznych aspektów wytwarzania tego biomateriału. Przy czym, w badaniach tych kierowałam się nie tylko aspektem ekonomicznym, ale również ekologicznym – źródła składników odżywczych dla bakterii syntetyzujących celulozę poszukiwałam wśród surowców naturalnych i odpadowych. Wytwarzanie BC z użyciem surowców naturalnych i odpadowych (np. soków owocowych z pomarańczy, ananasów, jabłek, kokosa, winogron, soku sizalowego, ścieków z procesu produkcji kandyzowanej jujuby, serwatki, łusek ryżu, łodyg kukurydzy) było już wcześniej opisywane w literaturze (Kongruang, 2007; Goelzer i wsp., 2009; Kurosumi i wsp., 2009; Li i wsp., 2015; Lima i wsp., 2017; Revin i wsp., 2018; Abol-Fotouh i wsp., 2020). Jednakże, zgodnie z powyżej wymienionymi pracami, aby otrzymać wysoki uzysk BC, pożywka produkcyjna powinna być uzupełniona o dodatkowe źródła azotu i węgla. Ponadto często konieczna jest również wstępna obróbka wykorzystywanych surowców, np. hydroliza termiczna, kwasowa lub enzymatyczna, co dodatkowo wydłuża proces syntezy BC i zmniejsza opłacalność ekonomiczną takiego rozwiązania.

Mając na uwadze wyżej wymienione kwestie oraz dokonując szczegółowego przeglądu literatury, w swoich badaniach postanowiłam wykorzystać sok komórkowy z bulw ziemniaków. Ziemniaki to warzywa o wysokiej wartości odżywczej uprawiane w wielu krajach na całym świecie, co przekłada się na ich łatwą dostępność i niską cenę w całym cyklu rocznym (Bradshaw i Bonierable, 2010). Obecnie, sok ziemniaczany jest najpowszechniej stosowany jako źródło białka w żywieniu zwierząt. Ponadto, w ostatnim czasie zyskuje on również popularność jako środek do łagodzenia objawów choroby wrzodowej żołądka i dwunastnicy lub innych problemów w obrębie układu trawiennego (Kowalczewski i wsp., 2012).

Przemysł ziemniaczany generuje znaczną ilość odpadów, w tym przede wszystkim wycierkę ziemniaczaną oraz wodę sokową (w przemyśle skrobiowym na 1 tonę skrobi przypada 3,5 tony odpadów). Ich zagospodarowanie wciąż stanowi istotny problem technologiczny (Grommers i van der Krogt, 2009; Fang i wsp., 2011). Jedynym raportem opisującym wykorzystanie takich odpadów do produkcji BC jest praca Abdelraof'a i wsp. (2019), w której do produkcji pożywki użyto skórek ziemniaczanych. Podejście to wymagało jednak zastosowania hydrolizy kwasowej z użyciem dodatkowych odczynników chemicznych, a proces prowadzony był w wysokiej temperaturze, co w rezultacie ograniczało potencjalne zastosowanie przemysłowe oraz opłacalność tej metody.

W ramach prowadzonych badań opracowałam pożywkę produkcyjną na bazie soku komórkowego z bulw ziemniaków (PJ, ang. *potato juice*) jako samodzielnego źródła składników odżywczych dla bakterii *K. xylinus* (**publikacja D-2**). Przeprowadziłam proces optymalizacji przygotowywania pożywki PJ z uwzględnieniem otrzymania jak największego uzysku BC. Następnie, pożywka PJ została przeze mnie scharakteryzowana pod względem zawartości cukrów, białek i pozostałości skrobi. Przeprowadzone analizy wykazały obecność

glukozy, fruktozy i sacharozy (w ilościach ok. 3,5 g/L, 2,4 g/L i 4 g/L), które mogą stanowić źródła węgla dla bakterii *K. xylinus*, białek (w ilości ok. 1,6 g/L), które z kolei mogą zostać wykorzystane jako źródło azotu oraz znikomych ilości skrobi (<0,1 g/L).

Zróżnicowany skład cukrowy pożywki PJ ma kluczowe znaczenie dla jej zastosowania w hodowlach produkcyjnych prowadzonych z wykorzystaniem różnych szczepów bakteryjnych, które najczęściej charakteryzują się odmiennym optimum pod względem zapotrzebowania na źródło energii i węgla (Singhsa i wsp., 2018; Chen i wsp., 2019). Ponadto, warto również zwrócić uwagę, że glukoza, która jest najpowszechniej wykorzystywanym składnikiem pożywek produkcyjnych, jest przetwarzana nie tylko na cząsteczki celulozy, ale również na kwas glukonowy, co obniża pH pożywki, a tym samym zmniejsza wydajność biosyntezy BC (Aswini i wsp., 2020). Na podstawie przeprowadzonych badań ustaliłam, że stężenie kwasu glukonowego w pożywce PJ, zmierzone po zakończeniu procesu biosyntezy BC, było znacznie mniejsze w porównaniu do konwencjonalnej pożywki H-S, co skutkowało wyższym pH w całym okresie hodowli. Poza składem cukrowym, uzyskane wyniki potwierdziły również, że zawartość białka w pożywce PJ, chociaż mniejsza niż w H-S, była wystarczająca dla utrzymania wysokiej efektywności biosyntezy BC.

Kinetyka wzrostu bakterii *K. xylinus* i dynamika produkcji BC są kluczowymi czynnikami pozwalającymi na dobór optymalnego czasu i warunków hodowli, w rezultacie mając wpływ również na ekonomiczny aspekt tego bioprocesu (Abdelraof i wsp., 2019). Z tego powodu, przeanalizowałam kinetykę wzrostu bakterii *K. xylinus* podczas 7-dniowej hodowli w pożywce H-S oraz w pożywce PJ. Podczas tych badań nie wykazałam różnic w dynamice wzrostu pomiędzy hodowlami prowadzonymi w obu testowanych pożywkach, co oznaczało, że komórki bakteryjne nie wymagały dłuższej adaptacji w przypadku opracowanej przeze mnie pożywki PJ. Ponadto wykazałam, że uzysk BC, który był decydującym czynnikiem determinującym zasadność stosowania pożywki PJ, był porównywalny z uzyskiem otrzymanym przy zastosowaniu pożywki H-S (4,26 g/L v. 4,28 g/L).

Mając na uwadze dużą zmienność szlaków metabolicznych zaangażowanych w biosyntezę BC wśród różnych szczepów *K. xylinus* (Lei i wsp., 2012; La China i wsp., 2020), w prowadzonych badaniach uwzględniłam ocenę możliwości zastosowania pożywki PJ w hodowlach produkcyjnych prowadzonych z wykorzystaniem 8 różnych szczepów *K. xylinus*. Ustaliłam, że w przypadku 4 z 8 testowanych szczepów uzysk BC był porównywalny do procesu prowadzonego z użyciem pożywki H-S, natomiast dla pozostałych 4 szczepów pożywka PJ nie zapewniała optymalnej efektywności produkcji BC, mimo zawartości różnych cukrów. Zmienność tych wyników potwierdziła, że wydajność produkcji BC jest zależna od szczepu *K. xylinus* i ściśle związana z jego preferencyjnym źródłem węgla.

Ustaliłam również, że BC wytworzona w pożywce PJ nie różniła się pod względem analizowanych parametrów fizykochemicznych (mikrostruktury, czystości chemicznej, parametrów związanych z chłonnością i utrzymaniem wody, gęstości oraz właściwości mechanicznych) od BC uzyskanej w pożywce H-S. Ponadto, BC otrzymywana w pożywce PJ nie wykazywała cytotoksyczności względem komórek fibroblastów, a po wysyceniu antyseptykiem charakteryzowała się podobnymi właściwościami przeciwdrobnoustrojowymi jak BC otrzymana w pożywce H-S.

Aby oszacować korzyści ekonomiczne wynikające z zastosowania pożywki PJ przeprowadziłam kalkulację zakładającą wykorzystanie ziemniaków jako surowca specjalnie zakupionego do produkcji pożywki. Ustaliłam, że koszt 1000 litrów takiej pożywki wyniósłby 900 - 1400 zł, biorąc pod uwagę wahania cen ziemniaków w trakcie roku (https://www.tridge.com/intelligences/potato/price), natomiast koszt 1000 litrów pożywki H-S ustalony w oparciu o oferty cenowe zebrane od firm pośredniczących w sprzedaży odczynników chemicznych, wahałby się w granicach 6500 - 9000 zł. Należy jednak podkreślić, że w przypadku soku komórkowego z bulw ziemniaków istnieje możliwość jego pozyskania

jako odpadu przemysłu skrobiowego, co praktycznie całkowicie eliminuje koszty związane z przygotowaniem pożywki PJ.

W celu wykazania dodatkowych korzyści wynikających z zastosowania opracowanej pożywki PJ, przeprowadziłam hodowle produkcyjne z wykorzystaniem pożywek przygotowanych na bazie innych surowców naturalnych i odpadów rolno-przemysłowych (skórki ziemniaków i pomarańczy, buraki, jabłka). Pożywki te przygotowane zostały w sposób analogiczny jak w przypadku pożywki PJ. Wykazałam, że barwa zastosowanych surowców miała wpływ na pigmentację membran BC, co utrudniało i wydłużało proces ich oczyszczania. Co więcej, niektóre pożywki cechowały się obecnością trudnych do usunięcia cząstek stałych, które wiązały się z celulozą i pozostawały w jej strukturze nawet po oczyszczeniu, co jest istotnym problemem w przypadku stosowania surowców naturalnych i odpadowych.

Podsumowując, wyniki powyższego etapu badań wykazały, że sok komórkowy z bulw ziemniaków (bez żadnej obróbki wstępnej oraz suplementacji) jest odpowiednim źródłem składników odżywczych dla bakterii syntetyzujących celulozę, umożliwiając wydajną oraz korzystną z punktu widzenia ekonomicznego i ekologicznego produkcję BC o doskonałych właściwościach i wysokiej czystości.

Podczas prowadzenia badań związanych z **publikacją D-2** nawiązałam współpracę z mgr inż. Michałem Brodą z Pomorsko-Mazurskiej Hodowli Ziemniaka w Strzekęcinie. Pozwoliło mi to na przebadanie 25 różnych odmian ziemniaków jako potencjalnych surowców do przygotowania pożywki produkcyjnej do wytwarzania BC z wykorzystaniem różnych szczepów *K. xylinus* i różnych warunków hodowli.

Dodatkowo, na podstawie wyników badań zaprezentowanych w **publikacji D-2**, przygotowałam zgłoszenie patentowe:

Ciecholewska-Juśko, D., Fijałkowski, K., Broda, M. Sposób otrzymywania inokulum do wytwarzania celulozy bakteryjnej oraz sposób wytwarzania celulozy bakteryjnej z wykorzystaniem pożywki pochodzenia roślinnego, nr P.433327, 2020.

Etap 3

Obecność biofilmu w ranach przewlekłych u ludzi i zwierząt powoduje duże problemy terapeutyczne, ponieważ hamuje on procesy zapalne, które są kluczowe dla gojenia oraz uszkadza tkankę w wyniku wydzielania szeregu enzymów przez komórki bakteryjne (Percival i wsp., 2015; Omar i wsp., 2017). Mając na uwadze obiecujące wyniki moich badań zamieszczone w **publikacji D-1**, wysnułam hipotezę, że opracowane przeze mnie materiały mogą spełniać wymogi stawiane nowoczesnym opatrunkom. Z tego względu, postanowiłam ocenić użyteczność BC modyfikowanej za pomocą reakcji krzyżowego sieciowania, wytworzonej z użyciem pożywki PJ oraz impregnowanej substancją o działaniu przeciwdrobnoustrojowym jako materiału opatrunkowego skierowanego przeciwko biofilmom bakteryjnym *S. aureus* i *P. aeruginosa,* które są oportunistycznymi patogenami często występującymi w zakażonych ranach (**publikacja D-3**). Do impregnacji BC w celu nadania jej właściwości przeciwdrobnoustrojowych użyłam szeroko stosowanego antyseptyku na bazie dichlorowodorku oktenidyny (OCT). Stosowanie środków antyseptycznych zamiast antybiotyków stało się powszechne w terapii i profilaktyce miejscowych zakażeń związanych z biofilmem, ze względu na ich mechanizm działania, który zmniejsza ryzyko pojawienia się szczepów opornych (Norman i wsp., 2016). Bazując na ustalonych korzystnych właściwościach modyfikowanej BC, zwłaszcza dużych zdolnościach sorpcyjnych oraz spowolnionym uwalnianiu wody z jej wnętrza (względem niemodyfikowanej BC), założyłam, że materiał ten

po impregnacji OCT zapewni jego przedłużone uwalnianie, co umożliwi skuteczną eradykację biofilmów, nawet w obecności dużych ilości wysięku. Ponadto założyłam, że modyfikowana, funkcjonalizowana BC będzie charakteryzowała się utrzymywaniem wilgotnego środowiska w łożysku rany oraz wydajnym pochłanianiem wysięku.

Standardowo, po procesie modyfikacji za pomocą reakcji krzyżowego sieciowania BC jest suszona (MBC_d, ang. *dry, modified bacterial cellulose*), co zapewnia jej trwałość i stabilność mikrobiologiczną. Jednakże, ponieważ wykazałam, że każde suszenie modyfikowanej BC obniża jej właściwości sorpcyjne, w prowadzonych badaniach wykorzystałam również materiały które nie zostały wysuszone po procesie odpłukiwania reagentów wykorzystywanych podczas procesu modyfikacji (MBC_w, *wet, modified bacterial cellulose*). Dlatego w badaniach, których wyniki zebrałam w **publikacji D-3** zastosowałam modyfikowaną BC suszoną i nie suszoną po procesie modyfikacji i porównałam je z niemodyfikowaną BC (uwodnioną i suchą; BC_w i BC_d, ang. *wet/dry bacterial cellulose*).

Wyniki przeprowadzonych przeze mnie badań wykazały, że po procesie impregnacji w roztworze OCT, materiały MBC_w zawierały znaczne ilości tego antyseptyku (jednak mniejsze niż BC_w), natomiast materiały MBC_d wykazywały znacznie większe zdolności pochłaniania OCT w porównaniu z BC_d. Warto również zauważyć, że w przypadku materiałów mokrych (BC_w, MBC_w) proces pochłaniania zachodzi na drodze wymiany cieczy, dlatego dla tych prób nie zaobserwowałam wzrostu współczynnika pęcznienia (SR%) podczas impregnacji. Wszystkie materiały mokre zaimpregnowane OCT (OCT-BC_w, OCT-MBC_w) oraz OCT-MBC_d były również w stanie wydajnie pochłaniać wysięk. Materiały na bazie modyfikowanej BC (OCT-MBC_w, OCT-MBC_d) charakteryzowały się również wydłużonym w porównaniu do niemodyfikowanej BC (OCT-BC_w, OCT-BC_d) utrzymywaniem OCT w swojej strukturze.

W dalszej kolejności przeprowadziłam analizę kinetyki uwalniania OCT z testowanych przeze mnie materiałów. W wyniku tych analiz otrzymałam dwa profile uwalniania – jeden wspólny dla materiałów modyfikowanych i drugi dla materiałów niemodyfikowanych. Ustaliłam, że modyfikacja za pomocą reakcji krzyżowego sieciowania istotnie wpływa na wydłużenie uwalniania OCT, dzięki zachowaniu przez BC warstwowej struktury z wieloma przestrzeniami powietrznymi w których utrzymywana jest ciecz. Jest to ważne, ponieważ obecnie badania nad opatrunkami skupiają się na poszukiwaniu matryc pozwalających na przedłużone uwalnianie substancji czynnych, aby zapewnić ich odpowiednie stężenie przez cały okres trwania leczenia (Gámez-Herrera i wsp., 2020). Dla porównania, materiały OCT-BC_w i OCT-BC_d charakteryzowały się początkowym gwałtownym uwalnianiem, co w przypadku materiałów opatrunkowych jest zjawiskiem niepożądanym, ze względu na możliwość nagromadzenia się substancji czynnej i wywołania efektu toksycznego. Taki efekt wydaje się szczególnie prawdopodobny w przypadku materiału OCT-BC_w, który pochłaniał zdecydowanie największe ilości OCT spośród wszystkich badanych materiałów.

Powyższe wyniki zostały potwierdzone w analizach z wykorzystaniem zmodyfikowanej metody dyfuzyjno-krążkowej, gdzie również zaobserwowałam wydłużone uwalnianie OCT z BC modyfikowanej, oraz intensywne i bardziej gwałtowne uwalnianie z BC niemodyfikowanej. Materiały mokre (OCT-BC_w, OCT-MBC_w) oraz OCT-MBC_d, wykazywały również silne działanie przeciwdrobnoustrojowe wobec komórek planktonicznych *S. aureus* i *P. aeruginosa* po 1, 3 i 7 dniach eksperymentu.

Analiza aktywności przeciwbiofilmowej materiałów na bazie BC impregnowanych OCT wobec biofilmów *S. aureus* i *P. aeruginosa* była badana z wykorzystaniem opracowanego przeze mnie modelu łożyska rany. Zgodnie z danymi literaturowymi, modele biofilmu *in vitro* są niezbędne w badaniach przesiewowych środków przeciwdrobnoustrojowych, ponieważ odzwierciedlają złożoną naturę ran przewlekłych (Hill i wsp., 2010; Latka i Drulis-Kawa, 2020). Jednocześnie, mimo postępu technologicznego, opracowanie i zoptymalizowanie

takiego modelu stanowią ciągle duże wyzwanie dla badaczy (Latka i Drulis-Kawa, 2020). Idealny model biofilmu *in vitro* powinien charakteryzować się powtarzalnością, opłacalnością oraz możliwością szybkiego wykonania (Thaarup i Bjarnsolt, 2021). Opracowany przeze mnie model pozwolił na prowadzenie długotrwałych analiz z jednoczesną symulacją produkcji wysięku, jaka zachodzi w ranie. Wykazałam, że mimo niższej zawartości antyseptyku w OCT-MBC_w i OCT-MBC_d w porównaniu z OCT-BC_w, wszystkie te materiały charakteryzowały się porównywalnie wysoką aktywnością przeciwbiofilmową. Dodatkowo, nie stwierdziłam statystycznie istotnych różnic między OCT-MBC_w a OCT-BC_w, co sugeruje, że zarówno hydrożelowa struktura natywnej BC jak i gąbczasta struktura modyfikowanej BC pozwalają na zapewnienie ilości OCT wystarczających dla osiągnięcia silnego efektu przeciwdrobnoustrojowego, przy czym modyfikowana BC charakteryzuje się zrównoważonym uwalnianiem substancji czynnej, dzięki czemu nie dochodzi do gwałtownego przyrostu jej stężenia determinującego efekt cytotoksyczny.

W dalszych etapach badań, potwierdziłam nietoksyczność opracowanych przeze mnie materiałów oraz ustaliłam, że charakteryzują się one dobrym przyleganiem do zakrzywionych powierzchni, w przeciwieństwie do OCT- BC_d.

Podsumowując, na podstawie uzyskanych wyników wykazałam, że opracowana przeze mnie metoda modyfikacji z wykorzystaniem reakcji krzyżowego sieciowania pozwala na zniwelowanie ograniczeń wynikających ze stosowania natywnej BC. Największe różnice zaobserwowałam między materiałami MBC_d i BC_d, co wskazuje na znaczenie reakcji krzyżowego sieciowania w poprawie właściwości suchej BC pod kątem wymogów stawianych nowoczesnym opatrunkom. Dodatkowo, materiały MBC_d przed impregnacją substancją przeciwdrobnoustrojową mogą być przechowywane przez dłuższy czas bez utraty korzystnych właściwości. Wyniki zebrane w **publikacji D-3** wskazują, że BC wytworzona w ekologicznej i niedrogiej pożywce PJ, modyfikowana za pomocą reakcji krzyżowego sieciowania oraz zaimpregnowana OCT może być szczególnie obiecującym materiałem opatrunkowym, zwłaszcza w leczeniu ran z dużym wysiękiem, zakażonych drobnoustrojami produkującymi biofilm.

Etap 4

Mimo wykazania relatywnie wysokiej skuteczności przeciwbiofilmowej opracowanych przeze mnie materiałów na bazie modyfikowanej BC zaimpregnowanej OCT, miałam na uwadze fakt, że w związku ze specyfiką ran przewlekłych, w tym ich skomplikowaną strukturą, biofilm jest w stanie przetrwać proces konwencjonalnego leczenia i odbudować swoją strukturę w stosunkowo krótkim czasie (Zhao i wsp., 2013). Z tego względu, poszukuje się metod, które pozwoliłyby ukierunkować procesy zachodzące podczas stosowania opatrunków przeciwbiofilmowych, umożliwiając np. kontrolowanie czasu i ilości uwolnionej substancji oraz docieranie nawet w trudno dostępne miejsca w ranie. Co ważne, zastosowanie takich metod mogłoby pomóc w eliminacji ograniczeń wynikających ze stosowania niemodyfikowanej BC. Jednym z czynników który może mieć wpływ na uwalnianie substancji aktywnych z polimerowych nośników może być RMF. Dlatego, w ramach kolejnej pracy (**publikacji D-4**), podjęłam się analizy wpływu RMF (o częstotliwości 5 i 50 Hz) na uwalnianie OCT z nośnika na bazie suchej, niemodyfikowanej BC i jego penetrację przez warstwy biofilmu.

W ramach grantu OPUS 14 finansowanego ze źródeł Narodowego Centrum Nauki realizowanego w Katedrze Mikrobiologii i Biotechnologii ZUT w Szczecinie pn. „Analiza mechanizmów zwiększonej efektywności substancji przeciwdrobnoustrojowych względem biofilmów w obecności wirującego pola magnetycznego" uczestniczyłam w szeregu badań dotyczących RMF i jego wpływu na komórki bakteryjne oraz działanie środków

przeciwdrobnoustrojowych. We wcześniejszych pracach, zespół badawczy skupiający specjalistów wielu dyscyplin z którym współpracuję wykazał, że RMF oddziałuje na naładowane cząsteczki np. jony substancji przeciwdrobnoustrojowych, wpływając na procesy mieszania i dyfuzji oraz wpływa na wzrost, aktywność metaboliczną i proces formowania biofilmu u różnych szczepów i gatunków drobnoustrojów (Fijałkowski i wsp., 2013; Fijałkowski i wsp., 2015; Rakoczy i wsp., 2017). Udowodniono także, że żywotność komórek w biofilmach *S. aureus* i *P. aeruginosa* przy jednoczesnej ekspozycji na działanie RMF oraz środków przeciwdrobnoustrojowych jest znacznie obniżana w porównaniu do prób nieeksponowanych na RMF (Junka i wsp., 2018).

Wiedząc, że RMF może mieć wpływ na ruch naładowanych cząsteczek uwalnianych z nośnika założyłam, że ekspozycja suchej BC zaimpregnowanej OCT na RMF może pomóc w zintensyfikowaniu działania przeciwbiofilmowego takich materiałów, poprzez kontrolę uwalniania OCT i jego wzmożoną penetrację przez warstwy biofilmu. W celu przeprowadzenia badań dotyczących aktywności przeciwbiofilmowej nośników na bazie BC zaimpregnowanych OCT i eksponowanych na RMF zastosowałam wielopoziomowy model biofilmu *in vitro,* składający się z trzech ułożonych na sobie krążków agarowych, umieszczonych w coraz większej odległości od BC zaimpregnowanej roztworem OCT. Model ten jest częścią metody A.D.A.M. (ang. *Antibiofilm Dressing's Activity Measurement*), opracowanej wcześniej przez zespół naukowy z którym współpracuję (Junka i wsp., 2017). Metoda ta umożliwia pomiar aktywności opatrunku przeciwbiofilmowego z wykorzystaniem układu, który odzwierciedla złożoną i wielopoziomową naturę biofilmu. Jako nośnika dla OCT użyłam niemodyfikowanej, suchej BC, która w moich wcześniejszych badaniach (**publikacje D-1, D-3**) charakteryzowała się najsłabszymi właściwościami chłonnymi i spełniała najmniej wymogów stawianych nowoczesnym opatrunkom, dzięki czemu mogłam sprawdzić znaczenie RMF dla zwiększenia przydatności takich materiałów.

Wyniki badań wykazały, że OCT uwolniony z BC w ciągu 3 godzin kontaktu nośnika z układem nieeksponowanym na RMF nie miał znaczącego wpływu na redukcję komórek bakteryjnych *S. aureus* i *P. aeruginosa* tworzących biofilm. Podobnie, zastosowanie jedynie RMF o częstotliwościach 5 i 50 Hz przez 1, 2 i 3 godziny nie wpływało znacząco na żywotność komórek w biofilmach. W dalszych etapach badań udowodniłam, że jednoczesne zastosowanie BC zaimpregnowanej OCT oraz ekspozycji na RMF istotnie zwiększa efekt przeciwbiofilmowy. Natężenie tego efektu zależało głównie od czasu ekspozycji na RMF, gatunku bakterii oraz krążka agarowego, na którym znajdował się biofilm (krążek kontaktowy, środkowy, dolny). Wykazałam, że RMF wpływało na intensyfikację procesu uwalniania OCT z BC oraz zwiększało efektywność jego przenikania do poszczególnych warstw biofilmu sprawiając, że jego stężenie w układzie było wyższe w porównaniu z kontrolą nieeksponowaną na RMF.

Dodatkowo, przeprowadzone przeze mnie analizy wykazały, że RMF, zastosowany zarówno samodzielnie jak i w kombinacji z OCT uwolnionym z BC, istotnie wpływa na komórki znajdujące się w biofilmach *S. aureus* i *P. aeruginosa* poprzez osłabienie ich ścian/błon komórkowych, zaburzanie morfologii komórek czy utratę turgoru. Zmiany te dotyczyły wszystkich warstw biofilmu. Przeprowadziłam również analizy wpływu RMF na macierze biofilmów które wykazały, że w wyniku ekspozycji na RMF, zwiększała się ich porowatość. Zmiany zachodziły także w składzie cukrowym macierzy.

Podsumowując, wyniki **publikacji D-4** sugerują, że zastosowanie materiałów na bazie BC zaimpregnowanych OCT z jednoczesną ekspozycją na RMF może być szczególnie obiecujące w eliminowaniu biofilmów zlokalizowanych w trudno dostępnych obszarach rany, gdzie fizyczne przeszkody ograniczają działanie antyseptyczne. Dodatkowo, można przypuszczać, że dzięki RMF będzie możliwe zniszczenie nawet podstawowych warstw

biofilmu, przy użyciu stosunkowo niskich stężeń środka antyseptycznego oraz w znacznie krótszym czasie kontaktu niż w przypadku braku ekspozycji na RMF.

6. Wnioski

Na podstawie wyników uzyskanych podczas badań prowadzonych w ramach rozprawy doktorskiej sformułowałam następujące wnioski:

1. Reakcja krzyżowego sieciowania przeprowadzona z wykorzystaniem kwasu cytrynowego oraz katalizatorów, które podczas rozkładu termicznego i w reakcjach z kwasami wydzielają duże ilości gazów (w szczególności mieszaniny wodorofosforanu disodu oraz wodorowęglanu sodu), pozwala na zachowanie trójwymiarowej struktury BC w stanie suchym, powodując tworzenie się przestrzeni między warstwami BC oraz pęcherzyków wypełnionych powietrzem (**publikacja D-1**).

2. Reakcja krzyżowego sieciowania przeprowadzona z wykorzystaniem kwasu cytrynowego oraz katalizatorów, które podczas rozkładu termicznego i w reakcjach z kwasami wydzielają duże ilości gazów (w szczególności mieszaniny wodorofosforanu disodu oraz wodorowęglanu sodu), znacząco zwiększa zdolność BC do pochłaniania i utrzymywania cieczy w porównaniu z suchą, niemodyfikowaną BC (**publikacja D-1**).

3. BC modyfikowana w procesie krzyżowego sieciowania z wykorzystaniem kwasu cytrynowego oraz katalizatorów, które podczas rozkładu termicznego i w reakcjach z kwasami wydzielają duże ilości gazów, nie wykazuje cytotoksyczności wobec komórek fibroblastów (**publikacja D-1**).

4. Sok komórkowy z bulw ziemniaków stanowi dobrą pożywkę produkcyjną do efektywnego wytwarzania BC z wykorzystaniem szczepów *K. xylinus*, umożliwiając otrzymanie porównywalnych ilości tego biopolimeru jak w przypadku zastosowania konwencjonalnej pożywki H-S (**publikacja D-2**).

5. BC wytwarzana z wykorzystaniem pożywki produkcyjnej na bazie soku komórkowego z bulw ziemniaków, nie wykazuje różnic w parametrach fizykochemicznych w porównaniu z BC otrzymaną z użyciem konwencjonalnej pożywki H-S, a także nie wykazuje cytotoksyczności wobec komórek fibroblastów (**publikacja D-2**).

6. Materiały na bazie BC wytworzonej w pożywce produkcyjnej z soku komórkowego z bulw ziemniaków, modyfikowanej za pomocą reakcji krzyżowego sieciowania z wykorzystaniem kwasu cytrynowego oraz mieszaniny wodorofosforanu disodu i wodorowęglanu sodu jako katalizatorów oraz zaimpregnowanej antyseptykiem (dichlorowodorkiem oktenidyny), charakteryzują się zdolnością do absorbcji wysięku zachodzącej na drodze wymiany cieczy przez okres do 5 dni (**publikacja D-3**).

7. Materiały na bazie BC wytworzonej w pożywce produkcyjnej z soku komórkowego z bulw ziemniaków oraz modyfikowanej za pomocą reakcji krzyżowego sieciowania z wykorzystaniem kwasu cytrynowego oraz mieszaniny wodorofosforanu disodu i wodorowęglanu sodu jako katalizatorów, charakteryzują się wydłużonym czasem uwalniania antyseptyku (dichlorowodorku oktenidyny), w porównaniu do niemodyfikowanej BC (**publikacja D-3**).

8. Materiały na bazie BC wytworzonej w pożywce produkcyjnej z soku komórkowego z bulw ziemniaków, modyfikowanej za pomocą reakcji krzyżowego sieciowania z wykorzystaniem kwasu cytrynowego oraz mieszaniny wodorofosforanu disodu i wodorowęglanu sodu jako katalizatorów oraz zaimpregnowanej antyseptykiem (dichlorowodorkiem oktenidyny), charakteryzują się wysoką aktywnością przeciwdrobnoustrojową (utrzymującą się przez min. 7 dni) wobec *S. aureus* i *P. aeruginosa* w hodowlach planktonicznych oraz w formie biofilmów *in vitro* (**publikacja D-3**).

9. RMF zwiększa efektywność działania antyseptyku (dichlorowodorku oktenidyny) względem biofilmów wytwarzanych przez *S. aureus* i *P. aeruginosa in vitro*, poprzez zwiększenie stopnia jego uwalniania z BC, a następnie penetracji przez kolejne warstwy biofilmu oraz osłabianie ścian komórkowych bakterii i zwiększanie porowatości macierzy biofilmu (**publikacja D-4**).

7. Cytowana literatura

1. Omar, A., Wright, J. B., Schultz, G., Burrell, R., & Nadworny, P. (2017). Microbial biofilms and chronic wounds. *Microorganisms*, *5*(1), 9.

2. Moormeier, D. E., & Bayles, K. W. (2017). Staphylococcus aureus biofilm: a complex developmental organism. *Molecular microbiology*, *104*(3), 365-376.

3. Wolcott, R. D., Hanson, J. D., Rees, E. J., Koenig, L. D., Phillips, C. D., Wolcott, R. A., ... & White, J. S. (2016). Analysis of the chronic wound microbiota of 2,963 patients by 16S rDNA pyrosequencing. *Wound repair and regeneration*, *24*(1), 163-174.

4. Bassetti, M., Vena, A., Croxatto, A., Righi, E., & Guery, B. (2018). How to manage Pseudomonas aeruginosa infections. *Drugs in context*, *7*.

5. Shettigar, K., Jain, S., Bhat, D. V., Acharya, R., Ramachandra, L., Satyamoorthy, K., & Murali, T. S. (2016). Virulence determinants in clinical Staphylococcus aureus from monomicrobial and polymicrobial infections of diabetic foot ulcers. *Journal of medical microbiology*, *65*(12), 1392-1404.

6. Bjarnsholt, T. (2013). The role of bacterial biofilms in chronic infections. *Apmis*, *121*, 1-58.

7. Sauer, K., Stoodley, P., Goeres, D. M., Hall-Stoodley, L., Burmølle, M., Stewart, P. S., & Bjarnsholt, T. (2022). The biofilm life cycle: expanding the conceptual model of biofilm formation. *Nature Reviews Microbiology*, 1-13.

8. Wu, H., Moser, C., Wang, H. Z., Høiby, N., & Song, Z. J. (2015). Strategies for combating bacterial biofilm infections. *International journal of oral science*, *7*(1), 1.

9. Clutterbuck, A. L., Woods, E. J., Knottenbelt, D. C., Clegg, P. D., Cochrane, C. A., & Percival, S. L. (2007). Biofilms and their relevance to veterinary medicine. *Veterinary microbiology*, *121*(1-2), 1-17.

10. Percival, S. L., McCarty, S. M., & Lipsky, B. (2015). Biofilms and wounds: an overview of the evidence. *Advances in wound care*, *4*(7), 373-381.

11. G. Armstrong, D., Bauer, K., Bohn, G., Carter, M., Snyder, R., & Serena, T. E. (2020). Principles of Best Diagnostic Practice in Tissue Repair and Wound Healing: An Expert Consensus. *Diagnostics*, *11*(1), 50.

12. Shahriari-Khalaji, M., Hong, S., Hu, G., Ji, Y., & Hong, F. F. (2020). Bacterial nanocellulose-enhanced alginate double-network hydrogels cross-linked with six metal cations for antibacterial wound dressing. *Polymers*, *12*(11), 2683.

13. Zheng, L., Li, S., Luo, J., & Wang, X. (2020). Latest advances on bacterial cellulose-based antibacterial materials as wound dressings. *Frontiers in Bioengineering and Biotechnology*, *8*, 593768.

14. Swingler, S., Gupta, A., Gibson, H., Kowalczuk, M., Heaselgrave, W., & Radecka, I. (2021). Recent advances and applications of bacterial cellulose in biomedicine. *Polymers*, *13*(3), 412.

15. Darvishi, S., Tavakoli, S., Kharaziha, M., Girault, H. H., Kaminski, C. F., & Mela, I. (2022). Advances in the Sensing and Treatment of Wound Biofilms. *Angewandte Chemie International Edition*, *61*(13), e202112218.

16. Gámez-Herrera, E., García-Salinas, S., Salido, S., Sancho-Albero, M., Andreu, V., Perez, M., ... & Mendoza, G. (2020). Drug-eluting wound dressings having sustained release of antimicrobial compounds. *European Journal of Pharmaceutics and Biopharmaceutics*, *152*, 327-339.

17. Massarelli, E., Silva, D., Pimenta, A. F. R., Fernandes, A. I., Mata, J. L. G., Armês, H., ... & Serro, A. P. (2021). Polyvinyl alcohol/chitosan wound dressings loaded with antiseptics. *International Journal of Pharmaceutics*, *593*, 120110.

18. Teixeira, M. A., Paiva, M. C., Amorim, M. T. P., & Felgueiras, H. P. (2020). Electrospun nanocomposites containing cellulose and its derivatives modified with specialized biomolecules for an enhanced wound healing. *Nanomaterials*, *10*(3), 557.

19. Lahiri, D., Nag, M., Dutta, B., Dey, A., Sarkar, T., Pati, S., ... & Ray, R. R. (2021). Bacterial cellulose: Production, characterization, and application as antimicrobial agent. *International Journal of Molecular Sciences*, *22*(23), 12984.

20. Czaja, W., Krystynowicz, A., Bielecki, S., & Brown Jr, R. M. (2006). Microbial cellulose—the natural power to heal wounds. *Biomaterials*, *27*(2), 145-151.

21. Sulaeva, I., Henniges, U., Rosenau, T., & Potthast, A. (2015). Bacterial cellulose as a material for wound treatment: Properties and modifications. A review. *Biotechnology advances*, *33*(8), 1547-1571.

22. Saska, S., Barud, H. S., Gaspar, A. M. M., Marchetto, R., Ribeiro, S. J. L., & Messaddeq, Y. (2011). Bacterial cellulose-hydroxyapatite nanocomposites for bone regeneration. *International journal of biomaterials*, *2011*.

23. Zaborowska, M., Bodin, A., Bäckdahl, H., Popp, J., Goldstein, A., & Gatenholm, P. (2010). Microporous bacterial cellulose as a potential scaffold for bone regeneration. *Acta biomaterialia*, *6*(7), 2540-2547.

24. Bielecki, S., Kalinowska, H., Krystynowicz, A., Kubiak, K., Kołodziejczyk, M., & De Groeve, M. (2012). Wound dressings and cosmetic materials from bacterial nanocellulose. *Bact. Nanocellulose*.

25. Portela, R., Leal, C. R., Almeida, P. L., & Sobral, R. G. (2019). Bacterial cellulose: A versatile biopolymer for wound dressing applications. *Microbial biotechnology*, *12*(4), 586-610.

26. de Amorim, J. D. P., da Silva Junior, C. J. G., de Medeiros, A. D., do Nascimento, H. A., Sarubbo, M., de Medeiros, T. P. M., ... & Sarubbo, L. A. (2022). Bacterial Cellulose as a Versatile Biomaterial for Wound Dressing Application. *Molecules*, *27*(17), 5580.

27. Wei, B., Yang, G., & Hong, F. (2011). Preparation and evaluation of a kind of bacterial cellulose dry films with antibacterial properties. *Carbohydrate Polymers*, *84*(1), 533-538.

28. Ul-Islam, M., Khan, T., & Park, J. K. (2012). Water holding and release properties of bacterial cellulose obtained by in situ and ex situ modification. *Carbohydrate Polymers*, *88*(2), 596-603.

29. Hanna, D. H., Lotfy, V. F., Basta, A. H., & Saad, G. R. (2020). Comparative evaluation for controlling release of niacin from protein-and cellulose-chitosan based hydrogels. *International journal of biological macromolecules*, *150*, 228-237.

30. Stumpf, T. R., Yang, X., Zhang, J., & Cao, X. (2018). In situ and ex situ modifications of bacterial cellulose for applications in tissue engineering. *Materials Science and Engineering: C*, *82*, 372-383.

31. Rajwade, J. M., Paknikar, K. M., & Kumbhar, J. V. (2015). Applications of bacterial cellulose and its composites in biomedicine. *Applied microbiology and biotechnology*, *99*(6), 2491-2511.

32. Torres, F. G., Arroyo, J. J., & Troncoso, O. P. (2019). Bacterial cellulose nanocomposites: An all-nano type of material. *Materials Science and Engineering: C*, *98*, 1277-1293.

33. He, W., Zhang, Z., Chen, J., Zheng, Y., Xie, Y., Liu, W., ... & Mosselhy, D. A. (2021). Evaluation of the anti-biofilm activities of bacterial cellulose-tannic acid-magnesium chloride composites using an in vitro multispecies biofilm model. *Regenerative biomaterials*, *8*(6), rbab054.

34. Zhao, G., Usui, M. L., Lippman, S. I., James, G. A., Stewart, P. S., Fleckman, P., & Olerud, J. E. (2013). Biofilms and inflammation in chronic wounds. *Advances in wound care*, *2*(7), 389-399.

35. Kim, P. J., & Steinberg, J. S. (2012, June). Wound care: biofilm and its impact on the latest treatment modalities for ulcerations of the diabetic foot. In *Seminars in vascular surgery* (Vol. 25, No. 2, pp. 70-74). WB Saunders.

36. Lázaro-Martínez, J. L., Álvaro-Afonso, F. J., García-Álvarez, Y., Molines-Barroso, R. J., García-Morales, E., & Sevillano-Fernández, D. (2018). Ultrasound-assisted debridement of neuroischaemic diabetic foot ulcers, clinical and microbiological effects: a case series. *Journal of Wound Care*, *27*(5), 278-286.

37. Junka, A. F., Rakoczy, R., Szymczyk, P., Bartoszewicz, M., Sedghizadeh, P. P., & Fijałkowski, K. (2018). Application of rotating magnetic fields increase the activity of antimicrobials against wound biofilm pathogens. *Scientific reports*, *8*(1), 1-12.

38. Gupta, T. T., & Ayan, H. (2019). Application of non-thermal plasma on biofilm: a review. *Applied Sciences*, *9*(17), 3548.

39. Konopacki, M., & Rakoczy, R. (2019). The analysis of rotating magnetic field as a trigger of Gram-positive and Gram-negative bacteria growth. *Biochemical Engineering Journal*, *141*, 259-267.

40. Luo, Q., Wang, H., Zhang, X., & Qian, Y. (2005). Effect of direct electric current on the cell surface properties of phenol-degrading bacteria. *Applied and environmental microbiology*, *71*(1), 423-427.
41. Rakoczy, R., Przybył, A., Kordas, M., Konopacki, M., Drozd, R., & Fijałkowski, K. (2017). The study of influence of a rotating magnetic field on mixing efficiency. *Chemical Engineering and Processing: Process Intensification*, *112*, 1-8.
42. Revin, V., Liyaskina, E., Nazarkina, M., Bogatyreva, A., & Shchankin, M. (2018). Cost-effective production of bacterial cellulose using acidic food industry by-products. *brazilian journal of microbiology*, *49*, 151-159.
43. Abol-Fotouh, D., Hassan, M. A., Shokry, H., Roig, A., Azab, M. S., & Kashyout, A. E. H. B. (2020). Bacterial nanocellulose from agro-industrial wastes: Low-cost and enhanced production by Komagataeibacter saccharivorans MD1. *Scientific reports*, *10*(1), 1-14.
44. Goelzer, F. D. E., Faria-Tischer, P. C. S., Vitorino, J. C., Sierakowski, M. R., & Tischer, C. A. (2009). Production and characterization of nanospheres of bacterial cellulose from Acetobacter xylinum from processed rice bark. *Materials Science and Engineering: C*, *29*(2), 546-551.
45. Kurosumi, A., Sasaki, C., Yamashita, Y., & Nakamura, Y. (2009). Utilization of various fruit juices as carbon source for production of bacterial cellulose by Acetobacter xylinum NBRC 13693. *Carbohydrate Polymers*, *76*(2), 333-335.
46. Bradford, M. M. (1976). A rapid and sensitive method for the quantitation of microgram quantities of protein utilizing the principle of protein-dye binding. *Analytical biochemistry*, *72*(1-2), 248-254.
47. Sulistyarti, H., Fardiyah, Q., & Febriyanti, S. (2015). A simple and safe spectrophotometric method for iodide determination. *Makara Journal of Science*, *19*(2), 1.
48. Rahman, M. R., Lai, J. C. H., Hamdan, S., Ahmed, A. S., Baini, R., & Saleh, S. F. (2013). Combined styrene/MMA/nanoclay cross-linker effect on wood-polymer composites (WPCs). *BioResources*, *8*(3), 4227-4237.
49. Junka, A. F., Żywicka, A., Szymczyk, P., Dziadas, M., Bartoszewicz, M., & Fijałkowski, K. (2017). ADAM test (Antibiofilm Dressing's Activity Measurement)—Simple method for evaluating anti-biofilm activity of drug-saturated dressings against wound pathogens. *Journal of microbiological methods*, *143*, 6-12.
50. Meftahi, A., Khajavi, R., Rashidi, A., Rahimi, M. K., & Bahador, A. (2018). Preventing the collapse of 3D bacterial cellulose network via citric acid. *Journal of Nanostructure in Chemistry*, *8*(3), 311-320.
51. Frone, A. N., Panaitescu, D. M., Nicolae, C. A., Gabor, A. R., Trusca, R., Casarica, A., ... & Salageanu, A. (2020). Bacterial cellulose sponges obtained with green cross-linkers for tissue engineering. *Materials Science and Engineering: C*, *110*, 110740.
52. Gyawali, D., Nair, P., Zhang, Y., Tran, R. T., Zhang, C., Samchukov, M., ... & Yang, J. (2010). Citric acid-derived in situ crosslinkable biodegradable polymers for cell delivery. *Biomaterials*, *31*(34), 9092-9105.
53. Ye, T., Wang, B., Liu, J., Chen, J., & Yang, Y. (2015). Quantitative analysis of citric acid/sodium hypophosphite modified cotton by HPLC and conductometric titration. *Carbohydrate polymers*, *121*, 92-98.
54. El Fawal, G. F., Abu-Serie, M. M., Hassan, M. A., & Elnouby, M. S. (2018). Hydroxyethyl cellulose hydrogel for wound dressing: Fabrication, characterization and in vitro evaluation. *International journal of biological macromolecules*, *111*, 649-659.
55. Sotolářová, J., Vinter, Š., & Filip, J. (2021). Cellulose derivatives crosslinked by citric acid on electrode surface as a heavy metal absorption/sensing matrix. *Colloids and Surfaces A: Physicochemical and Engineering Aspects*, *628*, 127242.
56. Qi, H., Huang, Y., Ji, B., Sun, G., Qing, F. L., Hu, C., & Yan, K. (2016). Anti-crease finishing of cotton fabrics based on crosslinking of cellulose with acryloyl malic acid. *Carbohydrate polymers*, *135*, 86-93.
57. Keshk, S. M. (2014). Bacterial cellulose production and its industrial applications. *J Bioprocess Biotech*, *4*(2), 150.
58. Shao, W., Wu, J., Liu, H., Ye, S., Jiang, L., & Liu, X. (2017). Novel bioactive surface functionalization of bacterial cellulose membrane. *Carbohydrate polymers*, *178*, 270-276.
59. Crépy, L., Miri, V., Joly, N., Martin, P., & Lefebvre, J. M. (2011). Effect of side chain length on structure and thermomechanical properties of fully substituted cellulose fatty esters. *Carbohydrate polymers*, *83*(4), 1812-1820.
60. Schilling, M., Bouchard, M., Khanjian, H., Learner, T., Phenix, A., & Rivenc, R. (2010). Application of chemical and thermal analysis methods for studying cellulose ester plastics. *Accounts of chemical research*, *43*(6), 888-896.
61. Gatenholm, P., & Klemm, D. (2010). Bacterial nanocellulose as a renewable material for biomedical applications. *MRS bulletin*, *35*(3), 208-213.

62. de Oliveira Barud, H. G., da Silva, R. R., da Silva Barud, H., Tercjak, A., Gutierrez, J., Lustri, W. R., ... & Ribeiro, S. J. (2016). A multipurpose natural and renewable polymer in medical applications: Bacterial cellulose. *Carbohydrate Polymers*, *153*, 406-420.
63. Widsten, P., Dooley, N., Parr, R., Capricho, J., & Suckling, I. (2014). Citric acid crosslinking of paper products for improved high-humidity performance. *Carbohydrate polymers*, *101*, 998-1004.
64. Kongruang, S. (2007). Bacterial cellulose production by Acetobacter xylinum strains from agricultural waste products. In *Biotechnology for Fuels and Chemicals* (pp. 763-774). Humana Press.
65. Li, Z., Wang, L., Hua, J., Jia, S., Zhang, J., & Liu, H. (2015). Production of nano bacterial cellulose from wastewater of candied jujube-processing industry using Acetobacter xylinum. *Carbohydrate Polymers*, *120*, 115-119.
66. Lima, H. L. S., Nascimento, E. S., Andrade, F. K., Brígida, A. I. S., Borges, M. D. F., Cassales, A. R., ... & Rosa, M. D. F. (2017). Bacterial cellulose production by Komagataeibacter hansenii ATCC 23769 using sisal juice-An agroindustry waste. *Brazilian Journal of Chemical Engineering*, *34*, 671-680.
67. Bradshaw, J. E., & Bonierbale, M. (2010). Potatoes. In *Root and tuber crops* (pp. 1-52). Springer, New York, NY.
68. Kowalczewski, P., Celka, K., Białas, W., & Lewandowicz, G. (2012). Antioxidant activity of potato juice. *Acta Scientiarum Polonorum Technologia Alimentaria*, *11*(2), 175-181.
69. Grommers, H. E., & van der Krogt, D. A. (2009). Potato starch: production, modifications and uses. In *Starch* (pp. 511-539). Academic Press.
70. Fang, C., Boe, K., & Angelidaki, I. (2011). Biogas production from potato-juice, a by-product from potato-starch processing, in upflow anaerobic sludge blanket (UASB) and expanded granular sludge bed (EGSB) reactors. *Bioresource technology*, *102*(10), 5734-5741.
71. Abdelraof, M., Hasanin, M. S., & El-Saied, H. (2019). Ecofriendly green conversion of potato peel wastes to high productivity bacterial cellulose. *Carbohydrate polymers*, *211*, 75-83.
72. Singhsa, P., Narain, R., & Manuspiya, H. (2018). Physical structure variations of bacterial cellulose produced by different Komagataeibacter xylinus strains and carbon sources in static and agitated conditions. *Cellulose*, *25*(3), 1571-1581.
73. Chen, G., Wu, G., Chen, L., Wang, W., Hong, F. F., & Jönsson, L. J. (2019). Comparison of productivity and quality of bacterial nanocellulose synthesized using culture media based on seven sugars from biomass. *Microbial Biotechnology*, *12*(4), 677-687
74. Aswini, K., Gopal, N. O., & Uthandi, S. (2020). Optimized culture conditions for bacterial cellulose production by Acetobacter senegalensis MA1. *BMC biotechnology*, *20*(1), 1-16.
75. Lei, L., Li, S., & Gu, Y. (2012). Cellulose synthase complexes: composition and regulation. *Frontiers in plant science*, *3*, 75.
76. La China, S., Bezzecchi, A., Moya, F., Petroni, G., Di Gregorio, S., & Gullo, M. (2020). Genome sequencing and phylogenetic analysis of K1G4: a new Komagataeibacter strain producing bacterial cellulose from different carbon sources. *Biotechnology letters*, *42*(5), 807-818.
77. Norman, G., Dumville, J. C., Mohapatra, D. P., Owens, G. L., & Crosbie, E. J. (2016). Antibiotics and antiseptics for surgical wounds healing by secondary intention. *Cochrane Database of Systematic Reviews*, (3).
78. Hill, K. E., Malic, S., McKee, R., Rennison, T., Harding, K. G., Williams, D. W., & Thomas, D. W. (2010). An in vitro model of chronic wound biofilms to test wound dressings and assess antimicrobial susceptibilities. *Journal of Antimicrobial Chemotherapy*, *65*(6), 1195-1206.
79. Latka, A., & Drulis-Kawa, Z. (2020). Advantages and limitations of microtiter biofilm assays in the model of antibiofilm activity of Klebsiella phage KP34 and its depolymerase. *Scientific reports*, *10*(1), 1-12.
80. Thaarup, I. C., & Bjarnsholt, T. (2021). Current in vitro biofilm-infected chronic wound models for developing new treatment possibilities. *Advances in Wound Care*, *10*(2), 91-102.
81. Fijałkowski, K., Nawrotek, P., Struk, M., Kordas, M., & Rakoczy, R. (2013). The effects of rotating magnetic field on growth rate, cell metabolic activity and biofilm formation by Staphylococcus aureus and Escherichia coli. *Journal of Magnetics*, *18*(3), 289-296.
82. Fijałkowski, K., Nawrotek, P., Struk, M., Kordas, M., & Rakoczy, R. (2015). Effects of rotating magnetic field exposure on the functional parameters of different species of bacteria. *Electromagnetic biology and medicine*, *34*(1), 48-55.

8. Omówienie pozostałych osiągnięć naukowo-badawczych

Działalność naukową rozpoczęłam w 2017 roku w Katedrze Toksykologii, Technologii Mleczarskiej i Przechowalnictwa Żywności na Wydziale Nauk o Żywności i Rybactwa Zachodniopomorskiego Uniwersytetu Technologicznego w Szczecinie, prowadząc badania w ramach pracy dyplomowej realizowanej podczas studiów magisterskich pt.: „Wpływ różnych metod grillowania na zawartość wybranych metali ciężkich w mięśniach pstrąga tęczowego". Praca została wykonana pod kierunkiem dr inż. Moniki Rajkowskiej-Myśliwiec i rozszerzona o kolejne wyniki badań w celu przygotowania publikacji naukowej, która ukazała się w 2021 roku (**publikacja A-1**). Po obronie pracy magisterskiej, z dniem 1 października 2018 r., rozpoczęłam naukę na studiach doktoranckich. Badania w ramach pracy doktorskiej wykonywałam w Katedrze Mikrobiologii i Biotechnologii Wydziału Biotechnologii i Hodowli Zwierząt Zachodniopomorskiego Uniwersytetu Technologicznego w Szczecinie pod kierunkiem dr hab. inż. Karola Fijałkowskiego, prof. ZUT, czego efektem jest niniejsza rozprawa doktorska składająca się z cyklu czterech publikacji naukowych.

W trakcie mojej działalności badawczej zgromadziłam dorobek naukowy na który składa się 16 publikacji, 1 patent, 3 zgłoszenia patentowe oraz 1 rozdział w monografii naukowej. Byłam również stypendystką w 3 projektach realizowanych w Katedrze Mikrobiologii i Biotechnologii ZUT w Szczecinie, w tym w grancie OPUS 14 finansowanym ze źródeł Narodowego Centrum Nauki pn. „Analiza mechanizmów zwiększonej efektywności substancji przeciwdrobnoustrojowych względem biofilmów w obecności wirującego pola magnetycznego" oraz 2 grantów badawczo-rozwojowych realizowanych w ramach Regionalnego Programu Operacyjnego Województwa Zachodniopomorskiego pn. „Biodegradowalne, przeciwbakteryjne i przeciwwirusowe filtry na bazie bionanocelulozy do zastosowania w maseczkach ochronnych" oraz „Testowanie w warunkach rzeczywistych innowacyjnych maseczek ochronnych (NanoBioCell) z bionanocelulozy". Podczas studiów doktoranckich odbyłam 2 staże krajowe - w Pomorsko-Mazurskiej Hodowli Ziemniaka w Strzekęcinie oraz w Instytucie Hodowli i Aklimatyzacji Roślin w Boninie. Brałam także czynny udział w wielu konferencjach o zasięgu krajowym i międzynarodowym (m.in. FEMS, World Microbe Forum, International Seminar on Sustainability, Economics and Safety, Międzyuczelniane Sympozjum biotechnologiczne „Symbioza", Interdycyplinarna Konferencja Nano&Biomateriały i inne). W celu podniesienia swoich kwalifikacji odbyłam także 6 certyfikowanych szkoleń, w tym szkoleń z obsługi specjalistycznego sprzętu. Jestem również aktywnym członkiem Koła Naukowego „BioReaktor" działającego w Katedrze Mikrobiologii i Biotechnologii ZUT oraz członkiem Polskiego Towarzystwa Mikrobiologów.

[A-1] Rajkowska-Myśliwiec, M., Pokorska-Niewiada, K., Witczak, A., Balcerzak, M., **Ciecholewska-Juśko, D**. (2021). Health benefits and risks associated with element uptake from grilled fish and fish products. *Journal of the Science of Food and Agriculture, 102*(3), 957-964.

IF_{2022} – 3.638, 100 pkt. MEiN

8.1. Osiągnięcia naukowe związane z produkcją i wykorzystywaniem celulozy bakteryjnej

Na początkowych etapach działalności badawczej w Katedrze Mikrobiologii i Biotechnologii ZUT w Szczecinie zapoznałam się z procesem wytwarzania BC stosując opracowane wcześniej przez dr inż. Annę Żywicką oraz dr hab. inż. Karola Fijałkowskiego,

prof. ZUT, optymalne parametry hodowli *K. xylinus*, zarówno stacjonarnej jak i mieszanej, z wykorzystaniem różnego rodzaju naczyń hodowlanych, w tym również bioreaktorów. Konsekwencją tych działań było między innymi wybranie szczepu referencyjnego *K. xylinus* wykorzystywanego podczas moich badań prowadzonych w ramach rozprawy doktorskiej.

Analizowałam także podstawowe parametry fizykochemiczne otrzymanej BC oraz możliwości jej zastosowania, np. jako nośnik do immobilizacji drożdży w procesie produkcji kwasu cytrynowego (CA, ang. *citric acid*, **publikacja A-2**). Wyniki tych badań wykazały, że drożdże *Yarrowia lipolytica* unieruchomione na BC wykorzystywały więcej glukozy w procesie fermentacji w porównaniu do wolnych komórek, a ich aktywność metaboliczna, a co za tym idzie – produkcja CA, utrzymywała się na stabilnym poziomie przez 4 kolejne cykle fermentacji, podczas gdy w przypadku wolnych komórek obserwowano spadek aktywności metabolicznej i produkcji CA z każdym kolejnym cyklem. Dodatkowo, ogólne stężenie otrzymanego CA było wyższe w przypadku drożdży immobilizowanych w porównaniu z wolnymi komórkami. Przedstawione wyniki wykazały, że zastosowanie nośnika BC do immobilizacji wykazuje wysoki potencjał biotechnologiczny.

Od początku swojej działalności naukowej w Katedrze Mikrobiologii i Biotechnologii byłam również zaangażowana w badania nad obniżeniem kosztów produkcji BC lub zwiększeniem wydajności jej biosyntezy. Jednym z badanych przeze mnie sposobów na zwiększenie wydajności produkcji BC na dużą skalę było zastosowanie bioreaktora wspomaganego magnetycznie (RMF) z pętlą zewnętrzną (EL-ALB, ang. *external-loop airlift bioreactor*) do przygotowania inokulum *K. xylinus* (**publikacja A-3**). Fermentacja prowadzona w takim bioreaktorze pozwoliła na uzyskanie inokulum o ponad 200-krotnie większej gęstości komórkowej w porównaniu z metodami klasycznymi, przy jednoczesnym zachowaniu zdolności do wydajnej produkcji BC o powtarzalnych właściwościach. Dodatkowo, wytworzone inokulum charakteryzowało się wysoką i stabilną aktywnością metaboliczną podczas procesu fermentacji, a zastosowanie EL-ALB wspomaganego RMF nie indukowało tworzenia mutantów *K. xylinus* nie produkujących celulozy.

[A-2] Żywicka, A., Junka, A., **Ciecholewska-Juśko, D**., Migdał, P., Czajkowska, J., & Fijałkowski, K. (2020). Significant enhancement of citric acid production by *Yarrowia lipolytica* immobilized in bacterial cellulose-based carrier. *Journal of Biotechnology*, *321*, 13-22.

IF_{2022} – 3,503, 70 pkt. MEiN

[A-3] Żywicka, A., **Ciecholewska-Juśko, D**., Drozd, R., Rakoczy, R., Konopacki, M., Kordas, M., Junka, A., Migdał, B., Fijałkowski, K. (2021). Preparation of *Komagataeibacter xylinus* inoculum for bacterial cellulose biosynthesis using magnetically assisted external-loop airlift bioreactor. *Polymers, 13*.

IF_{2022} – 4,329, 100 pkt. MEiN

8.2. Osiągnięcia naukowe związane z zastosowaniem celulozy bakteryjnej jako nośnika dla substancji przeciwdrobnoustrojowych w celu eradykacji biofilmów bakteryjnych.

Ważnym etapem prowadzonych przeze mnie badań była ocena możliwości wykorzystania BC jako nośnika dla substancji o działaniu przeciwdrobnoustrojowym – zarówno syntetycznych (antybiotyki, antyseptyki), jak i naturalnych (olejki eteryczne,

bioaktywne metabolity roślin leczniczych) w celu zwalczania zarówno komórek planktonicznych jak i biofilmowych.

Problematyką biofilmów interesowałam się już przed otwarciem przewodu doktorskiego uczestnicząc w badaniach, których celem była analiza m.in. zdolności gronkowców izolowanych z produktów mięsnych do wytwarzania biofilmu (**publikacja A-4**).

Mając na uwadze skomplikowaną naturę biofilmu bakteryjnego oraz mnogość czynników mogących wpływać na jego parametry takie jak ilość biomasy czy aktywność metaboliczna, brałam udział w badaniach, których wyniki wykazały duży wpływ stosowanej pożywki hodowlanej na wspomniane parametry biofilmu gronkowcowego. Co więcej, w badaniach tych wykazano, że rodzaj pożywki stosowanej w hodowli biofilmów wpływa również na skuteczność przeciwdrobnoustrojową środków antyseptycznych i antybiotyków uwalnianych z nośników celulozowych (**publikacja A-5**). Praca ta pozwoliła mi zwrócić szczególną uwagę na czynniki, jakie należy brać pod uwagę badając skuteczność opatrunków przeciwbiofilmowych, co wykorzystałam w swoich badaniach.

W badaniach, w które byłam zaangażowana wykazano również, że BC może być dobrym nośnikiem dla substancji naturalnych. W **publikacji A-6** oceniono potencjał do eradykacji biofilmów *P. aeruginosa* fazy lotnej i ciekłej olejków eterycznych z tymianku, drzewa herbacianego, bazylii, rozmarynu, eukaliptusa, mięty i lawendy, którymi wysycano nośniki BC. Wyniki wykazały, że nośniki BC wysycone olejkiem eterycznym z drzewa herbacianego charakteryzowały się wysoką aktywnością przeciwbiofilmową.

Oprócz standardowego procesu wysycania/impregnacji nośnika BC substancją o działaniu przeciwdrobnoustrojowym, można stworzyć również dwufunkcyjny system, w którym zaszczepia się komórki roślin produkujących substancje lecznicze na BC. Takie podejście zastosowano w **publikacji A-7**, zaszczepiając komórki rośliny leczniczej *Chelidonium majus* na nośniku BC. Podczas analizy wpływu BC zawierającej komórki *C. majus* na sekrecję cytokin (IL-1β, IL-8 i TNF-α) przez ludzkie neutrofile, wykazano działanie przeciwzapalne takiego nośnika. Wykazano również działanie przeciwdrobnoustrojowe i przeciwbiofilmowe przygotowywanych nośników względem *S. aureus, P. aeruginosa* i *C. albicans.*

[A-4] Woroszyło, M., Pendrak, K., **Ciecholewska, D.,** Padzik, N., Szewczuk, M., & Karakulska, J. (2019). Investigation of biofilm formation ability of coagulase-negative staphylococci isolated from ready-to-eat meat. *Acta Scientiarum Polonorum Zootechnica*, *17*(4), 27-34.

40 pkt. MEiN

[A-5] Paleczny, J., Junka, A., Brożyna, M., Dydak, K., Oleksy-Wawrzyniak, M., **Ciecholewska-Juśko, D**., Dziedzic, E., Bartoszewicz, M. (2021). The high impact of *Staphylococcus aureus* biofilm culture medium on in vitro outcomes of antimicrobial activity of wound antiseptics and antibiotic. *Pathogens*, *10*(11), 1385.

IF_{2022} – 3,492, 100 pkt. MEiN

[A-6] Brożyna, M., Paleczny, J., Kozłowska, W., Ciecholewska-Juśko, D., Parfieńczyk, A., Chodaczek, G., Junka, A. (2022). Chemical coposition and antibacterial activity of liquid and volatile phae of essential oils against planktonic and biofilm-forming cells of Pseudomonas aeruginosa. *Molecules*, *27*(13), 4096).

IF_{2022} – 4,412, 140 pkt. MEiN

[A-7] Zielińska, S., Matkowski, A., Dydak, K., Czerwińska, M. E., Dziągwa-Becker, M., Kucharski, M., Wójciak, M., Sowa, I., Plińska, S., Fijałkowski, K., **Ciecholewska-Juśko, D**., Broda, M., Gorczyca, D., Junka, A. (2021). Bacterial nanocellulose fortified with antimicrobial

and anti-inflammatory natural products from *Chelidonium majus* plant cell cultures. *Materials, 15*(1), 16.

IF_{2022} – 3,623, 140 pkt. MEiN

8.3. Osiągnięcia naukowe związane z wytwarzaniem przeciwdrobnoustrojowych filtrów na bazie celulozy bakteryjnej

Ze względu na pandemię wynikającą z globalnego rozprzestrzenienia się wirusa SARS-CoV-2 nastąpił znaczny wzrost zapotrzebowania na maseczki chirurgiczne, maski oddechowe oraz wszelkie urządzenia do filtrowania powietrza. Niestety fakt, że filtry te są wykonane z niebiodegradowalnych, syntetycznych polimerów oznacza, że gwałtowny wzrost ich produkcji doprowadził również do gwałtownego zwiększenia ilości odpadów na bazie tworzyw sztucznych. W celu opracowania biodegradowalnych, przeciwbakteryjnych i przeciwwirusowych filtrów na bazie BC, w Katedrze Mikrobiologii i Biotechnologii ZUT prowadzono badania, które były częścią 2 grantów badawczo-rozwojowych realizowanych w ramach Regionalnego Programu Operacyjnego Województwa Zachodniopomorskiego pn. „Biodegradowalne, przeciwbakteryjne i przeciwwirusowe filtry na bazie bionanocelulozy do zastosowania w maseczkach ochronnych" oraz „Testowanie w warunkach rzeczywistych innowacyjnych maseczek ochronnych (NanoBioCell) z bionanocelulozy". Technologia produkcji filtrów na bazie BC obejmowała proste i ekologiczne procesy, w tym wytwarzanie BC przy użyciu opracowanej przeze mnie pożywki produkcyjnej na bazie soku komórkowego z bulw ziemniaków oraz oczyszczanie, homogenizację, liofilizację i obróbkę niskociśnieniową plazmą argonową (LPP-Ar, ang. *low-pressure argon plasma*) (**publikacja A-8**). Otrzymany materiał na bazie BC funkcjonalizowany LPP-Ar wykazywał silne właściwości przeciwbakteryjne i przeciwwirusowe oraz brak cytotoksyczności wobec mysich fibroblastów *in vitro*. Ponadto filtry składające się z trzech warstw opracowanego materiału charakteryzowały się skutecznością filtracji bakterii i wirusów na poziomie >99%, przy zachowaniu wystarczająco niskiego oporu przepływu powietrza, aby umożliwić swobodne oddychanie. Co więcej, w ramach weryfikacji koncepcji, udało nam się przygotować 80 masek z filtrem na bazie BC funkcjonalizowanym za pomocą LPP-Ar, które były testowane przez personel medyczny. Zdecydowana większość użytkowników (~85%) oceniła testowane maseczki jako dobre lub bardzo dobre pod względem komfortu. Tak przygotowane nowatorskie, ekologiczne, biodegradowalne filtry na bazie BC są odpowiednie dla osobistego sprzętu ochrony dróg oddechowych (PPE), takiego jak maski chirurgiczne i maski oddechowe. Ponadto, w miarę zwiększania skali, mogą być przystosowane do filtracji powietrza wewnętrznego w szpitalach lub szkołach.

Podczas badań prowadzonych w ramach 2 wyżej wymienionych grantów powstały 2 zgłoszenia patentowe:

1. Fijałkowski, K., El Fray, M., Drozd, R., Żywicka, A., Sobolewski, P., **Ciecholewska-Juśko, D.**, Szymańska, M. Sposób wytwarzania modyfikowanej celulozy bakteryjnej o właściwościach przeciwdrobnoustrojowych, nr zgłoszenia: P.430149, 2021.

2. Fijałkowski, K., El Fray, M., Drozd, R., Żywicka, A., Sobolewski, P., **Ciecholewska-Juśko, D.**, Szymańska, M. Sposób wytwarzania biodegradowalnych materiałów filtracyjnych na bazie bionanocelulozy, nr zgłoszenia: P.430150, 2021.

[A-8] Żywicka, A., **Ciecholewska-Juśko, D.**, Szymańska, M., Drozd, R., Sobolewski, P., Junka, A., Gorgieva, S., El Fray, M., Fijałkowski, K. (2022). Argon plasma-modified bacterial cellulose filters for protection against respiratory pathogens.

- obecnie w recenzji

8.4. Osiągnięcia naukowe związane z wpływem wirującego pola magnetycznego na efektywność działania substancji przeciwdrobnoustrojowych względem biofilmów

W ramach grantu OPUS 14 dofinansowanego ze źródeł Narodowego Centrum Nauki realizowanego w Katedrze Mikrobiologii i Biotechnologii pn. „Analiza mechanizmów zwiększonej efektywności substancji przeciwdrobnoustrojowych względem biofilmów w obecności wirującego pola magnetycznego" uczestniczyłam, jako wykonawca części zadań badawczych, w analizach dotyczących wpływu RMF na komórki bakteryjne i działanie środków przeciwdrobnoustrojowych (**publikacje A-9, A-10, A-11**).

Metycylinooporne szczepy *S. aureus* (MRSA) stały się globalnym problemem dla systemów opieki zdrowotnej ze względu na ich oporność na większość antybiotyków β-laktamowych, której często towarzyszy oporność na inne klasy antybiotyków. Podczas realizacji grantu OPUS przeanalizowano wpływ jednoczesnego stosowania RMF z różnymi klasami antybiotyków (β-laktamami, glikopeptydami, makrolidami, linkozamidami, aminoglikozydami, tetracyklinami i fluorochinolonami) na 9 szczepów MRSA (8 metycylinoopornych i 1 wrażliwy na metycylinę) (**publikacja A-9**). Wyniki wykazały, że zastosowanie RMF w połączeniu z antybiotykami ingerującymi w ściany komórkowe (zwłaszcza β-laktamami) intensyfikuje efekt przeciwdrobnoustrojowy. Wykazano także, że RMF powoduje zaburzenia w ścianach komórkowych bakterii, co zwiększa skuteczność antybiotyków. Ponieważ największe zmiany w efekcie przeciwdrobnoustrojowym względem kontroli nieeksponowanych zaobserwowano w przypadku antybiotyków β-laktamowych, w następnym etapie przeanalizowano wpływ RMF w połączeniu z antybiotykami β-laktamowymi na 28 szczepów MRSA (**publikacja A-10**). Ponownie odnotowano znacznie silniejszy efekt bakteriobójczy w porównaniu z kontrolą nieeksponowaną na RMF. Zaobserwowano również spadek liczby komórek z nienaruszonymi ścianami komórkowymi i bez wyraźnie zmienionej morfologii po ekspozycji na RMF.

Zazwyczaj, badania nad wpływem pól magnetycznych na drobnoustroje są prowadzone z wykorzystaniem różnych gatunków lub różnych grup drobnoustrojów, ale nie z wykorzystaniem różnych szczepów należących do jednego gatunku. Dlatego, celem **publikacji A-11** była ocena wpływu RMF o częstotliwości 5 i 50 Hz na wzrost i aktywność metaboliczną komórek ośmiu gatunków bakterii: *S. aureus, P.aeruginosa, Proteus mirabilis, Klebsiella pneumoniae, Enterococcus faecalis , Enterobacter cloacae, Moraxella catarrhalis i Bacillus cereus,* z których każdy był reprezentowany przez co najmniej 4 różne szczepy. Wyniki wykazały zróżnicowany wpływ RMF na dynamikę wzrostu i aktywność metaboliczną komórek bakteryjnych, co zależało w największej mierze od szczepu. Stwierdzono, że w odniesieniu do eksponowanego szczepu tego samego gatunku, wpływ RMF może być pozytywny lub negatywny. W niektórych przypadkach nie zaobserwowano żadnego wpływu RMF na aktywność komórek. Badania wykazały zatem, że oprócz opisanych wcześniej czynników związanych przede wszystkim z parametrami fizycznymi pola magnetycznego, jednym z kluczowych parametrów wpływających na końcowy wynik jego oddziaływania jest zmienność wewnątrzgatunkowa bakterii.

[A-9] Woroszyło, M., **Ciecholewska-Juśko, D**., Junka, A., Wardach, M., Chodaczek, G., Dudek, B., Fijałkowski, K. (2021). The effect of rotating magnetic field on susceptibility

profile of methicillin-resistant *Staphylococcus aureus* strains exposed to activity of different groups of antibiotics. *International Journal of Molecular Sciences*, *22*(21), 11551.

IF_{2022} – 5,923, 140 pkt. MEiN

[A-10] Woroszyło, M., **Ciecholewska-Juśko, D**., Junka, A., Drozd, R., Wardach, M., Migdał, P., Szymczyk-Ziółkowska, P., Styburski, D., Fijałkowski, K. (2021). Rotating Magnetic Field increases β-lactam antibiotic susceptibility of methicillin-resistant Staphylococcus aureus strains. *International Journal of Molecular Sciences*, *22*(22), 12397.

IF_{2022} – 5,923, 140 pkt. MEiN

[A-11] Woroszyło, M., **Ciecholewska-Juśko, D**., Junka, A., Pruss, A., Kwiatkowski, P., Wardach, M., Fijałkowski, K. (2021). The impact of intraspecies variability on growth rate and cellular metabolic activity of bacteria exposed to rotating magnetic field. *Pathogens*, *10*(11), 1427.

IF_{2022} – 3,492, 100 pkt. MEiN

Zachodniopomorski Uniwersytet Technologiczny w Szczecinie

Wydział Biotechnologii i Hodowli Zwierząt

Załącznik 1

Kopie publikacji naukowych wchodzących w skład cyklu stanowiącego rozprawę doktorską

Daria Ciecholewska-Juśko

Rozprawa doktorska

OPRACOWANIE I CHARAKTERYSTYKA MATERIAŁÓW BIONANOCELULOZOWYCH DO ZAPOBIEGANIA KOLONIZACJI PRZEZ DROBNOUSTROJE PATOGENNE ORAZ DO ERADYKACJI BIOFILMÓW BAKTERYJNYCH

Carbohydrate Polymers 253 (2021) 117247

Contents lists available at ScienceDirect

Carbohydrate Polymers

journal homepage: www.elsevier.com/locate/carbpol

Superabsorbent crosslinked bacterial cellulose biomaterials for chronic wound dressings

Daria Ciecholewska-Juśko [a], Anna Żywicka [a], Adam Junka [b], Radosław Drozd [a], Peter Sobolewski [c], Paweł Migdał [d], Urszula Kowalska [e], Monika Toporkiewicz [f], Karol Fijałkowski [a,*]

[a] Department of Microbiology and Biotechnology, Faculty of Biotechnology and Animal Husbandry, West Pomeranian University of Technology, Szczecin, Piastów 45, 70-311 Szczecin, Poland
[b] Department of Pharmaceutical Microbiology and Parasitology, Wrocław Medical University, Borowska 211A, 50-556 Wrocław, Poland
[c] Department of Polymer and Biomaterials Science, Faculty of Chemical Technology and Engineering, West Pomeranian University of Technology, Szczecin, Piastów 45, 70-311 Szczecin, Poland
[d] Department of Environment, Hygiene and Animal Welfare, Faculty of Biology and Animal Science, Wrocław University of Environmental and Life Sciences, Chełmońskiego 38C, 51-630 Wrocław, Poland
[e] Centre of Bioimmobilization and Innovative Packaging Materials, West Pomeranian University of Technology, Szczecin, Janickiego 35, 71-270 Szczecin, Poland
[f] Laboratory of Confocal Microscopy, Łukasiewicz Research Network - PORT Polish Center for Technology Development, Stabłowicka 147, 54-066 Wrocław, Poland

ARTICLE INFO

Keywords:
Bacterial cellulose
Biopolymer
Crosslinking
Water-related properties
Wound dressings

ABSTRACT

In this work, we present a novel *ex situ* modification of bacterial cellulose (BC) polymer, that significantly improves its ability to absorb water after drying. The method involves a single inexpensive and easy-to-perform process of BC crosslinking, using citric acid along with catalysts, such as disodium phosphate, sodium bicarbonate, ammonium bicarbonate or their mixtures. In particular, the mixture of disodium phosphate and sodium bicarbonate was the most promising, yielding significantly greater water capacity (over 5 times higher as compared to the unmodified BC) and slower water release (over 6 times as compared to the unmodified BC). Further, our optimized crosslinked BC had over 1.5x higher water capacity than modern commercial dressings dedicated to highly exuding wounds, while exhibiting no cytotoxic effects against fibroblast cell line L929 *in vitro*. Therefore, our novel BC biomaterial may find application in super-absorbent dressings, designed for chronic wounds with imbalanced moisture level.

1. Introduction

A wide spectrum of health issues, frequently referred to as "lifestyle diseases," poses an increasing threat to modern western societies, due to their serious health complications (Egger & Dixo, 2014). In particular, chronic wounds are among the most persistent and serious, because they do not follow the natural trajectory of healing and, if infected, threaten the life of the patient (Frykberg & Banks, 2015). Due to their persistence, chronic wound treatment is a significant burden for patients, their families, and health-care professionals, as well as healthcare systems in general (Järbrink et al., 2017). Therefore, prevention and treatment of chronic wounds is one of the most important challenges of contemporary medicine. To date, a number of approaches to managing chronic wounds have been developed, including T.I.M.E. (Tissue, Infection, Moisture, Epithelialization), B.B.W.C. (Biofilm-Based Wound Care), and W.A.R. (Wounds at Risk) (Dissemond et al., 2011; Falanga, 2004; Percival, Vuotto, Donelli, & Lipsky, 2015). Although these strategies address the process of wound healing from different angles, they share a common denominator: maintenance of proper moisture level. In western medicine, keeping wounds dry was the conventional wisdom until landmark work by George Winter in 1962, who unquestionably demonstrated that moist wounds heal better than dry ones (Winter, 1962). Winter's paper became the basis for the moist wound-healing concept, which is generally accepted and has been further developed

* Corresponding author.
E-mail addresses: daria.ciecholewska@zut.edu.pl (D. Ciecholewska-Juśko), anna.zywicka@zut.edu.pl (A. Żywicka), adam.junka@umed.wroc.pl (A. Junka), radoslaw.drozd@zut.edu.pl (R. Drozd), psobolewski@zut.edu.pl (P. Sobolewski), pawel.migdal@upwr.edu.pl (P. Migdał), urszula.kowalska@zut.edu.pl (U. Kowalska), monika.toporkiewicz@port.pl (M. Toporkiewicz), karol.fijalkowski@zut.edu.pl (K. Fijałkowski).

https://doi.org/10.1016/j.carbpol.2020.117247
Received 28 June 2020; Received in revised form 31 August 2020; Accepted 12 October 2020
Available online 19 October 2020

ever since.

While dressings are commonly used to deliver moisture to a wound, wounds also possess intrinsic moisture, referred to as "exudate" (Vowden, Bond, & Meuleneire, 2015). In acute wounds, exudate accelerates the healing process, but in chronic wounds capillary leakage, failure of the patient's lymphatic system or oedema can result in excessive amount of wound exudate. Thus, in chronic wounds both the under- and over-production of exudate can occur, with both having a negative effect. Therefore, maintenance of the proper amount of exudate in chronic wounds is crucial for healing (Han & Ceilley, 2017).

Additionally, to provide the appropriate healing conditions, the wound itself should be protected from microbial contamination and other external factors. Presently, there is a wide range of modern dressings dedicated to protecting either dry, low-exuding or highly exuding wounds (Bernard, Barault, Juchaux, Laurensou, & Apert, 2005; Dhaliwal & Lopez, 2018; Pott, Meier, Stocco, Crozeta, & Ribas, 2014; Yadie & Hu, 2015). Nonetheless, there is still an ongoing search for a dressing material that would yield quick closure of chronic wounds regardless of type and amount of exudate.

One of the candidates for such an ideal dressing material is bacterial cellulose (BC). This polymer is biosynthesized primarily by acetic acid bacteria (Shao et al., 2017), of which Gram-negative *Komagataeibacter xylinus* is the most effective producer (Gullo, La China, Falcone, & Giudici, 2018). The high purity, crystallinity and density, binding capacity, shape, and water retention (Bielecki et al., 2012; El-Saied, El-Diwany, Basta, Atwa, & El-Ghwas, 2008; Ruka, Simon, & Dean, 2012) of BC has drawn extensive interest of research teams from all over the world. This is reflected by the rapidly increasing number of scientific reports on BC [https://www.ncbi.nlm.nih.gov/pubmed/?term=bacterial+cellulose], particularly over the past 15 years, investigating its wide range of potential applications in many branches of industry (Lin et al., 2013). In the biomedical field, this multifaceted material has already been used, among others, in drug-delivery carriers (Picheth et al., 2012) and in wound dressings for patients with extensive burns (Bielecki et al., 2012). These applications are possible thanks to the structure of BC, consisting of thin, loosely arranged fibrils, separated by "empty" spaces (Ul-Islam, Khan, & Park, 2012). This affects the liquid absorption of BC, which depends primarily on fibril arrangement, surface area, and porosity. Overall, the more space is available between the BC fibrils, the more liquid penetrates and adsorbs into the material. It has been estimated that approx. 97–98 % of total BC weight consists of water (Lin, Hsu, Chen, & Chen, 2009; Schrecker & Gostomski, 2005).

However, from the point of view of product development, dry materials offer several practical advantages, from permitting simpler packaging and lowering shipping costs, as well as offering greater shelf stability, prolonging the expiration date and improving the microbiological safety profile. While BC can be subjected to dehydration, the evaporation of water from the interfibrillar spaces causes the collapse of the BC structure (Ul-Islam et al., 2012a; Vasconcellos & Farinas, 2018). This irreversible process deprives BC of its most unique properties. After dehydration, the three-dimensional polymer network is unable to regenerate and its ability to re-swell and absorb liquid is significantly reduced, as compared to never-dried cellulose (Pa'e et al., 2018; Shezad, Khan, Khan, & Park, 2010). Therefore, dried BC is less useful within the scope of biomedical applications (Ul-Islam et al., 2012a, 2013). For this reason, several ex situ modifications have been proposed to counteract the disadvantageous consequences of BC dehydration, for example the production of BC-fibrin or BC-gelatin composites, decreasing BC crystallinity, or freeze drying (Brown, Laborie, & Zhang, 2012; Chang, Chen, Lin, & Chen, 2012; Fijałkowski et al., 2015; Torres, Arroyo, & Troncoso, 2019; Ul-Islam et al., 2013). Crosslinking is another type of *ex situ* modification method, typically obtained by linking at least two hydroxyl groups of single cellulose molecule or two or more hydroxyl groups of adjacent cellulose molecules. As a result, the material becomes stiffer and preserves its three-dimensional structure (Qi et al., 2016; Widsten, Dooley, Parr, Capricho, & Suckling, 2014; Young, 2002). Crosslinking efficiency can be further increased by using compounds that act as catalysts (CATs) for the reaction (Yang, 1991).

Crosslinking reactions have been used to modify numerous biopolymers; however, to date only two scientific publications by Meftahi, Khajavi, Rashidi, Rahimi, and Bahador (2018) and Frone et al. (2020) describe the use of crosslinking to modify cellulose produced by microorganisms. The first work describes crosslinking of BC in its native state (as a membrane), while the second one concerns crosslinking of the BC that underwent a disintegration and silanization process. In the first, more relevant work, Meftahi et al. reported that the use of citric acid (CA) as a crosslinking reagent, with sodium hypophosphite (SHP) catalyst (CAT), resulted in significantly enhanced (up to 3 times) levels of re-hydration of previously dried BC. CA and SHP have also already been used in a number of polymer studies involving crosslinking of hydrogels, plant cellulosic materials, and bio-composites (El Fawal, Abu-Serie, Hassan, & Elnouby, 2018; Gyawali et al., 2010; Meftahi et al., 2018; Yang, Chen, Guan, & He, 2010; Ye, Wang, Liu, Chen, & Yang, 2015).

CA is a particularly promising crosslinker not only because of its safety and non-toxicity, but also because of the stable crosslinking bonds it forms with cellulose. Importantly, CA is easily accessible and inexpensive, making this reagent commercially attractive. On the other hand, the use of SHP in chemical reactions can be problematic, because thermal SHP decomposition results in the formation of phosphine, a highly toxic and extremely flammable gas (Lewis, 2004). Further, SHP itself can have a negative environmental impact, because leached hydrogen phosphide compounds can contaminate surface waters (Feng, Xiao, Sui, Wang, & Xie, 2014).

In the present work, our primary goal was to obtain dry BC, displaying very high water-related parameters, which can be used as a super-absorbent dressing for chronic wounds. Towards this aim, we crosslinked BC with CA and tested a range of compounds as catalysts, the majority of which have never been used for this purpose. Importantly, focusing on biomedical applications and safety, we selected reagents that are all on the list of substances generally recognized as safe (GRAS), according to the U.S. Food and Drug Administration and are widely used in the food industry, for example as chemical leavening in baking (Brodie & Godber, 2001). This fact served as the basis for our study: these compounds release large amount of gases during reactions with acids and as a result of thermal decomposition. We hypothesized that released gas would fill the spaces between the crosslinked fibrils and BC layers, preventing them from collapsing during dehydration. Further, we assumed that the released gases could form new cavities within the BC matrix, additionally increasing water sorption capacity. Finally, in order to facilitate future translation and commercialization, we also assessed the specific CATs from the point of view of their potential impact on the environment, cytotoxicity, and cost-efficiency.

2. Materials and methods

2.1. Bacterial cellulose synthesis and purification

To obtain BC in a form of pellicles of consistent shape and diameter, the cellulose-producing *Komagataeibacter xylinus* strain (American Type Culture Collection - ATCC 53524) was cultured in 50 mL plastic tubes (Becton Dickinson and Company, USA), 24- or 96-well cell culture plates (Nest Scientific USA Inc., USA) under stationary conditions using Hestrin-Schramm (H-S) culture medium, over 7 days at 28 °C. Obtained BC samples were purified from bacteria and culture medium components using 0.1 M sodium hydroxide solution at 80 °C for 90 min, followed by rinsing with distilled water until the pH was neutral. The diameter of the BC pellicles obtained in plastic tubes was 2.5 cm, the average thickness was 0.9 cm, and the average weight was 4.5 g, whereas the diameter, average thickness and weight of BC pellicles obtained from 24- and 96-well plates were 1.25 cm, 0.4 cm, and 0.9 g and 0.6 cm, 0.15 cm and 0.3 g, respectively.

2.2. Crosslinking procedure

The crosslinking reaction was carried out using aqueous solutions of CA and different CATs. Six substances were used as CATs: disodium phosphate (later referred to as CAT1), sodium bicarbonate (later referred to as CAT2), disodium phosphate and sodium bicarbonate (1:1 mass ratio, later referred to as CAT3), ammonium bicarbonate (later referred to as CAT4), disodium phosphate and ammonium bicarbonate (1:1 mass ratio, later referred to as CAT5), sodium bicarbonate and ammonium bicarbonate (1:1 mass ratio, later referred to as the CAT6). Sodium hypophosphite (later referred to as CAT7) was used as a reference, because it is well described in the literature related to crosslinking of plant and also bacterial cellulose (Ji, Qi, Yan, & Sun, 2016; Meftahi et al., 2018; Stoyanov & Miller, 2017; Yang, 2001). As additional controls, we conducted reactions using: just 20 % CA, without any CAT, and each of the individual CATs, but without CA. All of the chemicals were purchased from POCH, Poland.

The entire crosslinking procedure consisted of four stages (see Fig. 1): ***i)*** impregnation of BC with CA and CAT for 24 h at 28 °C, ***ii)*** incubation at high temperature to induce the crosslinking reaction, ***iii)*** purification with distilled water until the pH stabilized at 7.0 for 24 h, in order to remove unbounded CA and CATs molecules, ***iv)*** drying at room temperature.

The BC samples obtained as a result of aforementioned modifications were referred as M1-M7, depending on the CAT used (CAT1-CAT7, respectively). As a control, BC treated with just distilled water, without CA or CAT, was used (later referred to as C).

2.2.1. Optimization of the BC crosslinking reactions

The first parameters to be optimized were the concentrations of CA and CATs. The following final concentrations (in distilled water, m/v) were used for BC impregnation: CA – 30 %, 20 %, 10 %, 5 %; CAT – 15 %, 10 %, 5%, 2.5 %. Additionally, a reaction using 20 % CA without any CAT was performed as a comparative control setting. The initial CA to CAT mass ratio (2:1) and reaction temperature (160 °C) were selected based on the previously published conditions (Stoyanov & Miller, 2017; Yang, 2001; Yang et al., 2010). The reaction was carried out until BC was completely dehydrated, that is until the weight of the sample stabilized.

Following the determination of the optimal concentrations of CA and CATs, we optimized the remaining parameters: CA to CAT mass ratio, reaction time and temperature. The following mass ratios between defined optimal concentrations of CA and CAT were tested: 1:1, 1.5:1, 2:1, 2.5:1, 3:1, 1:2. The role of crosslinking reaction temperature was assessed in the range between 120 and 180 °C and the following reaction times: 5, 15, 30, 60, 75 and 90 min. Further analyzes, presented below, were carried out for BC crosslinked in the optimal conditions.

2.3. Evaluation of the properties of BC crosslinked under optimal conditions using various catalysts

2.3.1. Analysis of the BC macrostructure – stereoscopic microscope

The macromorphological structure of modified and unmodified (control) BC samples was evaluated using stereoscopic microscope (Leica S9i, Leica Microsystems, Wetzlar, Germany). The analyzes were performed for dry and wet (rehydrated) BC samples. Both, the surface and the layer structure visible in cross-section were assessed.

2.3.2. Analysis of the BC microstructure – scanning electron microscope

Modified BC samples were fixed in glutaraldehyde (POCH, Poland) for 0.5 h and washed in the following concentrations of ethanol (POCH, Poland): 10 %, 25 %, 50 %, 60 %, 70 %, 80 %, 90 %, 100 %, respectively, 5 min at each concentration. Subsequently, the BC was subjected to sputtering with Au/Pd (60:40) using EM ACE600, Leica sputter (Leica Microsystems, Wetzlar, Germany). Both the surface and the layer structure visible in cross-section were assessed. The surfaces of the sputtered samples were examined using Auriga 60 Scanning Electron Microscope (SEM, Auriga 60, Zeiss, Oberkochen, Germany), whereas cross sections of the samples were analyzed using VEGA3 scanning electron microscope (VEGA3, Tescan, Brno, Czech Republic). The BC microfibril diameters were analyzed using software integrated with

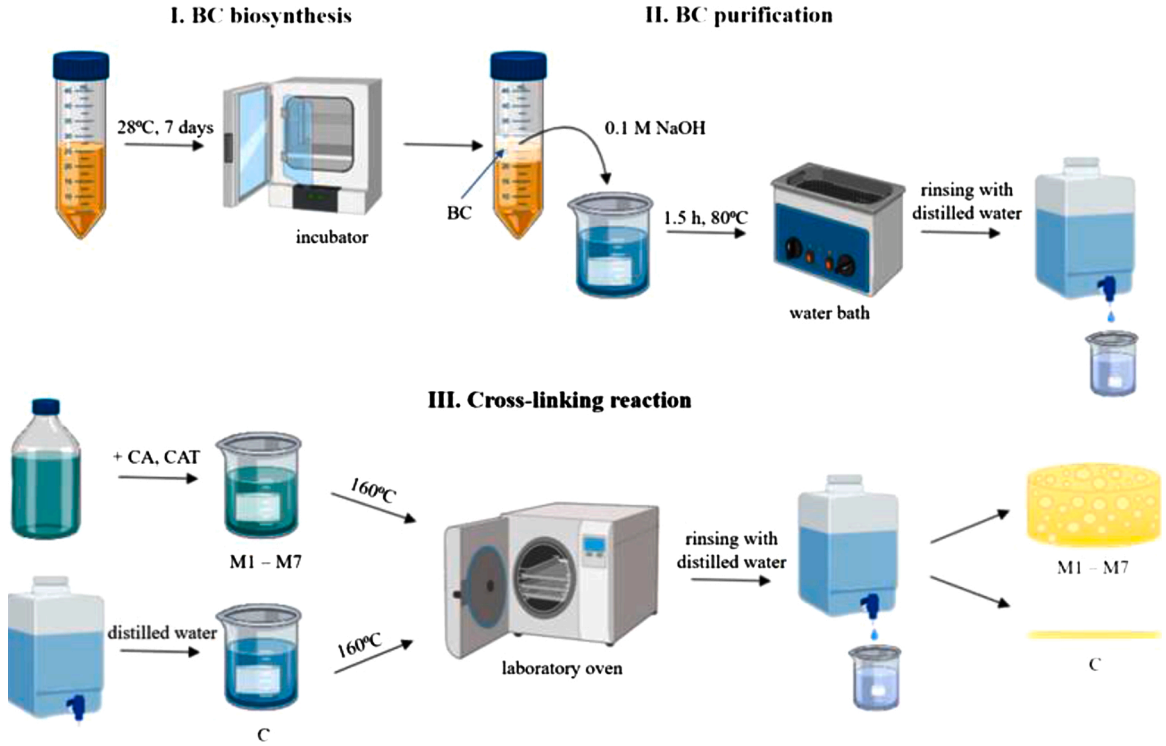

Fig. 1. BC modification procedure (created by BioRender.com).
C – control BC sample; CA – citric acid; CAT – catalyst; M1-M7 – modified BC samples.

Auriga 60 SEM, while micro-pore size was analyzed using ImageJ software (Schneider, Rasband, & Eliceiri, 2012).

2.3.3. Elemental analysis of BC surface – energy-dispersive X-ray spectroscopy

Samples were placed on aluminum tables, sputtered with gold (20 nm) using EM ACE600, Leica sputter (Leica Microsystems, Wetzlar, Germany), and placed in the scanning electron microscope chamber (Auriga 60, Zeiss, Oberkochen, Germany). X-ray microanalysis (EDX) was carried out using an EDX Oxford detector (Oxford Instruments, Abingdon, United Kingdom). The working distance was 5 mm and the voltage 20 kV. For characterization of sample composition, the AZtec system (Oxford Instruments, Abingdon, United Kingdom) was used.

2.3.4. Determination of chemical composition of the BC – Attenuated Total Reflectance Fourier Transform Infrared (ATR-FTIR) spectral studies

The assessment of the chemical composition of the BC samples was performed using a Bruker Alpha FTIR spectrometer with diamond ATR adapter. Spectra (32 scans) were collected over wavenumber range of 4000−400 cm^{-1} with a resolution of 4 cm^{-1}. The obtained ATR-FTIR spectra were analyzed using the Spectragryph 1.2 software. Additionally, the 2DShige© v1.3 program was used to preform 2D correlation analysis. 2D correlation spectra were visualized using OriginPro 8 software (Origin Software Solutions, United Kingdom) (Morita & Ozaki, 2004; Noda, 2004).

The chemometric principal component analysis (PCA) of all spectra was performed with using R software and the *FactoMineR* and *Factorextra* packages via RStudio software (Lê, Josse, & Husson, 2008). Prior to the analysis, the spectra in the of range 1850 cm^{-1} to 850 cm^{-1} were normalized to the peak area at 1200 cm^{-1}. The areas of integrated peaks were used as input data for PCA.

2.3.5. Determination of water swelling ratio

To determine the swelling ratio (SR (%)), BC pellicles were first dried at room temperature to completely remove water content. The dry BC samples were then immersed in distilled water and weighed – first after 1 min, and then every 10 min up to 60 min. After 60 min, the BC samples were left in water and their weight was measured after 24 h. The percentage of water absorption was calculated using the Eq. 1 (Pandey, Mohamad, & Amin, 2014):

$$SR\ (\%) = \frac{(W_w - W_d)}{W_d} * 100 \quad (1)$$

where, W_w is the weight of the swollen BC and W_d is the dry weight of the sample.

2.3.6. Determination of water holding capacity

Dry BC pellicles were weighed, immersed in distilled water for 24 h to obtain maximum absorption level, and then weighed again. The ability to hold water was determined using two methods: by centrifugation and by drying. In the former method, BC samples were arranged on cell strainers placed in 50 mL tubes, centrifuged (5804R, Eppendorf, Germany) at 200 *g* for 10 min, and then weighed. This procedure was repeated 10 times; in total, each sample was centrifuged 100 min. In the other method, BC samples were placed in an incubator at 37 °C and weighted every 10 min for 240 min. Water holding capacity (WHC (%)) was calculated using the Eq. 2:

$$WHC(\%) = \frac{W_{rw}}{W_w - W_d} * 100 \quad (2)$$

where, W_{rw} is the weight of water retained in BC during drying/centrifuging, W_w is the initial weight of wet BC, and W_d is the dry weight of the sample.

2.3.7. Determination of the BC density

The density of the BC samples was determined using hydrostatic balance (XA 52/Y, Radwag, Poland) in methanol as a standard liquid. The weight of samples was measured at room temperature in air, as well as in methanol. The sample density was determined using the Eq. 3 (Pratten, 1981):

$$\rho = \frac{W_d}{W_d - W_m} * \rho_{methanol} \quad (3)$$

where, W_d is the weight of the dry sample in the air, W_m is the weight of the sample in methanol, and $\rho_{methanol}$ is the density of methanol.

2.4. Evaluation of the crosslinking efficiency under optimal conditions using various catalysts

The BC crosslinking efficiency under optimal, defined reaction conditions was assessed as the BC weight percent gain (WPG (%)) compared to the weight of unmodified BC (control) and calculated according to the Eq. 4 (Rahman et al., 2013):

$$WPG\ (\%) = \frac{W_m - W_u}{W_u} * 100 \quad (4)$$

where: W_m is the dry weight of modified BC, and W_u is the dry weight of unmodified BC.

2.5. Determination of the cytotoxicity of BC crosslinked under optimal conditions using various catalysts

2.5.1. Direct contact assay

All cell culture reagents and cell lines were purchased from Sigma-Aldrich (Poznań, Poland). For direct contact assay based on the ISO 10993-5:2009 standard, 1×10^4 L929 cells (mouse fibroblasts) were seeded per well in a 96-well plate. Following 24 h of culture in Dulbecco's Modified Eagle Medium (DMEM) containing 10 % fetal bovine serum (FBS), 2 mM L glutamine, 100 U/mL penicillin, and 100 μg/mL streptomycin (hereafter referred to as "complete growth media") in an incubator (5% CO_2, 37 °C), the cells were assessed to be ~50 % confluent, the medium was aspirated, and previously autoclaved modified BC pellicles with a diameter of 6 mm were placed on top of the cell layer. Each disc was pretreated by soaking in 2 mL of complete growth medium for 1 h. CellCrown tissue culture inserts were then placed on top of the discs to prevent them from floating and media was replaced. As a sham control, CellCrown tissue culture insert was placed directly into the well. After another 24 h of culture in 5% CO_2 at 37 °C, wells were examined using inverted light microscope (Delta Optical IB-100, Poland) and then resazurin stock (0.15 mg/mL) was added to each well (1:6 dilution) (Riss et al., 2016). After 4 h of incubation the viability was assessed using fluorescent plate reader (Synergy HTX, Biotek, USA) at wavelengths of 540 nm excitation and 590 nm emission. Complete growth media in an empty well was used as a blank. The results were expressed as percent of cell viability, and calculated by the Eq. 5 (Park & Xian, 2015):

$$\%\ of\ cell\ viability = \left(\frac{FLs - FLb}{FLc - FLb}\right) * 100 \quad (5)$$

where FL is the fluorescence intensity (arbitrary units) and indexes *s, b,* and *c* refer to sample, blank, and control, respectively.

2.5.2. Extract assay

Extracts of crosslinked BC were prepared according to the ISO 10993-5:2009 standard. Briefly, for each tested material 8 BC pellicles were placed in a 24-well plate well and covered with 1.5 mL of complete growth medium. As a sham control, 1.5 mL of media was pipetted into an empty well. The plate was then placed into 37 °C CO_2 incubator for 24 h of extraction.

Simultaneously, 1 x 10^4 L929 cells were seeded per well in a 96-well plate. Following 24 h of culture in 5% CO_2 at 37 °C, the cells were assessed to be ~50 % confluent, the media was aspirated and replaced with 100 μL of extract – 5 technical replicates were performed per sample. After another 24 h of culture, cells were examined using inverted light microscope and then cell viability was assessed as described above.

2.5.3. Confocal microscopy analysis of fibroblast viability on BC pellicles

L929 fibroblasts were cultured on BC samples for 5 days, followed by fixation in 3.7 % formaldehyde solution and staining with SYTO-9 and Propidium Iodide (PI) dyes (a mix of both from ThermoFisher) to visualize DNA in live and dead cells, respectively. The samples were then imaged using an upright Leica SP8 confocal microscope (Leica Microsystems, Wetzlar, Germany). Stacks of confocal 8-bit images with a voxel size of 0.465 × 0.465 × 1.5 μm were acquired using a dry 20x objective (NA 0.75) with the pinhole was set to 1 AU. SYTO-9 was excited with 488 nm laser line and 492−526 nm emission range was collected, while PI fluorescence was excited with 552 nm laser line and 561−611 nm emission range was recorded. The presence of cellulose surface below cultured cells was confirmed in reflection mode using a 638 nm laser line. The acquisition was performed in sequential mode. Three-dimensional rendering was performed in Imaris software (Bitplane, United Kingdom).

2.6. Statistical analysis

Data are shown as means ± standard errors of the means (SEM) obtained from at least three different measurements (plus technical repetitions). Statistical differences between different BC samples were determined by one-way analysis of variance (ANOVA) and Tukey's post hoc test. All analyses were considered statistically significant when the P value was less than 0.05. Statistical tests were conducted using Statistica 9.0 (StatSoft, Poland).

3. Results and discussion

3.1. Optimization and determination of the BC crosslinking parameters

The primary aim of this work was to obtain super-absorbent biomaterial. Therefore, the water-swelling ratio (SR (%)) was used as the primary parameter to assess the effectiveness of each BC

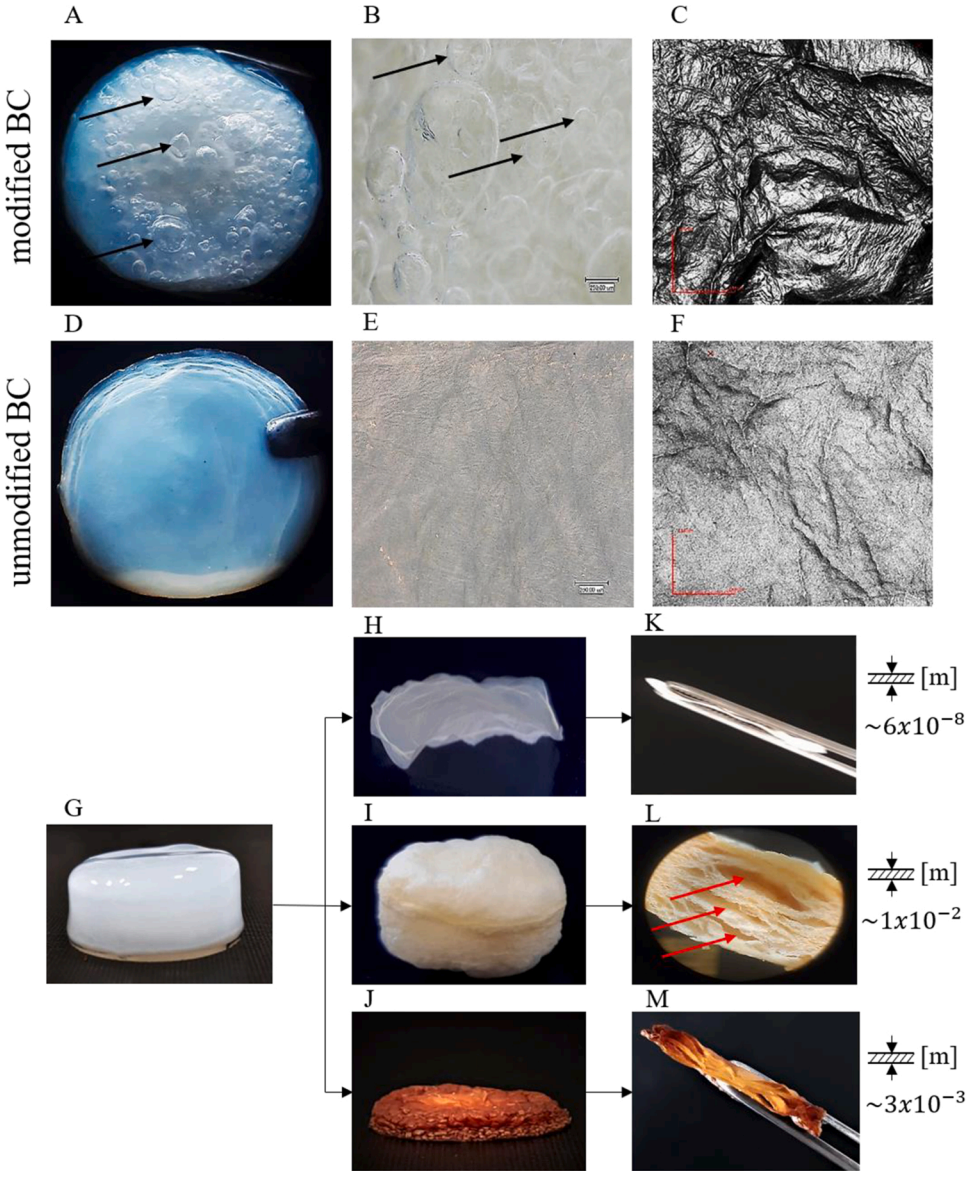

Fig. 2. The macromorphological differences in modified and unmodified BC.
A, B – top view of wet modified BC; C – surface of dry modified BC; D, E – top view of unmodified wet BC; F – surface of unmodified dry BC; G – side view of unmodified never-dried BC; H – side view of unmodified dry BC; I – side view of dry modified BC; J – side view of dry BC treated with 20 % CA w/o CAT; K – cross-section of unmodified dry BC, L – cross-section of dry modified BC, M – cross-section of dry BC treated with 20 % CA w/o CAT.

modification.

The SR (%) values for BC samples modified using different CATs under the same reaction conditions displayed a comparable trend. The most beneficial (for BC sorption properties) set of parameters for the crosslinking reaction was: 20 % CA concentration with 10 % of the appropriate CAT, 2:1 mass ratio of CA:CAT, reaction temperature of 160 °C, and reaction time of 75 min. The SR (%) results for entire data set of the results from the optimization of crosslinking process are presented in the Supplementary material (Fig. S1, Fig. S2, Tab. S1-S9). The water-related properties obtained under the most favorable conditions will be further discussed in section 3.4 Water-related properties and density of modified BC and efficiency of crosslinking reaction.

3.2. Macro and micromorphological characteristics of modified BC

Macromorphological examination demonstrated that dried, modified BCs, contrary to the unmodified samples, possess an arranged and multilayer structure regardless of CAT used (Fig. 2, Fig. S3).

This multilayer spatial arrangement of BC is directly related to the biological and physical processes of its polymer synthesis (Shao et al., 2017). Cellulose fibrils secreted by the bacterial cells into the extracellular space form a thin layer on the surface of the medium (Keshk, 2014). Over a time, a new cellulose layer appears on the surface, pushing the older one down and this process repeats until depletion of oxygen and nutrients in medium. The fact we observed multilayers in our crosslinked BC samples confirmed that the process successfully prevents the collapse of the 3D structure during drying.

Cross sections of the dried modified BC samples revealed the presence of empty spaces between the layers in all of the modified BC pellicles, but not in the case of unmodified BCs and BCs modified only with CA (Fig. 2G-K, Fig. S3). This provides strong evidence in support of our hypothesis that gas bubble formation occurs within the BC structure during crosslinking reaction with use of the tested thermo-sensitive catalysts (Fig. 2A, Fig. 2B, Fig. S4). Also, it is worth mentioning that the surface of the modified BC was also heavily folded, in contrast to the relatively smooth surface of unmodified BC, but no specific pattern of surface folding with different CATs was observed (Fig. 2A-F, Fig. S4, Fig. S5). Thus, the results of macromorphological examination help to explain why modified BC samples, particularly these crosslinked with addition of CAT3, displayed significantly higher SR (%) than unmodified BC (see Fig. S1, Tab. S1-S9).

Pictures of modified BC are presented on the example of M3 (BC modified with 20 % CA + 10 % CAT3). The pictures of cross section and surface of all modified BC samples are presented in Supplementary material (Fig. S3-S5). Black arrows (A, B) indicate air bubbles on the surface of the sample, whereas red arrows (K) indicate spaces between BC layers.

In order to assess the microscale architecture of crosslinked BC, we

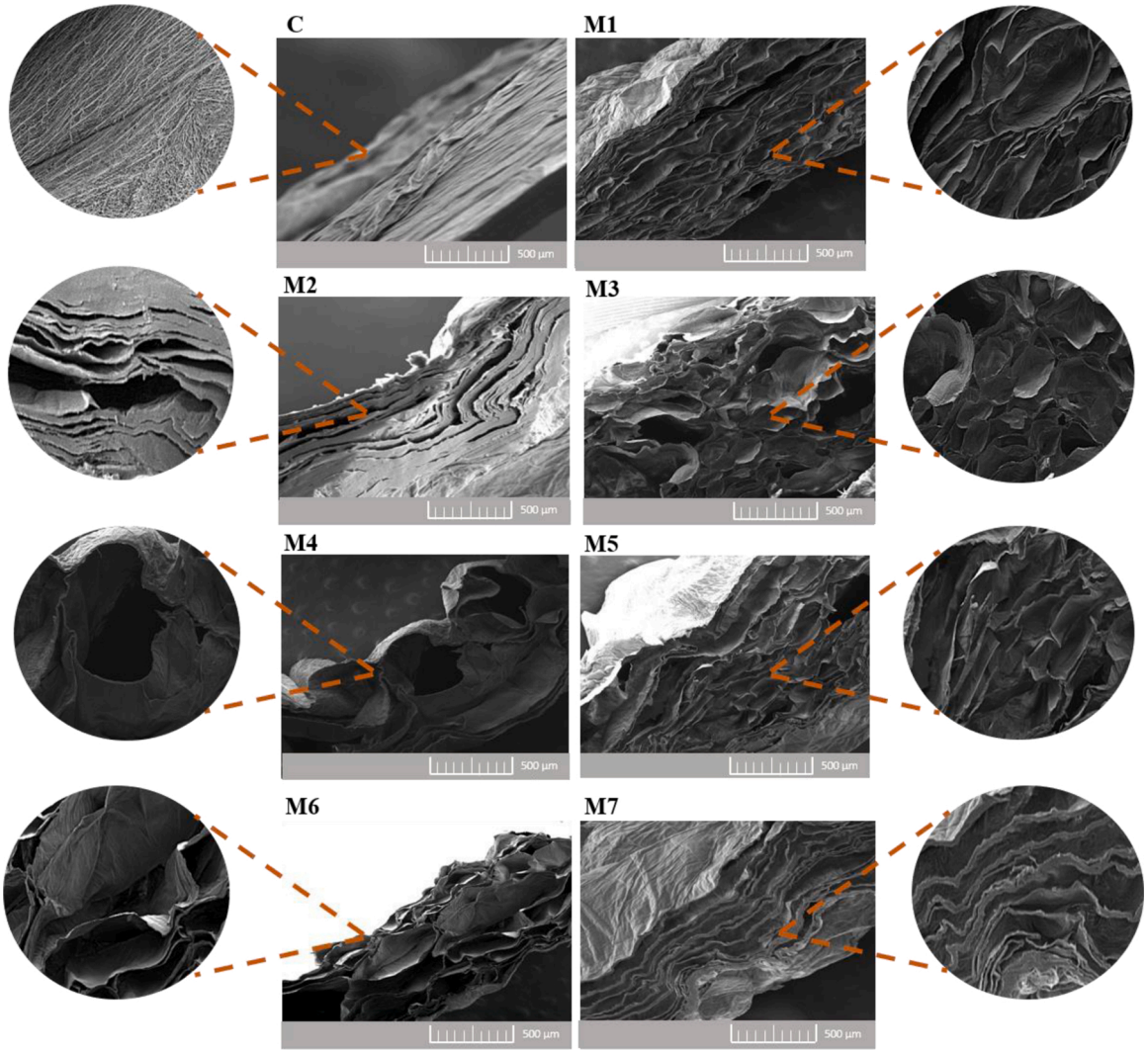

Fig. 3. Cross sections of BC pellicles visualized by scanning electron microscopy (SEM, VEGA3, Tescan, Brno, Czech Republic) at 500x and 2000x magnification for images in the center and on the edges of the figure, respectively. C – control BC sample; M1-M7 – modified BC samples.

used SEM imaging. Overall, SEM images of the surfaces of BC pellicles demonstrated that the micro-porosity and BC layer structure were preserved in all of the studied reaction conditions (Fig. S6). Fibril thickness and average pore diameter were comparable between all modified BC pellicles (regardless of CAT used) and control BC samples (Fig. S7-S9). In contrast, the SEM imaging of BC cross sections showed that morphology of stratification, as well as the formation of spaces between layers was CAT-specific (Fig. 3). In all modified BC pellicles, multiple spaces appeared as a result of delamination or blistering. However, we did not observe such stratification patterns in the case of control BC, which was characterized by a typical homogeneous structure throughout the entire section.

For the case of M1, SEM imaging of cross sections demonstrated regular corrugations of the matrix, as well as the presence of numerous, but relatively small, regular bubbles (air spaces) and moderate layer stratification (Fig. 3). In contrast, M2 was characterized by greater degree of corrugation, but instead of the bubbles present in M1, longitudinal air spaces were observed between the separate layers of M2. The structure of M3 resembled M1, except that the degree of folding was greater and the bubbles (visible as black spots) were larger and more deeply located. Meanwhile, M4 microstructure was characterized by a very high degree of folding and the presence of very large air spaces in the form of large, torn blisters. Further, the cellulose structure in M4 was also heavily altered. The structure of M5 resembled to some extent M1 and M3, but deep air channels were observed instead of bubbles. Cross sections of M6 were characterized by corrugated structure and numerous, very large, elongated air spaces, but due to their presence, delamination was not as clearly visible as in case of M2. Finally, cross sections of M7 exhibited a greater degree of stratification, as compared to M2. Further, large air spaces, but no air bubbles, were observed between layers of this modified BC. In contrast to all of the modified BC pellicles, the control BC had no layers or blisters and was characterized by regular, compact structure, with overlapping layers of cellulose clearly visible. Thus, in the process of dehydration, the unmodified cellulose fibers flatten, undergoing irreversible deformation – this is the reason that dried, unmodified BC has significantly reduced rehydration capacity.

In summary, SEM imaging revealed that crosslinking process results in two main changes in BC pellicle microstructure. The first is evident stratification, created by the air spaces between successive layers of cellulose (e.g. M2, M7). The second is deformation caused by the presence of large, spherical or ellipsoidal air spaces (bubbles) (e.g. M4, M6). However, the most favorable SR (%) values (see Fig. S1, Tab. S1-S9) were obtained for BC samples where both types of BC microstructure alteration occurred simultaneously (M1, M3, M5). We conclude that the final microstructure of modified BC depends on the amount of gas produced and on the pressure generated within the sample during drying of fibers. It may be assumed that gradual release of smaller amounts of gas leads to BC delamination, while the rapid release of larger amounts of gas, leads to the formation of larger bubbles. In future studies, we plan to further examine the mechanism and specific gas released during crosslinking.

Simultaneously with SEM imaging, energy-dispersive X-ray spectroscopy (EDX) analysis was performed to determine the specific elemental composition of modified and control BC surfaces (Fig. S10, Tab. S10). The measurements confirmed that carbon and oxygen were the main constituents of BC fibers, both in modified and unmodified samples. In the case of BC modified in the presence of CATs containing sodium salts (all the CATs except for CAT4), trace amount of sodium were also detected (0.2−0.5 w/w%). Somewhat surprisingly, nitrogen was not detected on the surface of BC modified with ammonium bicarbonate-based CATs (CATs 4–6). However, trace amounts of phosphorous were detected on M1, M3, and M5 samples, those that were modified with phosphorous-containing CATs (0.3−0.5 w/w%). It is worth noting, that in the case of the M7 sample (modified in the presence of sodium hypophosphite), the content of phosphorous was significantly higher (1.7 w/w%), as compared to the other aforementioned modifications.

3.3. Analysis of ATR-FTIR spectra of modified BC

Comparison of ATR-FTIR spectra of unmodified and modified BC indicated that all of the applied modification protocols had a major impact on BC chemical structure (Fig. 4A, Fig. S11). The primary difference as compared to non-treated BC was the appearance of a characteristic band at 1720 cm^{-1}, indicating the presence of a carbonyl group (C═O, stretching) (Crépy, Miri, Joly, Martin, & Lefebvre, 2011) – this can be considered a fingerprint of ester bonds and unreacted carboxylic groups of CA. The highest intensity of this band was observed following M5 modification, in which the combination of ammonium bicarbonate and disodium phosphate was used as catalyst, while for other the tested CATs the intensities were similar. Additionally, a second, characteristic and expected ester band appeared in all spectra of modified BC at approx. 1248 cm^{-1} (C—C—O asymmetric stretching) (Schilling et al., 2010); however, its intensity did not vary between modification variants. Further, 2D−COS spectra (all modifications) also revealed that crosslinking process had a high impact on band intensities in the spectral region of 1200 cm^{-1} to 850 cm^{-1} (Fig. 4B, C). In this region, the spectra are primarily shaped by C—O—C stretching ether linkages and pyranose backbone rings and carbon-oxygen bonds (C—OH), indicating presence of primary alcohols (He et al., 2018). The reduction in intensity of bands in this region could be also a consequence of ester bond formation between carboxyl groups of citric acid (CA) and C—OH of anhydrous glucose units in BC fibrils. The presence of negative cross-peaks in the synchronous spectrum 1720 cm^{-1} vs. 950 cm^{-1} also suggests the possibility of a significant influence of modification process on the crystallinity of BC (Drozd, Rakoczy, Konopacki, Frąckowiak, & Fijałkowski, 2017; Liu, Yuan, & Bhattacharyya, 2012).

Finally, PCA of ATR-FTIR data also confirmed successful modification of BC and showed differences in the impact of the different types of modifications on the BC structure. From all extracted principal components, the first three account for approx. 80 % of variance. In the PC1 (48.49 %) dimension, the main contribution, accounting for over 80 % of variance, was the result of changes at bands: 1320 cm^{-1}, 1108 cm^{-1}, 1277 cm^{-1}, 1313 cm^{-1}, 1427 cm^{-1}, 1160 cm^{-1}, 1248 cm^{-1}, 1364 cm^{-1}, 1720 cm^{-1}. The changes in the first six bands influenced PC1 to the greatest degree, with almost equal contributions (above 10 %). The PC2 (24.08 %) dimension was determined primarily by set of bands in the spectral range from 1002 cm^{-1} to 895 cm^{-1}, with the band at 980 cm^{-1} having the greatest influence on this dimension. The last dimension, PC3 (11.42 %) was primarily determined by bands at 1002 cm^{-1}, 1540 cm^{-1}, 1640 cm^{-1}, and 1720 cm^{-1}. The 3D plot of all dimensions indicated that samples of control BC were a significant distance from samples of modified BC (Fig. 4D). Further, samples of M1 and M2 were in similar region of space, in contrast to M5, M6, and M7. Finally, samples from M3 and M4 occupied the regions overlapping with previously listed modification variants.

Similar spectra were observed in the case of samples modified with CA but without the use of CAT (no additional bands specific for carbonyl group appeared) (Fig. S12). Meanwhile, in the case of samples modified with the use of just the individual CATs, without the addition of CA, the spectral region from to 1800 cm^{-1} to 800 cm^{-1} did not differ from the spectrum of unmodified BC. This indicates the key role of the CATs combined with CA, in both the process of macro- and microstructure modification and, to a lesser extent, in the introduction of functional groups, includingformation of ester bonds.

3.4. Water-related properties and density of modified BC and efficiency of crosslinking reaction

The biomedical applications of BC as a wound dressing material depend primarily on its water-related properties, including water

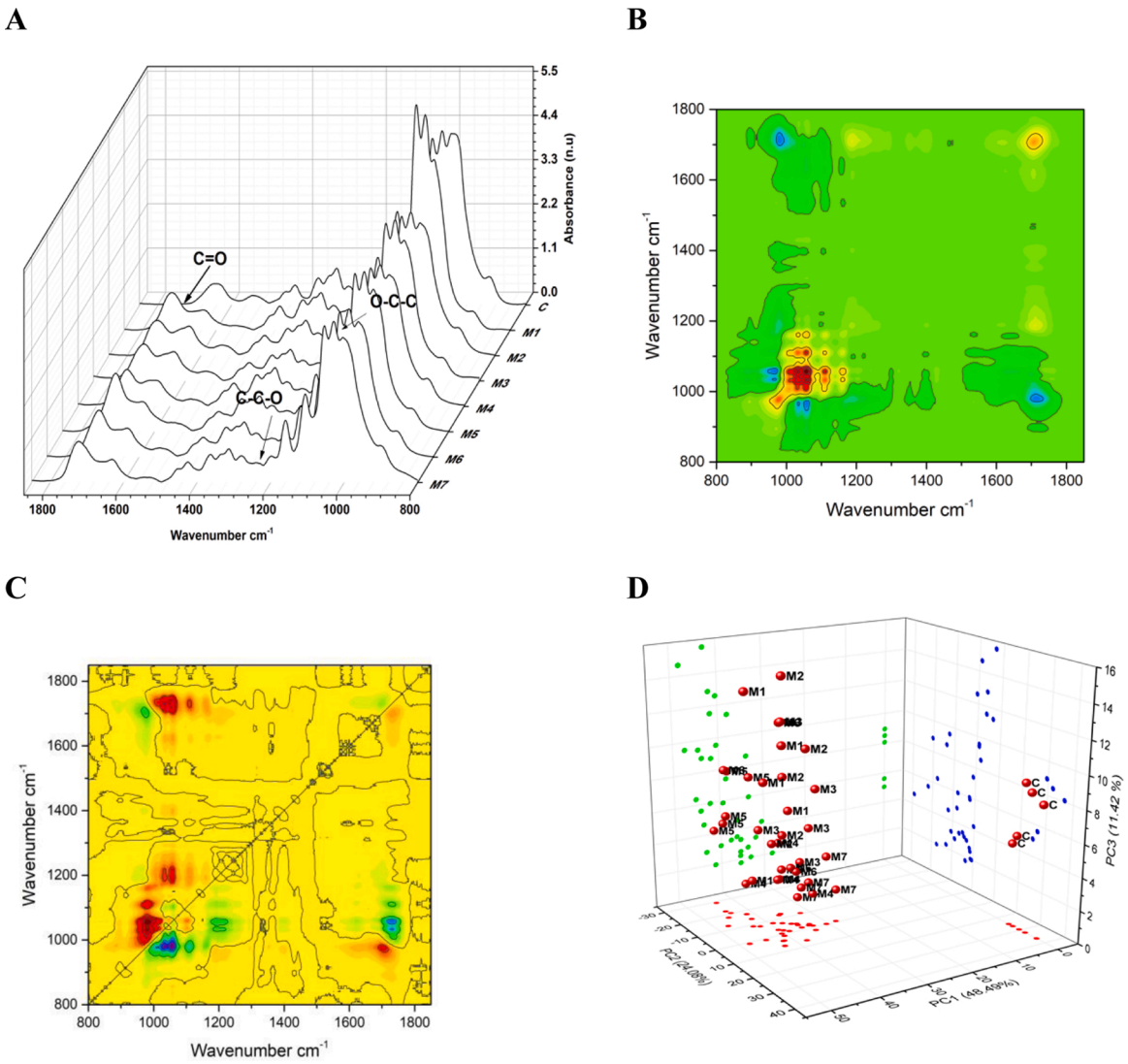

Fig. 4. Result of ATR-FTIR analysis of crosslinked BC. **A** - 1D spectra region form 1800 cm^{-1} to 800 cm^{-1} of modified BC with different CATs; **B** - 2D – COS synchronous spectra, **C** - 2D – COS asynchronous spectra; **D** - Result of PCA with plotted PC1, PC2 and PC3 dimensions. C – control BC sample; M1-M7 – modified BC samples.

swelling and holding capacity, as well as water release rate. These properties depend, in turn, on pore size, pore volume, and surface area (Gatenholm & Klemm, 2010; Zaborowska et al., 2010). The high liquid absorption capacity of BC is the primary driver for its application as a wound dressing material. Its excellent swelling capabilities not only help to absorb and sequestrate wound exudate, but also make dressing non-adherent to the wound bed. This latter feature is of paramount importance, not only with regard to easy, painless dressing removal, but also because it prevents the destruction of fresh, fragile granulation tissue (Portela, Leal, Almeida, & Sobral, 2019; Ul-Islam, Khan, & Park, 2012). Further, the adsorption capacity of BC for liquids and small particles also makes it an appropriate material for impregnation with antimicrobials; therefore, it can act as a drug carrier with excellent wound healing potential (de Oliveira Barud et al., 2016). As previously explained, fully swollen or completely dried BC is significantly devoid of ability to absorb fluids, including wound exudate. However, we hypothesized that following crosslinking, dried BC would have preserved micro-fibrous structure and maintained high water absorption capacity.

The results presented in Fig. 5A, (statistical analysis of these results is presented in Tab. S11) showed that after 60 min of incubation with water, SR (%) values for M1-M3 did not exceed twice the SR (%) value for the non-modified (control) BC. These samples were characterized by a slow, gradual increase in the SR (%) values over the entire period of 60 min and continued to absorb water up to 24 h (Fig. 5B, statistical analysis of these results is presented in Tab. S12). After this time, SR (%) values for samples M1-M3 were more than 3 times higher compared to the control BC, for which no increase of absorption was observed between 60 min and 24 h incubation in water. The highest values of SR (%) were obtained for M3: approx. 2 times higher after 60 min and over 5 times higher after 24 h of incubation in water, as compared to control BC. For M4 after both 60 min and 24 h, the values of SR (%) for did not differ statistically from the control BC – after 24 h incubation in water only a slight increase in this parameter as was noticed. Interestingly, over the 60 min incubation, the M5 material exhibited a much higher increase in SR (%) than the control (by over 4-fold), as well as other modified BC samples. However, after further incubation in water no additionally water sorption was observed (the difference between 60 min and 24 h did not exceeded 1%), meaning that the maximum water absorption capacity of the M5 was reached after 60 min. Somewhat similarly, M6 samples were also characterized by a much higher value of the SR (%) after 60 min, as compared to the control (by over 3 fold). The swelling capacity of M6 after 60 min was lower only than for the M5, although the dynamics of water absorption was comparable between these two modifications. After 24 h, similarly to the M5, only a

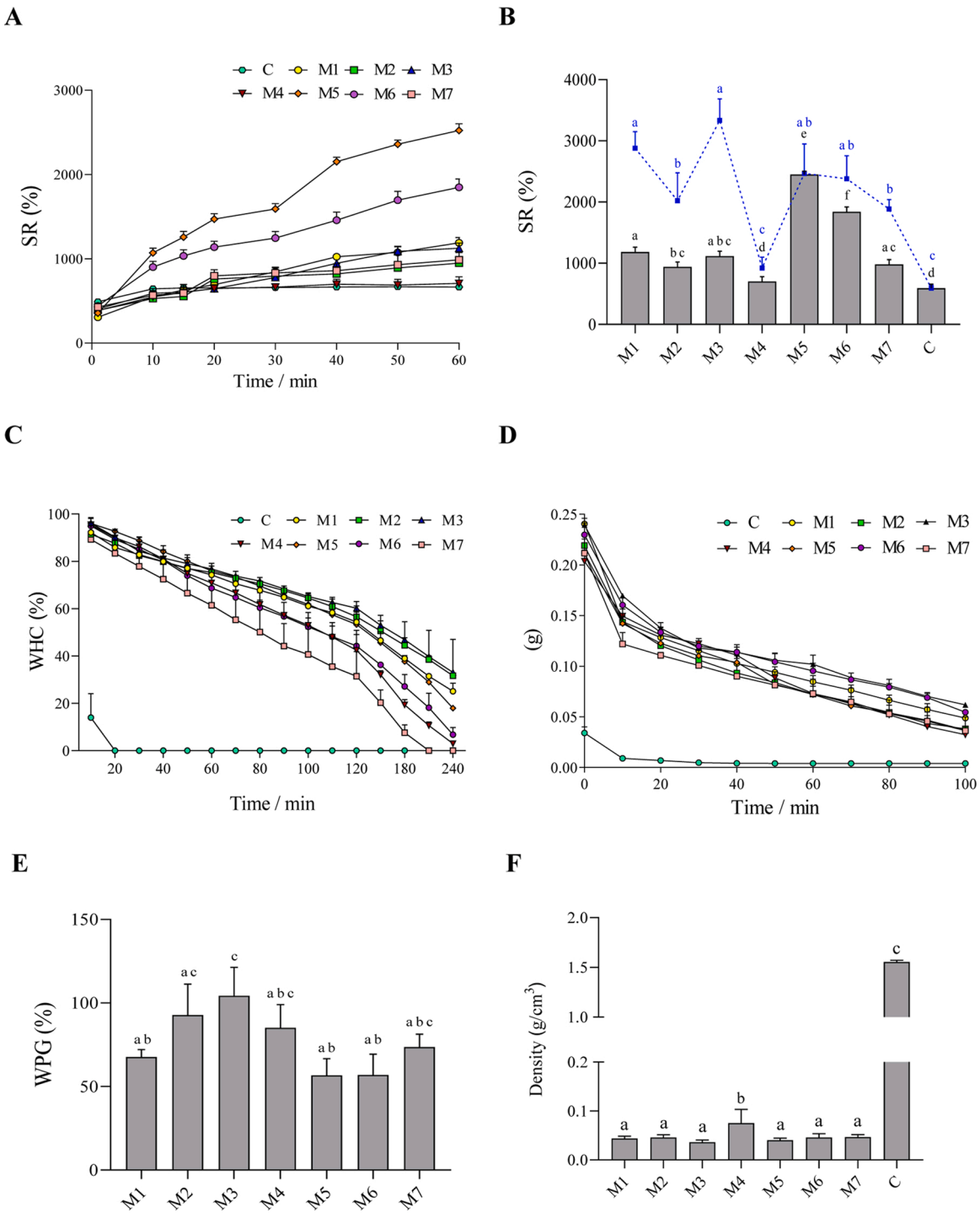

Fig. 5. **A -** Swelling ratio (%) of BC samples over 60 min of incubation in water; **B -** Swelling ratio (%) of BC samples after 60 min of incubation in water (column) compared to swelling ratio (%) after 24 h of incubation in water (line); **C -** Water holding capacity (%) of BC samples over 60 min of incubation at 37 °C; **D -** Weight loss of BC samples during centrifugation at 200 *g*; **E -** Efficiency of BC crosslinking reaction; **F -** Density of BC samples.

slight increase in SR (%) of M6 was found. The maximum SR (%) values of M6 were comparable with the M2 and M5. The sample modified with the reference catalyst (CAT7) after 60 min showed a degree of water absorption only slightly higher than the control. However, after 24 h, the SR (%) value for M7 sample was over 3 times higher as compared to the control. However, the maximum degree of water sorption for M7 was lower as compared to the M1 and M3 (approx. 1.5 and 1.7 times, respectively, with the differences being statistically significant), as well as to the M5 and M6 (approx. 1.3 times for both, but the differences were not statistically significant).

As previously discussed, the BC chemical modifications studied here relied on citric acid (CA) crosslinking, facilitated by the presence of the different CATs, which released gas during the reaction with CA and as a result of thermal decomposition. This co-effect resulted in the formation of additional space within the cellulose matrix, enabling the high water sorption capacity of the modified BC samples after drying. At the same time the micro-porosity of the BC pellicles was unchanged, as compared to the unmodified control BC (Fig. S8, Fig. S9B). As expected, using either reaction components individually (20 % CA or 10 % CAT), yielded materials without porosity and with poor SR values after 24 h, even

lower than for control, dried BC (see Supplementary data, section 1.5).

The water molecules are trapped physically on the surface and inside the BC matrix consisting of reticulated fibrils (Mohite & Patil, 2014). The more space is available between the BC fibrils, the more water can penetrate and adsorb onto the material. Further, the increase in the number and size of the pores results in an increase in surface area. The greater the surface area and the larger the pore size, the greater the capacity of BC to absorb water and swell (Guo & Catchmark, 2012; Meftahi et al., 2010).

Furthermore, in addition to an increase in swelling capacity, it was found that all of the modified BC samples demonstrated a significant increase in their capacity to hold water (Fig. 5C, Tab. S13). This favorable water holding capacity of modified BC can also be ascribed to the differences in microstructure obtained as a result of the crosslinking proceeding with the different CATs. For unmodified BC, total water loss was observed after just 20 min of incubation at 37 °C. Among modified samples, the quickest water loss was observed for the BC crosslinked with CAT7 (the WHC (%) reached 0 after 210 min). Samples M4 and M6 lost almost all absorbed water after 240 min, while BC modified with CATs 1–3 and CAT5 still held over 25 % of their initial water volume after 240 min. Overall, the highest water retention (33 %) after 240 min was observed for M3.

It has been demonstrated previously that the amount of water lost from BC matrix to the outer environment depends on the arrangement of cellulose microfibrils (Shezad et al., 2010). As demonstrated by Kaewnopparat, Sansernluk, and Faroongsarng (2008), only 10 % of the water in BC behaves like free bulk water. Thus, most of the water molecules within the cellulose are, more or less tightly, bound to the cellulose. According to Ul-Islam et al. (2012a), BC samples with smaller pore sizes are able to retain water longer than those with larger pores. This effect is due to the closely arranged microfibrils binding water molecules more efficiently, with the stronger hydrogen bonding interactions (Ougiya, Watanabe, Matsumura, & Yoshinaga, 1998; Shah, Ha, & Park, 2010).

Here, the gas released during the crosslinking reactions was responsible for the formation of numerous air cavities. It can be assumed that water filled up these spaces during WHC (%) analyses and exerted a pressure on the surrounding elastic cellulose fibrils, decreasing the pore sizes. This may explain why the modified samples M1-M3 in particular, absorbed water slowly, reaching maximum values of SR (%) after 24 h (Fig. 5B). These assumptions are consistent with the observations from our previous work, in which we used vegetable oil to *in situ* modify BC (Żywicka et al., 2018). There, we hypothesized that during the process of BC development, cellulose compressed oil droplets and had an impact on the overall morphology of the environment, with oil droplets adapting a funnel-type form within the cellulose. However, at the same time, the hydrophobic oil pushed back on the BC matrix, consisting of >98 % of water, thus compressing the fibrils and changing the overall morphology of the material.

Similarly, during centrifugation (200 *g*) the modified BC samples also held water significantly longer, as compared to the unmodified BC (Fig. 5D, Tab. S14). The control sample released all absorbed water after 30 min of centrifugation, whereas all of the modified BC, regardless of the CAT used, retained more than 50 % of the initial amount of water after 30 min of the process, and still retained some water after 100 min. However, in contrast to the experiment carried out with drying at 37 °C, in this experiment we did not observe any differences between BC samples modified using different CATs. Most likely, the forces affecting the material during centrifugation are much higher than those during evaporation at only modestly elevated temperature, and therefore the relatively small differences in the morphology of modified BC pellicles were not sufficient.

Finally, the efficiency of the crosslinking reactions in the presence of various CATs, expressed as weight percent gain (WPG (%)), was greatest for CAT3 (Fig. 5E). This result was also correlated with these samples having the highest SR (%) value (Fig. 5B). However, it should be noted that the M3 samples reached the maximum degree of water absorption after 24 h. Similar crosslinking efficiency was also found for reactions carried out in the presence of CAT2 and CAT4 (differences were statistically insignificant), but for the M4 modification, despite relatively similar efficiency, water absorption capacity was markedly lower (SR (%) values for M4 were comparable to unmodified control BC). Interestingly, the M5 and M6 modifications, which reached the maximum degree of water absorption after 60 min, had efficiency nearly 50 % lower than CAT3 and with similar efficiency as with CAT1. Because the highest efficiency of the crosslinking reaction was observed in the presence of CAT3 (mixture of CAT1 and CAT2), it can be stated that the use of catalyst combinations can be more efficient with regard to the parameters discussed than application of single catalyst. However, the results obtained using CAT4, 5 and 6 showed these mixtures decrease the crosslinking efficiency, but still yield desired water sorption properties. Therefore, it cannot be stated that the effectiveness of the crosslinking reaction, measured as the weight gain of the material due to the binding of citric acid (CA) molecules, correlates with the values of SR (%) coefficient. However, this data does support our hypothesis that the primary role of the crosslinking agent is to stiffen the BC structure, while the increased ability to absorb water is essentially caused by the gases released during thermal decomposition of CATs and the reaction of CA with CATs.

These considerations were supported by assessment of the densities of the modified BC pellicles (Fig. 5F, Tab. S15). The M3 and M5 samples, previously characterized by the greatest ability to absorb water, had the lowest densities (over 30 times lower as compared to control). Interestingly, M3 and M5 yielded BCs that differed in the kinetics of water absorption and the effectiveness of the crosslinking reactions were not equal, but these differences were not reflected in their densities. In contrast, the M4 samples displayed the highest density (over 2 times higher as compared to other modifications) and absorbed the lowest volume of water. It is noteworthy, that the density of dried, unmodified BC was more than 15 times greater than M4, but no differences in water absorption were observed between these samples. Further, the efficiency of the crosslinking reaction in the presence of CAT4 did not differ statistically from reactions carried out with CAT3 and CAT5. However, these results can be explained the differences in the macro- and microstructures of these samples. As described above, CAT4 yielded high degree of BC delamination with lack of structural continuity – the air spaces were torn apart. Thus, these results confirm the key role of the formation of air spaces within BC layers, in improving the sorption properties of modified BC biomaterials, as well as the role of the crosslinking agent, which stiffens the BC structure and prevents it from collapsing during drying.

Data are presented as mean ± standard error of the mean (SEM); values with different letters are significantly different ($p < 0.05$): a, b, c, d – statistically significant differences between the analyzed parameters. C – control BC sample; M1-M7 – modified BC samples.

3.5. Assessment of cytotoxicity of modified BC

In line with use in wound dressings (surface contact with the body), we screened for cytotoxicity of modified BC pellicles *in vitro* by performing both extract and direct contact tests based on ISO 10993-5, as well as by assessing L929 fibroblast viability after culture on BC pellicles for 5 days using confocal microscopy. No evidence of cytotoxicity of any of the modified BC samples was observed (Fig. 6A, Fig. S13, Tab. S17) after 24 h of culture of L929 fibroblasts with extracts (24 h, complete growth media, 37 °C). This indicated that no leachable toxic contaminants, such as residual citric acid or catalyst, were present, confirming that the purification protocol following modification was sufficient. Next, in the direct contact assay, where modified BC pellicle samples were placed on top of sub-confluent L929 cells in culture, we observed robust growth and normal cell morphology for control BC as well as M2, M3, M5, and M7 samples, while the cell density was somewhat reduced for the case of M1 and M6. However, for the case of M4 cell morphology

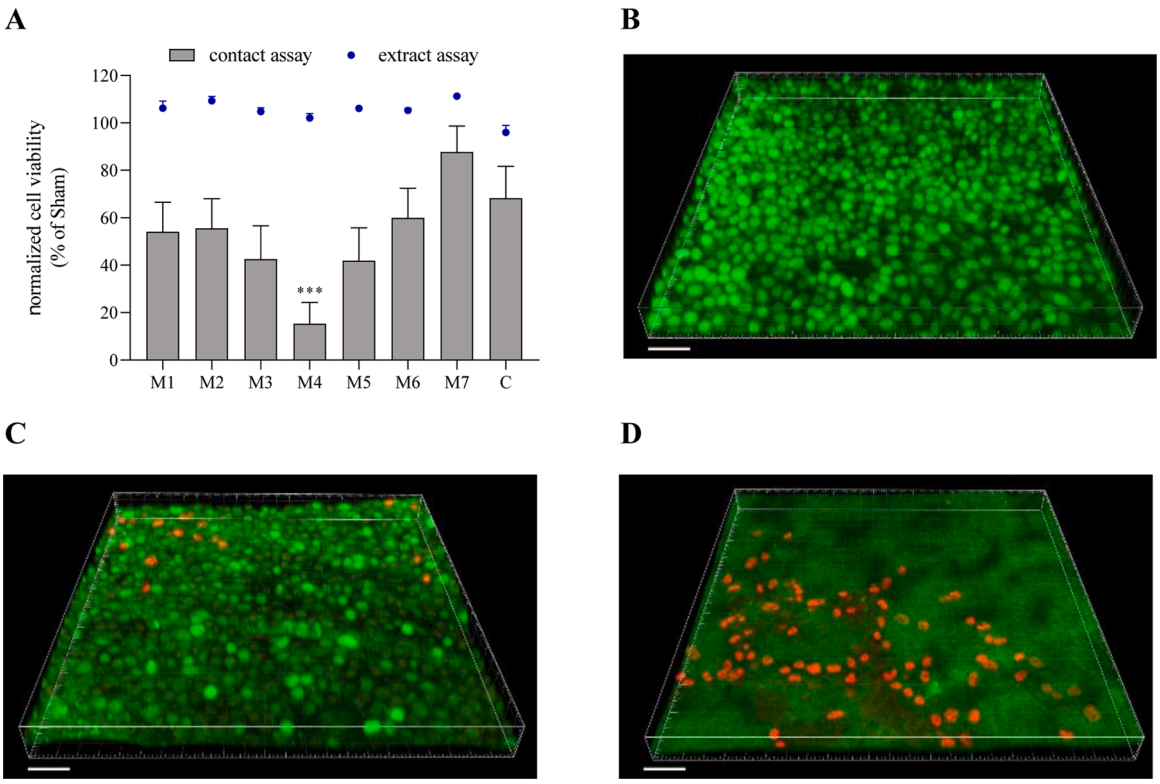

Fig. 6. A - Viability data for all tested BC samples normalized to Sham (CellCrown insert for direct contact or complete growth medium for extract) obtained with resazurin viability assay; data are presented as mean ± standard error of the mean (SEM); the '***' mark indicates statistical differences between modifications and control ($p < 0.001$). **B-D** - Visualization of L929 fibroblasts cultured on control BC (B), M2 (C) and M4 (D) samples, respectively. Green color – nuclei in live fibroblasts (SYTO-9 staining, bright green) and exposed cell-free cellulose (dim green); red color – nuclei in dead fibroblasts (propidium iodide). Scale bar =50 μm. C – control BC sample; M1-M7 – modified BC samples (For interpretation of the references to colour in this figure legend, the reader is referred to the web version of this article.).

was markedly altered and cell density was significantly lower (Fig. S14, Tab. S18, Tab. S19). These microscopic observations were confirmed with the resazurin viability assay (Fig. 6A). Overall, these results are consistent with the previous reports from Gyawali et al. (2010); El Fawal et al. (2018), that indicated that citric acid was safe and a nontoxic crosslinker for biomedical applications.

Finally, confocal microscopy (Fig. 6B–D) of L929 cells cultured on modified BC pellicles for 5 days confirmed presence of live (green) fibroblasts on the surface of control BC, and showed predominantly live cells on M2 sample, with only a few dead cells. However, for the case of M5, we observed a considerable amount of dead (red) fibroblasts. Thus, this additional experiment aimed at evaluating cytotoxicity risk over a longer time period directly confirmed the results the extract and direct contact assays. Overall, the promising results obtained thus far motivate further studies of these materials as wound dressings in animals, aimed at assessing risk of sensitization and irritation.

To summarize, we tested and optimized a series of crosslinking reactions of BC using citric acid and various catalysts. Based on the collected results, we can single out the use of a mixture of disodium phosphate and sodium bicarbonate (1:1 mass ratio, CAT3) as the most promising, yielding a SR (%) value of over 3300 % after 24 h. To our knowledge, the highest reported SR (%) value for modified BC was described by Figueiredo et al. (2015). As reported by these authors, BC samples were impregnated with 2-aminoethyl methacrylate (AEM) with and without addition of N, N-methylenbis(acrylamide) (MBA), yielding SR (%) values reaching 6200 %. However, in contrast to our modifications, the composites obtained by those authors were not dried before the swelling analyses. Additionally, while our highest SR (%) was lower as compared to the materials obtained by Figueiredo et al. (2015), our crosslinking approach has several advantages. First of all, the use of an additional polymer, AEM, filled the porous BC structure completely, which may reduce gas exchange, a feature crucial for wound closure (Sulaeva, Henniges, Rosenau, & Potthast, 2015). Meanwhile, our M3-modified BC had preserved structure, including micro-porosity, and also contained numerous air cavities (see Fig. 3, Fig. S3, Fig. S8). Another approach to obtain material with high sorption property described in the literature involves the use BC as a substrate for the production of hydrogel. As an example, Pandey, Amin, Igbal, Ahmad, and Abeer (2013) obtained a hydrogel composed of BC and acrylamide that was characterized by SR (%) at neutral pH of 2500 %, while Amin, Ahmad, Halib, and Ahmad (2012) synthetized BC/acrylic acid-based hydrogel with a SR (%) value exceeding 5000 %. However, to obtain these hydrogels, the BC had to be dissolved or ground into powder, and the synthesis process consisted of many stages. Additionally, it is important to consider the environmental health and safety aspects: acrylamide, acrylic acid and aminoethyl methacrylate are known to have toxic and irritant properties, limiting their applicability (in accordance with the guidelines of the National Institute for Occupational Safety and Health). Meanwhile, our M3 modification was obtained with use of simple and safe citric acid and disodium phosphate/sodium bicarbonate mixture. This fact cannot be neglected, especially considering the potential application of this BC material in wound dressings, where it will be in contact with fragile, exposed wound tissue.

To further assess the significance of our findings, we compared the swelling capacity of our M3-modified BC material, displaying the most promising features, to that of modern commercial dressings dedicated to highly exuding wounds. We found that the water swelling capacity of M3 (SR (%) over 3300 %) was greater than that displayed by the market-leading modern dressings, e.g. polyacrylate fiber superabsorbent

dressing [http://www.urgomedical.com] with SR (%) of 1400 % or hydrofiber superabsorbent dressing [https://www.convatec.com] with SR (%) of 2600 % (Tab. S20-S22).

4. Conclusions

The use of citric acid crosslinker combined with the various inorganic CATs provides an important novel technique yielding significant improvement in BC water-related properties after drying. Our work and findings are of high impact for virtually all types of biomedical applications of BC. The compounds we tested as catalysts, with the exception of sodium hypophosphite, have never been used for crosslinking of BC and only disodium phosphate was previously used as bridging agent in general. We demonstrated that the formation of air cavities within the BC matrix played a key role in facilitating the absorption of large volumes of water. At the same time, our novel BC biomaterials released the absorbed water slowly, thanks to preserved micro-porous structure. These properties make the developed BC materials very promising for applications as wound dressings not only for highly-exuding, but also dry wounds (Alvarez, Phillips, Menzoian, Patel, & Andriessen, 2012; Stephen-Haynes, Callaghan, Wibaux, Johnson, & Carty, 2014). Moisture is an essential factor of wound healing process. However, excessive amount of exudate can macerate the wound bed, degrading peri-wound skin and growth factors, and increase the risk of inflammation (Adderley, 2010). Our modified BC, in the dry state, may be applied as a "super-absorbent" wound dressing for exudate sequestration and maintenance of moisture levels appropriate for wound healing. Additionally, prior to drying, it is easy to envision loading the modified BC matrix with anti-inflammatory or antimicrobial drugs to be released as the dressing absorbs exudate. Existing cellulose-based dressings saturated with such aqueous antimicrobial as polyhexanide (PHMB) or octenidine (OCT) are already used in the clinical setting (Moritz et al., 2014; Wild et al., 2012).

We are aware that findings presented in this work are of *in vitro* character and require thorough testing in animal models before clinical trials may be performed. However, it should be emphasized that the application of cellulose-based dressings for purpose of exudate management is presently one of the most promising directions in chronic wound treatment (Keshk, 2014; Lin et al., 2013). Bearing this in mind, the excellent results for materials using our novel modification, as compared to commercial dressings, indicate that the developed method has great potential to facilitate the design of innovative new dressings dedicated to chronic wound management.

CRediT authorship contribution statement

Daria Ciecholewska-Juśko: Conceptualization, Methodology, Formal analysis, Writing - original draft, Investigation, Visualization. **Anna Żywicka:** Writing - review & editing. **Adam Junka:** Investigation, Writing - review & editing. **Radosław Drozd:** Investigation, Writing - review & editing. **Peter Sobolewski:** Investigation, Writing - review & editing. **Paweł Migdał:** . **Urszula Kowalska:** Investigation. **Monika Toporkiewicz:** Investigation. **Karol Fijałkowski:** Conceptualization, Methodology, Formal analysis, Project administration, Investigation, Writing - original draft, Visualization, Supervision.

Declaration of Competing Interest

The authors report no declarations of interest.

Acknowledgements

This work was supported by the National Centre for Research and Development in Poland (grant number LIDER/011/221/L-5/13/NCBR/2014))and the National Science Center in Poland (grant number 2017/27/B/NZ6/02103).

Appendix A. Supplementary data

Supplementary material related to this article can be found, in the online version, at doi:https://doi.org/10.1016/j.carbpol.2020.117247.

References

Adderley, U. J. (2010). Managing wound exudate and promoting healing. *British Journal of Community Nursing, 15*(Sup1), S15–S20.

Alvarez, O. M., Phillips, T. J., Menzoian, J. O., Patel, M., & Andriessen, A. (2012). An RCT to compare a bio-cellulose wound dressing with a non-adherent dressing in VLUs. *Journal of Wound Care, 21*(9), 448–453.

Amin, M. C. I. M., Ahmad, N., Halib, N., & Ahmad, I. (2012). Synthesis and characterization of thermo-and pH-responsive bacterial cellulose/acrylic acid hydrogels for drug delivery. *Carbohydrate Polymers, 88*(2), 465–473.

Bernard, F. X., Barault, C., Juchaux, F., Laurensou, C., & Apert, L. (2005). Stimulation of the proliferation of human dermal fibroblasts *in vitro* by lipidocolloid dressing. *Journal of Wound Care, 14*(5), 215–220.

Bielecki, S., Kalinowska, H., Krystynowicz, A., Kubiak, K., Kołodziejczyk, M., & De Groeve, M. (2012). Wound dressings and cosmetic materials from bacterial nanocellulose. In M. Gama, P. Gatenholm, & D. Klemm (Eds.), *Bacterial nanocellulose: A sophisticated multifunctional material, perspectives in nanotechnology* (pp. 157–174). Boca Raton, Florida: CRC Press.

Brodie, J., & Godber, J. (2001). Bakery processes, chemical leavening agents. *Kirk-othmer encyclopedia of chemical technology*. New York: John Wiley & Sons, Inc.. https://doi.org/10.1002/0471238961.0308051303082114.a01.pub2

Brown, E. E., Laborie, M. P. G., & Zhang, J. (2012). Glutaraldehyde treatment of bacterial cellulose/fibrin composites impact on morphology, tensile and viscoelastic properties. *Cellulose, 19*, 127–137.

Chang, S. T., Chen, L. C., Lin, S. B., & Chen, H. H. (2012). Nano-biomaterials application: Morphology and physical properties of bacterial cellulose/gelatin composites via crosslinking. *Food Hydrocolloids, 27*(1), 137–144.

Crépy, L., Miri, V., Joly, N., Martin, P., & Lefebvre, J. M. (2011). Effect of side chain length on structure and thermomechanical properties of fully substituted cellulose fatty esters. *Carbohydrate Polymers, 83*(4), 1812–1820.

de Oliveira Barud, H. G., da Silva, R. R., da Silva Barud, H., Tercjak, A., Gutierrez, J., Lustri, W. R., et al. (2016). A multipurpose natural and renewable polymer in medical applications: Bacterial cellulose. *Carbohydrate Polymers, 153*, 406–420.

Dhaliwal, K., & Lopez, N. (2018). Hydrogel dressings and their application in burn wound care. *British Journal of Community Nursing, 23*(Sup9), S24–S27.

Dissemond, J., Assadian, O., Gerber, V., Kingsley, Kramer, A., Leaper, D. J., et al. (2011). Classification of wounds at risk and their antimicrobial treatment with polihexanide: A practice-oriented expert recommendation. *Skin Pharmacology and Physiology, 24*(5), 245–255.

Drozd, R., Rakoczy, R., Konopacki, M., Frąckowiak, A., & Fijałkowski, K. (2017). Evaluation of usefulness of 2DCorr technique in assessing physicochemical properties of bacterial cellulose. *Carbohydrate Polymers, 161*, 208–218.

Egger, G., & Dixo, J. (2014). Beyond obesity and lifestyle: A review of 21st century chronic disease determinants. *BioMed Research International, 2014*, Article 731685. https://doi.org/10.1155/2014/731685

El Fawal, G. F., Abu-Serie, M. M., Hassan, M. A., & Elnouby, M. S. (2018). Hydroxyethyl cellulose hydrogel for wound dressing: Fabrication, characterization and *in vitro* evaluation. *International Journal of Biological Macromolecules, 111*, 649–659.

El-Saied, H., El-Diwany, A. I., Basta, A. H., Atwa, N. A., & El-Ghwas, D. E. (2008). Production and characterization of economical bacterial cellulose. *BioResources, 3*(4), 1196–1217.

Falanga, V. (2004). Wound bed preparation: Science applied to practice. In S. Calne (Ed.), *Wound bed preparation in practice* (pp. 2–5). London: MEP Ltd.

Feng, X., Xiao, Z., Sui, S., Wang, Q., & Xie, Y. (2014). Esterification of wood with citric acid: The catalytic effects of sodium hypophosphite (SHP). *Holzforschung, 68*(4), 427–433.

Figueiredo, A. R., Figueiredo, A. G., Silva, N. H., Barros-Timmons, A., Almeida, A., Silvestre, A. J., et al. (2015). Antimicrobial bacterial cellulose nanocomposites prepared by in situ polymerization of 2-aminoethyl methacrylate. *Carbohydrate Polymers, 123*, 443–453.

Fijałkowski, K., Żywicka, A., Drozd, R., Niemczyk, A., Junka, A. F., Peitler, D., et al. (2015). Modification of bacterial cellulose through exposure to the rotating magnetic field. *Carbohydrate Polymers, 133*, 52–60.

Frone, A. N., Panaitescu, D. M., Nicolae, C. A., Gabor, A. R., Trusca, R., Casarica, A., et al. (2020). Bacterial cellulose sponges obtained with green cross-linkers for tissue engineering. *Materials Science and Engineering C, 110*, Article 110740.

Frykberg, R. G., & Banks, J. (2015). Challenges in the treatment of chronic wounds. *Advanced Wound Care (New Rochelle), 4*(9), 560–582.

Gatenholm, P., & Klemm, D. (2010). Bacterial nanocellulose as a renewable material for biomedical applications. *MRS Bulletin, 35*(3), 208–213.

Gullo, M., La China, S., Falcone, P. M., & Giudici, P. (2018). Biotechnological production of cellulose by acetic acid bacteria: Current state and perspectives. *Applied Microbiology and Biotechnology, 102*(16), 6885–6898.

Guo, J., & Catchmark, J. M. (2012). Surface area and porosity of acid hydrolyzed cellulose nanowhiskers and cellulose produced by *Gluconacetobacter xylinus*. *Carbohydrate Polymers, 87*(2), 1026–1037.

Gyawali, D., Nair, P., Zhang, Y., Tran, R. T., Zhang, C., Samchukov, M., et al. (2010). Citric acid-derived in situ crosslinkable biodegradable polymers for cell delivery. *Biomaterials, 31*(34), 9092–9105.

Han, G., & Ceilley, R. (2017). Chronic wound healing: A review of current management and treatments. *Advances in Therapy, 34*(3), 599–610.
He, W., Ding, Y., Tu, J., Que, C., Yang, Z., & Xu, J. (2018). Thermal conversion of primary alcohols to disulfides via xanthate intermediates: An extension to the Chugaev elimination. *Organic & Biomolecular Chemistry, 16*(10), 1659–1666.
Järbrink, K., Ni, G., Sönnergren, H., Schmidtchen, A., Pang, C., Bajpai, R., et al. (2017). The humanistic and economic burden of chronic wounds: A protocol for a systematic review. *Systematic Reviews, 6*(1), 15.
Ji, B., Qi, H., Yan, K., & Sun, G. (2016). Catalytic actions of alkaline salts in reactions between 1, 2, 3, 4-butanetetracarboxylic acid and cellulose: I. Anhydride formation. *Cellulose, 23*(1), 259–267.
Kaewnopparat, S., Sansernluk, K., & Faroongsarng, D. (2008). Behavior of freezable bound water in the bacterial cellulose produced by *Acetobacter xylinum*: An approach using thermoporosimetry. *AAPS PharmSciTech, 9*(2), 701–707.
Keshk, S. M. (2014). Bacterial cellulose production and its industrial applications. *Journal of Bioprocessing & Biotechniques, 4*(2), 1.
Lê, S., Josse, J., & Husson, F. (2008). FactoMineR: A package for multivariate analysis. *Journal of Statistical Software, 25*(1), 1–18.
Lewis, R. J. (2004). *Sax's dangerous properties of industrial materials* (11th ed.). Hoboken (NJ): Wiley & Sons, Inc.. p. 3257.
Lin, S. P., Calvar, I. L., Catchmark, J. M., Liu, J. R., Demirci, A., & Cheng, K. C. (2013). Biosynthesis, production and applications of bacterial cellulose. *Cellulose, 20*(5), 2191–2219.
Lin, S. B., Hsu, C. P., Chen, L. C., & Chen, H. H. (2009). Adding enzymatically modified gelatin to enhance the rehydration abilities and mechanical properties of bacterial cellulose. *Food Hydrocolloids, 23*(8), 2195–2203.
Liu, D., Yuan, X., & Bhattacharyya, D. (2012). The effects of cellulose nanowhiskers on electrospun poly (lactic acid) nanofibers. *Journal of Materials Science, 47*(7), 3159–3165.
Meftahi, A., Khajavi, R., Rashidi, A., Rahimi, M. K., & Bahador, A. (2018). Preventing the collapse of 3D bacterial cellulose network via citric acid. *Journal of Nanostructure in Chemistry, 8*(3), 311–320.
Meftahi, A., Khajavi, R., Rashidi, A., Sattari, M., Yazdanshenas, M. E., & Torabi, M. (2010). The effects of cotton gauze coating with microbial cellulose. *Cellulose, 17*(1), 199–204.
Mohite, B. V., & Patil, S. V. (2014). Physical, structural, mechanical and thermal characterization of bacterial cellulose by G. Hansenii NCIM 2529. *Carbohydrate Polymers, 106*, 132–141.
Morita, S., & Ozaki, Y. (2004). Studies on Molecular Structure of Biocompatible Polymers by vibrational spectroscopy 1. ATR Spectra of Poly (2-hydroxyethyl methacrylate) (PHEMA). *Nippon Kagakkai Koen Yokoshu, 84*(2), 1191.
Moritz, S., Wiegand, C., Wesarg, F., Hessler, N., Müller, F. A., Kralisch, D., et al. (2014). Active wound dressings based on bacterial nanocellulose as drug delivery system for octenidine. *International Journal of Pharmaceutics, 471*(1-2), 45–55.
Noda, I. (2004). Advances in two-dimensional correlation spectroscopy. *Vibrational Spectroscopy, 36*(2), 143–165.
Ougiya, H., Watanabe, K., Matsumura, T., & Yoshinaga, F. (1998). Relationship between suspension properties and fibril structure of disintegrated bacterial cellulose. *Bioscience, Biotechnology and Biochemistry, 62*(9), 1714–1719.
Pa'e, N., Hamid, N. I. A., Khairuddin, N., Zahan, K. A., Seng, K. F., Siddique, B. M., et al. (2018). Effect of different drying methods on the morphology, crystallinity, swelling ability and tensile properties of nata de coco. *Sains Malaysiana, 43*(5), 767–773.
Pandey, M., Amin, M., Igbal, M. C., Ahmad, N., & Abeer, M. M. (2013). Rapid synthesis of superabsorbent smart-swelling bacterial cellulose/acrylamide-based hydrogels for drug delivery. *International Journal of Polymer Science*. https://doi.org/10.1155/2013/905471
Pandey, M., Mohamad, N., & Amin, M. C. I. M. (2014). Bacterial cellulose/acrylamide pH-sensitive smart hydrogel: Development, characterization, and toxicity studies in ICR mice model. *Molecular Pharmaceutics, 11*(10), 3596–3608.
Park, C. M., & Xian, M. (2015). Use of phosphorodithioate-based compounds as hydrogen sulfide donors. *Methods in Enzymology, 554*, 127–142.
Percival, S. L., Vuotto, C., Donelli, G., & Lipsky, B. A. (2015). Biofilms and wounds: An identification algorithm and potential treatment options. *Advanced Wound Care (New Rochelle), 4*(7), 389–397.
Picheth, G. F., Pirich, C. L., Sierakowski, M. R., Woehl, M. A., Sakakibara, C. N., de Souza, C. F., et al. (2012). Bacterial cellulose in biomedical applications: A review. *International Journal of Biological Macromolecules, 104*, 97–106.
Portela, R., Leal, C. R., Almeida, P. L., & Sobral, R. G. (2019). Bacterial cellulose: A versatile biopolymer for wound dressing applications. *Microbial Biotechnology, 12*, 586–610.
Pott, F. S., Meier, M. J., Stocco, J. G., Crozeta, K., & Ribas, J. D. (2014). The effectiveness of hydrocolloid dressings versus other dressings in the healing of pressure ulcers in adults and older adults: a systematic review and meta-analysis. *Revista Latino-Americana Enfermagem, 22*(3), 511–520.
Pratten, N. A. (1981). The precise measurement of the density of small samples. *Journal of Materials Science, 16*(7), 1737–1747.
Qi, H., Huang, Y., Ji, B., Sun, G., Qing, F. L., Hu, C., et al. (2016). Anti-crease finishing of cotton fabrics based on crosslinking of cellulose with acryloyl malic acid. *Carbohydrate Polymers, 135*, 86–93.
Rahman, M. R., Lai, J. C. H., Hamdan, S., Ahmed, A. S., Baini, R., & Saleh, S. F. (2013). Combined styrene/MMA/nanoclay cross-linker effect on wood-polymer composites (WPCs). *BioResources, 8*(3), 4227–4237.
Riss, T. L., Moravec, R. A., Niles, A. L., Duellman, S., Benink, H. A., Worzella, T. J., Minor, L., et al. (2016). In G. S (Ed.), *Assay guidance manual (internet)*. Bethesda (MD): Eli Lilly & Company and the National Center for Advancing Translational Sciences.
Ruka, D. R., Simon, G. P., & Dean, K. M. (2012). Altering the growth conditions of *Gluconacetobacter xylinus* to maximize the yield of bacterial cellulose. *Carbohydrate Polymers, 89*(2), 613–622.
Schilling, M., Bouchard, M., Khanjian, H., Learner, T., Phenix, A., & Rivenc, R. (2010). Application of chemical and thermal analysis methods for studying cellulose ester plastics. *Accounts of Chemical Research, 43*(6), 888–896.
Schneider, C. A., Rasband, W. S., & Eliceiri, K. W. (2012). NIH Image to ImageJ: 25 years of image analysis. *Nature Methods, 9*(7), 671–675.
Schrecker, S. T., & Gostomski, P. A. (2005). Determining the water holding capacity of microbial cellulose. *Biotechnology Letters, 27*(19), 1435–1438.
Shah, N., Ha, J. H., & Park, J. K. (2010). Effect of reactor surface on production of bacterial cellulose and water soluble oligosaccharides by *Gluconacetobacter hansenii* PJK. *Biotechnology and Bioprocess Engineering, 15*(1), 110–118.
Shao, W., Wu, J., Liu, H., Ye, S., Jiang, L., & Liu, X. (2017). Novel bioactive surface functionalization of bacterial cellulose membrane. *Carbohydrate Polymers, 178*, 270–276.
Shezad, O., Khan, S., Khan, T., & Park, J. K. (2010). Physicochemical and mechanical characterization of bacterial cellulose produced with an excellent productivity in static conditions using a simple fed-batch cultivation strategy. *Carbohydrate Polymers, 82*(1), 173–180.
Stephen-Haynes, J., Callaghan, R., Wibaux, A., Johnson, P., & Carty, N. (2014). Clinical evaluation of a thin absorbent skin adhesive dressing for wound management. *Journal of Wound Care, 23*(11), 532–542.
Stoyanov, A., & Miller, C. E. (2014). Cellulose fibers crosslinked with low molecular weight phosphorous containing polyacrylic acid and method U.S. Patent No. 8,722,797. Washington, DC: U.S. Patent and Trademark Office.
Sulaeva, I., Henniges, U., Rosenau, T., & Potthast, A. (2015). Bacterial cellulose as a material for wound treatment: Properties and modifications. A review. *Biotechnology Advances, 33*(8), 1547–1571.
Torres, F. G., Arroyo, J. J., & Troncoso, O. P. (2019). Bacterial cellulose nanocomposites: An all-nano type of material. *Materials Science and Engineering C, 98*, 1277–1293.
Ul-Islam, M., Khattak, W. A., Kang, M., Kim, S. M., Khan, T., & Park, J. K. (2013). Effect of post-synthetic processing conditions on structural variations and applications of bacterial cellulose. *Cellulose, 20*, 253–263.
Ul-Islam, M., Khan, T., & Park, J. K. (2012a). Water holding and release properties of bacterial cellulose obtained by in situ and ex situ modification. *Carbohydrate Polymers, 88*(2), 596–603.
Ul-Islam, M., Khan, T., & Park, J. K. (2012b). Nanoreinforced bacterial cellulose–montmorillonite composites for biomedical applications. *Carbohydrate Polymers, 89*(4), 1189–1197.
Vasconcellos, V., & Farinas, C. (2018). The effect of the drying process on the properties of bacterial cellulose films from *Gluconacetobacter hansenii*. *Chemical Engineering Transactions, 64*, 145–150.
Vowden, P., Bond, E., & Meuleneire, F. (2015). Managing high viscosity exudate. *Wounds International, 11*(1), 56–60.
Widsten, P., Dooley, N., Parr, R., Capricho, J., & Suckling, I. (2014). Citric acid crosslinking of paper products for improved high-humidity performance. *Carbohydrate Polymers, 101*, 998–1004.
Wild, T., Bruckner, M., Payrich, M., Schwarz, C., Eberlein, T., & Andriessen, A. (2012). Eradication of methicillin-resistant *Staphylococcus aureus* in pressure ulcers comparing a polyhexanide-containing cellulose dressing with polyhexanide swabs in a prospective randomized study. *Advances in Skin & Wound Care, 25*(1), 17–22.
Winter, G. D. (1962). Formation of the scab and the rate of epithelization of superficial wounds in the skin of the young domestic pig. *Nature, 193*, 293–294.
Yadie, Y., & Hu, H. (2015). A review on antimicrobial silver absorbent wound dressings applied to exuding wounds. *Journal of Microbial and Biochemical Technology, 7*, 228–233.
Yang, C. Q. (1991). FT-IR spectroscopy study of the ester crosslinking mechanism of cotton cellulose. *Textile Research Journal, 61*(8), 433–440.
Yang, C. Q. (2001). FTIR spectroscopy study of ester crosslinking of cotton cellulose catalyzed by sodium hypophosphite. *Textile Research Journal, 71*(3), 201–206.
Yang, C. Q., Chen, D., Guan, J., & He, Q. (2010). Cross-linking cotton cellulose by the combination of maleic acid and sodium hypophosphite. 1. Fabric wrinkle resistance. *Industrial & Engineering Chemistry Research, 49*(18), 8325–8332.
Ye, T., Wang, B., Liu, J., Chen, J., & Yang, Y. (2015). Quantitative analysis of citric acid/sodium hypophosphite modified cotton by HPLC and conductometric titration. *Carbohydrate Polymers, 121*, 92–98.
Young, R. A. (2002). Cross-linked cellulose and cellulose derivatives. *Textile Science and Technology, 13*, 233–281.
Zaborowska, M., Bodin, A., Bäckdahl, H., Popp, J., Goldstein, A., & Gatenholm, P. (2010). Microporous bacterial cellulose as a potential scaffold for bone regeneration. *Acta Biomaterialia, 6*(7), 2540–2547.
Żywicka, A., Junka, A. F., Szymczyk, P., Chodaczek, G., Grzesiak, J., Sedghizadeh, P. P., et al. (2018). Bacterial cellulose yield increased over 500% by supplementation of medium with vegetable oil. *Carbohydrate Polymers, 199*, 294–303.

International Journal of
Molecular Sciences

MDPI

Article

Potato Juice, a Starch Industry Waste, as a Cost-Effective Medium for the Biosynthesis of Bacterial Cellulose

Daria Ciecholewska-Juśko [1], Michał Broda [1,2], Anna Żywicka [1], Daniel Styburski [3], Peter Sobolewski [4], Krzysztof Gorący [4], Paweł Migdał [5], Adam Junka [6] and Karol Fijałkowski [1,*]

1 Department of Microbiology and Biotechnology, Faculty of Biotechnology and Animal Husbandry, West Pomeranian University of Technology, Szczecin, Piastów 45, 70-311 Szczecin, Poland; daria.ciecholewska@zut.edu.pl (D.C.-J.); michal.broda@zut.edu.pl (M.B.); anna.zywicka@zut.edu.pl (A.Ż.)
2 Pomeranian-Masurian Potato Breeding Company, 76-024 Strzekęcino, Poland
3 Laboratory of Chromatography and Mass Spectroscopy, Faculty of Biotechnology and Animal Husbandry, West Pomeranian University of Technology, Szczecin, Klemensa Janickiego 29, 71-270 Szczecin, Poland; daniel.styburski@zut.edu.pl
4 Department of Polymer and Biomaterials Science, Faculty of Chemical Technology and Engineering, West Pomeranian University of Technology, Szczecin, Piastów 45, 70-311 Szczecin, Poland; psobolewski@zut.edu.pl (P.S.); krzysztof.goracy@zut.edu.pl (K.G.)
5 Department of Environment, Hygiene and Animal Welfare, Faculty of Biology and Animal Science, Wroclaw University of Environmental and Life Sciences, Chełmońskiego 38C, 51-630 Wrocław, Poland; pawel.migdal@upwr.edu.pl
6 Department of Pharmaceutical Microbiology and Parasitology, Faculty of Pharmacy, Medical University of Wroclaw, Borowska 211a, 50-534 Wrocław, Poland; adam.junka@umed.wroc.pl
* Correspondence: karol.fijalkowski@zut.edu.pl; Tel.: +48-91-449-6714

Citation: Ciecholewska-Juśko, D.; Broda, M.; Żywicka, A.; Styburski, D.; Sobolewski, P.; Gorący, K.; Migdał, P.; Junka, A.; Fijałkowski, K. Potato Juice, a Starch Industry Waste, as a Cost-Effective Medium for the Biosynthesis of Bacterial Cellulose. *Int. J. Mol. Sci.* **2021**, *22*, 10807. https://doi.org/10.3390/ijms221910807

Academic Editor: Jeannine M. Coburn

Received: 10 September 2021
Accepted: 4 October 2021
Published: 6 October 2021

Abstract: In this work, we verified the possibility of valorizing a major waste product of the potato starch industry, potato tuber juice (PJ). We obtained a cost-effective, ecological-friendly microbiological medium that yielded bacterial cellulose (BC) with properties equivalent to those from conventional commercial Hestrin–Schramm medium. The BC yield from the PJ medium (>4 g/L) was comparable, despite the lack of any pre-treatment. Likewise, the macro- and microstructure, physicochemical parameters, and chemical composition showed no significant differences between PJ and control BC. Importantly, the BC obtained from PJ was not cytotoxic against fibroblast cell line L929 in vitro and did not contain any hard-to-remove impurities. The PJ-BC soaked with antiseptic exerted a similar antimicrobial effect against *Staphylococcus aureus* and *Pseudomonas aeruginosa* as to BC obtained in the conventional medium and supplemented with antiseptic. These are very important aspects from an application standpoint, particularly in biomedicine. Therefore, we conclude that using PJ for BC biosynthesis is a path toward significant valorization of an environmentally problematic waste product of the starch industry, but also toward a significant drop in BC production costs, enabling wider application of this biopolymer in biomedicine.

Keywords: bacterial cellulose; green technology; potato tuber juice; starch industry; waste product; biomaterials

1. Introduction

Bacterial cellulose (BC) is a versatile biopolymer, most effectively synthesized by non-pathogenic bacteria, *Komagataeibacter xylinus*. Similar to plant cellulose, BC is a linear polysaccharide consisting of β-1,4-glucan chains [1]. However, in contrast to plant-derived cellulose, BC is characterized by flexibility and high chemical purity. Moreover, it does not contain lignins, pectins, or hemicelluloses, the presence of which significantly prolongs the purification process of cellulose from plants [2–4]. Additionally, BC has high mechanical strength and water holding capacity owing to its dense fiber structure [5]. Importantly, BC can be considered biocompatible and non-toxic, as well as biodegradable, owing to the

activity of cellulase-producing organisms. As a result, BC is safe with regard to industrial applications, as well as for the environment [1,2]. Thanks to the above-mentioned unique properties, BC is versatile, having numerous and diverse applications: in food, cosmetics, pharmaceutical/biomedical, paper, and textile industries [1–7].

In the laboratory setting, BC production is a well-established, straightforward process. Given the proper media and growth conditions, bacteria eagerly produce cellulose membranes. Further, the whole process can be mechanized and, at least partially, automated. However, BC production on an industrial scale needs a reduction in costs due to the relatively expensive medium—typically Hestrin–Schramm (HS)—required for its biosynthesis. From an economic point of view, the less expensive the medium is, the higher the potential profits will be. In this regard, the optimal solution would be the use of industrial waste, which is dispensable for the manufacturer. Furthermore, this strategy has additional benefits from an environmental perspective, and therefore, repurposing waste products represents added value. In this context, Kurosumi et al. examined the possibility of effective BC production (up to 6 g/L of dry BC weight) from various waste fruit juices from oranges, pineapples, apples, grapes, and Japanese pears [8]. However, to obtain a high yield of the BC, additional nitrogen sources (such as yeast extract) had to be introduced to the aforementioned juices. Otherwise, BC yields were more than 3 times lower. Lima et al. optimized the method of obtaining BC in static culture, using sisal juice (an agro-industrial residue) as a substrate to produce a culture medium supplemented with sugars and yeast extract [9]. Revin et al. showed that the use of wheat or whey decoction can enable up to 3 times higher BC yield after 3 days of biosynthesis under dynamic conditions, as compared with conventional media [10]. In turn, Kongruang proposed a way to reduce the cost of BC production by using coconut and pineapple juices (rich in proteins, carbohydrates, and microelements) [11]. However, again, these media had to be supplemented with yeast extract. For the same reasons, Li et al. investigated the possibility of using wastewater from the process of candied jujube production [12]. The results of their research have shown that such post-production water was inexpensive to obtain; however, it required acid pre-treatment in order to obtain sufficient glucose content. The 3 h hydrolysis at 80 °C resulted in a 58% higher glucose content in the raw material, which translated into a high BC yield. Other natural ingredients, reported by several research groups, included *hydrolysates of* corn stalks or wheat, rice husk pre-treated with enzymatic hydrolysis, fruit and vegetable peels [8,11,13–16]. Summarizing the above information, it can be concluded that the main issues with the application of natural or waste substrates are related to the mandatory pre-processing stage or insufficient nutritional content. Both of these issues may significantly increase the total cost and extend the BC production process.

With these aspects in mind, we turned our attention to the potato industry. Potatoes are vegetables with high nutritional value and their extensive cultivation in Eastern Europe, China, and India translates into high availability and low price throughout the year cycle [17]. At the same time, the potato agro-industry generates substantial waste. Recently, Abdelraof et al. described their efforts to utilize potato peel waste for obtaining substrates for BC biosynthetic media [18]. To our knowledge, this is the only report concerning the use of potatoes or potato waste to produce BC. However, the processing of potato peels in order to obtain sufficient sugar content also required the use of acidic hydrolysis, with additional reagents, and high energy consumption (the hydrolysis process was carried out at a temperature of 100 °C). As a result, the potential industrial applicability and cost-effectiveness of this approach are limited.

In our approach, we selected potato tuber juice (PJ), another significant potato agro-industrial waste product. The most prominent producer is the starch industry, which in the European Union produces over 10 million tons of starch and starch derivatives, and more than 5 million tons of proteins and fibers each year [19]. During the manufacture of a single ton of potato starch, approximately 3.5 tons of PJ waste is produced. Further, the proper management of PJ and other post-production waste is a significant and unresolved technological problem for this industry [20,21]. Given the growing challenges presented by

climate change and other global environmental problems, the proper management of potato agro-industrial waste should be considered a key public policy target for governments and the private sector. Thus far, only the use of potato wastewater to irrigate agricultural fields has been explored; however, it creates problems with soil clogging, loss of water permeability, and water eutrophication [22].

Therefore, the goal of the current study was to investigate if PJ can be used as the medium for BC synthesis. We compared the yield, morphology, chemical composition, sorption properties, mechanical strength, and cytotoxicity of BC obtained from PJ-based cultures with those in a dedicated HS medium. In this fashion, we demonstrate an environmentally friendly strategy toward valorizing a major agro-industrial waste product and the possibility of a significant drop in costs related to BC synthesis, which should correlate with the wider application of this biopolymer in a wide range of industrial branches, including biomedicine.

2. Results and Discussion

2.1. Characterization of PJ Medium

In the current study, we used potato tuber juice (PJ) as a culture medium for BC biosynthesis. Importantly, the PJ was obtained in the same way as during the industrial production of starch. Further, the PJ medium required no pre-treatment process or any additional supplementation with nutrient sources, with the exception of the addition of 1% (*v*/*v*) ethanol. Ethanol is typically supplemented into HS media because it is a stimulating/initiating factor for BC biosynthesis by *K. xylinus* [7].

The lack of necessity of supplementing PJ with additional nutrients arises from the high content of various, easily absorbed nutrients present in potato tubers. While starch is the main component of the dry mass of potatoes (approx. 2%), tubers also contain (1) approx. 2% of proteins (a source of amino acids for bacterial cells), (2) 0.3 to 0.6% of sugars (a carbon source), and (3) a wide range of vitamins (e.g., A, C, B1, B2, B6) and minerals (e.g., potassium, phosphorus, magnesium, calcium, sodium, iron, zinc, and copper) [23,24]. Further, numerous other natural substances can also be found in potato tubers, including lipids, organic acids, polyphenols, fiber, and glycoalkaloids [24]. All of these compounds are also present in potato tuber juice [20,25]. Owing to its high nutritional value, potato tuber juice has already been considered a potential substrate for the *Lactobacillus casei* biomass production, as a food additive, or as an ingredient for functional food production [26,27]. The biological activity of PJ can also be of value; it can be used in the treatment of bowel diseases, reducing inflammatory symptoms [24].

In commercial media dedicated to BC production, such as HS, usually one specific sugar, typically glucose, is supplied as the carbon source [28,29]. However, in the case of media prepared from waste substrates, more complex composition and the presence of different sugars should be expected [16]. Our analysis of sugar content in PJ medium diluted with water in a 1:1 ratio showed the presence of sucrose (4.0 g/L), glucose (3.5 g/L), fructose (2.4 g/L), and starch (<0.1 g/L). Thus, in comparison with the HS medium, which has 20 g/L of glucose, the concentration of glucose alone and the total sugar content in the PJ medium were clearly lower (3.5 g/L and 9.9 g/L, respectively). However, our analysis indicated that diluted PJ contained a 25% higher concentration of proteins than HS medium (1.62 g/L v. 1.33 g/L). Finally, the initial pH of the PJ medium (6.08) was comparable to that of the HS medium (6.19)—neither required any further adjustment of this parameter.

2.2. Quantification of K. xylinus Cells and BC Yield

The kinetics of bacterial growth and the dynamics of BC production constitute crucial factors for adjusting the optimal time and conditions of bacterial cultivation. As a result, both have a major impact on the economic aspect of the bioprocess and its scale-up [18]. In Figure 1a, the growth curves of *K. xylinus* in HS and PJ media are presented. As can be seen, the growth curves are comparable. Importantly, for both media, the *K. xylinus* began to grow without a distinct lag phase, indicating that this microorganism did not require a

phase adjustment for replication. Molina-Ramirez et al. reported that the growth curve of cellulose-synthesizing bacteria correlates with an affinity for the carbon source [30]. Therefore, here, the affinity of *K. xylinus* American Type Culture Collection (ATCC) 53524strain for the carbon sources present in PJ medium was similar to glucose, the only carbon source in HS medium.

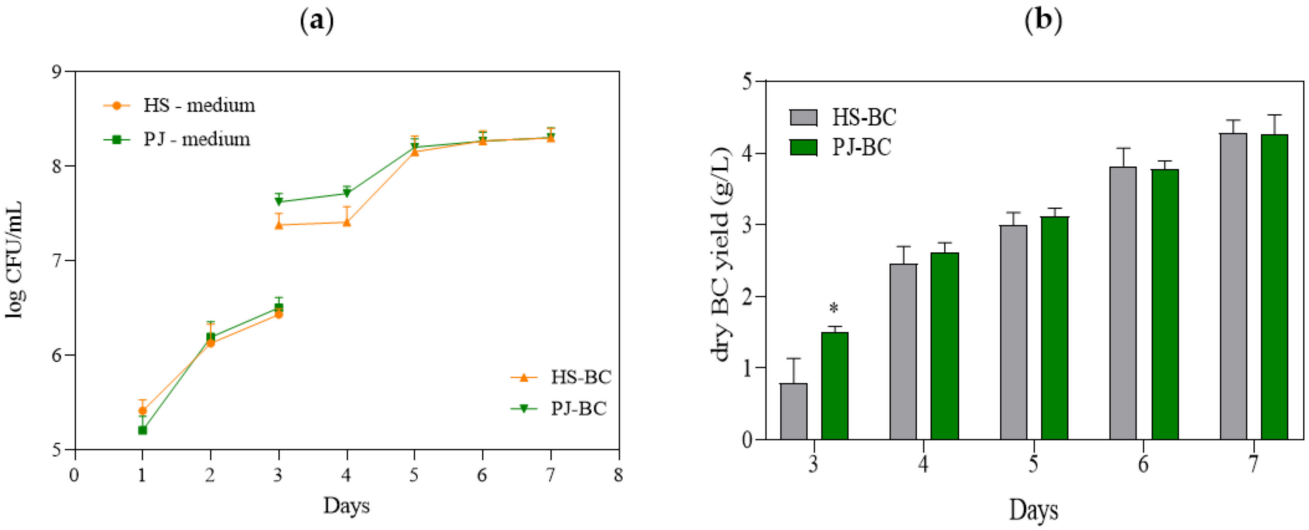

Figure 1. (**a**) Number of *K. xylinus* ATCC 53524cells in HS and PJ media and in BC pellicles; (**b**) yield of BC synthesized by *K. xylinus* ATCC 53524in HS and PJ media. Data are presented as a mean ± standard error of the mean (SEM). "*" indicates statistically significant difference between HS-BC and PJ-BC. HS—Hestrin–Schramm medium; PJ—potato juice medium; HS-BC—cellulose synthesized in HS; PJ-BC—cellulose synthesized in PJ.

The most important result of the present study was the yield of BC, which—despite the substantial differences in the chemical composition of PJ and HS media—was comparable (4.3 g/L) (Figure 1b). It can be noted that on the 3rd day of cultivation in the PJ medium, the BC yield was significantly higher. This is likely due to a corresponding higher bacterial cell density (Figure 1a).

As already mentioned, we supplemented both our developed PJ medium and the control HS medium with 1% (*v*/*v*) ethanol. The effect of ethanol on BC yield was comparable regardless of the type of medium (Table 1). Further, we show that for the most efficient production of the BC, potato juice should be diluted with water (Table 1). This result is of particular importance considering the industrial starch production process, in which, depending on the technology used, potato juice can be diluted with water during starch separation or purification [20].

Table 1. Dry BC yield of *K. xylinus* ATCC 53524depending on the degree of potato tuber juice dilution with water, the addition of ethanol, and starch content.

	Dry BC Yield (g/L)
PJ:water dilution ratio 1:1 *	4.26 ± 0.32
PJ:water dilution ratio 1:2	1.97 ± 0.11
PJ:water dilution ratio 2:1	2.27 ± 0.18
HS with 1% of ethanol	4.28 ± 0.18
HS without ethanol	2.04 ± 0.37
PJ with 1% of ethanol *	4.26 ± 0.32
PJ without ethanol	1.97 ± 0.53
non-centrifuged PJ medium containing starch solids (with 0.67 g/L starch content)	1.689 ± 0.143
PJ medium prepared with decantation and centrifugation (with <0.1 g/L starch content) *	4.26 ± 0.32

Data are presented as a mean ± standard error of the mean (SEM). * are the same conditions, presented separately for purposes of comparison.

2.3. The Changes in pH and Chemical Composition of PJ during Fermentation Process

It is well established that *K. xylinus* can metabolize a variety of sugars, regardless of the presence of the preferred one [31]. Glucose is one of the main components of the HS medium and is the primary substrate for the synthesis of cellulose (Figure 2a). It is incorporated in a four-step metabolic pathway. First, in the cytosol, glucose is converted to UDP-glucose by uridine–diphosphate–glucose pyrophosphorylase (EC 2.7.7.64, UDP-glucose pyrophosphorylase). In the next step, cellulose synthase (EC 2.4.1.12), located in the bacterial cell wall, catalyzes the polymerization of UDP-glucose to poly β-1-4 glucan [32]. However, although the BC is an anhydrous polymer of glucose, *K. xylinus* can use other monosaccharides and disaccharides, such as fructose, xylitol, sucrose, maltose, or lactose [33]. This feature is also apparent in the present study (Figure 2b). Importantly, the use of glucose as the primary carbon source for *K. xylinus* is associated with a drawback. These bacteria can readily convert glucose to gluconic acid, significantly decreasing the pH (<3.5) of the medium (Figure 2c). This, in turn, results in a decrease in intracellular pH. As a result, a high concentration of gluconic acid can change the activity of metabolic pathways responsible for BC synthesis, reducing the yield [34,35]. In contrast, when the culture medium contains fructose, *K. xylinus* cells convert this monosaccharide to acetic acid, which results in a lower drop in pH, as compared with gluconic acid [36]. Therefore, the use of PJ, containing a mixture of sugars, including fructose, with a relatively low concentration of glucose (3.5 g/L), compared with the HS (20 g/L), resulted in a significantly reduced concentration of gluconic acid produced during fermentation, and the pH remained above 4, even at the end to the fermentation process (Figure 2d). Meanwhile, in cultures with HS medium, the concentration of gluconic acid at the end of the fermentation process was approx. 10 times higher, and the pH dropped to 3.5 (Figure 2c,d).

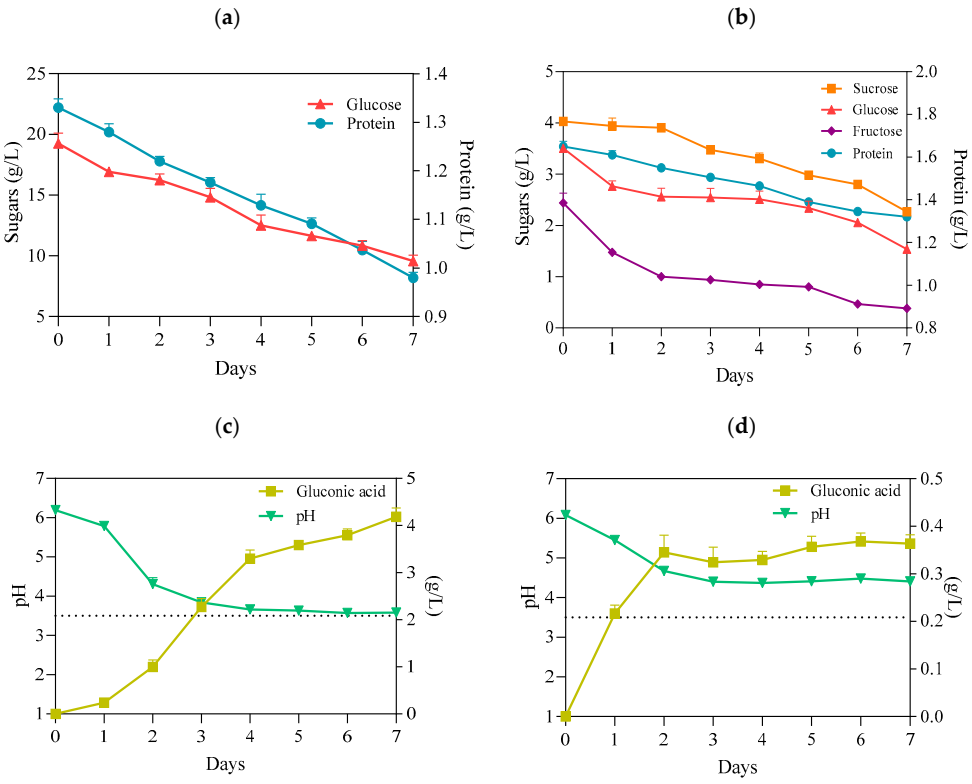

Figure 2. (**a**) Concentration of glucose and protein in HS medium; (**b**) concentration of sugars and protein in PJ medium; (**c**) pH and gluconic acid concentration in HS medium; (**d**) pH and gluconic acid concentration in PJ medium—all before and during BC biosynthesis by *K. xylinus* ATCC 53524. Data are presented as a mean ± standard error of the mean (SEM). critical pH value (3.5).

Nitrogen is a key component of proteins, making it necessary for cell metabolism. It comprises 8–14% of the dry cell mass of bacteria. Alongside carbon sources, proteinaceous nitrogen sources can also contribute to the enhancement of biomass production and BC synthesis, if suitably chosen [37]. The reports by several authors have shown that *K. xylinus* strains can utilize a wide range of protein and nitrogen sources, including casein hydrolysate, peptone, corn steep liquor, yeast extract, glutamate, soybean meal, glycine, and ammonium sulfate [7,37]. Likewise, in our present study, we observed that, although PJ and HS media differed in terms of qualitative and quantitative protein content, protein consumption during the BC biosynthesis process was similar (0.33 g/L v. 0.35 g/L) (Figure 2a,b).

The present study also confirmed that the starch was not metabolized during the BC biosynthesis process, as its concentration, 0.67 g/L, in media did not change during the cultivation of *K. xylinus*. Further, when using non-centrifuged PJ, containing starch solids, BC yield significantly decreased (Table 1).

2.4. The Role of Bacterial Strain and Presence of Sugars on BC Yield

The process of BC synthesis by bacterial cells is multilevel and includes many, tightly connected, metabolic pathways. A recent phylogenetic study of *Komagataeibacter* strains with defined genomes suggests that there is high variability in the structure of the pathways involved in BC synthesis [36]. The differences in structure and number of cellulose synthase operons in the genomes of *Komagataeibacter* strains are also considered the main reason behind inter-species differences in BC productivity and response to cultivation conditions [32,38]. Therefore, ideally, the culture medium used to produce BC should be adapted to the specific bacterial strain prior to the fermentation process [36,38]. On the other hand, considering the results reported by other authors related to the optimization of the culture medium, it can be noted that culture media with a more complex composition, particularly in terms of carbon and nitrogen sources, are more universal and result in relatively high yields of BC regardless of the bacterial strain used [7,30]. For this reason, we also aimed to determine whether the PJ medium can be considered universal for the cultivation of different *K. xylinus* strains. In four out of the eight tested strains (Figure 3a), BC yield using PJ medium was equivalent to HS medium. The variation in these results confirmed that BC production efficiency is strain dependent and closely related to the carbon source preference of the particular strain [31]. The role of intra-species variability in the effectiveness of synthesis of various biological-derived products, including BC, has been broadly discussed in the relevant literature [39–42]. Therefore, to enable replication and comparison with similar experiments by other research teams, we deliberately focused on the ATCC reference strains of *K. xylinus*.

Further, in order to determine which of the carbon sources present in the PJ plays a crucial role in the high BC yield, we prepared HS media supplemented with glucose, fructose, sucrose, or a combination of these sugars at the same concentrations as in PJ. The results showed that all of the sugars present in the PJ medium were metabolized and converted into BC by the *K. xylinus* ATCC 53524 strain (Figure 3b). The lowest BC yield was obtained when only a single sugar was present in the medium. Higher BC yields were observed for glucose–fructose and glucose–sucrose combinations. However, the highest BC yield (4.27 g/L) was obtained for the combination of glucose, fructose, and sucrose, which reflected the composition of the main sugars present in the PJ (Figure 2b v. Figure 3b). These results are in good agreement with previous studies that showed that the use of a combination of several different carbon sources in one medium resulted in substantially higher BC yields, as compared with the medium containing only a single one [43,44]. Further, among the reported carbon sources, glucose, fructose, and mannitol have been the best for BC production. One possible explanation for this is that cellulose-producing bacteria are able to convert structural glucose isomers (e.g., fructose) or the precursors of glucose (e.g., mannitol) into glucose [45]. An alternate sugar utilization strategy involves enzymatic cleavage of disaccharides to obtain glucose, which can explain

why some bacterial strains have better BC production efficiency via sucrose or lactose utilization [31,37,45]. Clearly, there is no single pattern among cellulose-producing bacteria, and the selection of the most appropriate carbon sources for a given strain is crucial for efficient BC production [45,46].

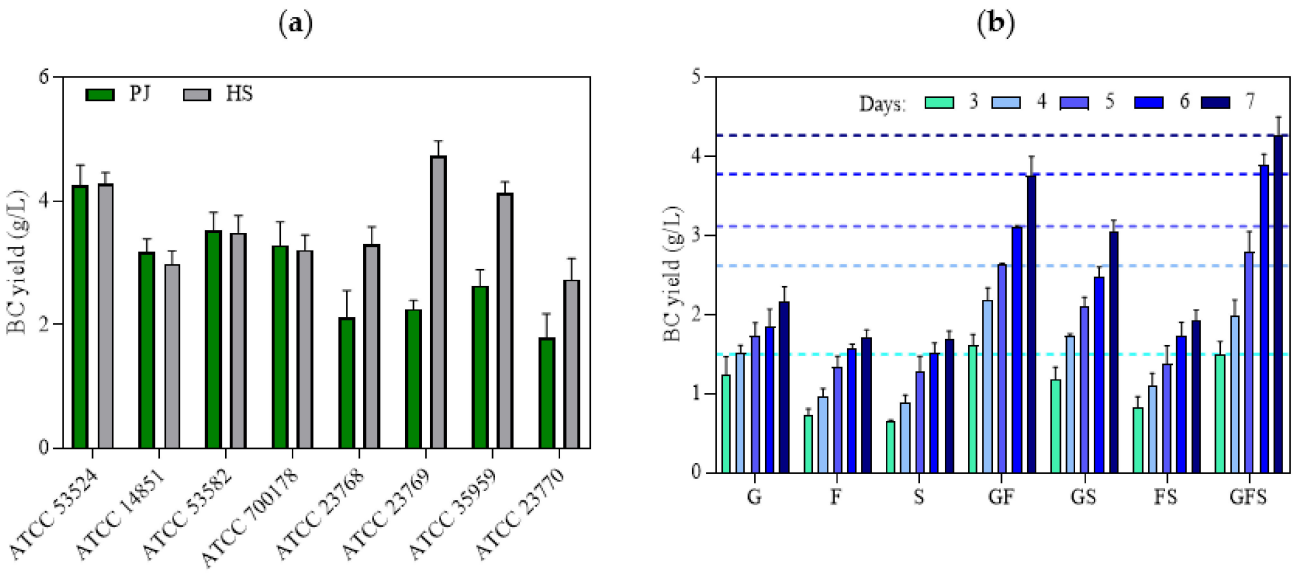

Figure 3. (**a**) BC yields of different *K. xylinus* strains in PJ and HS media after 7 days of cultivation; (**b**) BC yields of *K. xylinus* ATCC 53524 in HS medium with the addition of sugars at the same concentration as in PJ medium in the following days of cultivation. Data are presented as a mean ± standard error of the mean (SEM): G—glucose; F—fructose; S—sucrose. Horizontal lines in (**b**) indicate the BC yield of *K. xylinus* ATCC 53524 in PJ medium in the following days of cultivation.

2.5. Physicochemical Properties of BC Obtained from Potato Tuber Juice Medium

2.5.1. Macro- and Microstructure

Macromorphological assessment of PJ-BC indicated that it has a homogenous, smooth surface with no visible residues of the culture medium. In fact, the micromorphology was similar to the typical micromorphology of mature BC synthesized in the HS medium (Figure 4a,b,d,e). Likewise, the microstructure of PJ-BC was similar to that of HS-BC (Figure 4c,f) and was consistent with that described in the literature [47]. These observations are particularly important given that the PJ medium used is typically a waste product. A frequent issue encountered with the use of other agro-industrial wastes, such as fruit and vegetable peels or juices (besides the previously discussed issues of pre-processing and/or insufficient nutritional content), is the high content of artifacts, solids, and/or pigments present in the raw substrates. These will then also be present in the medium and then also in the BC obtained.

In order to assess the potential advantage of PJ over the other natural ingredient-based media, we prepared media from other food/agro-industry waste (potato peels, orange peels, beetroots, and apples) in the same fashion as the PJ media. We noted that, in terms of transparency, the PJ medium was comparable to the HS medium (Supplementary Figure S1). Further, for the case of PJ, there were fewer solids that had to be removed prior to the BC production. As was anticipated, the colors of the media prepared from the beetroots, apples, and even potato peels were also reflected in the pigmentation of the BC pellicles (Figure 5). This necessitated a longer purification process, as compared with the BC obtained from cultures in PJ or HS media (Figure 6). In the case of the BC obtained from an orange-peel-based medium, the yellow pigment was removed in the first stage of purification. However, in this case, the relative ease of pigment removal was likely due to the reduced thickness of the obtained cellulose membrane and its amorphous structure, which lowers its potential industrial applicability. In the case of other fruit-based media,

some residues of the fruits were tightly bound to the BC and remained, even after the purification process (Figure 7). In contrast, none of these issues were observed when the PJ medium was used for BC synthesis.

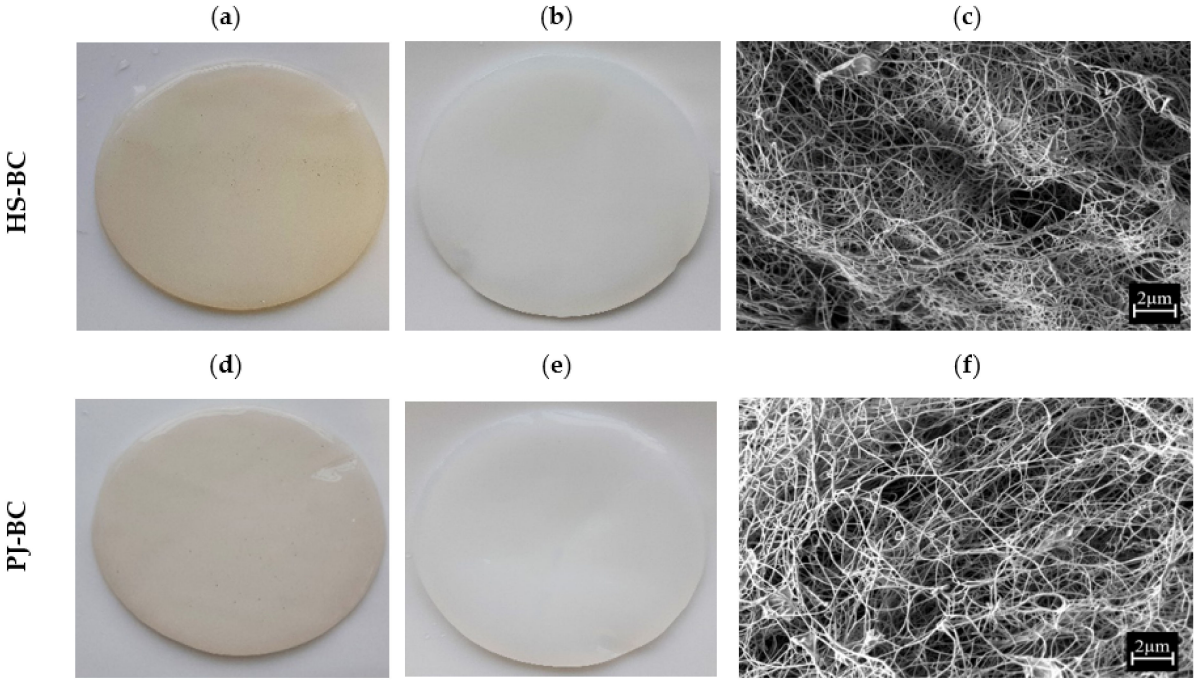

Figure 4. Macromorphology of BC from *K. xylinus* ATCC 53524: (**a**,**d**) before purification; (**b**,**e**) after purification; (**c**,**f**) micromorphology of BC from *K. xylinus* ATCC 53524 after purification, magnification 10,000× (SEM, Auriga 60, Zeiss, Oberkochen, Germany).

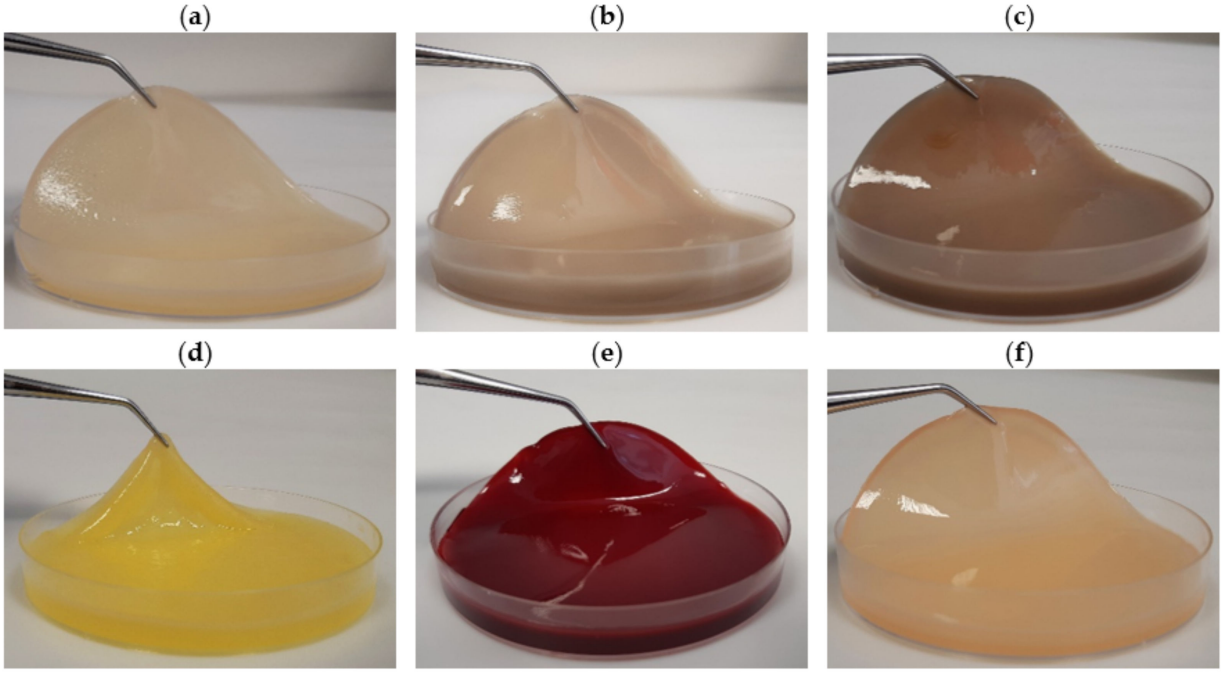

Figure 5. BC obtained from *K. xylinus* ATCC 53524 using (**a**) HS and natural ingredients-based media prepared from (**b**) potato juice, (**c**) potato peels, (**d**) orange peels, (**e**) beetroots, and (**f**) apples.

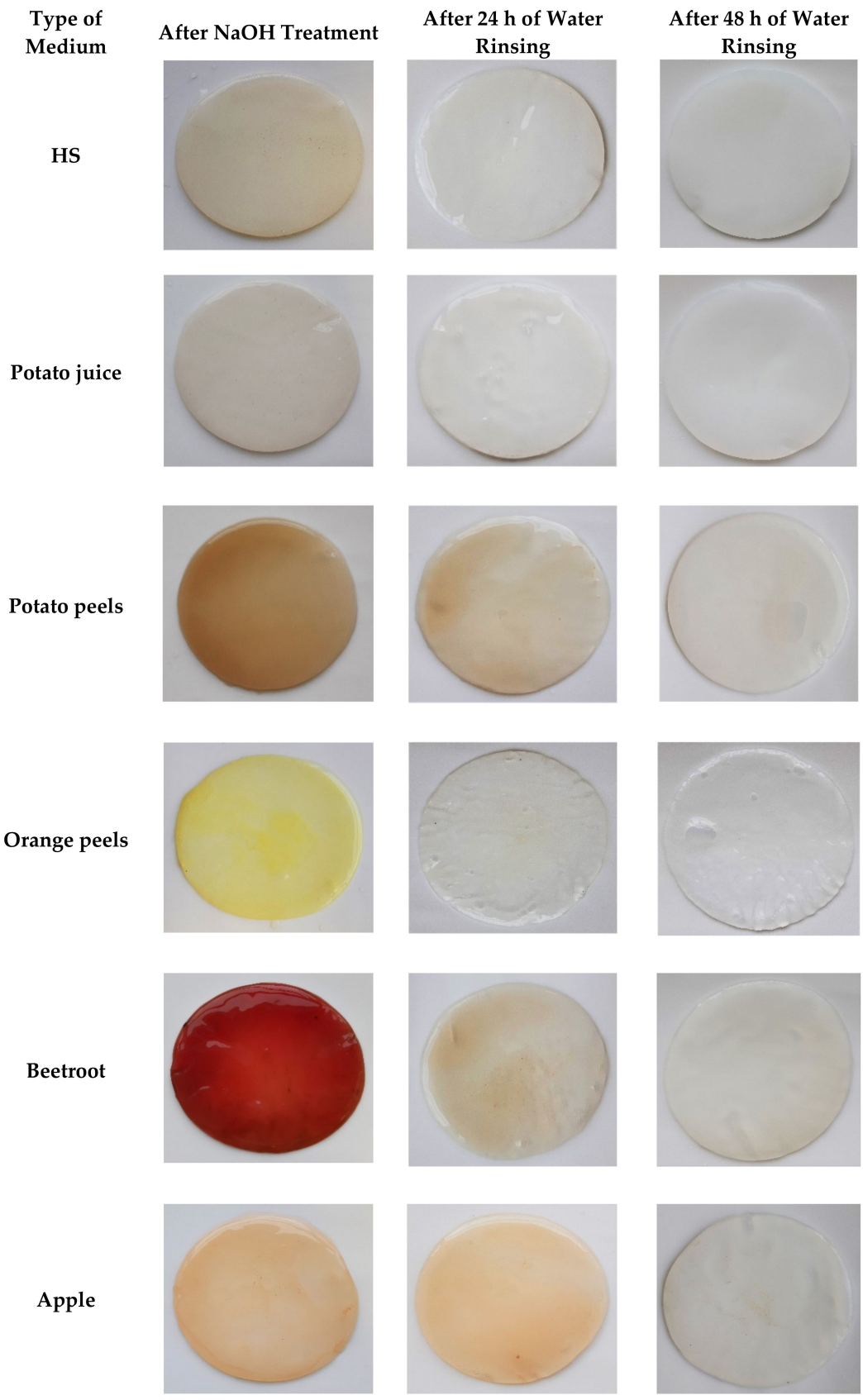

Figure 6. BC obtained from *K. xylinus* ATCC ATCC 53524 in HS and natural ingredients-based media in subsequent stages of purification.

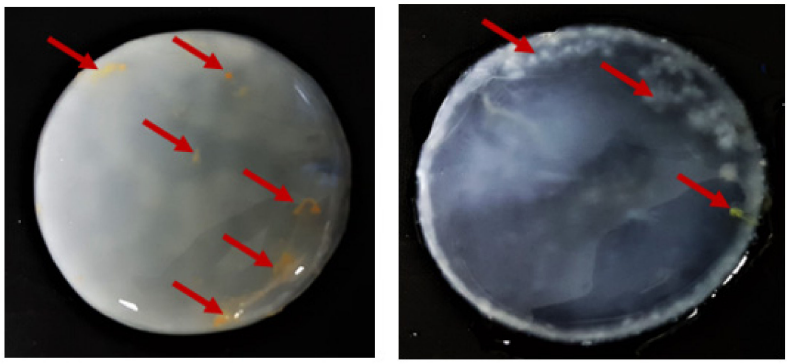

Figure 7. Purified BC from *K. xylinus* ATCC 53524 synthesized using natural (fruit) ingredients-based media. Red arrows indicate residues fragments (hard-to-remove impurities) of fruits bound in the BC membrane.

2.5.2. Analysis of ATR-FTIR Spectra

To further compare the BC obtained from PJ medium cultures to those in HS, we used infrared spectroscopy to examine chemical composition and crystallinity. The ATR-FTIR spectra of both HS-BC and PJ-BC exhibited all of the characteristic adsorption bands of cellulose functional groups (Supplementary Figure S2) that have been previously reported by other authors [48,49]. In all of the spectra, a pair of closely located bands at 710 cm^{-1} and 750 cm^{-1} was clearly visible and could be assigned to Iα and Iβ of BC microfibril allomorphs. All of the BC samples, regardless of the medium used, displayed a relatively high content of the Iα fraction (Table 2). Importantly, the use of the PJ medium did not influence the crystallinity indexes of the obtained BC, as compared with using HS. All of the samples exhibited high values of I.C. I1430/900. Likewise, the second crystallinity index, calculated as a ratio between the absorbance of the bands at 1370 cm^{-1} (CH bending) and 2900 cm^{-1} (CH and CH_2 stretching) was also similar, regardless of the medium used.

Table 2. Selected parameters of BC pellicles synthesized by *K. xylinus* ATCC 53524 in HS and PJ media.

	SR	WHC	EB	TS
HS-BC	299 ± 33	3.70 ± 1.24	20.0 ± 3.67	2.00 ± 0.26
PJ-BC	298 ± 33	4.07 ± 1.45	19.80 ± 3.28	2.05 ± 0.23
	Iα fraction	$I.C.1_{1370/2900}$	$I.C.2_{1430/900}$	ρ
HS-BC	0.44 ± 0.013	1.62 ± 0.21	1.04 ± 0.06	1.55 ± 0.02
PJ-BC	0.45 ± 0.018	1.57 ± 0.27	1.10 ± 0.11	1.49 ± 0.07

Data are presented as a mean ± standard error of the mean (SEM). SR—swelling ratio (%); WHC—water holding capacity after 8 min at 60 °C (%); EB—elongation at break (%); TS—tensile strength (MPa); ρ—density of BC (g/m^3).

2.5.3. Water-Related Properties, Density, and Mechanical Properties of BC

For many applications, the water-related properties can be considered to be the most important features of BC, because they determine its absorption capacity and ability to retain and release liquid. Overall, our results (Table 2, Supplementary Figure S3) indicated that water-related parameters were comparable for both BC membranes, regardless of the medium used for their production. There were no statistically significant differences between the results of the total swelling ratio and water holding capacity. Likewise, regardless of culture medium, we observed no significant differences in density nor tensile mechanical properties (Table 2).

In summary, all of the obtained results were in good agreement with values reported in the literature for typical, unmodified BC [50]. In this context, it should be noted that the physicochemical properties of BC are influenced by many factors, such as the cultivation conditions and time, in addition to the composition of the culture medium [51,52].

Therefore, the lack of any negative impact of PJ medium ingredients on BC properties is of paramount value for its future applications. This is of particular importance in the case of biomedical applications, such as wound healing materials, in which especially both BC liquid capacity and mechanical properties play essential roles [51,53].

2.6. BC Cytotoxicity Screening

BC has numerous potential biomedical applications including use as a biomaterial in tissue engineering, wound healing, and drug delivery [1,2]. In this context, it is important to note that BC is considered non-toxic. Therefore, it was important to confirm that BC obtained from PJ medium cultures was also not cytotoxic. We conducted extract and direct contact in vitro cytotoxicity assays, based on ISO 10993-5. In the extract tests, we observed robust growth of L929 cells exposed to all extracts. None of the tested materials resulted in viability below 70%, the threshold for cytotoxicity according to ISO 10993-5 (Figure 8a). There was no difference between PJ-BC and HS-BC. A similar trend was also observed in the direct contact assay. Importantly, the results of the viability assay were directly confirmed using fluorescence microscopy, with only live (stained green) cells observed (Figure 8b). Likewise, the morphology of L929 cells was not altered by either BC (Supplementary Figure S4). The results are in good agreement with our previous studies on BC-based materials [54]. However, we cannot compare our results with the BC obtained other by-product or waste media [10,11,16], because cytotoxicity studies are not (yet) a standard research practice in this context. We conclude that, from a cytotoxicity standpoint, the BC obtained from the PJ medium is equivalent to that obtained from conventional culture, making it suitable for biomedical applications.

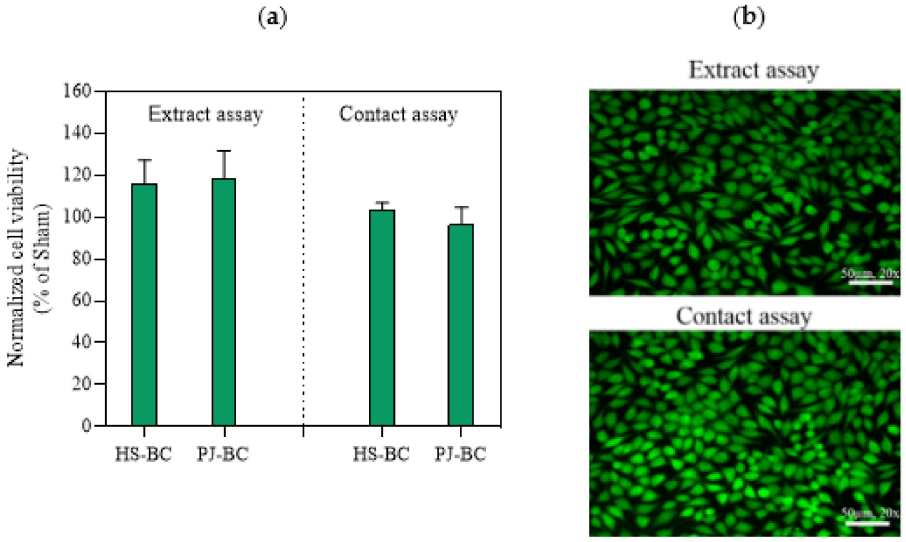

Figure 8. (**a**) L929 fibroblast viability data, as a percentage of the sham; (**b**) fluorescence live/dead visualization of L929 fibroblasts exposed PJ-BC for 24 h (extract and direct contact) and stained with Syto 9 (green, live) and propidium iodide dyes (red, dead). Data are presented as mean ± standard error of the mean (SEM); HS-BC—BC biosynthesized in HS medium; PJ-BC—BC biosynthesized in PJ medium.

2.7. The In Vitro Activity of PJ-BC and HS-BC Soaked with Antimicrobial against Two Species of Opportunistic Pathogens

The use of BC for preparing primary wound dressings is one of the most thoroughly investigated and promising applications of this biopolymer in medicine. BC features flexibility, biocompatibility, and favorable water properties, thereby meeting the most crucial criteria and expert guidelines for modern dressings designed to treat chronic wounds. The relatively easy-to-perform introduction of locally active antiseptic into BC provides an additional promising avenue for chronic wound treatment. In fact, a number

of studies have shown a high level of eradication of wound pathogens by antiseptic molecules released from BC, both in vitro and in vivo [54–58]. Further, an increasing number of such antiseptic-containing BC dressings are commercially available and applied in clinical practice [59]. Thus, we aimed to confirm that BC obtained from PJ media was also suitable in this context. We soaked PJ-BC and HS-BC with a modern antiseptic product (Octenisept®), containing octenidine dihydrochloride as the active ingredient, and assessed the antimicrobial activity against two species of opportunistic wound pathogens (*S. aureus* and *P. aeruginosa*) using a modification of the standard disk-diffusion assay. We observed no differences in the zones of growth inhibition, as a result of the octenidine released from PJ-BC or HS-BC (Figure 9). Thus, given the significantly lower cost of PJ-based medium, as compared with that of conventional HS medium, the overall advantage of the PJ-BC obtained here is clear. We conclude that PJ medium, particularly obtained as a waste from the potato starch industry, offers a cost-effective path toward broader and more common application of BC in biomedicine.

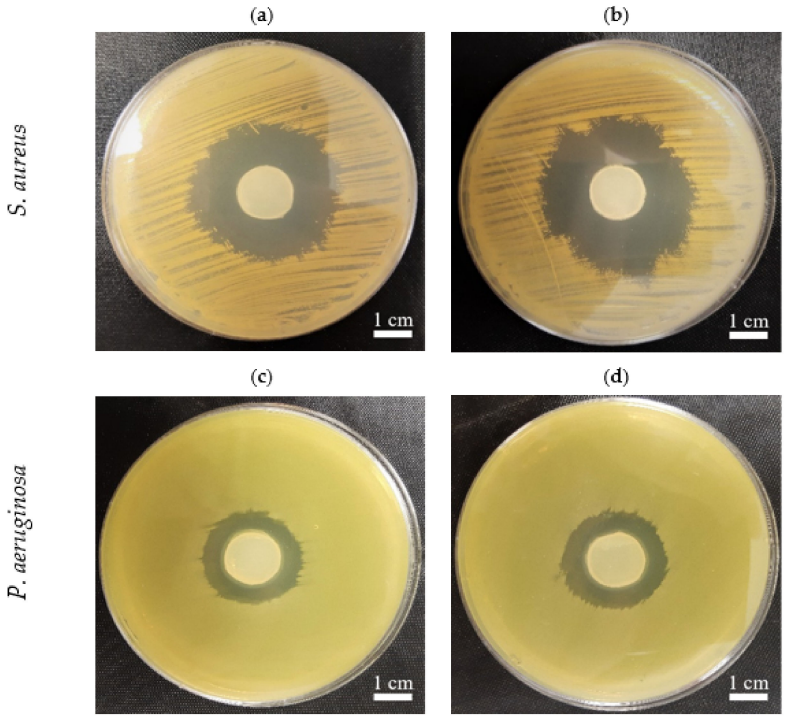

Figure 9. The growth inhibition zones in *S. aureus* (ATCC 6538) and *P. aeruginosa* (ATCC 15442) cultures, incubated with BC samples from *K. xylinus* ATCC 53524 soaked with an octenidine-containing antiseptic: (**a**,**c**) HS-BC; (**b**,**d**) PJ-BC. The comparable sizes of growth inhibition zones are seen with regard to specific pathogens independently from the type (PJ, HS-BC) of cellulose in which the sorption of octenidine was performed.

3. Materials and Methods

3.1. Preparation of Culture Medium

For the current study, we selected the Tajfun variety potato (average dry matter content: 22%, average starch content: 16%), because it is one of the varieties used by the starch industry. Potato tubers were obtained from Pomeranian-Masurian Potato Breeding Company (Strzekęcino, Poland). Prior to use, the tubers were stored at 4 °C but for no longer than 4 weeks. Potatoes were washed, peeled, and then PJ was obtained using a high-speed juicer (Bosch, MES3500, Gerlingen, Germany). Following juicing, the PJ was left at room temperature for 60 min to enable the starch residues to settle, and then the potato juice was decanted. The decanted PJ was then diluted with distilled water in a 1:1 ratio, sterilized by autoclaving at 121 °C, centrifuged for 10 min at 1500× *g* to remove

the remains of precipitated solids, and finally enriched with 1 *v*/*v*% of ethanol to yield the final PJ medium (Figure 10).

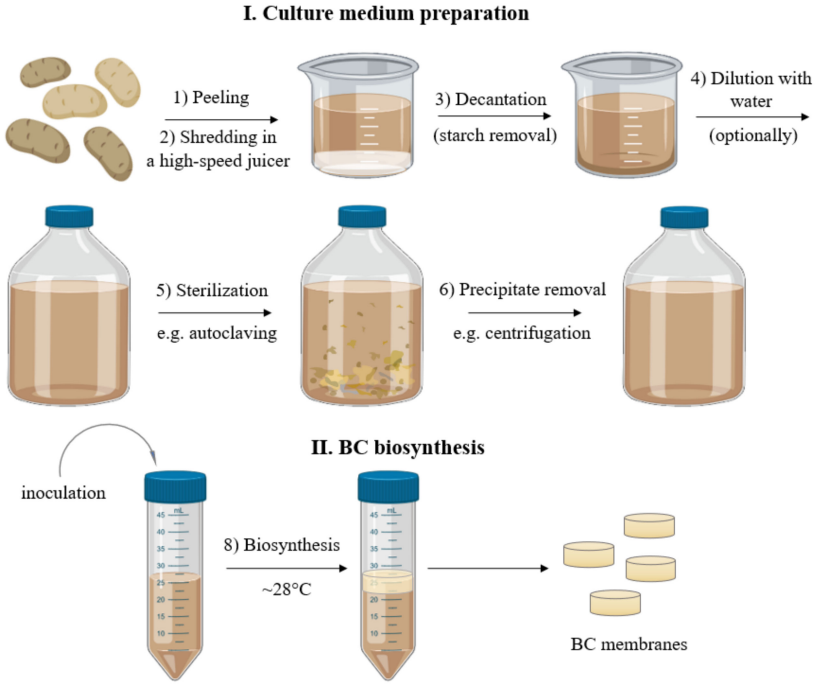

Figure 10. Scheme of the culture medium preparation and BC biosynthesis process.

3.2. Determination of pH, Protein, and Carbohydrate Concentration in PJ Medium

The concentration of sugars, including sucrose, glucose, fructose in PJ medium was determined by liquid chromatography–tandem mass spectrometry (LC–MS/MS) technique (1260 Infinity II Series Liquid Chromatograph, Agilent, USA). An InfinityLab Poroshell 120 EC-C18 column (Agilent, Santa Clara, CA, USA), with a particle diameter of 2.7 µm, equipped with a guard column was used for the chromatographic separation. The mass spectrometer (Ultivo G6465B, Agilent, Santa Clara, CA, USA) coupled to the chromatograph was used to detect and identify the tested analytes. Quantitative analysis was performed based on calibration curves prepared with the use of high purity sugar standards (MilliporeSigma, Burlington, MA, USA).

The concentration of total protein was measured using the Bradford protein assay with bovine serum albumin as a standard [60]. The starch concentration was measured using the iodine starch method [61]. The measurements for both of these assays were performed spectrophotometrically at 595 nm and 615 nm, respectively, using an Infinite 200 PRO NanoQuant Microplate Reader (Tecan, Männedorf, Switzerland). The pH of the PJ medium was assessed using a laboratory pH meter (Elmetron, Zabrze, Poland).

3.3. Microorganisms and Culture Conditions

For BC production, a reference strain of *Komagataeibacter xylinus* (American Type Culture Collection, ATCC 53524) was used. A bacterial suspension of cell density equal to 2×10^5 CFU/mL was used to inoculate 25 mL of medium in 50 mL plastic tubes (3.8 cm diameter, Polypropylene Conical Centrifuge Tube, Becton Dickinson and Company, Franklin Lakes, NJ, USA). Next, BC synthesis was conducted for 7 days at 28 °C. As a control, the standard HS medium (consisting of 2 *w*/*v*% glucose, 0.5 *w*/*v*% yeast extract, 0.5 *w*/*v*% peptone, 0.115 *w*/*v*% citric acid, 0.27 *w*/*v*% Na_2HPO_4, 0.05 *w*/*v*% $MgSO_4 \cdot 7H_2O$), enriched with 1 *v*/*v*% ethanol, was used.

In order to fully assess the possibility of using the PJ medium and the full spectrum of its potential advantages, several additional experiments were performed in an analogous

fashion. These included cultures of 7 additional *K. xylinus* strains from ATCC: 53582, 23770, 700178, 23768, 23769, 35959, 14851, as well as tests of several HS and PJ media combinations (PJ diluted with distilled water in 1:2 and 2:1 ratio; PJ and HS media without the addition of ethanol; non-centrifuged PJ containing starch solids; HS medium supplemented with the sucrose, glucose, fructose, and combination of these sugars at the same concentrations as in PJ). Additionally, we prepared and tested several media containing other ingredients that are agro-industrial wastes, including potato peels, orange peels, beetroot, and apples. The method of preparation of these media was analogous to the one applied for the preparation of the PJ medium. Finally, we also tested the use of other culture vessels such as Petri dishes 15 mm × 20 mm; the BC obtained from Petri dishes was also used for evaluation of its mechanical properties.

3.4. Determination of BC Yield

Starting from the 3rd day of cultivation, BC pellicles synthesized in HS (HS-BC) and in PJ media (PJ-BC) were harvested, purified by treating with 0.1 M NaOH solution at 80 °C for 90 min, and then rinsed with distilled water until pH became neutral (6.5–7.5). The obtained samples were then weighed on an analytical balance (accuracy 0.0001 g, WTB 2000 Radwag, Radom, Poland), dried at 60 °C, and weighed again. BC yield was expressed as dry mass (g) of BC/volume of culture medium (L).

3.5. Quantification and Viability Assessment of K. xylinus Cells

The quantity and viability of bacterial cells were determined in PJ and HS media (from 1st day of cultivation) and in PJ-BC and HS-BC pellicles (from 3rd day of cultivation) after their enzymatic digestion with cellulase, using alamarBlue Cell Viability assay (ThermoFisher, Waltham, MA, USA). AlamarBlue Cell Viability Reagent is a ready-to-use resazurin-based solution that functions as cell viability and metabolic activity indicator. For the digestion, the pellicles were washed in distilled water, transferred to 25 mL of the cellulase solution in citrate buffer (0.05 mol/L, pH 4.8), and incubated with shaking for 24 h at 30 °C. Next, the samples consisting of either culture medium or cell suspensions obtained from enzymatic hydrolysis of pellicles were centrifuged for 10 min at 3300× *g*. The resulting pellets were washed in phosphate-buffered saline (PBS, MilliporeSigma, Burlington, MA, USA), centrifuged again under the same conditions, and restored to their original volume with PBS. The bacterial suspensions (200 µL) were then transferred into wells of 96-well fluorescence microtiter plates (Becton Dickinson and Company, Franklin Lakes, NJ, USA), and 20 µL of alamarBlue reagent was added, followed by incubation for 1 h at 30 °C, in dark. The fluorescence was measured using a microplate fluorescence reader (Synergy HTX, Biotek, Winooski, VT, USA), using 540 nm excitation and 590 nm emission filters. Sterile PBS was used as the blank. As *K. xylinus* cells may show different metabolic activity depending on whether they are isolated from the medium or from the BC pellicle, dedicated standard curves were prepared separately for the cells obtained from the culture medium and the BC pellicles (Supplementary Figure S5). Using these standard curves, the fluorescence data were converted into log CFU/mL.

3.6. Assessment of pH, Protein, Sucrose, Glucose, Fructose, and Gluconic Acid Concentration during BC Biosynthesis

Each day of the fermentation process, samples of the culture media were taken and centrifuged for 1 h at 15,000× *g*. The supernatant was then separated from the pellet, filtered (PES 0.22 µm, MiliporeSigma, Burlington, MA, USA), and, if dedicated for LC-MS/MS analyses, additionally diluted with water (1:1000). All of the measurements were performed as previously described in Section 3.2 (Determination of pH, protein, and carbohydrate concentration in potato juice medium).

3.7. Evaluation of Physical and Chemical Properties of BC Obtained from PJ Medium

3.7.1. Analysis of Microstructure Using Scanning Electron Microscopy (SEM)

Purified PJ-BC and HS-BC pellicles obtained after 7 days of culture were fixed in 1% (*v*/*v*) aqueous solution of glutaraldehyde for 0.5 h at room temperature and dehydrated using an ethanol dilution series from 10% to 100% (*v*/*v*) (5 min at each concentration). Subsequently, the samples were dried at room temperature for 15 min, coated with a 15 nm layer of carbon using a high vacuum carbon coater (ACE 600, Leica, Mannheim, Germany), and imaged with the ZEISS Auriga 60 scanning electron microscope (SEM, Auriga 60, Zeiss, Jena, Germany).

3.7.2. Determination of Chemical Composition of BC Pellicles Using Attenuated Total Reflectance Fourier Transform Infrared (ATR-FTIR) Spectroscopy

Infrared spectra of purified PJ-BC and HS-BC pellicles obtained from 7 days cultures were evaluated using the ATR-FTIR technique, with an ALPHA FT-IR Spectrometer (Bruker Co., Leipzig, Germany) with a DTGS detector and the platinum–ATR-sampling module with a robust diamond crystal and variable angle incidence beam. For each BC pellicle, 32 scans at 4 cm^{-1} resolution were recorded over the spectral range of 4000–400 cm^{-1}. Initial spectral data processing was performed using the Spectragryph 1.2 software package.

The crystallinity index was calculated using the ratio of absorbance values for peaks 1430/900 (Cr.R1) and 1370/2900 (Cr.R2). The fraction of the cellulose Iα was calculated from ATR-FTIR spectra according to Equation (1) [62]. The area of the peaks at A710 (710 cm^{-1}) for Iβ and at A750 (750 cm^{-1}) for Iα was determined from the spectra deconvoluted using Peakfit software. The following equation was used:

$$f_\alpha = A750/(A750 + A710) \quad (1)$$

3.7.3. Determination of Water Swelling Ratio

Purified PJ-BC and HS-BC pellicles obtained from 7 days cultures were dried at 60 °C for 6 h to remove any water, weighed, immersed in distilled water for 24 h, and weighed again. The swelling ratio as a percent of dry mass (SR%) was then calculated using Equation (2) as follows:

$$SR\ (\%) = (W_w - W_d)/W_d \times 100 \quad (2)$$

where W_w is the weight of the swollen BC and W_d is the dry weight of the sample.

3.7.4. Determination of Water Holding Capacity

Purified and dried PJ-BC and HS-BC pellicles obtained from 7 days cultures were weighted, immersed in distilled water for 24 h to obtain maximum absorption level, and weighed again. The ability to hold water was determined using a moisture analyzer (Radwag, Radom, Poland) at 60 °C until the weight of BC was equal to the initial value (dry weight before hydration). Weight measurements were made automatically every 2 min. Water holding capacity (WHC) was then calculated using Equation (3) as follows:

$$WHC\ (\%) = W_{rw}/(W_w - W_d) \times 100 \quad (3)$$

where W_{rw} is the weight of water retained in BC during drying, W_w is the initial weight of wet BC, and W_d is the dry weight of the sample.

3.7.5. Determination of Density

The density of the dry, purified PJ-BC and HS-BC pellicles obtained from 7 days cultures was determined using a hydrostatic balance (XA 52/Y, Radwag, Radom, Poland) with methanol as a standard liquid. The weight of samples was measured at room temperature in the air as well as in methanol. The sample density was calculated using Equation (4) [63] as follows:

$$\rho = \rho_{methanol} \times W_d/(W_d - W_m) \quad (4)$$

where W_d is the weight of the dry sample in the air, and W_m is the weight of the sample in methanol.

3.7.6. Evaluation of Mechanical Properties

The tensile tests were performed according to PN-EN ISO 527-1 using Instron Universal Testing Machine (Instron, Norwood, MA, USA). For this purpose, purified wet PJ-BC and HS-BC pellicles were obtained from 7 days cultures in Petri dishes, which were cut into 2.5 × 10 cm strips. Prior to testing, samples were gently pressed to remove excess water and obtain a uniform thickness of 4.5 to 5 mm. Tensile tests were then carried out at room temperature, with a crosshead speed of 10 mm/min. The average values of tensile strength and elongation at break were calculated from the stress–strain curves. All measurements were performed in four replicates.

3.8. Cytotoxicity Screening

In vitro cytotoxicity screening of the purified PJ-BC and HS-BC pellicles was performed using extract and direct contact assays, based on ISO 10993-5:2009 using ATCC CCL-1 (L929) murine fibroblasts (passages 10-28), as described previously [64]. L929 cell line, Dulbecco's modified Eagle medium (DMEM), fetal bovine serum (FBS), L-glutamine, penicillin, streptomycin, and all other cell culture reagents were purchased from MilliporeSigma (MilliporeSigma, Burlington, MA, USA). All cell culture plasticware and disposables were purchased from VWR (VWR, USA). L929 cells were maintained and cultured in DMEM supplemented with 10% FBS, 2 mM L-glutamine, 100 U/mL penicillin. and 100 µg/mL streptomycin. For all cell culture assays, BC pellicles were sterilized by autoclaving.

3.8.1. Extract Assay

For extract assay, 5 pellicles (~10 cm^2) of each material were placed in a 6-well plate well, covered with 5 mL of growth media, and incubated for 24 h in a cell culture CO_2 incubator at 37 °C. For dried HS-BC/PJ-BC films, 5 discs (~10 cm^2) were covered with 3 mL of media. Finally, just media incubated in the same fashion served as a sham extract, while extracts of medical-grade PCL (CAPA 6430) and nitrile glove served as negative and positive (toxic) controls, respectively. In parallel, a 96-well plate was seeded with 1×10^4 L929 cells per well and incubated for 24 h to allow for cell adhesion and spreading. At this point, the media was replaced with 100 µL of each extract, with 6 technical replicates performed per material. The plate was then returned to the incubator and cells were cultured for an additional 24 h, after which cells were examined using an inverted light microscope (Delta Optical IB-100). Cell viability was evaluated using resazurin assay [64]. Fluorescence measurements were performed using a fluorescent plate reader (Synergy HTX, Biotek, Winooski, VT, USA) at 540 nm excitation and 590 nm emission. Complete growth media in an empty well was used as a blank. The results were expressed as the percent of cell viability relative to control (sham) and were calculated using Equation (5) as follows:

$$\% \text{ of cell viability} = 100 \times (FL_s - FL_b)/(FL_c - FL_b) \quad (5)$$

where FL is the fluorescence intensity (arbitrary units) and indexes s, b, and c refer to sample, blank, and control, respectively.

3.8.2. Direct Contact Assay

For the direct contact assay, 5×10^4 L929 cells were seeded per well of a 24-well plate and incubated for 24 h to allow for cell adhesion and spreading. After this time, the media was replaced with fresh media, and BC pellicles (~2 cm^2) that had been presoaked in cell culture media were placed directly on top of the cell monolayer (n = 5 pellicles per material). After a further 24 h of incubation, pellicles were carefully removed, and cell

viability was evaluated as described above, using both light microscopy and the resazurin viability assay.

3.8.3. Visualization of Fibroblast Viability

L929 fibroblasts cultured and treated as for the extract and direct cytotoxicity assays were stained for 15 min. with 3 µL of Syto 9 and Propidium iodide (PI) dyes (ThermoFisher Scientific, Waltham, MA, USA) 1000-fold diluted in PBS (MilliporeSigma, Burlington, MA, USA). Next, the dye-containing buffer was removed, and the cells were gently rinsed 3× times with PBS. Images of stained cells were captured using Lumascope 620 (Etaluma, Carlsband, CA, USA) at magnification ×20.

3.9. The In Vitro Activity of PJ-BC and HS-BC Soaked with Antimicrobial against Two Species of Opportunistic Pathogens

PJ-BC and HS-BC membranes were placed into wells of 24-well plates (F type, Nest Scientific Biotechnology, Wuxi, China) containing 1 mL of Octenisept® (Schülke-Mayr, Norderstedt, Germany). The samples were incubated overnight at 4 °C. Cultures of reference *S. aureus* ATCC 6538 and *P. aeruginosa* ATCC 15442 (24 h in Tryptic Soya Broth medium (Biomaxima, Lublin, Poland)) were diluted in sterile 0.9% saline (Stanlab, Lublin, Poland) to 0.5 McF (DensiLaMeter II, Erba Lachema, Brno, Czech Republic) and spread evenly throughout Mueller–Hinton agar plates (Biomaxima, Lublin, Poland). The previously prepared PJ- and HS-BC soaked with Octenisept® were then placed on top of the plates. The cultures were incubated overnight at 37 °C. The next day, the growth inhibition zones were recorded with the use of a digital camera.

3.10. Statistical Analyses

The data obtained in this study are presented as mean values ± standard error of the mean (SEM). Statistical differences between BC samples obtained in cultures using HS and PJ media were determined by one-way analysis of variance (ANOVA) and Tukey's post hoc test. The cultures were conducted in triplicate and all experiments were repeated at least three times. Differences were considered significant at a level of $p < 0.05$. The statistical analyses were conducted using GraphPad Prism 9.0 (GraphPad Software Inc., San Diego, CA, USA).

4. Conclusions

Our results demonstrate that PJ (without any pre-treatment) is suitable as a source of nutrients for cellulose-producing *K. xylinus* bacteria. Most importantly, after diluting PJ with water 1:1 to prepare the medium, the yield of BC was equivalent to that obtained from a commercial HS medium. Further, the PJ-BC obtained in this study did not differ from conventionally produced HS-BC in terms of its physical and chemical properties and was not cytotoxic. Additionally, the release of the antimicrobial agent from both types of BC resulted in the similar growth inhibition of two opportunistic pathogens. As a result, PJ-BC should be able to be used in the same applications as commercially produced BC. Importantly, converting the BC production process to use PJ medium at an industrial scale should be relatively easy to implement, thanks to the high availability and low cost of PJ, a by-product of the potato starch industry.

Supplementary Materials: The following are available online at https://www.mdpi.com/article/10.3390/ijms221910807/s1.

Author Contributions: Conceptualization, D.C.-J., M.B. and K.F.; methodology, D.C.-J., M.B. and K.F.; formal analysis, D.C.-J. and K.F.; investigation, D.C.-J., M.B., D.S., P.S., K.G. and P.M.; writing—original draft preparation, D.C.-J. and K.F.; writing—review and editing, A.Ż., P.S. and A.J.; visualization, D.C.-J., P.S. and K.F.; supervision, K.F.; project administration, K.F. All authors have read and agreed to the published version of the manuscript.

Funding: This research received no external funding.

Institutional Review Board Statement: Not applicable.

Informed Consent Statement: Not applicable.

Data Availability Statement: The data that support the findings of this study are available from the corresponding author upon reasonable request.

Conflicts of Interest: The authors declare no conflict of interest.

References

1. Czaja, W.; Krystynowicz, A.; Bielecki, S.; Brown, R.M., Jr. Microbial cellulose-the natural power to heal wounds. *Biomaterials* **2006**, *27*, 145–151. [CrossRef]
2. Sannino, A.; Demitri, C.; Madaghiele, M. Biodegradable cellulose-based hydrogels: Design and applications. *Materials* **2009**, *2*, 353–373. [CrossRef]
3. Rana, A.K.; Frollini, E.; Thakur, V.K. Cellulose nanocrystals: Pretreatments, preparation strategies, and surface functionalization. *Int. J. Biol. Macromol.* **2021**, *182*, 1554–1581. [CrossRef]
4. Beluns, S.; Gaidukovs, S.; Platnieks, O.; Gaidukova, G.; Mierina, I.; Grase, L.; Starkowa, O.; Brazdausks, P.; Thakur, V.K. From wood and hemp biomass wastes to sustainable nanocellulose foams. *Ind. Crops Prod.* **2021**, *170*, 113780. [CrossRef]
5. Ullah, H.; Badshah, M.; Correia, A.; Wahid, F.; Santos, H.A.; Khan, T. Functionalized bacterial cellulose microparticles for drug delivery in biomedical applications. *Curr. Pharm. Des.* **2019**, *25*, 3692–3701. [CrossRef] [PubMed]
6. Drozd, R.; Szymańska, M.; Przygrodzka, K.; Hoppe, J.; Leniec, G.; Kowalska, U. The Simple Method of Preparation of Highly Carboxylated Bacterial Cellulose with Ni-and Mg-Ferrite-Based Versatile Magnetic Carrier for Enzyme Immobilization. *Int. J. Mol. Sci.* **2021**, *22*, 8563. [CrossRef]
7. Chawla, P.R.; Bajaj, I.B.; Survase, S.A.; Singhal, R.S. Microbial cellulose: Fermentative production and applications. *Food Technol. Biotechnol.* **2009**, *47*, 107–124.
8. Kurosumi, A.; Sasaki, C.; Yamashita, Y.; Nakamura, Y. Utilization of various fruit juices as carbon source for production of bacterial cellulose by *Acetobacter xylinum* NBRC 13693. *Carbohydr. Polym.* **2009**, *76*, 333–335. [CrossRef]
9. Lima, H.L.S.; Nascimento, E.S.; Andrade, F.K.; Brígida, A.I.S.; Borges, M.; Cassales, A.R.; Muniz, C.R.; Filho, M.D.S.M.S.; Morais, J.P.S.; Rosa, M.D.F. Bacterial Cellulose Production by *Komagataeibacter hansenii* ATCC 23769 Using Sisal Juice-An Agroindustry Waste. *Braz. J. Chem. Eng.* **2017**, *34*, 671–680. [CrossRef]
10. Revin, V.; Liyaskina, E.; Nazarkina, M.; Bogatyreva, A.; Shchankin, M. Cost-effective production of bacterial cellulose using acidic food industry by-products. *Braz. J. Med. Biol. Res.* **2018**, *49*, 151–159. [CrossRef]
11. Kongruang, S. Bacterial cellulose production by *Acetobacter xylinum* strains from agricultural waste products. *Biotechnol. Fuels Chem.* **2007**, *148*, 763–774.
12. Li, Z.; Wang, L.; Hua, J.; Jia, S.; Zhang, J.; Liu, H. Production of nano bacterial cellulose from waste water of candied jujube-processing industry using *Acetobacter xylinum*. *Carbohydr. Polym.* **2015**, *120*, 115–119. [CrossRef]
13. Abol-Fotouh, D.; Hassan, M.A.; Shokry, H.; Roig, A.; Azab, M.S.; Kashyout, A.B. Bacterial nanocellulose from agro-industrial wastes: Low-cost and enhanced production by *Komagataeibacter saccharivorans* MD1. *Sci. Rep.* **2020**, *10*, 1–14.
14. Cheng, Z.; Yang, R.; Liu, X.; Liu, X.; Chen, H. Green synthesis of bacterial cellulose via acetic acid pre-hydrolysis liquor of agricultural corn stalk used as carbon source. *Bioresour. Technol.* **2017**, *234*, 8–14. [CrossRef]
15. Goelzer, F.D.E.; Faria-Tischer, P.C.S.; Vitorino, J.C.; Sierakowski, M.R.; Tischer, C.A. Production and characterization of nanospheres of bacterial cellulose from *Acetobacter xylinum* from processed rice bark. *Mat. Sci. Eng. C* **2009**, *29*, 546–551. [CrossRef]
16. Hussain, Z.; Sajjad, W.; Khan, T.; Wahid, F. Production of bacterial cellulose from industrial wastes: A review. *Cellulose* **2019**, *26*, 2895–2911. [CrossRef]
17. Bradshaw, J.E.; Bonierbale, M. Potatoes. In *Root and Tuber Crops*; Bradshaw, J.E., Ed.; Springer: New York, NY, USA, 2010; Volume 7, pp. 1–52.
18. Abdelraof, M.; Hasanin, M.S.; El-Saied, H. Ecofriendly green conversion of potato peel wastes to high productivity bacterial cellulose. *Carbohydr. Polym.* **2019**, *211*, 75–83. [CrossRef] [PubMed]
19. The European Starch Industry. Available online: https://starch.eu/the-european-starch-industry/ (accessed on 22 May 2021).
20. Fang, C.; Boe, K.; Angelidaki, I. Biogas production from potato-juice, a by-product from potato-starch processing, in upflow anaerobic sludge blanket (UASB) and expanded granular sludge bed (EGSB) reactors. *Bioresour. Technol.* **2011**, *102*, 5734–5741. [CrossRef]
21. Grommers, H.E.; van der Krogt, D.A. Potato starch: Production, modifications and uses. *Starch* **2009**, *11*, 511–539.
22. Kot, A.M.; Pobiega, K.; Piwowarek, K.; Kieliszek, M.; Błażejak, S.; Gniewosz, M.; Lipińska, E. Biotechnological methods of management and utilization of potato industry waste-a review. *Potato Res.* **2020**, *63*, 431–447. [CrossRef]
23. Jayanty, S.S.; Diganta, K.; Raven, B. Effects of cooking methods on nutritional content in potato tubers. *Am. J. Potato Res.* **2019**, *96*, 183–194. [CrossRef]
24. Kowalczewski, P.Ł.; Olejnik, A.; Białas, W.; Rybicka, I.; Zielińska-Dawidziak, M.; Siger, A.; Kubiak, P.; Lewandowicz, G. The nutritional value and biological activity of concentrated protein fraction of potato juice. *Nutrients* **2019**, *11*, 1523. [CrossRef] [PubMed]

25. Kowalczewski, P.; Celka, K.; Białas, W.; Lewandowicz, G. Antioxidant activity of potato juice. *Acta Sci. Pol. Technol. Aliment.* **2012**, *11*, 175–181.
26. Han, G.P.; Lee, K.R.; Han, J.S.; Kozukue, N.; Kim, D.S.; Kim, J.; Bae, J.H. Quality characteristics of the potato juice-added functional white bread. *Korean J. Food Sci. Technol.* **2004**, *36*, 924–929.
27. Kim, N.J.; Jang, H.L.; Yoon, K.Y. Potato juice fermented with *Lactobacillus casei* as a probiotic functional beverage. *Food Sci. Biotechnol.* **2012**, *21*, 1301–1307. [CrossRef]
28. Jozala, A.F.; Pértile, R.A.N.; dos Santos, C.A.; de Carvalho Santos-Ebinuma, V.; Seckler, M.M.; Gama, F.M.; Pessoa, A. Bacterial cellulose production by *Gluconacetobacter xylinus* by employing alternative culture media. *Appl. Microbiol. Biotechnol.* **2015**, *99*, 1181–1190. [CrossRef] [PubMed]
29. Sperotto, G.; Stasiak, L.G.; Godoi, J.P.M.G.; Gabiatti, N.C.; De Souza, S.S. A review of culture media for bacterial cellulose production: Complex, chemically defined and minimal media modulations. *Cellulose* **2021**, *28*, 2649–2673. [CrossRef]
30. Molina-Ramírez, C.; Castro, M.; Osorio, M.; Torres-Taborda, M.; Gómez, B.; Zuluaga, R.; Gómez, C.; Ganan, P.; Rojas, O.J.; Castro, C. Effect of different carbon sources on bacterial nanocellulose production and structure using the low pH resistant strain *Komagataeibacter medellinensis*. *Materials* **2017**, *10*, 639. [CrossRef]
31. Singhsa, P.; Narain, R.; Manuspiya, H. Physical structure variations of bacterial cellulose produced by different *Komagataeibacter xylinus* strains and carbon sources in static and agitated conditions. *Cellulose* **2018**, *25*, 1571–1581. [CrossRef]
32. Lei, L.; Li, S.; Gu, Y. Cellulose synthase complexes: Composition and regulation. *Front. Plant Sci.* **2012**, *3*, 75–84. [CrossRef]
33. Chen, G.; Wu, G.; Chen, L.; Wang, W.; Hong, F.F.; Jönsson, L.J. Comparison of productivity and quality of bacterial nanocellulose synthesized using culture media based on seven sugars from biomass. *Microb. Biotechnol.* **2019**, *12*, 677–687. [CrossRef] [PubMed]
34. Aswini, K.; Gopal, N.O.; Uthandi, S. Optimized culture conditions for bacterial cellulose production by *Acetobacter senegalensis* MA1. *BMC Biotechnol.* **2020**, *20*, 46. [CrossRef]
35. Embuscado, M.E.; Marks, J.S.; BeMiller, J.N. Bacterial cellulose. I. Factors affecting the production of cellulose by *Acetobacter xylinum*. *Food Hydrocoll.* **1994**, *8*, 407–418. [CrossRef]
36. Drozd, R.; Szymańska, M.; Żywicka, A.; Kowalska, U.; Rakoczy, R.; Kordas, M.; Konopacki, M.; Junka, A.F.; Fijałkowski, K. Exposure to non-continuous rotating magnetic field induces metabolic strain-specific response of *Komagataeibacter xylinus*. *Biochem. Eng. J.* **2020**, *166*, 107855. [CrossRef]
37. Ramana, K.V.; Tomar, A.; Singh, L. Effect of various carbon and nitrogen sources on cellulose synthesis by *Acetobacter xylinum*. *World J. Microbiol. Biotechnol.* **2000**, *16*, 245–248. [CrossRef]
38. La China, S.; Bezzecchi, A.; Moya, F.; Petroni, G.; Di Gregorio, S.; Gullo, M. Genome sequencing and phylogenetic analysis of K1G4: A new *Komagataeibacter* strain producing bacterial cellulose from different carbon sources. *Biotechnol. Lett.* **2020**, *42*, 807–818. [CrossRef] [PubMed]
39. Brugnoli, M.; Robotti, F.; La China, S.; Anguluri, K.; Haghighi, H.; Bottan, S.; Ferrari, A.; Gullo, M. Assessing effectiveness of *Komagataeibacter* strains for producing surface-microstructured cellulose via guided assembly-based biolithography. *Sci. Rep.* **2021**, *11*, 19311. [CrossRef] [PubMed]
40. Kechkar, M.; Sayed, W.; Cabrol, A.; Aziza, M.; Ahmed Zaid, T.; Amrane, A.; Djelal, H. Isolation and identification of yeast strains from sugarcane molasses, dates and figs for ethanol production under conditions simulating algal hydrolysate. *Braz. J. Chem. Eng.* **2019**, *36*, 157–169. [CrossRef]
41. Ruiz, P.; Izquierdo, P.M.; Seseña, S.; Palop, M.L. Intraspecific genetic diversity of lactic acid bacteria from malolactic fermentation of Cencibel wines as derived from combined analysis of RAPD-PCR and PFGE patterns. *Food Microbiol.* **2008**, *25*, 942–948. [CrossRef]
42. Zeidan, A.A.; Poulsen, V.K.; Janzen, T.; Buldo, P.; Derkx, P.M.; Øregaard, G.; Neves, A.R. Polysaccharide production by lactic acid bacteria: From genes to industrial applications. *FEMS Microbiol. Rev.* **2017**, *41*, S168–S200. [CrossRef]
43. Hungund, B.; Prabhu, S.; Shetty, C.; Acharya, S.; Prabhu, V.; Gupta, S.G. Production of bacterial cellulose from *Gluconacetobacter persimmonis* GH-2 using dual and cheaper carbon sources. *J. Microb. Biochem. Technol.* **2013**, *5*, 31–33. [CrossRef]
44. Hungund, B.S.; Gupta, S.G. Improved production of bacterial cellulose from Gluconacetobacter persimmonis GH-2. *J. Microb. Biochem. Technol.* **2010**, *2*, 127–133. [CrossRef]
45. Wang, S.S.; Han, Y.H.; Chen, J.L.; Zhang, D.C.; Shi, X.X.; Ye, Y.X.; Chen, D.-L.; Li, M. Insights into bacterial cellulose biosynthesis from different carbon sources and the associated biochemical transformation pathways in *Komagataeibacter* sp. W1. *Polymers* **2018**, *10*, 963. [CrossRef]
46. Tabaii, M.J.; Emtiazi, G. Comparison of bacterial cellulose production among different strains and fermented media. *Appl. Food Biotechnol.* **2016**, *3*, 35–41.
47. Klemm, D.; Schumann, D.; Udhardt, U.; Marsch, S. Bacterial synthesized cellulose artificial blood vessels for microsurgery. *Prog. Polym. Sci.* **2001**, *26*, 1561–1603. [CrossRef]
48. Algar, I.; Fernandes, S.C.; Mondragon, G.; Castro, C.; Garcia-Astrain, C.; Gabilondo, N.; Retegi, A.; Eceiza, A. Pineapple agroindustrial residues for the production of high value bacterial cellulose with different morphologies. *J. Appl. Polym. Sci.* **2015**, *132*, 1–17. [CrossRef]
49. Huang, H.C.; Chen, L.C.; Lin, S.B.; Hsu, C.P.; Chen, H.H. In situ modification of bacterial cellulose network structure by adding interfering substances during fermentation. *Bioresour. Technol.* **2010**, *101*, 6084–6091. [CrossRef] [PubMed]

50. Markiewicz, E.; Hilczer, B.; Pawlaczyk, C. Dielectric and acoustic response of biocellulose. *Ferroelectrics* **2004**, *304*, 39–42. [CrossRef]
51. Lin, W.C.; Lien, C.C.; Yeh, H.J.; Yu, C.M.; Hsu, S.H. Bacterial cellulose and bacterial cellulose–chitosan membranes for wound dressing applications. *Carbohydr. Polym.* **2013**, *94*, 603–611. [CrossRef]
52. Zhijiang, C.; Guang, Y. Bacterial cellulose/collagen composite: Characterization and first evaluation of cytocompatibility. *J. Appl. Polym. Sci.* **2011**, *120*, 2938–2944. [CrossRef]
53. Sulaeva, I.; Henniges, U.; Rosenau, T.; Potthast, A. Bacterial cellulose as a material for wound treatment: Properties and modifications. A review. *Biotechnol. Adv.* **2015**, *33*, 1547–1571. [CrossRef] [PubMed]
54. Junka, A.; Fijałkowski, K.; Ząbek, A.; Mikołajewicz, K.; Chodaczek, G.; Szymczyk, P.; Smutnicka, D.; Żywicka, A.; Sedghizadeh, P.P.; Dziadas, M.; et al. Correlation between type of alkali rinsing, cytotoxicity of bio-nanocellulose and presence of metabolites within cellulose membranes. *Carbohydr. Polym.* **2017**, *157*, 371–379. [CrossRef]
55. Wiegand, C.; Moritz, S.; Hessler, N.; Kralisch, D.; Wesarg, F.; Müller, F.A.; Fischer, D.; Hipler, U.C. Antimicrobial functionalization of bacterial nanocellulose by loading with polihexanide and povidone-iodine. *J. Mater. Sci. Mater. Med.* **2015**, *26*, 245. [CrossRef]
56. De Mattos, I.B.; Nischwitz, S.P.; Tuca, A.C.; Groeber-Becker, F.; Funk, M.; Birngruber, T.; Mautner, S.I.; Kamolz, L.P.; Holzer, J.C.J. Delivery of antiseptic solutions by a bacterial cellulose wound dressing: Uptake, release and antibacterial efficacy of octenidine and povidone-iodine. *Burns* **2020**, *46*, 918–927. [CrossRef] [PubMed]
57. Dydak, K.; Junka, A.; Dydak, A.; Brożyna, M.; Paleczny, J.; Fijałkowski, K.; Kubielas, G.; Aniołek, O.; Bartoszewicz, M. In vitro efficacy of bacterial cellulose dressings chemisorbed with antiseptics against biofilm formed by pathogens isolated from chronic wounds. *Int. J. Mol. Sci.* **2021**, *22*, 3996. [CrossRef]
58. Napavichayanun, S.; Ampawong, S.; Harnsilpong, T.; Angspatt, A.; Aramwit, P. Inflammatory reaction, clinical efficacy, and safety of bacterial cellulose wound dressing containing silk sericin and polyhexamethylene biguanide for wound treatment. *Arch. Derm. Res.* **2018**, *310*, 795–805. [CrossRef]
59. Zheng, L.; Li, S.; Luo, J.; Wang, X. Latest advances on bacterial cellulose-based antibacterial materials as wound dressings. *Front Bioeng. Biotechnol.* **2020**, *8*, 1334. [CrossRef]
60. Bradford, M.M. A rapid and sensitive method for the quantitation of microgram quantities of protein utilizing the principle of protein-dye binding. *Anal. Biochem.* **1976**, *72*, 248–254. [CrossRef]
61. Sulistyarti, H.; Fardiyah, Q.; Febriyanti, S. A simple and safe spectrophotometric method for iodide determination. *Makara J. Sci.* **2015**, *19*, 43–48. [CrossRef]
62. Kataoka, Y.; Kondo, T. Quantitative analysis for the cellulose *Iα* crystalline phase in developing wood cell walls. *Int. J. Biol. Macromol.* **1999**, *24*, 37–41. [CrossRef]
63. Ciecholewska-Juśko, D.; Żywicka, A.; Junka, A.; Drozd, R.; Sobolewski, P.; Migdał, P.; Kowalska, U.; Toporkiewicz, M.; Fijałkowski, K. Superabsorbent crosslinked bacterial cellulose biomaterials for chronic wound dressings. *Carbohydr. Polym.* **2021**, *253*, 117247. [CrossRef] [PubMed]
64. Riss, T.L.; Moravec, R.A.; Niles, A.L.; Duellman, S.; Benink, H.A.; Worzella, T.J.; Minor, L. Cell Viability Assays. In *Assay Guidance Manual*; Sittampalam, G., Coussens, N., Eds.; Eli Lilly & Company and the National Center for Advancing Translational Sciences: Bethesda, MD, USA, 2004; pp. 1–23.

Microbiological Research 263 (2022) 127125

Contents lists available at ScienceDirect

Microbiological Research

journal homepage: www.elsevier.com/locate/micres

The cross-linked bacterial cellulose impregnated with octenidine dihydrochloride-based antiseptic as an antibacterial dressing material for highly-exuding, infected wounds

Daria Ciecholewska-Juśko [a], Adam Junka [b], Karol Fijałkowski [a,*]

[a] Department of Microbiology and Biotechnology, Faculty of Biotechnology and Animal Husbandry, West Pomeranian University of Technology, Szczecin, Piastów 45, 70-311 Szczecin, Poland
[b] Department of Pharmaceutical Microbiology and Parasitology, Faculty of Pharmacy, Medical University of Wroclaw, Borowska 211a, 50534 Wroclaw, Poland

ARTICLE INFO

Keywords:
Bacterial cellulose
Wound dressings
Antiseptic
Bacterial biofilm
Chronic wound treatment

ABSTRACT

The highly absorbent, antibacterial dressings with a sustained release of the antimicrobial are considered necessary measures to counteract chronic wound biofilm-based infections. This study aimed to analyze wet and dry bacterial cellulose (BC) materials, modified by chemical cross-linking, and impregnated with an antiseptic based on octenidine dihydrochloride (OCT) in the context of its antibiofilm/antibacterial activity, exudate absorption, and cytotoxicity. The native BC was obtained from cost-effective, ecological-friendly potato juice (leftover from the starch industry). The ability to absorb and retain OCT, exudate absorption capacity, the kinetics of OCT release as well as antibiofilm/antibacterial activity of modified BC materials against biofilm-forming and planktonic bacteria (*Staphylococcus aureus* and *Pseudomonas aeruginosa*) were investigated. The performed analyses revealed that modified BC materials, thanks to their layered structure with numerous air spaces, were characterized by sustained exudate absorption and OCT release profile, which allowed them to exhibit high antimicrobial activity for up to 7 days, with a reduction of planktonic and biofilm cells of 84–100% and 69–93%, respectively. The modified BC materials showed also no cytotoxicity against fibroblast cell line L929 in vitro and were characterized by firm adhesion to the curved surfaces. These results indicate that cross-linked BC impregnated with OCT may be a particularly promising dressing material (obtained using sustainable processes), especially in the treatment of biofilm-infected, highly-exuding wounds.

1. Introduction

The chronic, difficult-to-heal wounds affect millions of people worldwide every year, with the highest rate of occurrence in the geriatric populations of the western hemisphere (Cheng et al., 2018; Weller et al., 2020; Alam et al., 2021). The management of these pathological entities devoured USD 20.37 Million in the year 2021; with a forecast of USD 34.46 Million for the year 2030 (Sen, 2019; Wound Care Market Research Report, 2021). One of the most pivotal factors, protracting the wound healing, is referred to as the biofilm. This microbial community is enclosed within an extracellular matrix (ECM), providing microorganisms protection, nutrition source, and the framework for the efficient interchange of virulence factors. The tolerance of biofilm against the immune system and antimicrobial agents is significantly higher compared to the planktonic (non-adhered) cells of the same microbial strain (Omar et al., 2017). In the chronic wound, the presence of biofilm inhibits the inflammatory processes that are crucial for wound healing, e.g., reducing the ability of leukocytes to penetrate the biofilm, weakening their ability to produce reactive oxygen species (ROS), and preventing phagocytosis (Omar et al., 2017; Bayer et al., 1991; Malic et al., 2011). Moreover, by the secretion of such enzymes as proteases, lipases or elastases, the biofilm-forming microorganisms damage the wound tissue (Percival et al., 2015). Therefore, the improper treatment of a biofilm-infected wound increases significantly the risk of amputation and the occurrence of life-threatening systemic inflammation (Armstrong et al., 2020; Paleczny et al., 2021).

One of the pillars of chronic wound management is the application of the dressings to control the level of the exudate (the wound fluid), ensure adequate gas exchange, protect the wound site from the external contaminants, and also to eradicate the microorganisms from the wound

* Corresponding author.
E-mail addresses: daria.ciecholewska@zut.edu.pl (D. Ciecholewska-Juśko), adam.junka@umed.wroc.pl (A. Junka), karol.fijalkowski@zut.edu.pl (K. Fijałkowski).

https://doi.org/10.1016/j.micres.2022.127125
Received 23 June 2022; Received in revised form 5 July 2022; Accepted 9 July 2022
Available online 15 July 2022

bed (Gámez-Herrera et al., 2020; Zheng et al., 2020). A variety of polymers is applied as dressing materials to fulfill these above-mentioned, diversified purposes. Among them, the natural (biological) polymers are considered to display high biocompatibility, biodegradability, and the desired mechanical and physiochemical properties (Zheng et al., 2020). One of such biopolymers is referred to as bacterial cellulose (BC), which is produced by microorganisms belonging to genera *Komagataeibacter*, *Acetobacter*, *Rhizobium*, *Sarcina*, *Agrobacterium*, *Azotobacter, Enterobacter, Pseudomonas, Salmonella*. Among all microorganisms reported for BC biosynthesis, the non-pathogenic *Komagataeibacter xylinus* is considered one of the most efficient cellulose-producing species (Lahiri et al., 2021; Sperotto et al., 2021). The BC found already its application as a material for implants, stents, artificial blood vessels, and as an integral part of drug delivery systems (Rajwade et al., 2015; Ullah et al., 2016; Swingler et al., 2021; Nemati and Gholami, 2021). The BC can be also successfully used as a dressing material for chronic wounds, thanks to its desired properties with this regard (Portela et al., 2019; Volova et al., 2019). It was shown that the application of BC during long-term contact with the human organism does not lead to any toxic or allergenic effects (Zheng et al., 2020). The BC can be produced in virtually every shape and size; it is also highly formable, flexible, and transparent (Rajwade et al., 2015). The spatial structure of nanofibers, stabilized by hydrogen bonds, determines such BC properties as high crystallinity and the highest Young's modulus among all two-dimensional organic materials (Dayal and Catchmark, 2016). The high specific surface area and porosity ensure also efficient gas exchange and high liquid absorption capacity (Zheng et al., 2020).

The most frequently proposed BC dressings are based on the never-dried (wet) form of this polymer, which, being highly hydrated, provides a proper level of moisture, beneficial for wound healing (Nuutila and Eriksson, 2021). There are also several reports demonstrating the usability of partially or completely dried BC (Portela et al., 2019; Wei et al., 2011). Other research describes modifications of BC to improve its properties and meet all the necessary functional requirements for wound dressings (Sulaeva et al., 2015). Such modifications are most often related to the formation of composites with other substances/materials (Rajwade et al., 2015; Shahriari-Khalaji et al., 2020; He et al., 2021) and to facilitate the prolonged release of the bioactive substances or (in the case of dry BC) to ensure the proper level of gas permeability and re-hydration (Portela et al., 2019).

The BC is frequently fortified with the various types of antimicrobial agents, such as antibiotics or antiseptics, and also metal/metal oxide nanoparticles, carbon/silica nanomaterials as well as such organic compounds as chitosan, curcumin, amino acids, or plant-derived alkaloids (Moritz et al., 2014; Zheng et al., 2020; Swingler et al., 2021; Zielińska et al., 2021; Krasowski et al., 2021). The application of antimicrobial wound dressings significantly accelerates the wound closure by eradicating healing-protracting biofilm. As consequence, the patient's health status increases, while the economic burden related to the care of the chronic wound, decreases (Alavi et al., 2014; Shahriari-Khalaji et al., 2020).

In our previous research, we have shown that the BC materials modified in the simple and safe process of chemical crosslinking with citric acid and different catalysts have beneficial properties in terms of their application in medicine (Ciecholewska-Juśko et al., 2021a). As we demonstrated, the crosslinking process prevented cellulose fibers from collapsing during drying and allowed to obtain a sponge-like biopolymer which, even in a dry state, retained its three-dimensional structure, in contrast to dried, unmodified cellulose (Ciecholewska-Juśko et al., 2021a). Based on the established beneficial properties of crosslinked BC (especially its water-related properties), in this work, we assumed that the impregnation of such modified BC materials with an antimicrobial substance (octenidine dihydrochloride antiseptic) would provide its prolonged release and a high liquid holding capacity. We further assumed that such properties of BC materials would enable effective reduction of microbes and allow to maintain of a moist environment by release of fluid from and simultaneous absorption of exudate to the polymer. Taking into account the changes in the BC properties that occur during drying, the analyzes were performed using never-dried (wet) and dried materials. The unmodified BC materials served as the comparator of the study. Because the principal disadvantage of intensive large-scale commercial use of the BC-based materials is the high price of the conventional, culturing medium (Herstin-Schramm medium), we replaced it (for the first time in the context of dressing material development), with the cost-effective potato juice (starch industry waste), based on our previous research (Ciecholewska-Juśko et al., 2021b).

Therefore, the study aimed to characterize and evaluate the antibiofilm/antibacterial potential, ability to control the exudate level, and cytotoxicity of octenidine dihydrochloride-impregnated, crosslinked BC materials.

2. Materials and methods

2.1. Preparation of unmodified and modified BC materials

For BC production, *Komagataeibacter xylinus* (ATCC 53524) strain was cultured in polypropylene Petri dishes with a diameter of 9 cm, under stationary conditions, for 5 days at 28 °C using a potato juice medium prepared according to the methodology described in our previous publication (Ciecholewska-Juśko et al., 2021b). Then, BC membranes were purified by incubating with 0.1 M NaOH at 80 °C for 90 min and washed with distilled water until a neutral pH was obtained. Subsequently, the purified BC membranes were modified with a crosslinking reaction using citric acid as the crosslinking agent and disodium phosphate/sodium bicarbonate mixture as catalysts (2:1 w/w) according to the method described in our previous work (Ciecholewska-Juśko et al., 2021a). The modified samples were then rinsed with distilled water to remove unbound molecules of citric acid and catalysts until the pH became neutral. Half of the samples were left in the wet state (later referred to as the modified wet BC, or MBC_w materials), whereas the other part was dried at room temperature to a constant weight in the range of 5–7 days (later referred to as the modified dry BC, or MBC_d materials). Additionally, purified, unmodified wet BC (BC_w) and dry BC (BC_d) materials were used as comparative samples for modified materials. In the last step, all the BC materials were cut to a size of 5 × 5 cm or 1.5 × 1.5 cm and sterilized in an autoclave.

2.2. Swelling in OCT capacity

The wet and dry MBC and BC materials with dimensions of 5 × 5 cm were weighed on an analytical balance (WTB 2000 Radwag, Poland), immersed in 1% octenidine dihydrochloride solution (Schülke, Germany, later referred to as the OCT), and then weighed at time intervals for 8 h, and then after 24 h. The results were expressed as a swelling ratio (SR%) calculated using Eq. (1):

$$SR \quad (\%) = \quad \frac{W_w - W_i}{W_i} * 100 \tag{1}$$

Where W_w is the weight of swollen material and W_i is the initial weight of the material.

2.3. Impregnation with octenidine dihydrochloride solution

The MBC and BC materials were weighed on an analytical balance (WTB 2000 Radwag, Poland), immersed in OCT for 24 h at 4 °C, and weighed again. The wet materials (modified and unmodified) were immersed in OCT in the same conditions as in the case of the dry samples, however, the antiseptic solution was changed to a fresh portion every 2 h, until its absorbance (measured at a wavelength of 270 nm) reached the initial value (such a procedure let to replace the water

present in wet samples with the OCT and to obtain the same octenidine dihydrochloride concentration in all materials). To estimate the volume of OCT absorbed by the wet samples, part of them was weighed, dried, and weighed again. The materials impregnated with OCT were later referred to as the OCT-MBC or OCT-BC.

2.4. OCT holding capacity

The wet and dry OCT-MBC and OCT-BC materials with dimensions of 5 × 5 cm were weighed on an analytical balance (WTB 2000 Radwag, Poland). Then the materials were placed in the incubator (37 °C) and weighed every 10 min for 1 h, then every 1 h up to 8 h, and then again every 24 h up to 7 days. The results were expressed as OCT holding capacity (OCT-HC) calculated using Eq. (2):

$$\text{OCT-HC } (\%) = W_{rw}/(W_w - W_d) \text{ x } 100 \quad (2)$$

Where W_{rw} is the weight of OCT retained in the material during drying, W_w is the initial weight of the OCT impregnated material, and W_d is the weight of the material after drying.

2.5. Exudate absorption capacity

The OCT-MBC and OCT-BC materials with dimensions of 5 × 5 cm were weighed on an analytical balance (WTB 2000 Radwag, Poland), immersed in 20 mL of simulated wound fluid (SWF), composed of fetal bovine serum, NaCl, $NaHCO_3$, KCl, K_2HPO_4 x 3 H_2O, $MgCl_2$ x 6 H_2O, $CaCl_2$, Na_2SO_4, TRIS buffer and HCl (pH 7.4) (Petrauskaite et al., 2013) with the addition of 1 mg/mL Congo Red as an indicator of absorption (SWF-CR) (Mazeau and Wyszomirski, 2012; Thongsomboon et al., 2020) and incubated at room temperature under shaking conditions (160 rpm). The changes in concentration of SWF-CR (due to its absorption by the materials) and OCT (due to its release from the materials) were measured spectrophotometrically every hour for 8 h and then every 24 h for 7 days at the wavelength of 300 nm (determined based on the spectral scanning for the standard solutions of SWF-CR/OCT, Fig. S1). The SWF-CR (%) that remained in the solution (which was not absorbed by OCT-MBC and OCT-BC materials) was determined from the calibration curve for standard SWF-CR/OCT solutions (Fig. S2). The concentration of SWF-CR (%) that indicates maximum exchange with OCT present in the samples was also determined from the calibration curve taking into account the initial volume of OCT in the materials and the maximum value of absorbed OCT determined during the swelling analyses.

Additionally, to demonstrate the exchange between SWF-CR (pH 6.17) and OCT (pH 7.00) the pH of SWF-CR/OCT solutions was also measured at each time point.

2.6. The release of OCT into the artificial wound bed model

The OCT-MBC and OCT-BC materials (dimensions of 5 ×5 cm) were gently placed on the top of the plates (Petri dishes of a diameter of 90 mm) containing Tryptic Soy Agar (TSA, Graso Biotech, Poland) (with 4% of agar) with previously prepared round-shaped artificial wound beds (2.8 cm in diameter), filled with 3 mL of SWF and covered with a sterile Teflon mat to limit the penetration of OCT to the area of the artificial wound bed only (a detailed presentation of the set-up was included in the Supplementary material, Fig. S3).

Then the plates with OCT-containing materials were incubated at 37 °C with a humidity level of 98–99% to reduce evaporation during the analysis. The measurements of OCT released to the SWF in artificial wound beds were performed at time intervals, by transferring 10 μl of SWF to a microvolume plate (Take 3, Biotek, USA) and reading the absorbance at the wavelength of 270 nm (Synergy HTX, Biotek, USA). The measurements were carried out in a short release mode (lasting 8 h), and in a long release mode (lasting 7 days). In the long release mode, to simulate the continuous exudation that occurs in the wound, the artificial wound beds were replenished every 24 h with 1.5 mL of SWF (measurements were performed right before and immediately after the addition of the SWF, creating a release/dilution curve). The volume of SWF added was estimated according to the guidelines for the standard rate of exudate production for various types of wounds developed by the World Union of Wound Healing Societies (WUWHS, 2019).

2.7. Antimicrobial activity

Antimicrobial activity was assessed against two reference strains of bacteria with the high biofilm-formation potential, namely *Staphylococcus aureus* (ATCC 6538) and *Pseudomonas aeruginosa* (ATCC 15442). Additionally, for the modified disc diffusion test, four other clinical strains of staphylococci representing different species (*S. aureus*, *S. equorum*, *S. warneri*, *S. xylosus*) and four other clinical strains of *P. aeruginosa* were also used.

2.7.1. Disc diffusion test

The liquid cultures of bacteria were adjusted to 0.5 McFarland standard, corresponding to 1.5×10^8 CFU/mL, and spread evenly over the surface of 90 mm Mueller-Hinton (M-H) agar plates (Graso Biotech, Poland) using sterile cotton swabs. Then, OCT-MBC and OCT-BC materials with dimensions of 1.5 × 1.5 cm were placed in the center of the plate. The cultures were incubated for 18 h at 37 °C. After incubation, the diameters of growth inhibition zones were measured and presented in the mm.

2.7.2. Modified disc diffusion test

Bacterial suspensions and cultures were prepared according to the method described above, however, the OCT-containing materials were placed on the M-H agar plates with seeded bacterial cultures for 1 h and then transferred to another plate for another hour (the transfer of materials was performed 8 times; the plates were later referred to as the transfer 1–8). Each plate was then incubated for 18 h at 37 °C. The last plates (after the transfer number 8) were incubated together with the materials placed on them for 18 h at 37 °C (these plates were later referred to as the transfer number 9).

2.7.3. Liquid medium test

Initially, *S. aureus* and *P. aeruginosa* strains were plated on Brain Heart Infusion agar (BHI, Graso Biotech, Poland) and incubated for 24 h at 37 °C. After incubation, one colony-forming unit (CFU) of each strain was transferred into 10 mL Tryptic Soy Broth (TSB, Oxoid, UK) and incubated for 24 h at 37 °C with shaking (200 rpm). Next, cultures were diluted in TSB medium to obtain bacterial suspension equal to 1.5×10^8 CFU/mL and 1.5×10^5 CFU/mL. In the next step, OCT-MBC and OCT-BC materials (1.5 ×1.5 cm) were immersed in the 100 mL of the bacterial suspensions (of both densities) and incubated for 7 days at 37 °C with shaking (160 rpm). On days 1, 3, and 7, 1 mL of each bacterial suspension was collected into sterile 1.5 mL tubes; simultaneously 1 mL of fresh TSB medium was added to the experimental cultures (to maintain their constant volume). The collected suspensions were then centrifuged (5415 R, Eppendorf, Germany) for 10 min at 3300 x *g*, resulting pellets were washed with phosphate-buffered saline (PBS, MilliporeSigma, USA), centrifuged again, and restored to the original volume (1 mL) with PBS. Then, 100 μl of each sample was transferred to the wells of 96 well plates (Nest Scientific USA Inc., USA). In order to determine the number of metabolically active cells, the 3-(4,5-Dimethylthiazol-2-yl)− 2,5-diphenyltetrazolium bromide (MTT), reduction cell viability assay was performed using a 3 mg/mL solution of MTT (MilliporeSigma, USA) in PBS (Żywicka and Fijałkowski, 2017; Junka et al., 2017). The measurements were performed at a wavelength of 540 nm and a reference wavelength of 690 nm using a microplate reader (Synergy HTX, Biotek, USA). The results were presented as a percent reduction of viable bacteria (% of killed bacteria in liquid medium

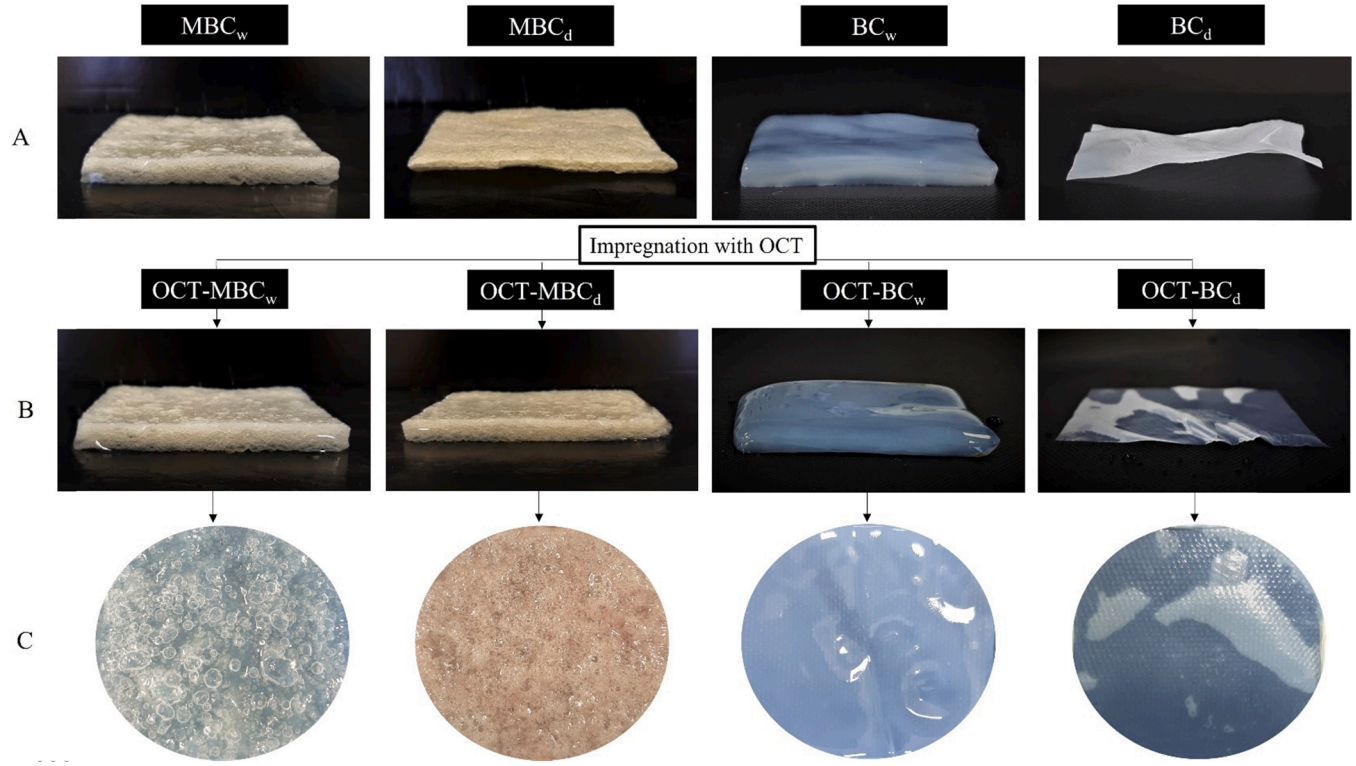

Fig. 1. MBC and BC materials before (A) and after impregnation with OCT (B); C - top view of the surface of OCT-containing materials.

incubated with OCT-MBC and OCT-BC materials in comparison to the bacteria incubated in a medium without the materials).

2.7.4. Biofilm culture test

In the first step, to obtain coatings with staphylococcal and pseudomonal biofilms, round pieces of sterile gauze (with a diameter of 2.5 cm) were cut and placed on the bottom of the wells of 6-well plates (Nest Scientific USA Inc., USA). Then, 3 mL of 1×10^6 CFU/mL bacterial suspension in TSB (GRASO, Poland) with the addition of 1% glucose was added into each well, and the plates were incubated at 37 °C for 48 h (after 24 h, the medium was replaced) (Fig. S4). After 48 h of incubation, gauzes with biofilm were carefully removed from the medium, placed into clean plates, and washed three times with PBS to remove bacterial cells not attached to the gauze.

2.7.4.1. Biofilm presence confirmation. To confirm the presence of biofilm on the gauze coatings, the samples were covered with 300 μl of MTT solution (3 mg/mL in PBS) and incubated at 37 °C for 30 min. During the incubation, changes of color due to the reduction of MTT by live biofilm cells to purple formazan crystals were observed and documented at time intervals (after 1, 5, 10, and 30 min). As a control, sterile gauze was used.

Additionally, a scanning electron microscopy (SEM) analysis was performed. Gauzes with staphylococcal and pseudomonal biofilms were washed gently with PBS and fixed by immersion in 3% glutaraldehyde (POCH, Poland) for 15 min at room temperature. In order to remove the fixative, the samples were washed two twice with PBS. Then, dehydration in increasing concentrations of ethanol (10%, 25%, 50%, 60%, 70%, 80%, 90%, and 100%; POCH, Poland) was performed (10 min per solution). The ethanol was then rinsed off and the samples were dried at room temperature. Next, the samples were covered with gold and palladium (60:40; sputter current 40 mA; sputter time 50 s) using a Quorum machine (Quorum International, USA) and examined under a Zeiss EVO MA25 scanning electron microscope (Carl Zeiss, Germany).

2.7.4.2. Assessment of cell reduction in biofilm – artificial wound bed model. After confirmation of the presence of staphylococcal and pseudomonal biofilms, the gauzes were first moistened with 50 μl of SWF to allow their proper adhesion, then placed at the bottom of the artificial wound bed prepared as described in Section 2.6 (Fig. S3) and poured with 3 mL of SWF (Fig. S4). In the next step, the OCT-MBC and OCT-BC materials (5 ×5 cm) were placed gently in the center of the plate. As the control, the same plates with the artificial wound bed model, however with no materials on their surface, were prepared. All the plates were incubated at 37 °C for 1, 3, and 7 days (Fig. S4), (the plates incubated for 3 and 7 days were replenished with 1.5 mL of SWF every day). After the incubation time, the OCT-containing materials and SWF were carefully removed, and the gauzes with biofilm were transferred to sterile 2 mL tubes (Eppendorf, Germany) with previously added 1 mL of PBS, and shaken vigorously for 10 min using a vortex mixer (DLAB Scientific Inc., USA) to detach the bacterial cells. Next, the gauzes were removed, the bacterial suspensions were centrifuged (5415 R, Eppendorf, Germany) for 10 min at 3300 x *g* and the resulting pellets were washed with PBS, centrifuged again, and restored to their original volume (1 mL) with PBS. Then, the MTT reduction cell viability assay was performed as described above. The results were presented as a percent reduction of viable bacteria (% of eradicated biofilm-forming cells incubated with OCT-MBC and OCT-BC materials in comparison to the bacterial biofilms incubated without the materials).

2.8. Cytotoxicity screening

In vitro cytotoxicity screening of the purified MBC and BC materials was performed using extract and direct contact assays, based on ISO 10993-5:2009 using ATCC CCL-1 (L929) murine fibroblasts (passages 10–28), as described previously (Ciecholewska-Juśko et al., 2021a). Dulbecco's modified Eagle medium (DMEM), fetal bovine serum (FBS), L-glutamine, penicillin, streptomycin, and all other cell culture reagents were purchased from MilliporeSigma (MilliporeSigma, USA). All cell culture plasticware and disposables were purchased from VWR (VWR,

Table1
Characterization of MBC and BC materials before and after impregnation with OCT.

	MBC_w	MBC_d	BC_w	BC_d
Initial thickness (mm)	3.20 ± 0.25	2.50 ± 0.10	4.00 ± 0.40	0.06 ± 0.01
Initial weight (g)	7.48 ± 0.32	0.27 ± 0.06	9.87 ± 0.16	0.08 ± 0.01
	OCT-MBC_w	OCT-MBC_d	OCT-BC_w	OCT-BC_d
Weight (g)	7.51 ± 0.20	5.03 ± 0.15	9.92 ± 0.18	0.30 ± 0.03
Volume of absorbed OCT (mL)	7.34 ± 0.20	4.76 ± 0.18	9.83 ± 0.18	0.22 ± 0.03

USA). L929 cells were maintained and cultured in DMEM supplemented with 10% fetal bovine serum, 2 mM L-glutamine, 100 U/mL penicillin, and 100 μg/mL streptomycin. The cell viability was evaluated using a resazurin assay (Riss et al., 2016). As the control, L929 cells culture incubated without MBC and BC materials was used. The results were expressed as a percent of cell viability (% of the viability of the control setting).

For the visualization of fibroblast viability, L929 cells cultured and treated as for the extract and direct assays were stained with 3 μl of Syto 9 and Propidium iodide (PI) dyes (ThermoFisher Scientific, USA) 1000-fold diluted in PBS for 15 min. Next, the dye-containing buffer was removed, and the cells were gently rinsed 3 times with PBS. The images of stained cells were captured using Lumascope 620 (Etaluma, USA) at magnification × 20.

2.9. Statistical analysis

Data obtained in this study were presented as mean values ± standard error of the mean (SEM) calculated from at least three different measurements. Statistical differences between different samples were determined using a two-way analysis of variance (ANOVA). The Tukey's HSD (Hostly Significant Difference) post-hoc test was used for multiple comparisons of means. All differences were considered statistically significant when the P-value was less than 0.05. Statistical tests were conducted using GraphPad Prism 9.0 (GraphPad Software Inc., USA).

3. Results and discussion

3.1. Characteristics of MBC and BC materials

The analysis of the surface of the MBC and BC samples revealed that both BC_w and BC_d materials had smooth structures and were translucent, whereas MBC_w and MBC_d materials had a sponge-like, layered, non-translucent structure with numerous air bubbles (OCT-filled in the case of the antiseptic-impregnated materials) (Fig. 1).

The weight measurements (Table 1) indicated that modification of BC materials by the crosslinking significantly increased (by over 300%) its dry weight as compared to the weight of the unmodified BC samples (BC_d, Table 1), which resulted from the binding of citric acid molecules with cellulose fibers. After impregnation with OCT, the MBC_d materials were expanded as the result of filling its cavities and spaces between layers (with a weight increase of over 1700%). In the process of drying, the structure of the unmodified BC materials collapses irreversibly (and significantly loses its thickness). Therefore, BC_d materials were characterized by the lowest rehydration (with OCT solution) capacity (with a 280% weight increase after impregnation) (Fig. 1, Table1).

Among all the tested samples, the MBC_d materials were characterized by the highest swelling ratio (SR%). They were also the only type of materials, which swelled in OCT solution throughout the entire period (8 h) of the experiment (Fig. 2A) and showed a statistically significant difference in the SR% between 8 and 24 h (Fig. S5). In comparison, BC_d materials swelled in OCT solution only for the first 20 min. The wet BC materials were already saturated with water (during the purification process); therefore, they did not show any increase in weight and SR coefficient (Fig. 2A).

The results of OCT-holding capacity presented in Fig. 2B showed that the OCT-BC_w materials were characterized by the highest holding capacity of OCT solution as compared to the remaining types of samples, reaching dry weight on the 7th day of the incubation (as a result of further incubation for 24 h, no additional reduction in the weight of these materials was found) (Fig. 2B, Tab. S1). In contrast, OCT-BC_d materials achieved their dry weight after only 30 min. Therefore, its collapsed and flattened structure translated into poor liquid absorption and holding capacity. Such properties should be considered a significant limitation of the BC_d materials use as a dressing for highly-exuding wounds. The OCT-MBC_w and OCT-MBC_d materials, despite a significantly lower OCT content as compared to the OCT-BC_w materials (of 24% and 52%, respectively; Table 1), thanks to their multi-layer and multi-gap structure, retained OCT solution up to 6th and 5th day, respectively (Fig. 2B, Tab. S1). It was also found that the OCT-MBC materials retained OCT solution significantly longer as compared to the OCT-BC materials (Fig. 2B).

3.2. Exudate absorption capacity

The ability to absorb an abundant volume of exudate is one of the desirable properties of a dressing because the proper level of moisture is obligatory for the wound healing and closure process. Moreover, it allows for reducing the frequency of the dressing change, which is often associated with the pain sensation in the patient (Han and Ceilley, 2017; Bazbouz and Tronci, 2019, Swingler et al., 2021, Zheng et al., 2020).

The ability of OCT-MBC and OCT-BC materials to absorb exudate was

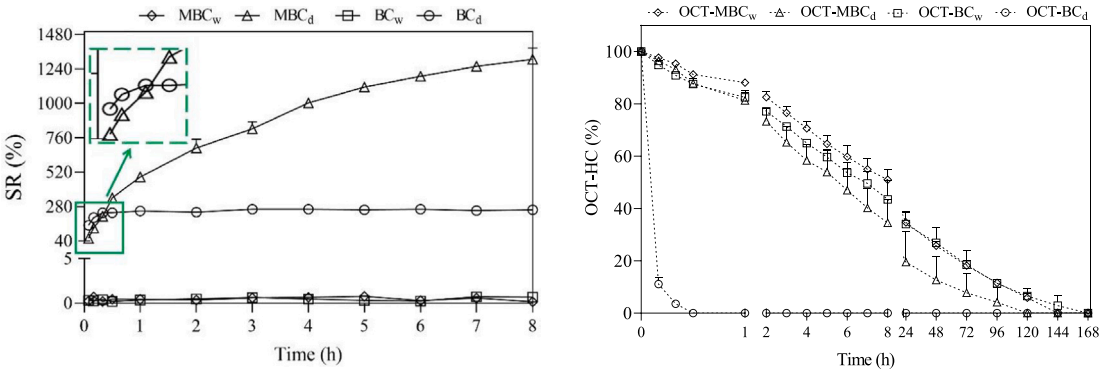

Fig. 2. A - Swelling in OCT ratio (%), B - OCT holding capacity (%) of MBC and BC materials.

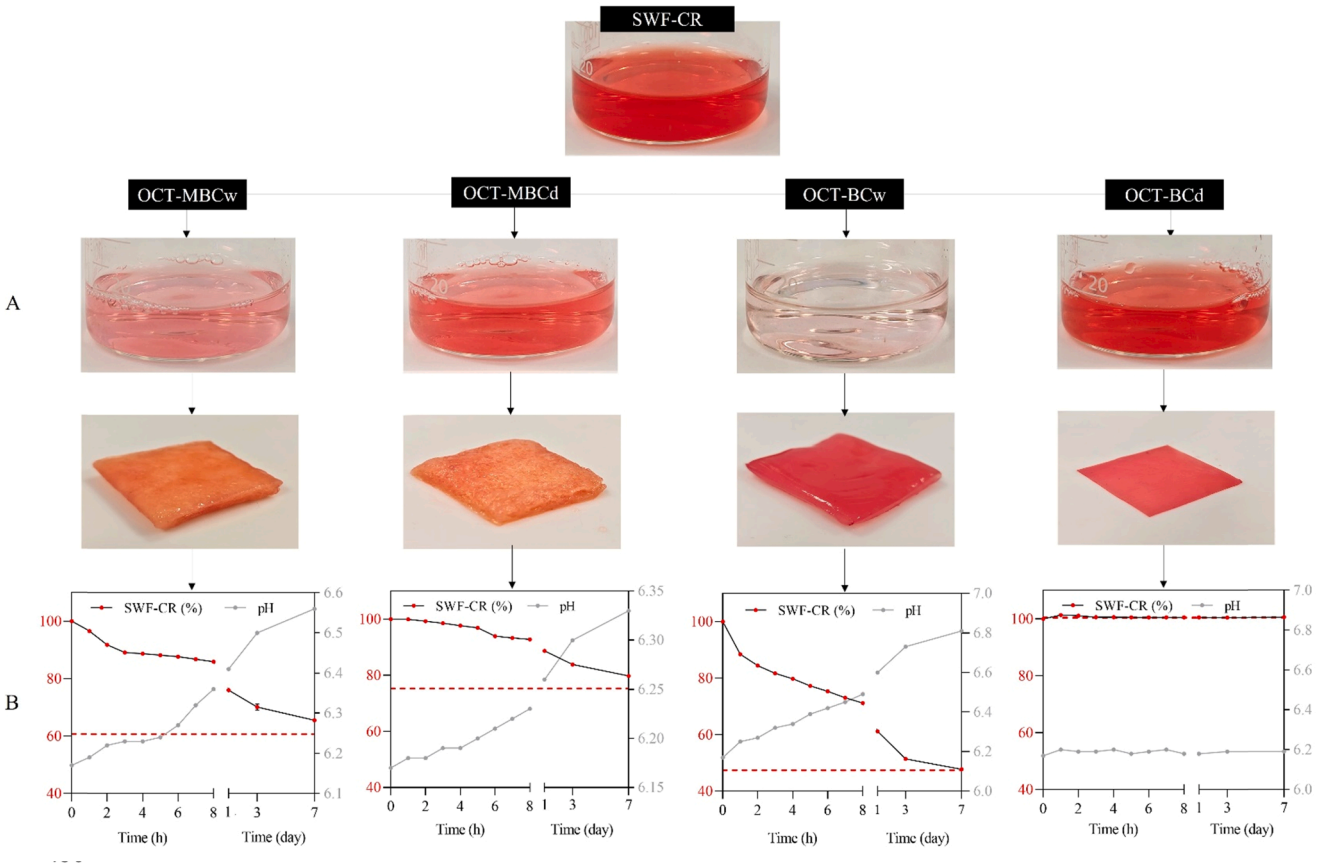

Fig. 3. Exudate absorption by OCT-MBC and OCT-BC materials; A - Discoloration of the SWF-CR solution, B - Changes in concentration of SWF-CR (%) and pH in time. Red dotted lines represent the concentration of SWF-CR (%) after a maximum exchange with OCT present in OCT-MBC and OCT-BC materials.

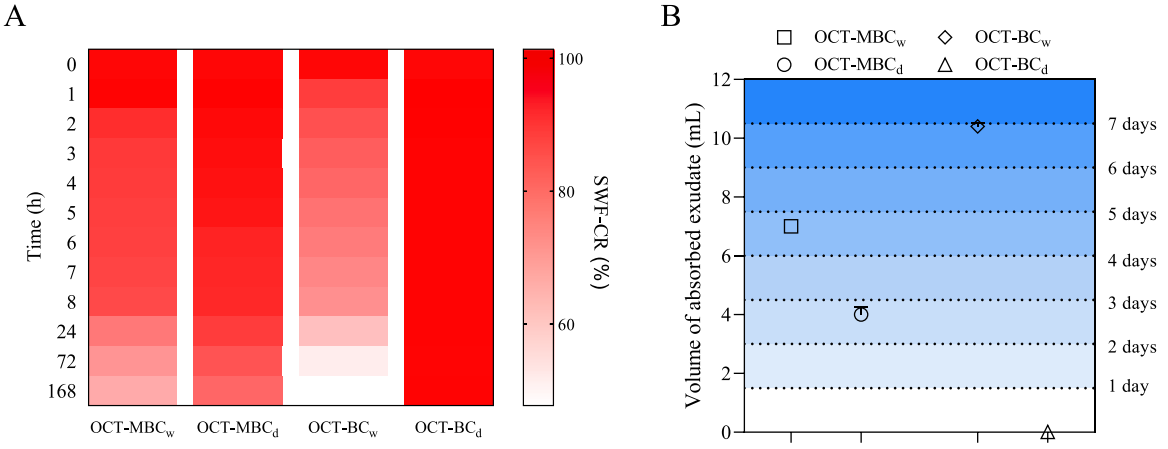

Fig. 4. A - Graphic presentation of SWF-CR concentration in time during the exudate absorption test, B - Exudate absorption capacity of OCT-MBC and OCT-BC materials in comparison with the average volume of exudate that is secreted into the wound with a diameter of 2.8 cm. Dotted lines represent the volume of exudate secreted in subsequent days.

determined based on the changes in the absorbance of the SWF-CR solution (in which the materials were incubated). The CR anionic diazo dye can stain, among others, such polysaccharides as cellulose (Thongsomboon et al., 2020). Since BC materials used in the current study were already impregnated with the OCT solution, the absorption of SWF-CR could only take place at the expense of the OCT solution release into the exudate. Therefore, the decrease in SWF-CR concentration indicated the exchange of the liquids i.e. OCT solution present in the materials and the exudate. In the case of MBC materials, the decrease in the SWF-CR concentration (reflected by the discoloration of the SWF-CR solution and change in absorbance) after the 8 h of measurements reached the values of 36% and 32% (for OCT-MBC_w and OCT-MBC_d materials, respectively). The most significant decrease was found for the OCT-BC_w material (of 55%), while in the case of the OCT-BC_d material, no significant changes in SWF-CR concentration were observed throughout the entire measurement period (Fig. 3, Fig. 4A). Except for OCT-BC_d material, the measurements which were taken after 1, 3, and 7 days showed comparable trends between different samples, however, only the OCT-BC_w materials reached the maximum level of exchange between the liquids on the day 7 (Fig. 3, Fig. S2). Also within 8 h, the

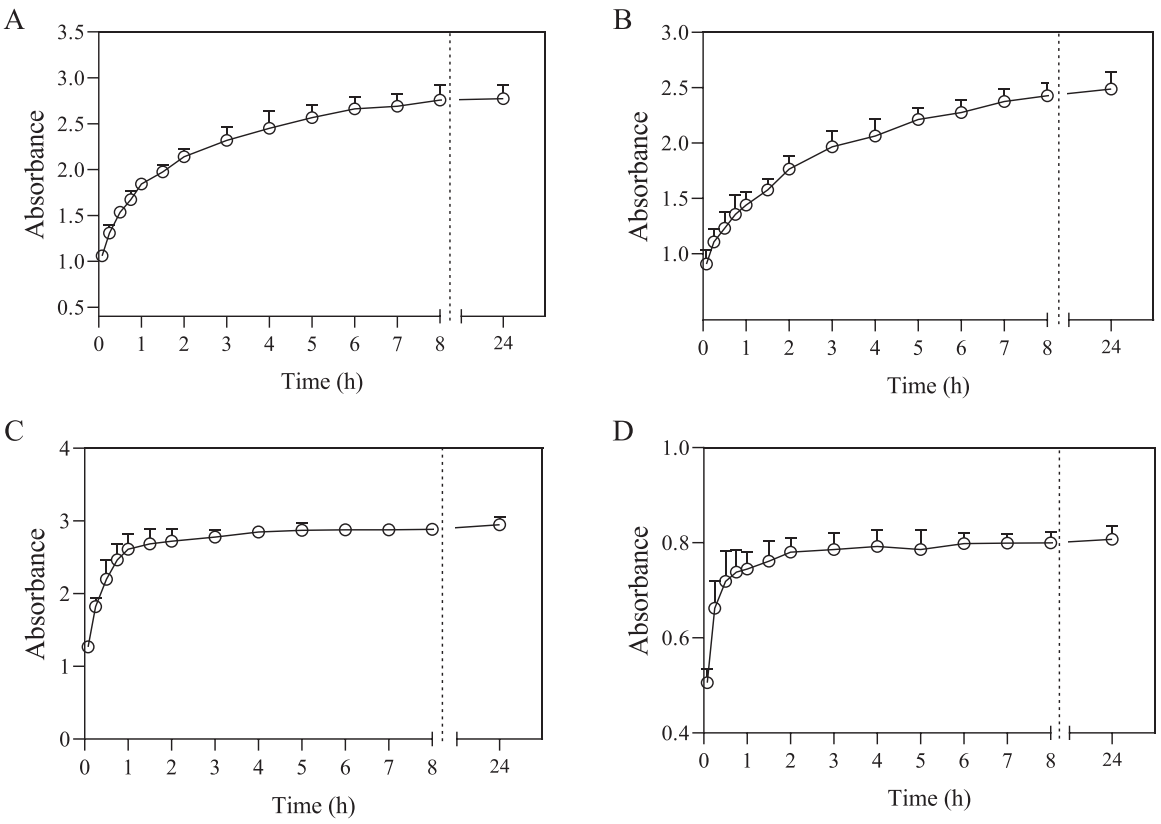

Fig. 5. The kinetics of OCT releasing from MBC and BC materials - short release mode; A - OCT-MBC$_w$; B - OCT-MBC$_d$; C - OCT-BC$_w$; D - OCT-BC$_d$.

OCT-BC$_w$ materials absorbed the exudate more rapidly as compared to the OCT-MBC$_d$ and OCT-MBC$_w$ materials (Fig. 3).

The decrease in SWF-CR with a simultaneous increase in OCT corresponded also with the changes in pH of the solution. The highest value of pH of the exudate was recorded after 7 days of incubation with OCT-BC$_w$ (6.81), followed by OCT-MBC$_w$ (6.56) and OCT-MBC$_d$ materials (6.33). In the case of OCT-BC$_d$ materials, the pH of the solution remained constant throughout the measurement period which resulted from the low OCT content in these samples (Fig. 3).

The results of the exudate absorption capacity revealed that the differences between the OCT-MBC$_w$ and OCT-BC$_w$ materials were significantly lower than between OCT-MBC$_d$ and OCT-BC$_d$ materials. This confirms the key role of the crosslinking process (resulting in the formation of air spaces between subsequent BC layers) in the improvement of the sorption properties of MBC$_d$ as compared to the BC$_d$ materials.

Furthermore, based on the SWF-CR (%) remaining in the solution, the volume of SWF-CR absorbed (mL) by the OCT-MBC and OCT-BC materials was calculated and compared to the average volume of exudate secreted into the wound with a diameter of 2.8 cm, in accordance with World Union of Wound Healing Societies guidelines (WUWHS, 2019). This assessment was performed to determine the time in which the OCT-MBC and OCT-BC materials would be able to absorb the exudate without the need for a dressing change (Fig. 4B). The results indicated that OCT-MBC$_w$ materials would absorb the exudate for approx. 5 days; OCT-MBC$_d$ materials - for approx. 3 days and OCT-MBC$_d$ materials for 7 days. OCT-BC$_d$ materials, due to the low rehydration capacity, showed no ability to absorb the exudate released even after 1 day.

3.3. Release rate of OCT

The kinetics and duration of the release of active substances from porous carriers, including BC materials, depend on their porosity (including the size of pores and their distribution), specific surface area, and swelling capacity (Adepu and Khandelwal, 2020). Currently, research on wound dressings focuses on the design of sustained-release materials to ensure an adequate concentration of the active substances (e.g. antimicrobials) throughout the whole treatment period (Gámez-Herrera et al., 2020). The scope of research concerning modifications of BC materials to obtain an extended-release of antimicrobials has thus far been limited to its oxidation (Solomevich et al., 2020; Inoue et al., 2020) or formation of composites (Shah et al., 2013; Rajwade et al., 2015; Volova et al., 2018). In the current study, the BC materials were modified using widely available, safe reagents in a relatively simple, one-step process. It was shown that despite the differences in the volumes of OCT that were released from OCT-MBC and OCT-BC materials, there were two distant patterns of its short release profile – one characteristic for modified materials (OCT-MBC$_w$ and OCT-MBC$_d$) and the other one for unmodified materials (OCT-BC$_w$ and OCT-BC$_d$). In the case of OCT-MBC materials, thanks to their specific layered structure and numerous cavities, a sustained release of OCT throughout the experiment was observed with no apparent rapid increase in its concentration at any time point of the measurements (Fig. 4A,B). Contrary, OCT-BC materials, regardless of their hydration state, were characterized by a high rate of OCT release within the first hour. Then, within the next 4 h, the trend of OCT release stabilized and remained at a constant level until the end of the experiment (Fig. 4C,D). These observations are consistent with the reports of other authors on the releasing kinetics of bioactive substances from the BC (Moritz et al., 2014; Alkhatib et al., 2017; de Mattos et al., 2020). Moritz et al. (2014) investigated the release of octenidine from the never-dried, unmodified BC and, as in our

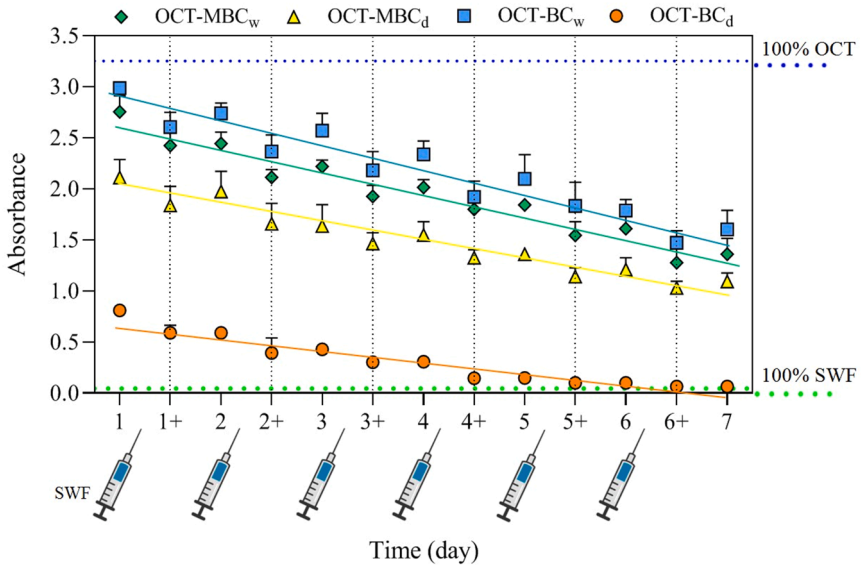

Fig. 6. The kinetics of OCT releasing from MBC and BC materials - long release mode.

research, also showed the rapid release of this antiseptic during the first 8 h. The initial burst release of liquid substances from the never-dried BC materials (i.e. OCT-BC$_w$) is determined, to the greatest extent, by the material's morphology and the volume of liquid trapped in the network of intertwined fibers, which weight does not exceed 1% of the total weight of the material (Hanna et al., 2020). On the other hand, in the case of the rehydrated BC materials (i.e. OCT-BC$_d$), the initial burst release rate may be related to the flattening of the layered network of cellulose fibers, which occurs in the drying process. In consequence, such materials of homogenous structure are in fact not impregnated but "covered" with the liquid, so during release, they drain off rapidly. Such a rapid release of drugs (i.e. antimicrobial solution), resulting in their high concentration, is considered a harmful phenomenon concerning the wound healing - irritating and damaging the tissue (Hanna et al., 2020; Solomevich et al., 2020) and also impairing the process of wound granulation and epithelialization (Hirsch et al., 2010).

In the long release mode experiment, all materials released OCT, and therefore its concentration increased in the artificial wound bed after 12 h, as compared to the concentration measured immediately after each SWF injection. In the case of OCT-BC$_d$ materials, the OCT concentration in SWF solution was increasing only for 3 days, while in the case of the remaining materials – for 7 days (entire experiment period) (Fig. 5). Moreover, the trends in the release/dilution curve for OCT-MBC$_w$, OCT-MBC$_d$, and OCT-BC$_w$ materials did not differ among themselves significantly (Fig. 5).

Although native BC has been extensively investigated in recent years, also in the context of its applicability as a dressing or drug delivery system, there are just a few long-term release studies (>48 h). An exception is a work of Alkhatib et al. (2017) in which the octenidine release profile was studied for 8 days using the native BC and BC/poloxamer hybrid carriers. According to those authors' reports, the native BC released octenidine for 48 h, while the BC/poloxamer, depending on the concentration and type of poloxamer used, for 96–196 h. However, it is also worth noting, that the addition of poloxamers caused a significant decrease in liquid absorption and retention capacity of the BC/poloxamer composite.

Values marked with "+ " on the X-axis indicate the measurements immediately after the SWF injection. The blue dotted line indicates absorbance for 100% OCT solution; the green dotted line indicates absorbance for 100% SWF solution; After each day, 1.5 mL of SWF was added to the artificial wound bed (marked with a syringe).

3.4. Determination of the BC material's antimicrobial activity

3.4.1. Disc diffusion method

In the case of the standard variant of the disc diffusion test

Table 2
Growth inhibition zones (mm) of staphylococci around OCT-MBC and OCT-BC materials depending on the subsequent transfers.

	Transfer	*S. aureus* (ATCC 6538)	*S. aureus*	*S. equorum*	*S. warneri*	*S. xylosus*
OCT-MBC$_w$	1	42 ± 5	52 ± 9	90 ± 0	65 ± 8	62 ± 6
	4	30 ± 4	31 ± 5	36 ± 4	39 ± 5	35 ± 8
	8	26 ± 2	22 ± 5	49 ± 8	35 ± 5	35 ± 6
	9	25 ± 2	30 ± 4	40 ± 7	29 ± 3	42 ± 8
OCT-MBC$_d$	1	39 ± 7	40 ± 5	56 ± 8	31 ± 3	40 ± 7
	4	28 ± 3	29 ± 3	24 ± 6	25 ± 4	34 ± 6
	8	22 ± 4	22 ± 3	37 ± 4	36 ± 6	41 ± 5
	9	20 ± 3	26 ± 4	36 ± 4	27 ± 7	41 ± 5
OCT-BC$_w$	1	62 ± 6	90 ± 0	90 ± 0	65 ± 7	66 ± 6
	4	23 ± 2	21 ± 3	45 ± 4	26 ± 5	33 ± 2
	8	20 ± 1	17 ± 2	35 ± 5	20 ± 4	25 ± 1
	9	18 ± 1	23 ± 4	31 ± 3	20 ± 3	24 ± 3
OCT-BC$_d$	1	19 ± 3	35 ± 6	40 ± 7	40 ± 3	35 ± 5
	4	15 ± 0	16 ± 2	16 ± 2	16 ± 4	16 ± 3
	8	15 ± 0	15 ± 1	15 ± 0	15 ± 0	15 ± 0
	9	15 ± 0	17 ± 4	16 ± 1	15 ± 0	15 ± 0

Table 3
Growth inhibition zones (mm) of pseudomonas around OCT-MBC and OCT-BC materials depending on subsequent transfers.

	Transfer	*P. aeruginosa*				
		(ATCC 15442)	1	2	3	4
OCT-MBC_w	1	25 ± 6	25 ± 4	18 ± 3	19 ± 2	19 ± 4
	4	21 ± 1	20 ± 2	15 ± 0	15 ± 0	16 ± 4
	8	17 ± 4	18 ± 2	15 ± 0	15 ± 0	15 ± 0
	9	20 ± 2	16 ± 3	15 ± 0	15 ± 0	15 ± 0
OCT-MBC_d	1	23 ± 4	24 ± 4	16 ± 0	16 ± 2	17 ± 3
	4	18 ± 4	17 ± 3	15 ± 0	15 ± 0	15 ± 0
	8	16 ± 2	16 ± 1	15 ± 0	15 ± 0	15 ± 0
	9	16 ± 2	16 ± 3	15 ± 0	15 ± 0	15 ± 0
OCT-BC_w	1	24 ± 4	28 ± 1	24 ± 3	17 ± 3	25 ± 4
	4	15 ± 0	15 ± 0	15 ± 0	16 ± 1	16 ± 3
	8	15 ± 0	15 ± 0	15 ± 0	15 ± 0	15 ± 0
	9	16 ± 2	15 ± 0	15 ± 0	15 ± 0	15 ± 0
OCT-BC_d	1	15 ± 0	15 ± 0	15 ± 0	15 ± 0	15 ± 0
	4	–	–	–	–	–
	8	–	–	–	–	–
	9	–	–	–	–	–

(continuous overnight incubation of bacterial cultures together with the OCT-impregnated materials) performed in the *S. aureus* cultures with the use of OCT-MBC materials, zones of growth inhibition with diameters of 42 and 38 mm (for OCT-MBC_w and OCT-MBC_d materials, respectively) were observed. The largest growth inhibition zones were observed as a result of the use of OCT-BC_w materials (45 mm), while for OCT-BC_d materials, zones with a diameter of 29 mm were recorded (Fig. 6, Tab. S2). In turn, in the *P. aeruginosa* cultures incubated with OCT-MBC_w, OCT-MBC_d and OCT-BC_w materials, there was no difference between the growth inhibition diameters (they all were 30 mm). In contrast, in cultures treated with the OCT-BC_d materials, the inhibition zones did not exceed 18 mm.

In the case of the modified disc diffusion test performed in the cultures with different species of staphylococci, the inhibition zones obtained after 1st application of the OCT-MBC materials (transfer 1) were 42–90 mm (OCT-MBC_w) and 31–56 mm (OCT-MBC_d). It is worth noting, that only after transfer 1 the average zones of growth inhibition for both OCT-MBC materials were smaller as compared to the OCT-BC_w materials (62–90 mm), whereas, after the remaining transfers, zones were larger (Table 2, Fig. S6-S10). In contrast, for OCT-BC_d materials, zones of growth inhibition with a diameter of 19–40 mm were recorded after transfer 1, with a significant decrease to 15–17 mm after the remaining transfers (Table 2, Fig. S6-S10). After transfer 9, depending on the bacterial strain, zones with a diameter of 25–42 mm for OCT-MBC_w materials and 20–41 mm for OCT-MBC_d materials were recorded, while for OCT-BC_w and OCT-BC_d materials, they were 18–31 mm and 15–17 mm, respectively. This provides evidence of prolonged OCT release, and hence extended bactericidal efficiency of the modified BC materials.

For *P. aeruginosa* cultures, the largest zones of growth inhibition were observed after transfer 1 (all materials), after which, in the case of OCT-BC_d materials, no growth inhibition was recorded, whereas for the remaining materials, only limited growth of bacteria only in the area directly under the material was spotted (Table 3, Fig. S11-S15). The exceptions were the results obtained in *P. aeruginosa* reference strain and isolate no.1 for the MBC_w and MBC_d materials, where zones of growth inhibition around these materials were observed also after transfer 4, 8, and 9 (16–21 mm and 16–18 mm, respectively).

3.4.2. Planktonic cells

The critical level of bacteria leading to infection is defined as 10^4-10^5 CFU per 1 g of wound tissue. If the number of bacteria rises above this level, the probability of infection increases significantly due to the fact that the host's immune system may no longer be able to control the proliferating microbes under these conditions (Farhan and Jeffery, 2021; Alves et al., 2021). For this reason, in the test of antimicrobial efficiency of OCT-MBC and OCT-BC materials against planktonic cells,

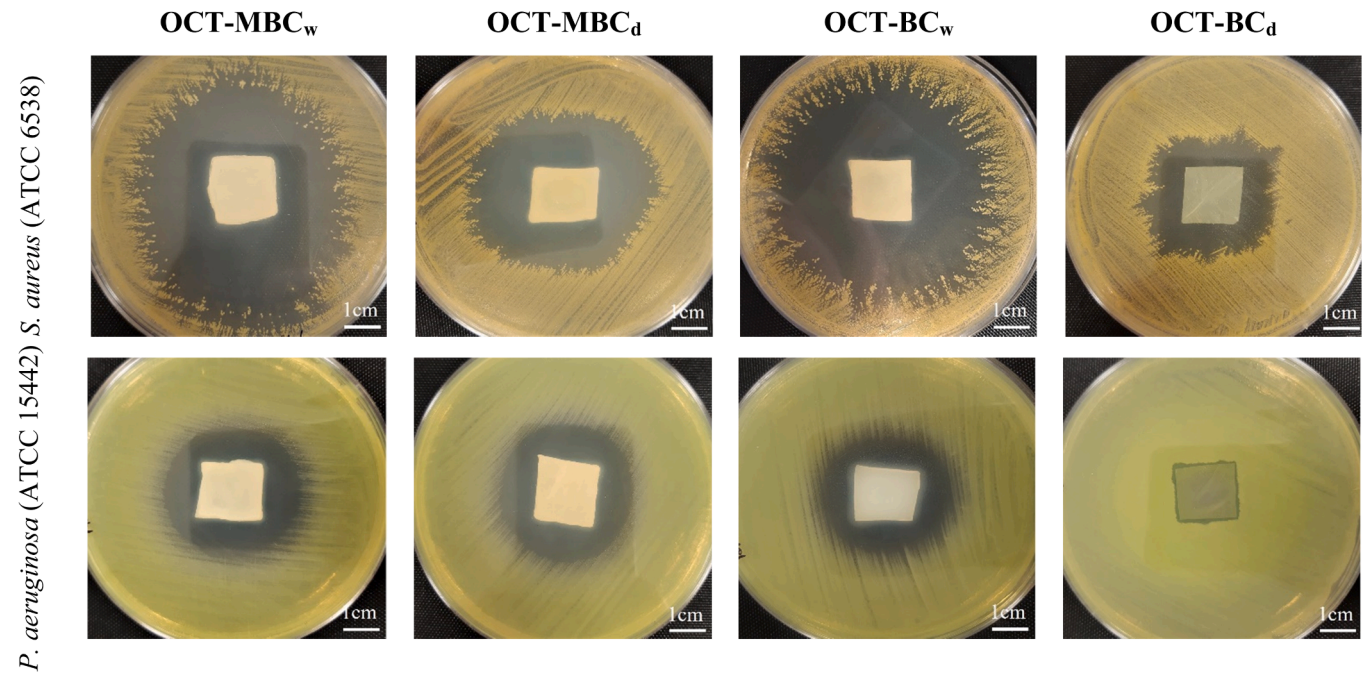

Fig. 7. Growth inhibition zones in *S. aureus* and *P. aeruginosa* cultures around OCT-MBC and OCT-BC materials.

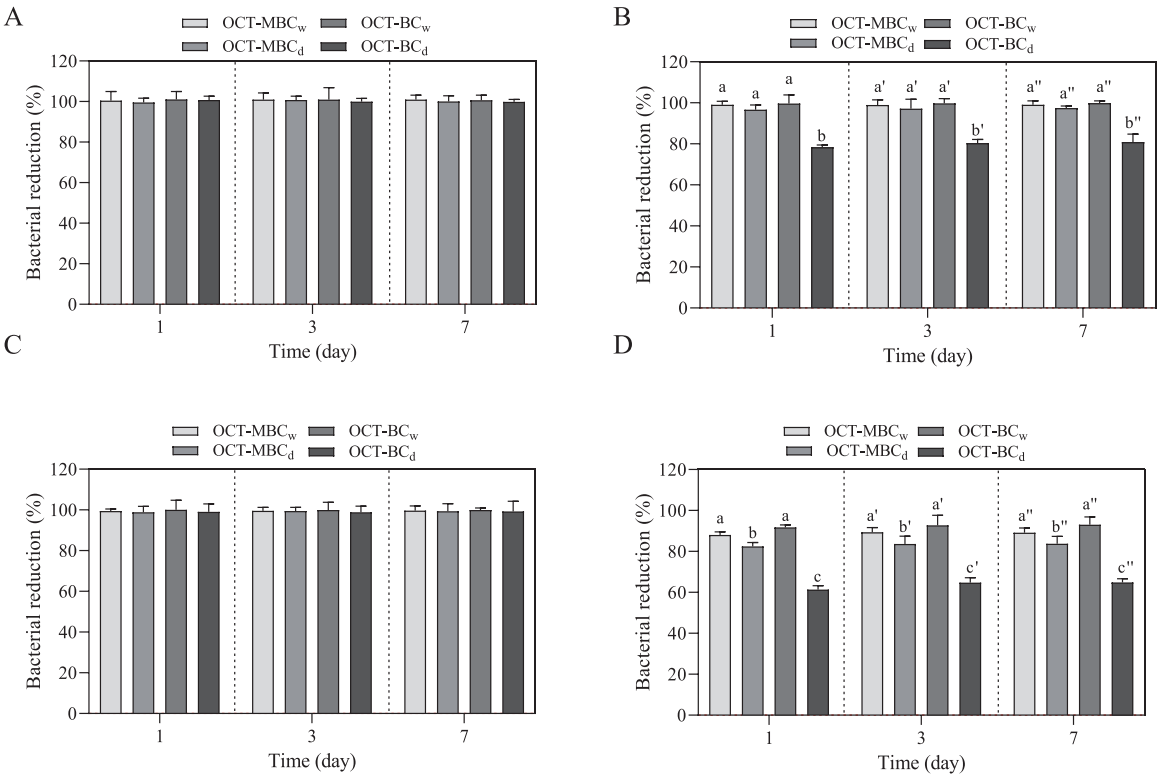

Fig. 8. Percentage of bacterial reduction after 1, 3, and 7 days of incubation for *S. aureus* (A, B) and *P. aeruginosa* (C, D), for cultures with a density of 10^5 CFU/mL (A, C) and 10^8 CFU/mL (B, D). Different letters indicate statistical differences ($p < 0.05$) between different materials.

bacterial cultures with an initial density of 10^5 CFU/mL and 10^8 CFU/mL were used to reflect the spread of the infection.

It was shown that regardless of the bacterial species and the incubation time, in the case of a culture of an initial density of 10^5 CFU/mL, both OCT-MBC and OCT-BC materials showed 100% antibacterial efficiency (Fig. 7A,C). However, in the case of *S. aureus* culture with an initial density of 10^8 CFU/mL, the OCT-BC$_d$ materials caused a significantly lower bacterial reduction (%) throughout the whole experiment (78–81%) as compared to the other materials, which retained the antibacterial efficiency above 95% (Fig. 7B). For *P. aeruginosa* suspension, lower values of reduction were obtained as compared to the *S. aureus*, however, the trend for the OCT-BC$_d$ materials was maintained (with results ranging between 60% and 65%). Compared to *S. aureus*, the degree of bacterial reduction in *P. aeruginosa* suspension caused by OCT-MBC and OCT-BC materials was lower by approx. 7–16% (depending on the analyzed material) (Fig. 7D).

3.4.3. Biofilms

Initially, it was confirmed that both investigated bacterial species were able to form biofilm structures on the gauzes prepared for the experimental settings applied. As proven through SEM (Fig. 8A,B) both microbial species formed adhered multi-cellular structures meeting the established criteria of biofilm formation, whereas the MTT assay showed a distribution of bacterial cells over the entire surface of the gauze (Fig. S16). After proving the presence of biofilms on the gauzes, we performed a series of experiments to investigate the antibiofilm activity of OCT-impregnated dressing materials.

To investigate the antibiofilm effectiveness of OCT-MBC and OCT-BC materials we constructed an in vitro model of a wound infected with biofilm-forming bacteria. Such models in different variants have already been used by other authors (Kucera et al., 2014; He et al., 2021). Because of the variety of species potentially infecting the factual wound, also the artificial wound bed should allow both Gram-positive and Gram-negative bacteria to proliferate in. (He et al., 2021). In the present study, TSA medium containing 4% agar was chosen, based on other reports on the matter (Chen et al., 2021; Alves et al., 2018). Additionally, the Teflon mat was applied as an artificial barrier that an intact epidermis would represent in vivo.

The results showed that OCT-MBC$_w$, OCT-MBC$_d$, and OCT-BC$_w$ materials caused a substantial reduction of both, *S. aureus* and *P. aeruginosa* biofilm-forming bacterial cells (Fig. 8C,D). In the case of *S. aureus*, bacterial reduction (%) after 24 h exceeded 96%, (there were no statistically significant differences between different materials) and it changed only slightly after 3 days (93–99%, depending on the type of the material) (Fig. 8C). Statistically significant differences between the results obtained for different materials were found only after 7 days of the experiment - OCT-MBC$_w$ - 89%, OCT-MBC$_d$ - 71%, and OCT-BC$_w$ - 93%. In contrast, OCT-BC$_d$ materials were characterized by a significantly lower percentage of bacterial reduction (<45% on the 1st and 3rd day of the experiment). Moreover, on the 7th day, the number of bacteria in biofilms incubated with OCT-BC$_d$ materials was even higher compared to the control (biofilm gauzes incubated without any dressing material), which proves the lack of sufficient concentration of antimicrobial reaching the biofilm. In the case of the settings with biofilm formed by *P. aeruginosa*, only slightly lower percentages of the bacterial reduction after 1st and 3rd day of incubation with the OCT-impregnated materials were recorded as compared to the results obtained for *S. aureus* biofilms. However, on day 7, the strongest bacterial reduction was found for OCT-MBC$_w$ (86%), then for the OCT-BC$_w$ (82%) and the OCT-MBC$_d$ materials (69%) (Fig. 8D). Similarly to *S. aureus* biofilms, OCT-BC$_d$ materials were characterized by the lowest antibiofilm activity throughout the whole experiment. Regardless of the contact time or bacterial species, no statistically significant differences were found between the OCT-MBC$_w$ and OCT-BC$_w$ materials. In contrast, in the case of the OCT-MBC$_d$ and OCT-BC$_d$ materials, the differences were significant at each time point of the bacterial viability measurements. Importantly, the results of antibiofilm analyses corresponded to the results obtained in the OCT releasing study (Fig. 4, Tab. S3).

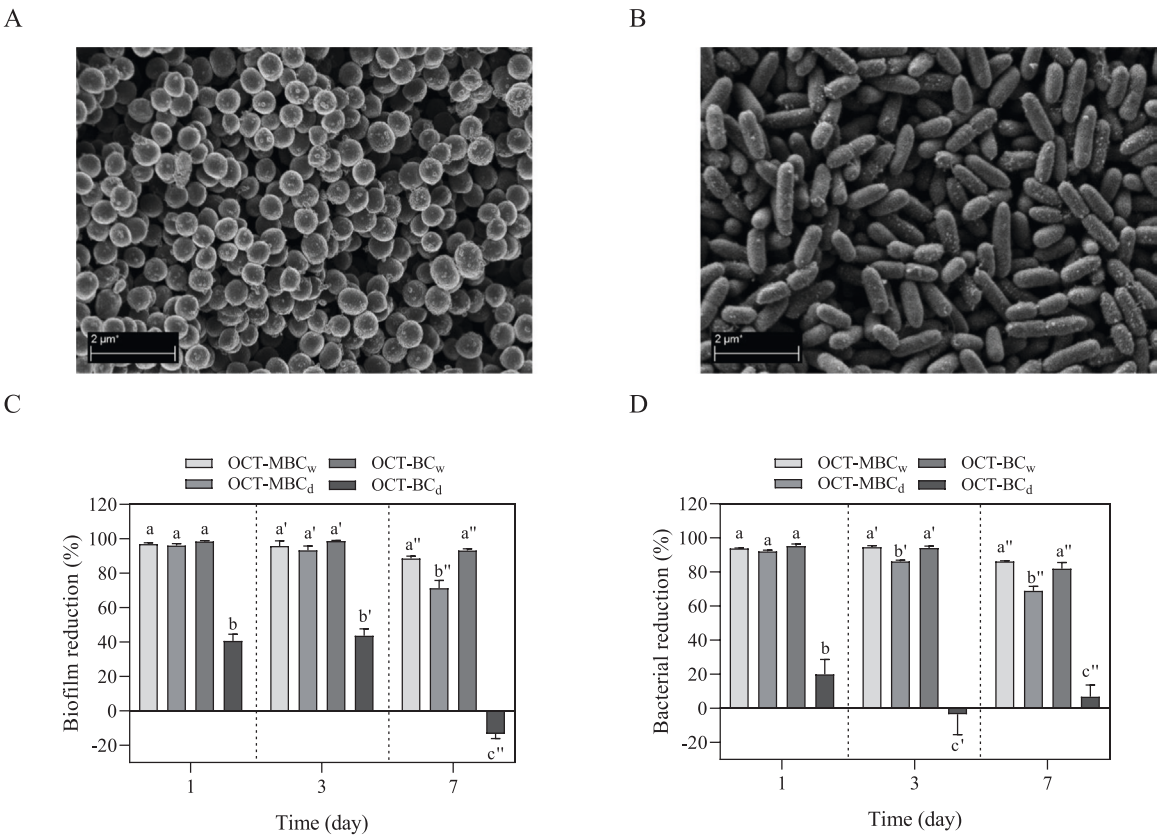

Fig. 9. A, B - Scanning electron microscopy images of *S. aureus* and *P. aeruginosa* biofilms, respectively. C, D - Percent of biofilm reduction after 1, 3, and 7 days of experiment for *S. aureus* and *P. aeruginosa,* respectively. Different letters indicate statistical differences ($p < 0.05$) between different materials.

Although there are numerous works concerning the use of BC combined with different antimicrobial substances as an antibacterial wound dressing, most of these reports describe the effect on liquid cultures rather than on bacteria in the form of a biofilm (Zhang et al., 2020; de Mattos et al., 2020; Shahriari-Khalaji et al., 2020; Moritz et al., 2014). Moreover, in the context of antimicrobial and/or antibiofilm activity, most authors described the use of BC-based composites rather than the BC in the native form (He et al., 2021; Zhang et al., 2020). As an example, Zmejkoski et al. (2021) evaluated the antibiofilm activity of BC composites with chitosan and chitosan nanoparticles obtained by gamma radiation and showed, that after 24 h, the bacterial reduction achieved 58–78% for *S. aureus* and 78–83% for *P.aeruginosa*, depending on the composite variant used. In turn, Zhang et al. (2020) used BC/tannic acid composites combined with $MgCl_2$ (BC-TA-Mg) in different solutions. In total, 4 variants of composites were tested, and the measurements were performed at 3 time points - 12, 24, and 48 h. In the case of *S. aureus*, the highest percentages of biofilm reduction were obtained after 12 h (approx. 80%), while after 24 h reduction decreased to 70%. In the case of *P. aeruginosa*, the highest results were obtained after 24 and 48 h (approx. 80%) (Zhang et al., 2020). Therefore, it can be assumed that the OCT-MBC and OCT-BC_w materials were characterized by high antibiofilm activity (despite the differences in the volume of the absorbed OCT), which was maintained for 7 days. Moreover, there were no statistically significant differences between OCT-MBC_w and OCT-BC_w materials during the whole experiment (for both tested species of bacteria), as well as between OCT-MBC_d and OCT-BC_w materials after 1 day for *S. aureus* and after 3 days for *P. aeruginosa.*

3.5. Assessment of cytotoxicity

In the case of both, extract and direct contact assays, none of the tested materials resulted in viability below 70%, which is the threshold for cytotoxicity according to ISO 10993–5 (Fig. 9A). The obtained results of the viability assay were confirmed by fluorescence microscopy (Fig. 9B), where only live cells (stained green with Syto 9) were observed. The results confirmed that both, the use of a medium for BC biosynthesis provided with leftover sources (potato juice) and the crosslinking modification in the presence of citric acid and catalysts did not result in cytotoxicity of the obtained materials, which is consistent with our previous studies (Ciecholewska-Juśko et al., 2021a, 2021b), as well as research of other authors (Gyawali et al., 2010; El Fawal et al., 2018).

To summarize, in the current study, for the first time the BC modified by chemical crosslinking reaction (in a wet and dry state) was compared to the never-dried and dry native BC in the context of use as a dressing material for infected, highly-exuding wounds.

The native, never-dried BC, (marked in this work as BC_w materials) has previously been considered an antibacterial dressing material (Moritz et al., 2014; Zheng et al., 2020). The main limitations of the use of this material are the absorption and release profiles of liquids (including antimicrobials), showing the rapid course of these processes in the first hours. In some cases, this may cause an initial accumulation of the active substance, which is perceived as harmful and may be irritating to surrounding tissues (Hanna et al., 2020; Solomevich et al., 2020). On the other hand, OCT-BC_w materials provide a moist environment recommended in the healing process, and due to a large volume of absorbed OCT, it shows high antibiofilm activity for up to 7 days. Dry BC is also well characterized in the literature, where its favorable properties related to mechanical strength, the safety of use, and biodegradability are raised (Wei et al., 2011; Portela et al., 2019). However, as shown in the present study, the absorption capacity of this material is too low to provide adequate absorption in the case of highly-exuding wounds, or a sufficient volume of active substance to ensure long-term antibacterial activity.

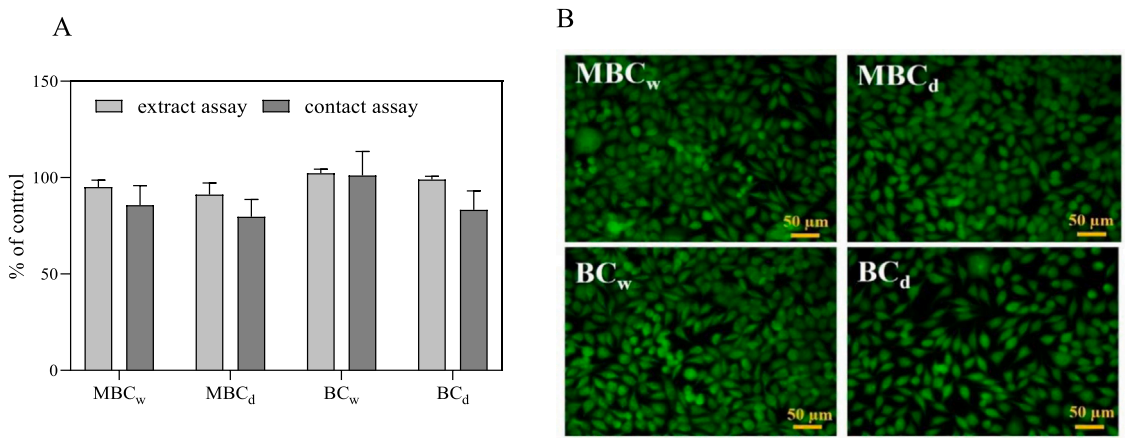

Fig. 10. The viability (A); and fluorescence live/dead visualization (B) of L929 fibroblasts exposed to MBC and BC materials.

	OCT-MBC_w	OCT-MBC_d	OCT-BC_w	OCT-BC_d
Non-toxicity	✓	✓	✓	✓
Fit and adherence to the wound	✓	✓	✓	✗
High exudate absorption capacity	✓	✓	✓	✗
Sustained release of OCT	✓	✓	✗	✗
High antimicrobial and antibiofilm activity	✓	✓	✓	✗
Possibility of unlimited storage time before impregnation with OCT	✗	✓	✗	✓

Fig. 11. Selected properties of OCT-MBC and OCT-BC materials.

Thanks to the modification process, OCT-MBC materials were characterized by improved, prolonged absorption and release profiles. The sustained release of antimicrobials from a carrier is especially important in the context of infected wounds, where the key goal for the proper course of the wound healing process is to maintain an effective concentration of the drug and also to sequester the abundant volumes of wound fluids (Gámez-Herrera et al., 2020). In the case of OCT-MBC materials, the sustained release of OCT was achieved thanks to its sponge-like structure containing numerous internal spaces and air bubbles. Such properties of the MBC materials resulted in a slower loss of moisture, as well as slower release of the antiseptic into the artificial wound bed (as compared to the unmodified BC materials) while maintaining high antimicrobial and antibiofilm activity.

The comprehensive approach to the characteristics of the MBC materials, performed in the current study, allowed us to conclude that these materials meet all of the most important requirements set for dressings intended to be applied on the infected and highly-exuding wounds (Fig. 10) (Dabiri et al., 2016). In addition, the use of MBC materials creates a possibility of controlled impregnation and thus optimization of the sustained antimicrobial release process, which allows the formation of dressing materials dedicated to specific patients. Such personalized treatment methods are now considered one of the main factors that guarantee the success of wound healing (Moritz et al., 2014; Teoh et al., 2022).

In addition to the macromorphological features and physicochemical properties that should be represented by dressing materials, much attention is paid to the direct and indirect costs associated with the treatment of chronic, difficult-to-heal wounds (Weller et al., 2020; Sen, 2019; Cheng et al., 2018). In this context, the MBC_d (as well as BC_d) as dry materials, can be stored for virtually unlimited time, significantly decreasing the economic cost related to its preservation. One of the factors significantly limiting the application of BC materials in large-scale production is also the cost of its synthesis with the use of the conventional, microbiological H-S medium. Therefore, in the current

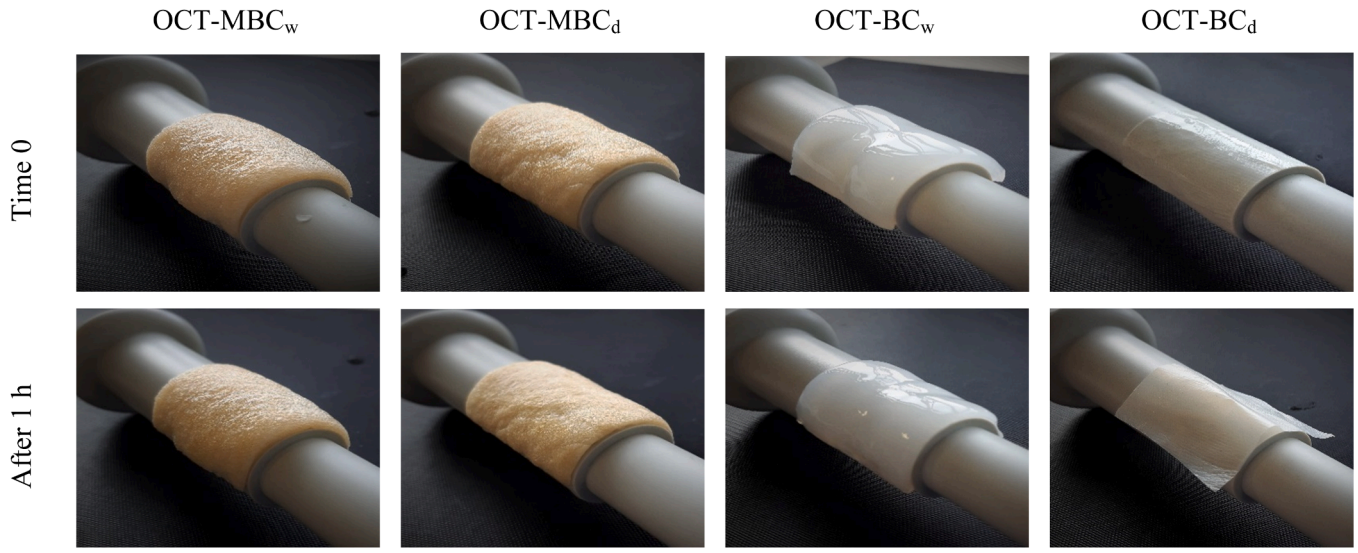

Fig. 12. Formability of OCT-MBC and OCT-BC materials.

study, we took advantage of our previous discovery indicating that potato juice (a leftover of the starch industry) is a convenient source of nutrients for cellulose biosynthesis by *K. xylinus* bacteria and enables large-scale production of BC without the costs incurred on culture media. The use of such a medium is safe and does not change the morphological or physicochemical properties of the produced cellulose (Ciecholewska-Juśko et al., 2021b), and it is profitable not only from an economic but also from the ecological point of view (Treesuppharat et al., 2017).

To further assess the significance of our findings, we evaluated the tested materials in terms of adhesion. For this purpose, we placed OCT-MBC and OCT-BC materials (5 ×5 cm) on a polypropylene roll with a diameter of 3 cm and observed them for 1 h (Fig. 11). During this time, different materials, including those based on BC, were loosening their moisture in the most abrupt manner, which can result in deformation or/and weakening of adhesion (Shah et al., 2013; Rajwade et al., 2015; Solomevich et al., 2020). Importantly, the proper adhesion is an important feature of dressings in the direct contact with the wound, also due to the location of wounds e.g., in the bends of the limbs. It was shown that both OCT-MBC, as well as OCT-BC_w materials, exhibited good adherence to the bent surface, whereas OCT-BC_d materials deformed and stopped adhering to the edges of the polypropylene roll within a 1 h due to the short drying time.

Finally, considering the complex nature of the wound environment and the fact that infection is most often the result of the coexistence of many types of bacteria (and also the underlying comorbidities of the patient), it is necessary to conduct further studies on multispecies biofilm and finally to perform the in vivo studies. Fig. 12.

At this stage of the investigation, the promising properties of modified BC materials, fortified with OCT antiseptic were shown explicitly. Already in 2003, the European societies of wound professionals proposed the algorithm referred to as the T.I.M.E., which covered the major factors of the efficient management of chronic wounds, namely: T - tissue; I - infection/inflammation; M - moisture, and E - edges/epithelialization (Schultz et al., 2004). The efficient dressing, intended for use in chronic wounds, should be compliant with the above-mentioned factors. The modified BC dressing materials presented in this study, display the desirable properties concerning all pillars of the algorithm - these related to the patient's tissue ("T" and "E") because they show no cytotoxicity against fibroblasts; concerning the pillar related to exudate ("M") as the dressings can sequester the abundance of liquid and maintain the proper moisture of wound, and finally with the pillar related with microorganisms, as the modified BC materials can release the antiseptic in the desired, prolonged mode. The concept of T.I.M.E., although commonly applied by wound professionals, has been also criticized for its tendency to focus mainly on the wound, neglecting at the same time the wider issues related to the patient and its surrounding (Moore et al., 2019). Therefore, the BC materials used in the current work were synthesized using a safe, ecological and cost-effective medium. In conclusion, although the aforementioned in vivo tests are required, the modified BC materials characterized in the current work, at the present stage of the investigation, meet all the expectations for the T.I.M.E.-compliant dressing intended for use in the highly-exuding, biofilm-infected chronic wounds.

Declaration of Competing Interest

The authors declare that they have no known competing financial interests or personal relationships that could have appeared to influence the work reported in this paper.

Acknowledgments

The present work was financially supported by the National Science Centre in Poland (Grant No. 2017/27/B/NZ6/02103, Opus 14, granted to Karol Fijałkowski).

CRediT authorship contribution statement

Daria Ciecholewska-Juśko: Conceptualization, Methodology, Investigation, Visualization, Formal analysis, Writing – original draft. **Adam Junka**: Writing – original draft, Writing – review & editing. **Karol Fijałkowski**: Conceptualization, Project administration, Funding acquisition, Writing – review & editing, Supervision. All the authors have reviewed the manuscript.

Appendix A. Supporting information

Supplementary data associated with this article can be found in the online version at doi:10.1016/j.micres.2022.127125.

References

Adepu, S., Khandelwal, M., 2020. Ex-situ modification of bacterial cellulose for immediate and sustained drug release with insights into release mechanism. Carbohydr. Polym. 249, 116816 https://doi.org/10.1016/j.carbpol.2020.116816.

Alam, W., Hasson, J., Reed, M., 2021. Clinical approach to chronic wound management in older adults. J. Am. Geriatr. Soc. 69 (8), 2327–2334. https://doi.org/10.1111/jgs.17177.

Alavi, A., Sibbald, R.G., Mayer, D., Goodman, L., Botros, M., Armstrong, D.G., Woo, K., Boeni, T., Ayello, E.A., Kirsner, R.S., 2014. Diabetic foot ulcers: Part II. Management. J. Am. Acad. Dermatol. 70 (1) https://doi.org/10.1016/j.jaad.2013.07.048.

Alkhatib, Y., Dewaldt, M., Moritz, S., Nitzsche, R., Kralisch, D., Fischer, D., 2017. Controlled extended octenidine release from a bacterial nanocellulose/Poloxamer hybrid system. Eur. J. Pharm. Biopharm. 112, 164–176. https://doi.org/10.1016/j.ejpb.2016.11.025.

Alves, D.R., Booth, S.P., Scavone, P., Schellenberger, P., Salvage, J., Dedi, C., Thet, N.T., Jenkins, A.T.A., Waters, R., Ng, K.W., Overall, A.D.J., Metcalfe, A.D., Nzakizwanayo, J., Jones, B.V., 2018. Development of a high-throughput ex-vivo burn wound model using porcine skin, and its application to evaluate new approaches to control wound infection. Front. Cell. Infect. Microbiol. 8, 196. https://doi.org/10.3389/fcimb.2018.00196.

Alves, P.J., Barreto, R.T., Barrois, B.M., Gryson, L.G., Meaume, S., Monstrey, S.J., 2021. Update on the role of antiseptics in the management of chronic wounds with critical colonisation and/or biofilm. Int. Wound J. 18 (3), 342–358. https://doi.org/10.1111/iwj.13537.

Armstrong, D.G., Bauer, K., Bohn, G., Carter, M., Snyder, R., Serena, T.E., 2020. Principles of best diagnostic practice in tissue repair and wound healing: an expert consensus. Diagnostics 11, 50. https://doi.org/10.3390/diagnostics11010050.

Bayer, A.S., Speert, D.P., Park, S., Tu, J., Witt, M., Nast, C.C., Norman, D.C., 1991. Functional role of mucoid exopolysaccharide (alginate) in antibiotic-induced and polymorphonuclear leukocyte mediated killing of Pseudomonas aeruginosa. Infect. Immun. 59, 302–308 https://doi.org/10.1128%2Fiai.59.1.302-308.1991.

Bazbouz, M.B., Tronci, G., 2019. Two-layer electrospun system enabling wound exudate management and visual infection response. Sensors 19 (5), 991. https://doi.org/10.3390/s19050991.

Chen, X., Lorenzen, J., Xu, Y., Jonikaite, M., Thaarup, I.C., Bjarnsholt, T., Kirketerp-Møller, K., Thomsen, T.R., 2021. A novel chronic wound biofilm model sustaining coexistence of Pseudomonas aeruginosa and Staphylococcus aureus suitable for testing of antibiofilm effect of antimicrobial solutions and wound dressings. Wound Repair Regen. 29 (5), 820–829. https://doi.org/10.1111/wrr.12944.

Cheng, Q., Gibb, M., Graves, N., Finlayson, K., Pacella, R.E., 2018. Cost-effectiveness analysis of guideline-based optimal care for venous leg ulcers in Australia. BMC Health Serv. Res 18 (1), 1–13. https://doi.org/10.1186/s12913-018-3234-3.

Ciecholewska-Juśko, D., Żywicka, A., Junka, A., Drozd, R., Sobolewski, P., Migdał, P., Kowalska, U., Toporkiewicz, M., Fijałkowski, K., 2021a. Superabsorbent crosslinked bacterial cellulose biomaterials for chronic wound dressings. Carbohydr. Polym. 253, 117247 https://doi.org/10.1016/j.carbpol.2020.117247.

Ciecholewska-Juśko, D., Broda, M., Żywicka, A., Styburski, D., Sobolewski, P., Gorący, K., Migdał, P., Junka, A., Fijałkowski, K., 2021b. Potato juice, a starch industry waste, as a cost-effective medium for the biosynthesis of bacterial cellulose. Int. J. Mol. Sci. 22 (19), 10807. https://doi.org/10.3390/ijms221910807.

Dabiri, G., Damstetter, E., Phillips, T., 2016. Choosing a wound dressing based on common wound characteristics. Adv. Wound Care 5 (1), 32–41. https://doi.org/10.1089/wound.2014.0586.

Dayal, M.S., Catchmark, J.M., 2016. Mechanical and structural property analysis of bacterial cellulose composites. Carbohydr. Polym. 144, 447–453. https://doi.org/10.1016/j.carbpol.2016.02.055.

El Fawal, G.F., Abu-Serie, M.M., Hassan, M.A., Elnouby, M.S., 2018. Hydroxyethyl cellulose hydrogel for wound dressing: Fabrication, characterization and in vitro evaluation. Int. J. Biol. Macromol. 111, 649–659. https://doi.org/10.1016/j.ijbiomac.2018.01.040.

Farhan, N., Jeffery, S., 2021. Diagnosing burn wounds infection: the practice gap & advances with MolecuLight bacterial imaging. Diagnostics 11 (2), 268. https://doi.org/10.3390/diagnostics11020268.

Gámez-Herrera, E., García-Salinas, S., Salido, S., Sancho-Albero, M., Andreu, V., Pérez, M., Luján, L., Irusta, S., Arruebo, M., Mendoza, G., 2020. Drug-eluting wound dressings having sustained release of antimicrobial compounds. Eur. J. Pharm. Biopharm. 152, 327–339. https://doi.org/10.1016/j.ejpb.2020.05.025.

Gyawali, D., Nair, P., Zhang, Y., Tran, R.T., Zhang, C., Samchukov, M., Makarov, M., Kim, H.K.W., Yang, J., 2010. Citric acid-derived in situ crosslinkable biodegradable polymers for cell delivery. Biomaterials 31 (34), 9092–9105. https://doi.org/10.1016/j.biomaterials.2010.08.022.

Han, G., Ceilley, R., 2017. Chronic wound healing: a review of current management and treatments. Adv. Ther. 34 (3), 599–610. https://doi.org/10.1007/s12325-017-0478-y.

Hanna, D.H., Lotfy, V.F., Basta, A.H., Saad, G.R., 2020. Comparative evaluation for controlling release of niacin from protein-and cellulose-chitosan based hydrogels. Int. J. Biol. Macromol. 150, 228–237. https://doi.org/10.1016/j.ijbiomac.2020.02.056.

He, W., Zhang, Z., Chen, J., Zheng, Y., Xie, Y., Liu, W., Wu, J., Mosselhy, D.A., 2021. Evaluation of the anti-biofilm activities of bacterial cellulose-tannic acid-magnesium chloride composites using an in vitro multispecies biofilm model. Regen. Biomater. 8 (6), rbab054. https://doi.org/10.1093/rb/rbab054.

Hirsch, T., Koerber, A., Jacobsen, F., Dissemond, J., Steinau, H.U., Gatermann, S., Al-Benna, S., Kesting, M., Seipp, H.M., Steinstraesser, L., 2010. Evaluation of toxic side effects of clinically used skin antiseptics in vitro. J. Surg. Res. 164 (2), 344–350. https://doi.org/10.1016/j.jss.2009.04.029.

Inoue, B.S., Streit, S., dos Santos Schneider, A.L., Meier, M.M., 2020. Bioactive bacterial cellulose membrane with prolonged release of chlorhexidine for dental medical application. Int. J. Biol. Macromol. 148, 1098–1108. https://doi.org/10.1016/j.ijbiomac.2020.01.036.

Junka, A.F., Żywicka, A., Szymczyk, P., Dziadas, M., Bartoszewicz, M., Fijałkowski, K., 2017. A.D.A.M. test (Antibiofilm Dressing's Activity Measurement) - Simple method for evaluating anti-biofilm activity of drug-saturated dressings against wound pathogens. J. Microbiol. Methods 143, 6–12. https://doi.org/10.1016/j.mimet.2017.09.014.

Krasowski, G., Junka, A., Paleczny, J., Czajkowska, J., Makomaska-Szaroszyk, E., Chodaczek, G., Majkowski, M., Migdał, P., Fijałkowski, K., Kowalska-Krochmal, B., Bartoszewicz, M., 2021. In vitro evaluation of polihexanide, octenidine and NaClO/HClO-based antiseptics against biofilm formed by wound pathogens. Membranes 11, 62. https://doi.org/10.3390/membranes11010062.

Kucera, J., Sojka, M., Pavlik, V., Szuszkiewicz, K., Velebny, V., Klein, P., 2014. Multispecies biofilm in an artificial wound bed-A novel model for in vitro assessment of solid antimicrobial dressings. J. Microbiol. Methods 103, 18–24. https://doi.org/10.1016/j.mimet.2014.05.008.

Lahiri, D., Nag, M., Dutta, B., Dey, A., Sarkar, T., Pati, S., Edinur, H.A., Abdul Kari, Z., Mohd Noor, N.H., Ray, R.R., 2021. Bacterial cellulose: production, characterization, and application as antimicrobial agent Int. J. Mol. Sci. 22 (23), 12984. https://doi.org/10.3390/ijms222312984.

Malic, S., Hill, K.E., Playle, R., Thomas, D.W., Williams, D.W., 2011. In vitro interactions of chronic wound bacteria in biofilms. J. Wound Care 20, 569–577. https://doi.org/10.12968/jowc.2011.20.12.569.

de Mattos, I.B., Nischwitz, S.P., Tuca, A.C., Groeber-Becker, F., Funk, M., Birngruber, T., Mautner, S.I., Kamolz, L.-P., Holzer, J.C., 2020. Delivery of antiseptic solutions by a bacterial cellulose wound dressing: uptake, release and antibacterial efficacy of octenidine and povidone-iodine. Burns 46 (4), 918–927. https://doi.org/10.1016/j.burns.2019.10.006.

Mazeau, K., Wyszomirski, M., 2012. Modelling of Congo red adsorption on the hydrophobic surface of cellulose using molecular dynamics. Cellulose 19 (5), 1495–1506. https://doi.org/10.1007/s10570-012-9757-6.

Moore, Z., Dowsett, C., Smith, G., Atkin, L., Bain, M., Lahmann, N.A., Schultz, G.S., Swanson, T., Vowden, P., Weir, D., Zmuda, A., Jaimes, H., 2019. TIME CDST: an updated tool to address the current challenges in wound care. J. Wound Care 28 (3), 154–161. https://doi.org/10.12968/jowc.2019.28.3.154.

Moritz, S., Wiegand, C., Wesarg, F., Hessler, N., Müller, F.A., Kralisch, D., Hipler, U.C., Fischer, D., 2014. Active wound dressings based on bacterial nanocellulose as drug delivery system for octenidine. Int. J. Pharm. 471 (1–2), 45–55. https://doi.org/10.1016/j.ijpharm.2014.04.062.

Nemati, E., Gholami, A., 2021. Nano bacterial cellulose for biomedical applications: A mini review focus on tissue engineering. AANBT 2(4), 93–101. https://doi.org/10.47277/AANBT/2(4)85.

Nuutila, K., Eriksson, E., 2021. Moist wound healing with commonly available dressings. Adv. Wound Care 10 (12), 685–698. https://doi.org/10.1089/wound.2020.1232.

Omar, A., Wright, J.B., Schultz, G., Burrell, R., Nadworny, P., 2017. Microbial biofilms and chronic wounds. Microorganisms 5, 9. https://doi.org/10.3390/microorganisms5010009.

Paleczny, J., Junka, A., Brożyna, M., Dydak, K., Oleksy-Wawrzyniak, M., Ciecholewska-Juśko, D., Dziedzic, E., Bartoszewicz, M., 2021. The high impact of staphylococcus aureus biofilm culture medium on in vitro outcomes of antimicrobial activity of wound antiseptics and antibiotic. Pathogens 10 (11), 1385. https://doi.org/10.3390/pathogens10111385.

Percival, S.L., McCarty, S.M., Lipsky, B., 2015. Biofilms and wounds: an overview of the evidence. Adv. Wound Care 4 (7), 373–381. https://doi.org/10.1089/wound.2014.0557.

Petrauskaite, O., Gomes, P.D.S., Fernandes, M.H., Juodzbalys, G., Stumbras, A., Maminskas, J., Liesiene, J., Cicciù, M., 2013. Biomimetic mineralization on a macroporous cellulose-based matrix for bone regeneration. Biomed. Res. Int. 2013. https://doi.org/10.1155/2013/452750.

Portela, R., Leal, C.R., Almeida, P.L., Sobral, R.G., 2019. Bacterial cellulose: a versatile biopolymer for wound dressing applications. Microb. Biotechnol. 12 (4), 586–610. https://doi.org/10.1111/1751-7915.13392.

Rajwade, J.M., Paknikar, K.M., Kumbhar, J.V., 2015. Applications of bacterial cellulose and its composites in biomedicine. Appl. Microbiol. Biotechnol. 99 (6), 2491–2511. https://doi.org/10.1007/s00253-015-6426-3.

Riss, T.L., Moravec, R.A., Niles, A.L., Duellman, S., Benink, H.A., Worzella, T.J., Minor, L., 2016. Cell viability assays. In: Markossian, S., Grossman, A., Brimacombe, K., et al. (Eds.), Assay Guidance Manual (Internet). Eli Lilly & Company and the National Center for Advancing Translational Sciences, Bethesda, pp. 1–23.

Schultz, G.S., Barillo, D.J., Mozingo, D.W., Chin, G.A., 2004. Wound Bed Advisory Board Members. Wound bed preparation and a brief history of TIME. Int. Wound J. 1 (1), 19–32. https://doi.org/10.1111/j.1742-481x.2004.00008.x.

Sen, C.K., 2019. Human wounds and its burden: an updated compendium of estimates. Adv. Wound Care 8 (2), 39–48. https://doi.org/10.1089/wound.2019.0946.

Shah, N., Ul-Islam, M., Khattak, W.A., Park, J.K., 2013. Overview of bacterial cellulose composites: a multipurpose advanced material. Carbohydr. Polym. 98 (2), 1585–1598. https://doi.org/10.1016/j.carbpol.2013.08.018.

Shahriari-Khalaji, M., Hong, S., Hu, G., Ji, Y., Hong, F.F., 2020. Bacterial nanocellulose-enhanced alginate double-network hydrogels cross-linked with six metal cations for antibacterial wound dressing. Polymers 12 (11), 2683. https://doi.org/10.3390/polym12112683.

Solomevich, S.O., Dmitruk, E.I., Bychkovsky, P.M., Nebytov, A.E., Yurkshtovich, T.L., Golub, N.V., 2020. Fabrication of oxidized bacterial cellulose by nitrogen dioxide in chloroform/cyclohexane as a highly loaded drug carrier for sustained release of cisplatin. Carbohydr. Polym. 248, 116745 https://doi.org/10.1016/j.carbpol.2020.116745.

Sperotto, G., Stasiak, L.G., Godoi, J.P.M.G., Gabiatti, N.C., De Souza, S.S., 2021. A review of culture media for bacterial cellulose production: complex, chemically defined and minimal media modulations. Cellulose 28 (5), 2649–2673. https://doi.org/10.1007/s10570-021-03754-5.

Sulaeva, I., Henniges, U., Rosenau, T., Potthast, A., 2015. Bacterial cellulose as a material for wound treatment: properties and modifications. A review. Biotechnol. Adv. 33, 1547–1571. https://doi.org/10.1016/j.biotechadv.2015.07.009.

Swingler, S., Gupta, A., Gibson, H., Kowalczuk, M., Heaselgrave, W., Radecka, I., 2021. Recent advances and applications of bacterial cellulose in biomedicine. Polymers 13, 412. https://doi.org/10.3390/polym13030412.

Teoh, J.H., Tay, S.M., Fuh, J., Wang, C.H., 2022. Fabricating scalable, personalized wound dressings with customizable drug loadings via 3D printing. J. Control. Release 341, 80–94. https://doi.org/10.1016/j.jconrel.2021.11.017.

Thongsomboon, W., Werby, S.H., Cegelski, L., 2020. Evaluation of phosphoethanolamine cellulose production among bacterial communities using Congo red fluorescence. J. Bacteriol. 202 (13), e00030–20. https://doi.org/10.1128/JB.00030-20.

Treesuppharat, W., Rojanapanthu, P., Siangsanoh, C., Manuspiya, H., Ummartyotin, S., 2017. Synthesis and characterization of bacterial cellulose and gelatin-based hydrogel composites for drug-delivery systems. Biotechnol. Rep. 15, 84–91. https://doi.org/10.1016/j.btre.2017.07.002.

Ullah, H., Santos, H.A., Khan, T., 2016. Applications of bacterial cellulose in food, cosmetics and drug delivery. Cellulose 23, 2291–2314. https://doi.org/10.1007/s10570-016-0986-y.

Volova, T.G., Shumilova, A.A., Shidlovskiy, I.P., Nikolaeva, E.D., Sukovatiy, A.G., Vasiliev, A.D., Shishatskaya, E.I., 2018. Antibacterial properties of films of cellulose composites with silver nanoparticles and antibiotics. Polym. Test. 65, 54–68. https://doi.org/10.1016/j.polymertesting.2017.10.023.

Volova, T.G., Shumilova, A.A., Nikolaeva, E.D., Kirichenko, A.K., Shishatskaya, E.I., 2019. Biotechnological wound dressings based on bacterial cellulose and degradable copolymer P (3HB/4HB). Int. J. Biol. Macromol. 131, 230–240. https://doi.org/10.1016/j.ijbiomac.2019.03.068.

Wei, B., Yang, G., Hong, F., 2011. Preparation and evaluation of a kind of bacterial cellulose dry films with antibacterial properties. Carbohydr. Polym. 84 (1), 533–538. https://doi.org/10.1016/j.carbpol.2010.12.017.

Weller, C.D., Team, V., Sussman, G., 2020. First-line interactive wound dressing update: a comprehensive review of the evidence. Front. Pharmacol. 11, 155. https://doi.org/10.3389/fphar.2020.00155.

World Union of Wound Healing Societies (WUWHS) Consensus Document. Wound exudate: effective assessment and management, 2019. Wounds International, London.

Wound Care Market Research Report 2021, https://www.researchandmarkets.com/reports/4085102/wound-care-market-research-report-by-product (accessed 28 March, 2022).

Zhang, Z.Y., Sun, Y., Zheng, Y.D., He, W., Yang, Y.Y., Xie, Y.J., Feng, Z.X., Qiao, K., 2020. A biocompatible bacterial cellulose/tannic acid composite with antibacterial and anti-biofilm activities for biomedical applications. Mater. Sci. Eng. C 106, 110249. https://doi.org/10.1016/j.msec.2019.110249.

Zheng, L., Li, S., Luo, J., Wang, X., 2020. Latest advances on bacterial cellulose-based antibacterial materials as wound dressings. Front. Bioeng. Biotechnol. 8, 1334. https://doi.org/10.3389/fbioe.2020.593768.

Zielińska, S., Matkowski, A., Dydak, K., Czerwińska, M.E., Dziągwa-Becker, M., Kucharski, M., Wójciak, M., Sowa, I., Plińska, S., Fijałkowski, K., Ciecholewska-Juśko, D., Broda, M., Gorczyca, D., Junka, A., 2021. Bacterial nanocellulose fortified with antimicrobial and anti-inflammatory natural products from chelidonium majus plant cell cultures. Materials 15 (1), 16. https://doi.org/10.3390/ma15010016.

Zmejkoski, D.Z., Zdravković, N.M., Trišić, D.D., Budimir, M.D., Marković, Z.M., Kozyrovska, N.O., Marković, B.M.T., 2021. Chronic wound dressings–Pathogenic bacteria anti-biofilm treatment with bacterial cellulose-chitosan polymer or bacterial cellulose-chitosan dots composite hydrogels. Int. J. Biol. Macromol. 191, 315–323. https://doi.org/10.1016/j.ijbiomac.2021.09.118.

Żywicka, A., Fijałkowski, K., 2017. Measurement of bacterial adhesion to metal surfaces with different chemical composition-evaluation of different methods. Environ. Biotechnol. 13 (2), 14–22. https://doi.org/10.14799/ebms28.

scientific reports

Check for updates

OPEN

The effects of rotating magnetic field and antiseptic on in vitro pathogenic biofilm and its milieu

Daria Ciecholewska-Juśko[1], Anna Żywicka[1], Adam Junka[2]✉, Marta Woroszyło[1], Marcin Wardach[3], Grzegorz Chodaczek[4], Patrycja Szymczyk-Ziółkowska[5], Paweł Migdał[6] & Karol Fijałkowski[1]✉

The application of various magnetic fields for boosting the efficacy of different antimicrobial molecules or in the character of a self-reliant antimicrobial agent is considered a promising approach to eradicating bacterial biofilm-related infections. The purpose of this study was to analyze the phenomenon of increased activity of octenidine dihydrochloride-based antiseptic (OCT) against *Staphylococcus aureus* and *Pseudomonas aeruginosa* biofilms in the presence of the rotating magnetic field (RMF) of two frequencies, 5 and 50 Hz, in the in vitro model consisting of stacked agar discs, placed in increasing distance from the source of the antiseptic solution. The biofilm-forming cells' viability and morphology as well as biofilm matrix structure and composition were analyzed. Also, octenidine dihydrochloride permeability through biofilm and porous agar obstacles was determined for the RMF-exposed versus unexposed settings. The exposure to RMF or OCT apart did not lead to biofilm destruction, contrary to the setting in which these two agents were used together. The performed analyses revealed the effect of RMF not only on biofilms (weakening of cell wall/membranes, disturbed morphology of cells, altered biofilm matrix porosity, and composition) but also on its milieu (altered penetrability of octenidine dihydrochloride through biofilm/agar obstacles). Our results suggest that the combination of RMF and OCT can be particularly promising in eradicating biofilms located in such areas as wound pockets, where physical obstacles limit antiseptic activity.

The ability to form biofilm is considered one of the most pivotal virulence factors enabling microorganisms adaptation to the environment of the infection site[1]. The biofilm is a highly organized, microbial community containing not only metabolically active but also slow-growing and dormant cells. This multi-cellular society of aggregated microorganisms is enclosed within a self-produced extracellular matrix (ECM). The matrix may account for even 90% of biofilm's dry mass and may consist of proteins, glycoproteins, polysaccharides, and extracellular DNA[1,2] in various proportions. The ECM provides bacteria protection, nutrition source, and the environment in which virulence factors or messenger molecules are interchanged rapidly and effectively. Moreover, bacteria distributed in various layers of ECM display metabolic differentiation. This phenomenon is considered an important component of observed high tolerance (reaching up to 1000 times) of biofilm against various antimicrobial agents compared to planktonic (non-adhered) cells of the same microbial strain[3].

The application of antiseptics (instead of antibiotics) has become successively common in the therapy and prophylaxis of topical, biofilm-related infections, especially these of skin and wounds[4]. The main rationale standing behind it, is antiseptics' mechanism of action, significantly decreasing the risk of resistant strains emergence. As an example, the molecular activity of octenidine dihydrochloride leads to the destruction of cellular walls and membranes, followed by cytoplasmic leakage, enzymatic malfunctions, and cell death, finally.

[1]Department of Microbiology and Biotechnology, Faculty of Biotechnology and Animal Husbandry, West Pomeranian University of Technology, Szczecin, Piastów 45, 70-311 Szczecin, Poland. [2]Department of Pharmaceutical Microbiology and Parasitology, Faculty of Pharmacy, Medical University of Wroclaw, Borowska 211a, 50-534 Wrocław, Poland. [3]Faculty of Electrical Engineering, West Pomeranian University of Technology, Szczecin, Sikorskiego 37, 70-313 Szczecin, Poland. [4]Laboratory of Confocal Microscopy, Łukasiewicz Research Network-PORT Polish Center for Technology Development, Stabłowicka 147, 54-066 Wrocław, Poland. [5]Centre for Advanced Manufacturing Technologies (CAMT/FPC), Faculty of Mechanical Engineering, Wroclaw University of Science and Technology, Łukasiewicza 5, 50-371 Wrocław, Poland. [6]Department of Environment, Hygiene and Animal Welfare, Faculty of Biology and Animal Science, Wroclaw University of Environmental and Life Sciences, Chełmońskiego 38C, 51-630 Wrocław, Poland. ✉email: adam.junka@umed.wroc.pl; karol.fijalkowski@zut.edu.pl

Although modern antiseptics are considered efficient antimicrobials, biofilm communities within chronic wounds are often able to survive the treatment and rebuild their structure within a relatively short time[5]. It is due to not only the aforementioned protective properties of biofilm structure but also due to the specificity of the chronic wound environment itself. The majority of chronic wounds produce an exudate, a turbid cellular fluid that dilutes antiseptic concentration, and also binds antiseptic molecules to proteins and/or blood cells (in the case of so-called "fresh bloody exudate") contained within[6]. Moreover, the topographical irregularities and niches in the wound are used by microbes as a shelter from unfavorable agents (i.e. their active substances cannot reach the site where biofilm develops or they reach there in decreased concentration)[7]. Lastly, such prevalent wound pathogens as *S. aureus*, developed the ability to use host fibrinogen and transform it into fibrin. These fibrin accretions form a physical object referred to as the clot, containing bacteria within it, and protecting them, to a specific extent (depending on the clot size) from antiseptics[8]. Noteworthy, the application of higher concentrations of antiseptics, which would overcome the above-mentioned processes and phenomena, leads to the cytotoxic effect on cells of the wound bed and inhibition of healing[9]. Therefore, the question which should be addressed at this point concerns the possibility of increasing antiseptics' antibiofilm efficacy without an increase in their concentration. Although such a claim seems to be hard to achieve, the application of various types of magnetic fields intended as an agent boosting the efficacy of different antimicrobial molecules[10–12] or in the character of a self-reliant antimicrobial agent[13,14] is considered to be a promising approach.

In our previous works, we have shown that the specific type of magnetic field, referred to as the rotating magnetic field (RMF), acts on the charged molecules (e.g. ions of antimicrobials present in a medium) moving them accordingly to the magnetic field rotation[15]. Furthermore, we previously demonstrated that the RMF displays an impact (of various nature—from negative to positive one) on the growth, metabolic activity, and biofilm formation of several different strains and species of microorganisms[16–18]. In a separate line of investigation, we analyzed the combined effect of RMF and different antibiotics and antiseptics against *S. aureus* and *P. aeruginosa* biofilms in a standard microplate model[19]. The obtained results indicated that the reduction of biofilms exposed to the RMF and antimicrobials was 50% higher as compared to biofilms exposed to antimicrobials only. We have also proved that RMF increases the bactericidal effect of different classes of antibiotics against *S. aureus*, especially methicillin-resistant strains (MRSA)[20]. The observed effect concerned, to the highest extent, these antibiotics, which affect and alter structures of the bacterial cell walls[21]. Although the aforementioned studies were performed not on the bacterial cells within biofilm structure, the obtained results provided us a strong empirical back-up concerning the matter analyzed and moved us to the performance of the present investigation line.

The purpose of this study was to investigate and understand the nature of the increased activity of octenidine dihydrochloride-based antiseptic in the presence of the RMF toward biofilm (including its components, i.e. cells and matrix) and the changes in octenidine dihydrochloride behavior in biofilm milieu (understood as the antiseptic penetrability through the surface the biofilm was cultured on). We hypothesized that the RMF can have an impact on all of the above components. Therefore, we evaluated the changes caused by the RMF (of two distinguished frequencies, 5 and 50 Hz) during the 1, 2, or 3 h exposure on the cell viability and morphology as well as on the structure and composition of biofilms formed by *S. aureus* and *P. aeruginosa* on agar discs, placed in increasing distance from the source of the antiseptic solution at a concentration below the bactericidal effect. Moreover, the penetrability of octenidine dihydrochloride through the porous, agar obstacles as well as the relationship between the RMF parameters and duration of the exposure with regard to the bacterial species (and thus the type of biofilm formed by them) were investigated.

Materials and methods

Bacterial strains and antimicrobial. For experimental purposes, the reference American Tissue and Cell Culture (ATCC, USA) strains of *P. aeruginosa* 15442 and *S. aureus* 6538 were used. The applied antimicrobial was an antiseptic containing 0.1% of octenidine dihydrochloride (Schulke-Mayr GmbH, Germany), later referred to as the "OCT".

Experimental setup. The exposure of biofilm to the RMF was carried out using self-designed RMF bioreactors, described in our previous works[18,20,21], and adopted for purposes of this research. One of the bioreactors was operated with the active RMF generator, while the second served as the control setup (without RMF). Each RMF bioreactor (Fig. 1) was constructed from a 3-phase, four-pole stator consisting of twelve groups of three coil sets. The internal dimensions of the process chamber (in which the incubation of microbiological samples took place) were 16 cm in diameter and 20 cm in height. A detailed description of the RMF generator parameters was provided in Supplementary Table S1. The frequency of alternating current (AC) supplied to the RMF generator was adjusted with the Unidrive M200 inverter (Control Techniques, Nidec Industrial Automation, Poland). The temperature inside the RMF process chamber was regulated and corrected using a thermostat (KISS K6, Huber, Germany) connected to a circulating pump system (Yonos Pico 2.0 25/1-6 25/60, Wilo, Ireland) and the heat exchanger equipped with temperature probes (LM-61B, National Semiconductor Corporation, USA). The homogeneous temperature distribution in the RMF bioreactors was maintained by air flow provided during exposure (1 L/min, 35 °C, RH 90%). The distribution of magnetic induction (B) in the process chamber was determined at 100 V and AC frequencies of 5 and 50 Hz using the Ansys Maxwell simulation software ver.19.1 (ANSYS Inc., USA) and measured using teslameter (SMS-102, Asonik, Poland).

Preparation of OCT containing carrier. The discs made of bacterial cellulose (later referred to as the carriers) synthesized, purified and dried as described in earlier works of our team[22,23] of 15 mm diameter and 0.015 mm thickness were saturated by immersion with OCT dilutions in PBS (Millipore Sigma, USA), (1:16 for *S. aureus* biofilm and 1:4 for *P. aeruginosa* biofilm) for 24 h at room temperature. Above dilutions were experi-

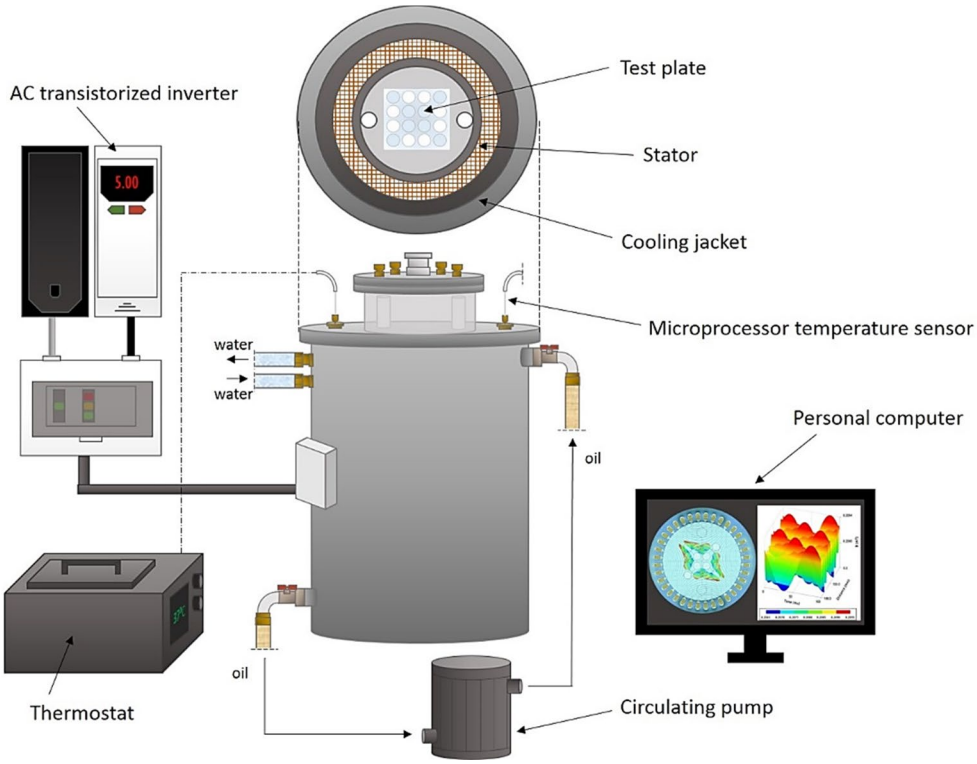

Figure 1. RMF generator with monitoring and control equipment.

mentally selected because they did not lead to an antibiofilm effect in 3 h contact time (Supplementary Fig. S1). Additionally, to prepare the control setting for the experiments based on using OCT, the carriers were soaked with PBS instead of the antimicrobial.

Based on the difference in weight (measured using an analytical balance, Radwag, AS 160.R2, Poland) between the dry and the impregnated carrier, it was found that the volume of the OCT solution (or PBS) absorbed by the disc was 25.0 µL.

Antibiofilm dressing's activity measurement test. To analyze the antibiofilm activity of the OCT released from the carrier, the Antibiofilm Dressing's Activity Measurement (A.D.A.M) test was performed according to the protocol originally devised in our laboratory[2,22] with minor modifications (concerning the concentration of microorganisms and the size of the agar discs). Briefly, *P. aeruginosa* ATCC 15442 and *S. aureus* ATCC 6538 colonies grown on the Columbia Agar (containing 5% sheep blood medium) were transferred into 5 mL of Tryptic Soy Broth (TSB) medium and incubated for 24 h at 37 °C with shaking (200 rpm). After incubation, cultures were diluted in TSB (Biomaxima, Poland) broth supplemented with 1% glucose to obtain the same optical density (OD) equals 1×10^3 CFU/mL. Simultaneously, agar discs of 6 mm in diameter and 4 mm high were cut out from the agar plate containing 2% (v/w) bacteriological agar (Graso Biotech, Poland), transferred to the wells of the 24-well plate, immersed in 2 mL of the bacterial suspension and incubated for 48 h at 37 °C to form a biofilm layer on their surface. After incubation, the discs were rinsed 3 times with 2 mL of 0.9% NaCl to remove non-adherent bacteria and transferred to the agar-filled wells of a trimmed 24-well plate with previously cut holes of diameters equal to the agar discs. Three biofilm-containing discs were placed one into another in each of the holes. The disc put on the bottom of the well are further referred to as the "B-disc" (bottom disc); the disc put directly on the B-disc, as the "M-disc" (middle disc); and the last disc put directly on the M-disc, as the C-disc (contact disc). Next, the carriers impregnated with OCT (or PBS) were placed directly on the C-disc and the plate was covered with a lid.

Exposure of biofilms to RMF. To ensure uniform exposure to the RMF, each 24-well plate (later referred to as the "test plate") was aseptically trimmed with two end columns (columns A and F) before the A.D.A.M test setting preparation. In turn, the biofilm-containing discs were placed only in the outer wells, excluding the corner wells. Thanks to such distribution, all biofilm samples exposed to the RMF were at the same distance from the stator. The test plate with biofilm was placed in the center of the RMF generator (thus subjected to the influence of a magnetic field characterized by the same parameters) and in the middle of the height of the RMF generator (where the magnetic induction value was maximal, Supplementary Fig. S2). The graphical presentation of the arrangement of the test plate during the exposure to the RMF is presented in Fig. 2.

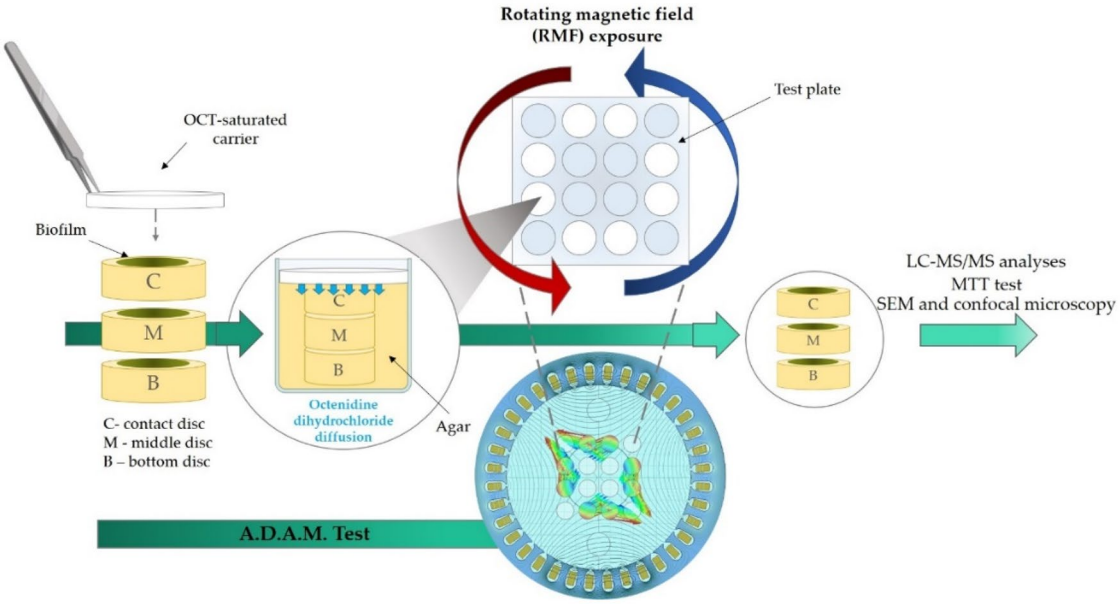

Figure 2. The graphical presentation of the A.D.A.M. test and the arrangement of the test plate during the exposure to rotating magnetic field (RMF).

The test plates were exposed to the RMF of 5 and 50 Hz (the minimal and maximal frequencies that can be set in the experimental setup) for 1, 2, or 3 h at 37 °C. In the case of exposure lasting for 1 and 2 h, the plates were further incubated until 3 h (for 2 and 1 h, respectively) maintaining the same conditions, however with the RMF generator switched off.

The control RMF-unexposed plates were incubated in the twin bioreactor, which had the RMF generator switched off (Supplementary Fig. S3). This RMF-off bioreactor was arranged approximately 2 m from the RMF-on bioreactor. As measured using a Hall probe (Smart Magnetic Sensor-102, Asonik, Poland), the source of the RMF did not affect the RMF-off bioreactor during the experiment (the magnetic induction (B) inside the RMF-off bioreactor was ≤ 0.05 mT).

Evaluation of bacterial viability in biofilm. After 3 h of RMF exposure and/or incubation, the carriers were removed, agar discs covered with biofilm were carefully transferred to a 24-well plate containing 2 mL of MTT (3-(4,5-dimethylthiazol-2-yl)-2,5-diphenyltetrazolium bromide, Millipore Sigma, USA) solution (3 mg/mL in TSB) and incubated in the dark for 1 h at 37 °C. After incubation, the discs were transferred to 2 mL of isopropanol and shaken vigorously using a plate shaker for 15 min to dissolve the formazan resulting from MTT reduction. After shaking, the MTT-formazan solution was aspired and transferred to the wells of a 96-well plate. Finally, the absorbance of the solution obtained was measured with a wavelength of 570 nm and a reference wavelength of 690 nm using a microplate reader (Tecan, Infinite 200 PRO NanoQuant, Switzerland).

Results were presented as % of living cells on successive agar discs for the experimental setting in comparison to the control setting calculated by the following formula (1):

$$\%\ of\ living\ cells = \left(\frac{\left(Abs_{experimental} - Abs_{background}\right)}{\left(Abs_{control} - Abs_{background}\right)} \right) \times 100 \quad (1)$$

where $Abs_{experimental}$ is the absorbance of MTT-formazan solution obtained for biofilms from the experimental settings, $Abs_{control}$ is the absorbance of MTT-formazan solution obtained for biofilms from the control settings, $Abs_{background}$ is the absorbance of the experimental or control samples containing no bacteria (biofilm).

Depending on the purpose of the analysis, different comparative experimental and control settings were used: (i) to determine the antibiofilm activity of OCT solution, results were calculated as % of living biofilm-forming cells on successive agar discs treated with OCT-saturated carriers (OCT-treated biofilms) in comparison to the setting with the carriers soaked with PBS instead of OCT (PBS-treated biofilms). In this setting all the biofilm samples were incubated in the control bioreactor (RMF-off generator), (ii) to determine the effect of RMF exposure on the viability of biofilm-forming bacteria, results were calculated as % of living biofilm-forming cells on agar discs exposed to RMF (RMF-exposed biofilms) in comparison to the setting unexposed to RMF (RMF-unexposed biofilms). In this setting all biofilm samples were treated with the carriers soaked with PBS (instead of OCT), (iii) to determine the influence of RMF on antibiofilm activity of OCT solution (main experimental settings), results were calculated as % of living biofilm-forming cells on agar discs treated with OCT-saturated carriers and exposed to RMF (OCT-treated/RMF-exposed biofilms) in comparison to the setting with the carriers soaked with OCT but unexposed to RMF (OCT-treated/RMF-unexposed biofilms).

Analysis of impact of RMF on penetration rate of octenidine dihydrochloride. In order to analyze the impact of RMF on the penetration rate of octenidine dihydrochloride (the main active component of applied antiseptic product) through successive agar discs, the same A.D.A.M.-based setting as the one used for the measurement of antibiofilm activity was exposed to the RMF generated at 5 and 50 Hz (or incubated in RMF-off condition). However, for this study, the agar discs (C, M, B) were not covered by biofilm and the carrier was impregnated with the original OCT solution (without a dilution). The remaining analysis conditions, including the temperature and humidity as well as exposure and incubation time, were the same as during the measurement of antibiofilm activity.

To extract the octenidine dihydrochloride, the agar discs were placed in 0.5 mL of methanol (Stanlab, Poland) in deionized water (1:1) and incubated with shaking (250 rpm; Biosan, PSU-10i, Latvia) for 3 h[20,21]. Next, the methanol–water mixtures with the extracted antiseptics were filtered through a syringe filter (0.22 µm pore diameter, Chromafil® Xtra, Macherey–Nagel, Germany) and analyzed by liquid chromatography–tandem mass spectrometry (LC–MS/MS) technique (1260 Infinity II Series Liquid Chromatograph, Agilent, USA). An InfinityLab Poroshell 120 EC-C18 column (Agilent, USA) with a particle diameter of 2.7 µm equipped with a guard column was used for chromatographic separation. A mass spectrometer (Ultivo G6465B, Agilent, USA) coupled to the chromatograph was used to detect and identify the assessed antiseptics. The quantitative analysis was based on calibration curves prepared with the use of octenidine dihydrochloride standards (Dishman Pharmaceuticals & Chemicals Ltd., UK). The results were presented as % of octenidine dihydrochloride extracted from successive agar discs exposed to RMF (or incubated in RMF off conditions) in comparison to its initial concentration in the carrier.

Visualization of cell wall integrity of biofilm-forming cells. In order to visualize the impact of RMF and OCT (together or as self-reliant agents) on microbial biofilm, the biofilm samples were immersed in 1 mL of Filmtracer™ LIVE/DEAD™ Biofilm Viability Kit (Invitrogen, Thermo Fisher Scientific, USA) solution and incubated at room temperature for 15 min[20,21]. After incubation, the solution was removed and the biofilms were gently rinsed once with sterile water. The biofilms were analyzed using a confocal microscope (Leica, SP8, Germany) with a 25x water dipping objective, using sequential mode for 488 nm laser line and 500–530 nm emission to detect SYTO-9 and 552 nm laser line and 575–627 nm emission to detect propidium iodide (PI) within microbial cells. The subsequent images (biofilm cross-sections) were collected with ~ 2 µm spacing in the Z dimension. The obtained biofilm images were further analyzed with Imaris 9 (Abingdon, UK) software, with the use of the maximum intensity projection method.

The following settings of this experiment were prepared: OCT-treated/RMF-exposed biofilms; OCT-treated/RMF-unexposed biofilms; PBS-treated/RMF-exposed biofilms; PBS-treated/RMF-unexposed biofilms. The analysis conditions, including OCT dilution, temperature and humidity as well as exposure and incubation time, were the same as during the measurement of antibiofilm activity (A.D.A.M. test).

Visualization of cells, structure of biofilm matrix and porosity of agar discs. To confirm the presence of biofilm formed on agar discs, to visualize the impact of RMF on the biofilm structure and cell status, and to visualize the porosity of agar discs, scanning electron microscopy (SEM) was applied. The PBS-treated/RMF-exposed and PBS-treated/RMF-unexposed biofilms prepared in the same conditions as in the A.D.A.M. test were rinsed with PBS and fixed by immersion in 3% glutarate (POCH, Poland) for 15 min at room temperature. Next, the biofilms were rinsed twice with PBS to remove the fixative. The dehydration in increasing concentrations of ethanol (POCH, Poland) (25%, 50%, 60%, 70%, 80%, 90%, and 100%) was performed for 10 min per solution. Then, the ethanol was rinsed off, and the biofilms were dried at room temperature. Next, biofilms were covered with gold and palladium (60:40; sputter current, 40 mA; sputter time, 50 s) using a Quorum machine (Quorum International, USA) and examined using the SEM (Carl Zeiss, EVO MA25, Germany). In the case of agar discs without biofilm (analysis of agar discs porosity), the procedures were analogical as in the case of biofilm-covered discs, the procedures of fixation and visualization were analogical as in the case of biofilm-covered discs, with the exception that the first step (rinsing with PBS) was omitted.

The SEM images of PBS-treated/RMF-exposed and PBS-treated/RMF-unexposed biofilms and agar surfaces were processed using ImageJ software (National Institutes of Health, USA). The images were converted into 16-bit images and considered Regions of Interest (ROIs). Next, the threshold was settled for ROIs in such a manner that fibrils were recognized as background ("Image/Adjust/Threshold" command), while the pores were recognized as the areas to be further analyzed. The "Process/Subtract" command was applied to manage the background pixels; the number of pores was calculated using the option of "Particles Analyses" with circularity from 0.00 to 1.00. The ferret diameters were calculated using the "Set measurements/Ferret Diameter" command from threshold 16-bit images; each setting was analyzed in six ROIs.

Determination of saccharide content in cell-free biofilm matrix. Initially, all the strains were plated onto the Columbia Agar (containing 5% sheep blood medium, Graso Biotech, Poland) and cultivated for 24 h at 37 °C. After incubation, one colony-forming unit (CFU) was transferred into 5 mL of Tryptic Soy Broth (TSB, Oxoid, UK) and incubated for another 24 h at 37 °C with shaking (200 rpm, Biosan, ES-20/60, Latvia). Next, cultures were diluted in TSB supplemented with 1% glucose to obtain bacterial suspension equal to 1×10^3 CFU/mL, which was then transferred to Petri dishes (20 mL/Petri dish) and incubated for 48 at 37 °C. After that time biofilms were exposed to the RMF of 5 and 50 Hz (RMF-exposed biofilms) or incubated in RMF-off conditions (RMF-unexposed biofilms) for 3 h. After exposure, the medium was gently removed, and the biofilm, remaining on the dish, was rinsed with 10 mL of PBS. In the next stage, the biofilm was collected using a tissue culture scraper, transferred to a 50 mL test tube, and mixed with 36% aqueous formaldehyde solution

(Millipore Sigma, USA). The formaldehyde solution was added in a proportion of 60 µL per 10 mL of biofilm. The resulting suspension was shaken (100 rpm, Biosan, PSU-10i, Latvia) at room temperature for 1 h, then mixed with 1 M NaOH solution (in the proportion of 4 mL of NaOH solution per 10 mL of biofilm suspension), shaken (100 rpm) at room temperature for a further 3 h and centrifuged at 4500 × g for 1 h at 4 °C (Eppendorf, Centrifuge 5804R, Germany). After centrifugation, the supernatants, containing biofilm matrices, were filtered through a syringe filter (0.22 µm pore diameter) and then dialyzed using dialysis membranes (molecular weight cut-off = 14,000, Millipore Sigma, USA) immersed in beakers containing 1 L of DI water. Dialysis was carried out for approx. 3 days at 4 °C (during dialysis, water was changed every 24 h) until the biofilm matrix suspensions reached the resistance of deionized water used for dialysis (resistivity < 1(MWxcm)).

The matrices were hydrolyzed with the use of 80% trifluoroacetic acid (TFA, Milipore Sigma, USA) and evaporated using SpeedVac device SRF110 (Thermo Fisher Scientific, USA). Next, dried samples were derivatized by heating (60 °C for 30 min) in the solution containing 1000 µL of anhydrous pyridine (Millipore Sigma, USA), *N*-Methyl-*N*-tert-butyldimethylsilyltrifluoroacetamide (MTBSTFA, Millipore Sigma, USA), and 100 µL of trimethylchlorosilane (TCMS, Millipore Sigma, USA). The 5 mg of D-sorbitol (Milipore Sigma, USA) was introduced to the solution as an internal standard.

The assessment of saccharide content in the cell-free biofilm matrix was performed using gas chromatography-mass spectrometer coupled with a mass spectrometer single quadrupole (GC–MS/MS, Shimadzu, QP 2010, Japan) with the TRACE™ TR-5MS capillary column (0.25 µm, 0.25 mm I.D., 30 m length, Thermo Fischer Scientific, USA). The mobile phase was helium 99.999% (LindeGas, Poland) with a linear velocity of 30 cm/s in constant flow mode. The dosing was set for 1 µL in splitless mode. The inlet temperature was set to 320 °C, ion source temperature was 300 °C. The initial oven temperature was set at 100 °C, increasing 10 °C/min to a final temperature of 320 °C with a 10-min hold time. The mass spectrometer was set to scan mode 10 000 scan/sec in the range 40–600 amu. The spectra were analyzed using GCMSsolution ver. 4.1 software (Shimadzu, Japan) with NIST 14 Library (National Institute of Standards and Technology, USA). All saccharides serving as comparative references were purchased from Milipore Sigma, USA.

Confirmation of a lack of cells within the biofilm matrix. To confirm that the purified biofilm matrix contained no cells within, the cryo-SEM technique was applied. The 10 µL of the matrix was placed on the cryo-SEM table. Next, the sample and the table were frozen in liquid nitrogen under vacuum conditions. A vacuum of 10^{-7} mbar was provided in the preparation chamber by a turbomolecular pumping system (Vacuubrand, Germany). The frozen table and the sample were transferred into a vacuum chamber of cryo-SEM attachment (Quorum, UK) and sputtered with a platinum layer. Such prepared sample was examined using SEM (Carl Zeiss, Auriga 60, Germany). The observation was performed at a working distance of 5 mm, EGT = 2 kV/m. The SEM cold stage was – 180 °C with temperature stability of < 0.5 °C.

Statistical analysis. The data were presented as mean values ± standard error of the mean (SEM) obtained from at least three different measurements (plus technical repetitions). Statistical differences between RMF-exposed and control settings were determined by one-way analysis of variance (ANOVA). Tukey's multiple comparisons test was used for multiple comparisons of means (the post-hoc analysis). Differences were considered significant at a level of $p < 0.05$. The statistical analyses were conducted using GraphPad Prism 9.0 (GraphPad Software Inc., USA).

Results

Biofilm formation on agar discs. Both investigated bacterial species were able to form biofilm structures in the experimental settings applied, as proven through SEM and confocal microscopy (Fig. 3). The observed share of extracellular matrix was higher in the case of *P. aeruginosa* ATCC 14452 than in the case of *S. aureus* ATCC 6538, nevertheless both microbial species formed adhered multi-cellular structures meeting the established criteria of biofilm formation. After proving the ability to produce biofilm in the applied experimental setting, we performed a series of experiments to investigate the impact of RMF combined with the OCT on overall antibiofilm activity, understood as activity against biofilm-forming cells and the ability to penetrate through physical obstacles and biofilm layers formed at different distances from the OCT source. The above analyzes were preceded by the assessment of the influence of OCT (without RMF) and RMF (without OCT) on changes in the viability of biofilm-forming cells.

Effect of OCT treatment on viability of biofilm-forming bacteria. It was found that during 3 h of contact time, the OCT released from the carrier had no significant impact on the % of viable biofilm-forming cells of both *S. aureus* and *P. aeruginosa* bacterial species, on any of the agar discs (C, M, B). However, the OCT released from the carrier significantly reduced the % of viable biofilm-forming cells when the contact time was exceeded (Fig. 4). In this case, the strongest bactericidal effect was noted for disc C (neighboring with OCT-containing carrier), then for disc M, while the lowest effect was found for disc B (placed in the greatest distance from OCT-containing carrier). The results from the setting applying contact time longer than 3 h (control of testing method usability) confirmed that OCT possesses the appropriate antibiofilm activity, contrary to setting when 3 h contact time was applied. Therefore 3 h of contact time was chosen for analyses of boosting effect of the RMF on OCT activity.

Effect of RMF exposure on viability of biofilm-forming bacteria. In the next stage of our research, the analysis covered the effect of exposure to the RMF of different frequencies (5 and 50 Hz) lasting 1, 2, and 3 h on changes in the viability of biofilm-forming bacteria on each of the agar discs. It was found that the exposure

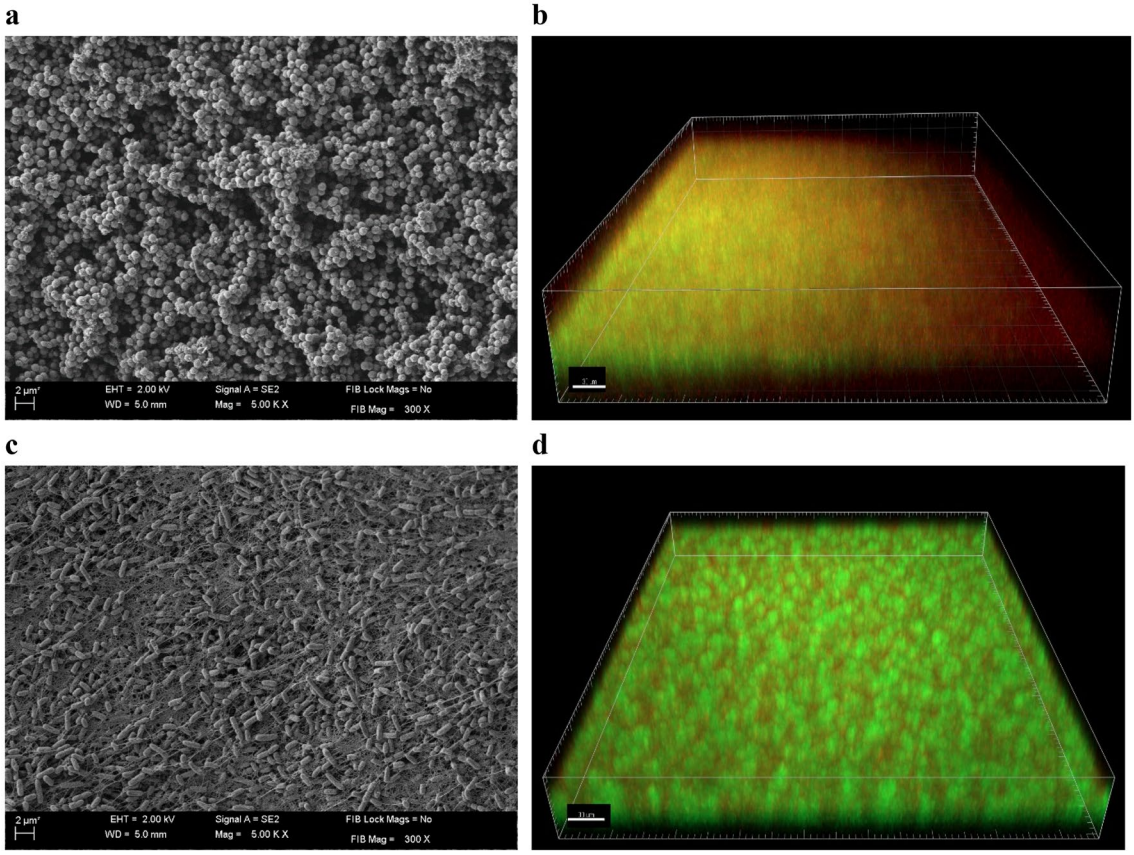

Figure 3. Structure of 48 h biofilm formed on agar discs visualized by scanning electron and confocal microscopy, (**a**, **b**) *S. aureus* and (**c**, **d**) *P. aeruginosa*. The magnification of pictures taken using SEM equals 5000× and confocal microscopy 40×.

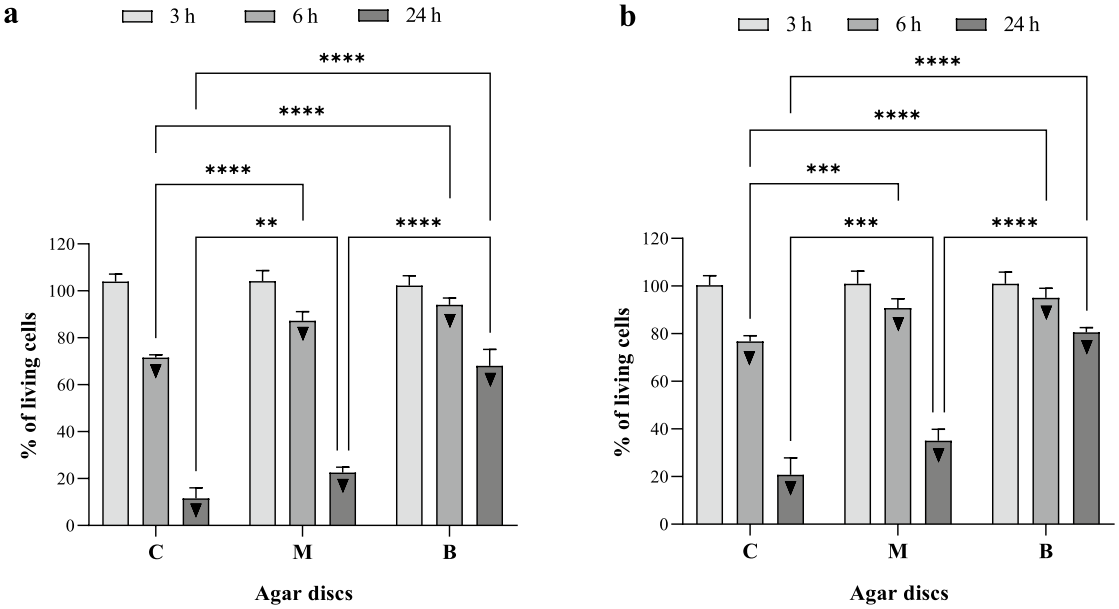

Figure 4. Percent of living (**a**) *S. aureus* and (**b**) *P. aeruginosa* biofilm-forming cells on successive agar discs incubated with OCT-saturated carriers. The results are presented as % reduction of living biofilm-forming cells on successive agar discs incubated with OCT-saturated carriers in comparison to the control setting with the carriers soaked with PBS instead of OCT and expressed as a mean ± SEM. The asterisks in the graphs indicate statistically significant differences between OCT-treated biofilms on successive agar discs (*$p < 0.05$, **$p < 0.01$, ***$p < 0.001$, ****$p < 0.0001$). ▼—statistically significant differences ($p < 0.05$) between OCT-treated and PBS-treated biofilms.

of biofilm samples to the RMF (PBS-treated and RMF-exposed biofilms) did not significantly affect the viability of *S. aureus* and *P. aeruginosa* cells regardless of the exposure duration and RMF frequencies (5 v. 50 Hz). There were also no statistically significant differences in the viability of RMF-exposed biofilm-forming cells between the individual agar discs (C, M, B), (Supplementary Fig. S4).

Influence of RMF on OCT antibiofilm activity. In the further stages of the experiment, it was shown that the exposure of biofilm samples to the RMF (regardless of its frequency) increased significantly the antibacterial effect caused by OCT against *S. aureus* and *P. aeruginosa* biofilms (Fig. 5). The effect was mainly dependent on the time of exposure to the RMF and on biofilm, with regard to the specific agar disc (C, M, B) it grew, and to a lesser extent on the biofilm-forming species or the RMF frequency. Although the observed antibacterial effect was proportional to the exposure time, even the exposure lasting 1 h (the shortest exposure time) caused a significant reduction in the number of viable cells in the *S. aureus* biofilm (formed on discs C and B) and in the case of *P. aeruginosa* biofilm (on the disc C). Nevertheless, the greatest RMF influence was found for the settings exposed for 3 and thereafter for 2 h, where the reduction in biofilm viability (regardless of species and frequency) was statistically significant in all analyzed agar discs (C, M, B). Moreover, the differences between 2 and 3 h exposure to the RMF were of relatively minor level and did not exceed 10%. In the case of a 3 h exposure, the *S. aureus* biofilm viability dropped, respectively, by approx. 45%, 40%, and 30% for the C, M, and B agar discs, and by 45%, 30%, and 20%, during 2 h of exposure. In the case of *P. aeruginosa* biofilm, especially in the 3 h exposure variant, the influence of the RMF frequency was of greater importance for the obtained results. Only the results concerning the biofilm on the C disc were similar for both frequencies (approx. 45%). In turn, in the case of the M and B discs, the differences in viability inhibition, depending on the RMF frequency, were approx. 10% (5 Hz, disc M—40%, disc B—30%; 50 Hz, disc M—30%, disc B—20%). The respective values recorded for 2 h exposure were less substantial and did not exceed 5%—the drop of viability was approx. 40% for the C disc; 25% for the M disc and 17% for the B disc. In the case of exposures lasting 1 h, regardless of the bacterial species and the frequency of RMF, the decrease in cell viability did not exceed 20%. Moreover, in the case of discs M and B, no statistically significant differences were found between the RMF-exposed and RMF-unexposed samples, and the reduction of viability was less than 10%.

Nevertheless, despite the observed differences between individual agar discs depending on the RMF frequency, the total antimicrobial effect of OCT and RMF on C, M, and B discs was comparable, and the differences were not statistically significant, regardless of the analyzed species of bacteria (Supplementary Fig. S5).

Influence of RMF on release and penetrability rate of octenidine dihydrochloride. It was found that the RMF altered the level of octenidine dihydrochloride penetration into the individual agar discs (Fig. 6). The most significant influence of the RMF was observed during continuous exposure for 3 h. In this case, the greater effect was observed as a result of exposure to the RMF of 50 Hz (all discs consisted of a total of 58% of octenidine dihydrochloride as compared to its initial concentration in the carrier), compared to exposure to the RMF of 5 Hz (43%) (Supplementary Fig. S6). When exposed to the RMF for a shorter time, the octenidine dihydrochloride concentration was also higher as compared to the unexposed control settings, but the differences did not exceed 3%, and significant differences occurred only for M discs, regardless of the RMF frequency. The greatest concentration of octenidine dihydrochloride was detected in disc C and the lowest in the disc placed at the bottom of the test plate (disc B). This trend was observed regardless of the time of exposure to the RMF.

Influence of RMF on biofilm-forming cells and biofilm matrix. The application of the RMF regardless of its frequencies increased the number of *S. aureus* and *P. aeruginosa* cells with altered (compromised) cell walls (Fig. 7; since no substantial differences were observed between the applied RMF frequencies, the results obtained for 50 Hz are presented in Supplementary Information, Supplementary Fig. S7). Comparable changes were observed across the whole structure of biofilm (from the upper, through the middle to the basal layers). Likewise, the incubation of biofilms with OCT-saturated carriers together with the exposure to RMF resulted in a significantly higher level of destructed cells (also in the whole cross-section of biofilm) compared to biofilms incubated with OCT-saturated carriers but unexposed to the RMF.

Because the results of the confocal microscopy indicated that the RMF can alter cell walls of biofilm-forming cells, in the next step of investigation we analyzed the character of these changes using the SEM. As can be seen in Fig. 8, the application of the RMF (of both 5 Hz and 50 Hz frequencies) correlated with a spectrum of changes in biofilm-forming cells of *P. aeruginosa* and *S. aureus*. These alterations included loss of turgor, a change of shape (particularly well-seen in *P. aeruginosa* cells); in the case of *S. aureus*, the increase in distance between cells was also observed. Following this last observation, we performed a parametric analysis of the RMF-induced changes in the pseudomonal and staphylococcal biofilm matrix. The results presented in Fig. 9 indicated that the number of pores in *S. aureus* and *P. aeruginosa* biofilm matrices were statistically higher ($p < 0.05$) compared to the RMF-unexposed biofilms. In turn, the differences between the number of pores in biofilms exposed to the RMF of 5 or 50 Hz, were statistically insignificant. The average pore number in *S. aureus* biofilm matrix, exposed to the RMF of 5 or 50 Hz, was 43% and 37% higher, respectively, compared to the RMF-unexposed biofilms. In the case of *P. aeruginosa* these values were 220% and 214%, for 5 and 50 Hz exposure respectively.

Influence of RMF on biofilm matrix composition. In subsequent analyses, we assessed the impact of the RMF on the biofilm matrix with regard to its molecular composition. Before the analysis, the cells and their leftovers were chemically removed from the biofilm; the effectiveness of this procedure was confirmed using the cryo-SEM technique and then, the cell-free matrix of biofilms exposed or unexposed to the RMF was subjected to GC–MS/MS analyses (Supplementary Fig. S8).

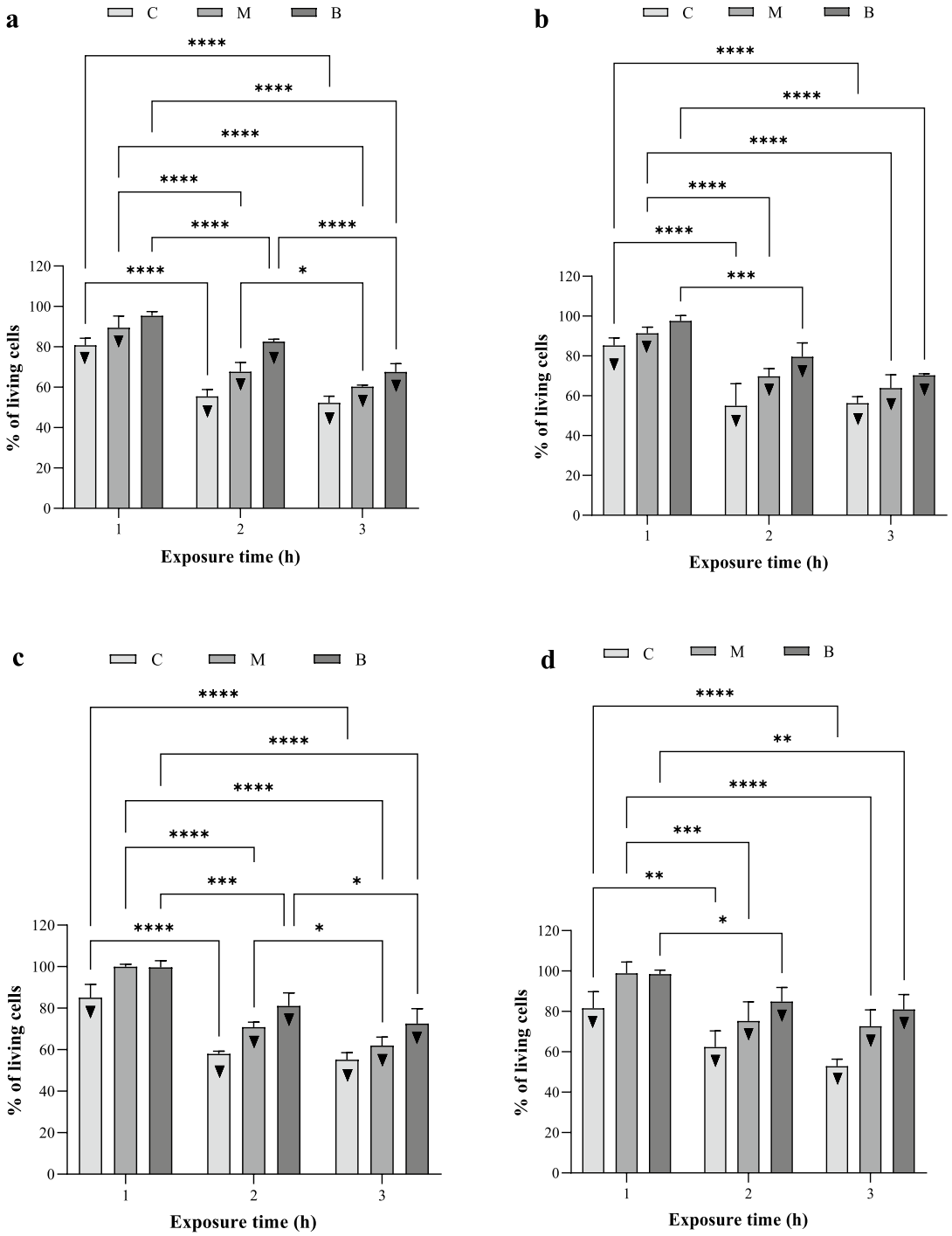

Figure 5. Percent of living biofilm-forming cells on successive agar discs treated with OCT-saturated carriers and exposed to RMF. (**a**) *S. aureus*—RMF of 5 Hz, (**b**) *S. aureus*—RMF of 50 Hz, (**c**) *P. aeruginosa*—RMF of 5 Hz and (**d**) *P. aeruginosa*—RMF of 50 Hz. The results are presented as % reduction of living biofilm-forming cells on successive agar discs treated with OCT-saturated carriers and exposed to RMF in comparison to the settings with the carriers soaked with OCT but unexposed to RMF and expressed as a mean ± SEM. The asterisks in the graphs indicate statistically significant differences between OCT-treated biofilms exposed to RMF for different time (*$p < 0.05$, **$p < 0.01$, ***$p < 0.001$, ****$p < 0.0001$). ▼—statistically significant differences ($p < 0.05$) between OCT-treated/RMF-exposed and OCT-treated/RMF-unexposed biofilms.

The GC–MS/MS analysis was targeted to sugars, considered one of the major components (in a form of polysaccharides) of both pseudomonal and staphylococcal biofilm matrices. It was found that the application of the RMF (5 and 50 Hz) altered the saccharide composition of both analyzed biofilms (Table 1). In the case

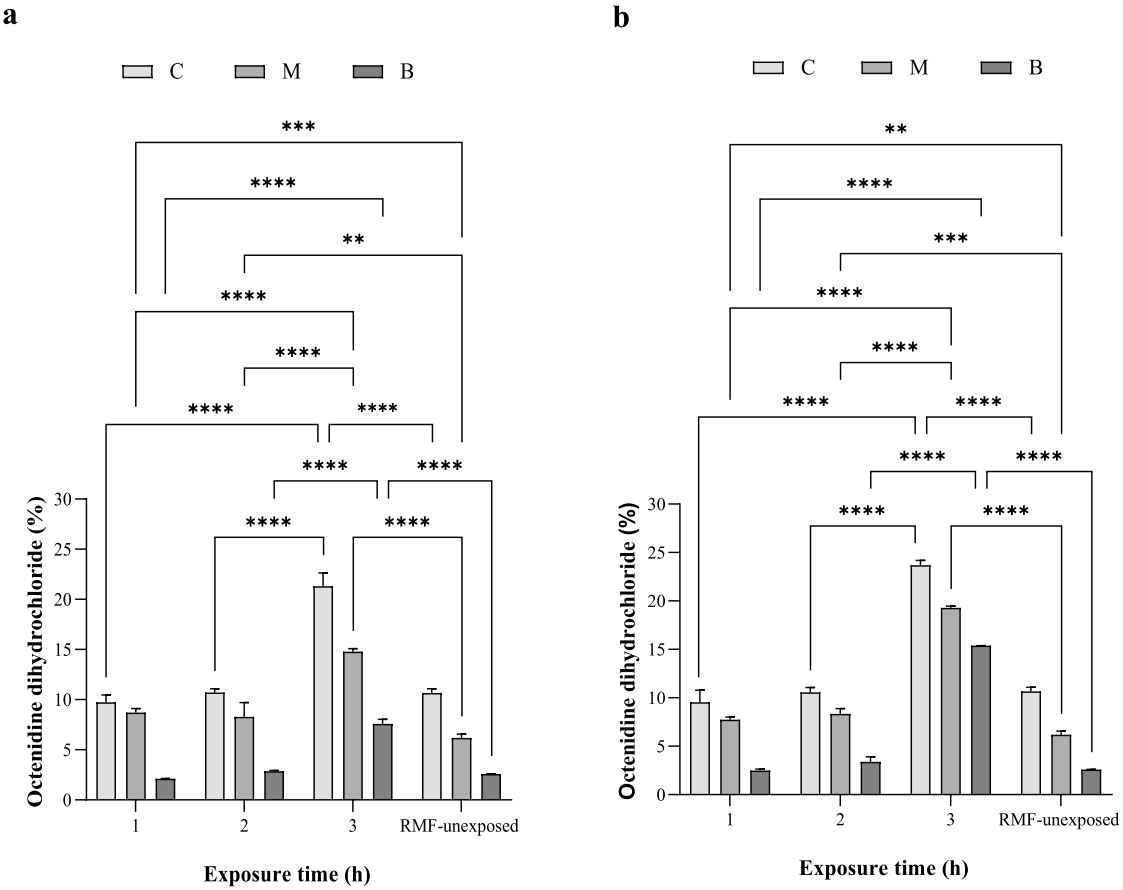

Figure 6. Percent of octenidine dihydrochloride extracted from successive agar discs exposed to RMF of (**a**) 5 Hz and (**b**) 50 Hz, in comparison to its initial concentration in the carrier. The results are presented as mean ± SEM. The asterisks in graphs indicate statistically significant differences between RMF-exposed and RMF-unexposed agar discs (*$p < 0.05$, **$p < 0.01$, ***$p < 0.001$, ****$p < 0.0001$).

of *P. aeruginosa*, a distinct trend was observed, i.e. the content of 11 (out of 13 detected) saccharides (and their isomers) was lower in the RMF-exposed biofilm compared to the RMF-unexposed setting; moreover, the drop of content in these 11 saccharides was stronger for the RMF of 5 Hz comparing to the RMF of 50 Hz. The saccharides which did not fit the above pattern were b-fucose and a-galacturonic acid. In the case of fucose, exposure to the RMF increased its content in comparison to the RMF-unexposed setting (to a higher extent at 50 Hz than at 5 Hz), while in the case of a-galacturonic acid, its content was basically the same in the matrix obtained from biofilm unexposed vs. exposed to the RMF 50 Hz (0.15 vs. 0.14 ng/mg, respectively) and higher (0.15 vs. 0.23 ng/mg) due to the exposure to the RMF of 5 Hz. In the case of the staphylococcal matrix, the drop of saccharide content was observed for 4 (out of 15 detected) saccharides: *a*-arabinose, *b*-rhamnose, *a*-fucose, and *b*-fucose. The content of the remaining 11 saccharides was higher in the matrix obtained from biofilm exposed to the RMF as compared to the RMF-unexposed setting; in the case of 7 (out of 11 saccharides matching the above pattern), the increase was higher in biofilm exposed to the RMF of 5 Hz comparing to the RMF of 50 Hz.

Discussion

The current study aimed to determine the factors standing behind the observed increased antibiofilm efficacy of octenidine dihydrochloride-based antiseptic in the presence of the RMF. We assumed, that the increased effectiveness of the antiseptic in the presence of RMF should be interpreted as the appearance of the antibiofilm effect observed in a shorter contact time and/or with the concentration of the active substance, which did not cause any bactericidal effect if the RMF was not applied. For this reason, we used the A.D.A.M. test, previously developed by our team[22], dedicated to the determination of the antibiofilm effect exerted by the active substance, penetrating the three biofilm structures separated by three porous obstacles (represented by 3 agar discs in test). Moreover, for the purposes of this study, it was necessary to apply such antiseptic dilution that displayed any or scanty antibiofilm effect during the particular (experimental) contact time but caused an antibiofilm effect if the contact time was extended. Such assumption was taken, based on the mechanism of action of octenidine dihydrochloride-based antiseptics, which (even when diluted), can cause a bactericidal effect if a sufficiently long contact time is provided[24]. Following the same thinking pattern, also the selected exposure time to the RMF (3 h), was too short to change significantly the viability of the biofilm-forming cells. Thus, if the antibiofilm effect occurred, it would be a result of the simultaneous effects displayed by the antiseptic and the RMF. For this

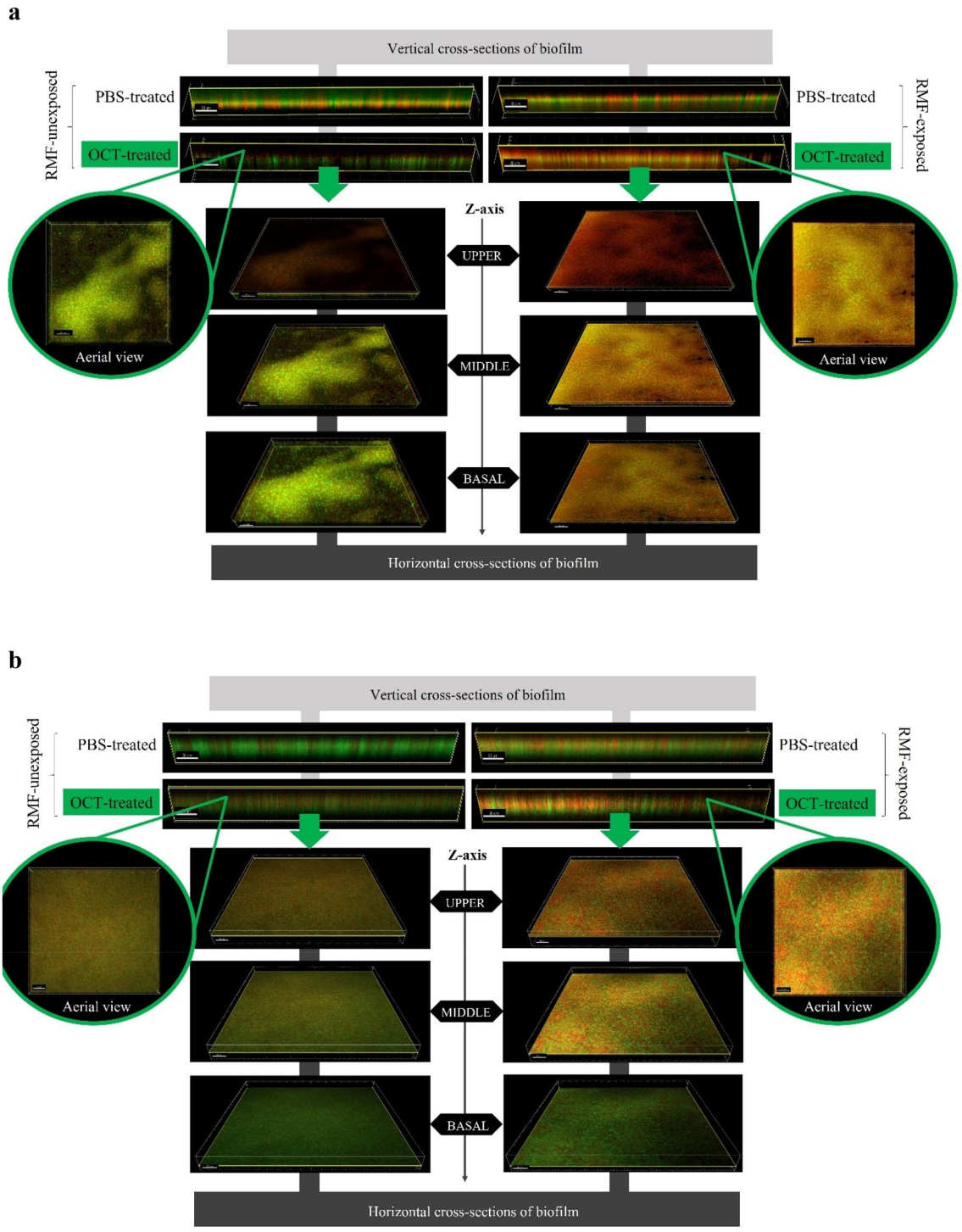

Figure 7. The spatial location of (**a**) staphylococcal and (**b**) pseudomonal cells within biofilm treated with OCT-saturated carriers and/or exposed to RMF (5 Hz). The cells with non-altered cell walls dye green (as a result of SYTO-9), while the cells with compromised cell walls dye red/orange (as a result of propidium-iodide incorporation).

reason, in the first stage of the study, it was confirmed that the application of antiseptic-saturated carrier did not translate into a drop of viable biofilm-forming cells of both *S. aureus* and *P. aeruginosa* bacterial species, on any of the agar discs (C, M, B) during the particular 3 h contact time. Simultaneously, the application of the same (with regard to antiseptic concentration) carriers reduced the percent of viable biofilm-forming cells when the contact time was exceeded over a 3 h period. The reduction in the number of live bacterial cells was particularly visible only in the case of biofilms incubated with antiseptic solutions for 24 h, which was most likely related to the relatively low concentration of the active substance applied solution and the acknowledged prolonged

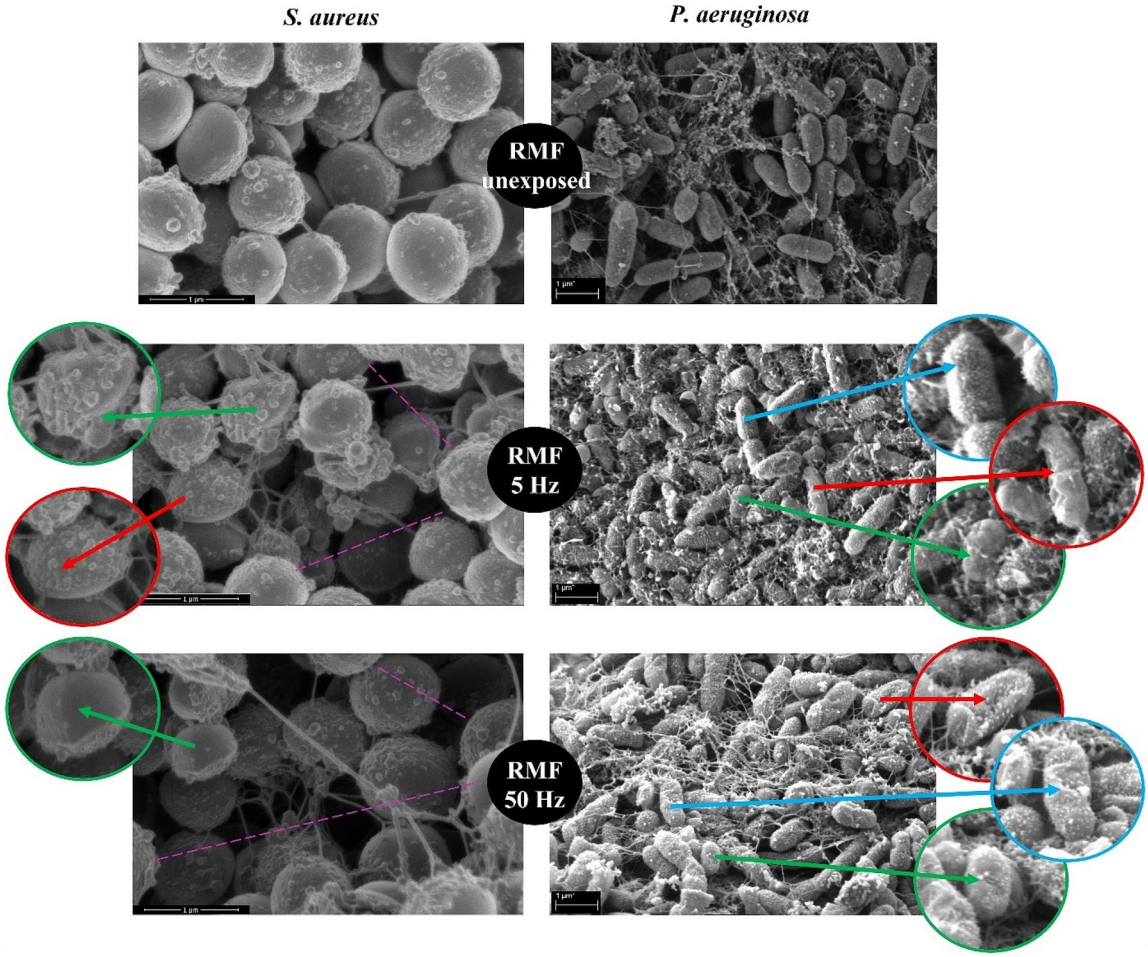

Figure 8. Morphology of (**a**) staphylococcal and (**b**) pseudomonal cells within biofilm structure exposed and unexposed to RMF. Green arrows indicate changes in cellular morphology; the red arrows indicate loss of turgor; blue arrows indicate granularities on the cell surface. The purple lines point out the increased distance between cells in biofilms exposed to the RMF. The magnification of staphylococcal biofilm equals 50,000× and pseudomonal biofilm 30,000×.

mechanism of the antiseptic action[24,25]. In addition, lower values of cell viability were found for *S. aureus* as compared to *P. aeruginosa*, which in turn could be related to the differences in the structure and composition of the biofilm matrix produced by these bacterial species. As shown in the SEM analysis, the *P. aeruginosa* biofilm contained significantly greater amounts of the protective matrix than *S. aureus* biofilm. Moreover, the biofilm matrix of *P. aeruginosa* contains not only exopolysaccharides[26,27] but also phospholipids, which are one of the main target sides of octenidine hydrochloride molecules[25], which may explain the observed differences in this antiseptic activity against biofilms formed by two different bacterial species.

The literature data indicated that various types of magnetic fields may influence the number of live bacterial cells, causing the reduction[28–31] or increase[32–34] in their number. There are also numerous studies where the application of magnetic fields did not alter the number of exposed bacteria[35–38]. It is widely recognized that the effect of the magnetic field is to a major extent related to its characteristics (e.g. frequency, intensity, and distribution of magnetic field lines) and time of exposure. Therefore, in our research, we analyzed the effect of exposure to the RMF of different frequencies (5 and 50 Hz) for 1, 2, and 3 h on changes in the viability of bacteria present on each of the agar discs in applied biofilm model. However, it was found, that the exposure of biofilm samples to the RMF (without the antiseptic) did not significantly affect the viability (measured by standard metabolic tests) of *S. aureus* and *P. aeruginosa* cells regardless of the exposure duration and RMF frequencies. There were also no statistically significant differences in the viability of RMF-exposed cells forming a biofilm on the specific (C, M, B) agar discs. In our previous studies, we showed that the RMF affected the cell viability of *S. aureus* and *P. aeruginosa*, but it has to be underlined that these studies were conducted for bacteria cultured in liquid cultures, during their phase of logarithmic growth[18]. In the present study, the exposed bacteria were immobilized on the surface of agar discs and anchored within the biofilm matrix. As it is commonly known, bacterial biofilm communities are characterized by a much greater resistance to all stressors (including antimicrobials) as compared to the same bacteria in liquid suspension (referred to as the planktonic phenotype)[39–41]. The access of biofilm-forming bacteria to nutrients and oxygen (in the case of aerobic species) is limited and thus regulated by the biofilm community itself by complex pathways of information exchange[42]. In this context, it can be said,

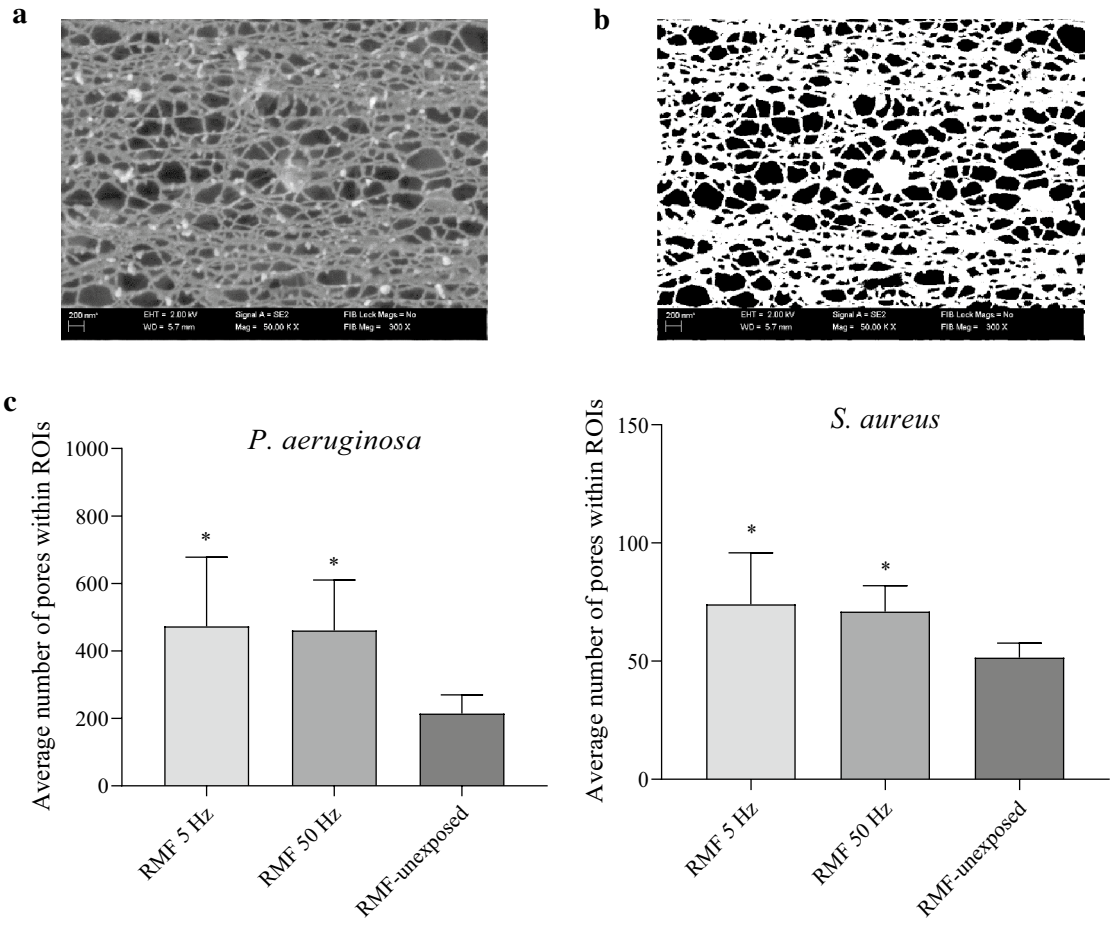

Figure 9. The porosity of biofilm matrix exposed and unexposed to RMF. (**a**) image of representative *P. aeruginosa* biofilm matrix, (**b**) image processing of matrix leading to differentiation of fibrils (white shapes) from matrix pores (black shapes), (**c**) average number of pores in *S. aureus* and *P. aeruginosa* biofilm matrix exposed and unexposed to RMF. The results are presented as mean ± SEM. The asterisks in graphs indicate statistical significance ($p < 0.05$) between respective average values.

	S. aureus			*P. aeruginosa*		
Sugar [ng/mg]	**RMF-unexposed**	**RMF 5 Hz**	**RMF 50 Hz**	**RMF-unexposed**	**RMF 5 Hz**	**RMF 50 Hz**
a-Arabinose	2.55 ± 0.24	1.68 ± 0.07	1.20 ± 0.12	0.32 ± 0.08	0.13 ± 0.04	0.27 ± 0.04
b-Arabinose	6.41 ± 0.32	8.22 ± 0.14	7.66 ± 0.72	0.76 ± 0.12	0.48 ± 0.16	0.60 ± 0.13
a-Galactose	5.56 ± 0.43	6.78 ± 0.31	7.65 ± 1.53	0.92 ± 0.2	0.25 ± 0.05	0.41 ± 0.06
b-Galactose	15.43 ± 0.56	17.40 ± 2.26	17.59 ± 3.62	0.00	0.00	0.00
a-Glucose	64.03 ± 3.56	79.24 ± 7.32	71.27 ± 7.07	1.88 ± 0.2	0.92 ± 0.21	1.57 ± 0.25
b-Glucose	33.89 ± 3.10	41.31 ± 4.34	40.23 ± 8.09	3.01 ± 0.14	0.91 ± 0.31	2.02 ± 0.31
a-Mannose	8.31 ± 0.14	12.33 ± 1.78	10.01 ± 0.61	2.95 ± 0.06	0.71 ± 0.17	1.78 ± 0.09
b-Mannose	15.44 ± 0.67	17.45 ± 1.67	17.63 ± 2.68	2.58 ± 0.2	1.21 ± 0.32	2.20 ± 0.27
a-Rhamnose	1.31 ± 0.21	3.10 ± 0.23	2.30 ± 0.34	3.92 ± 0.14	1.13 ± 0.07	2.82 ± 0.15
b-Rhamnose	3.67 ± 0.45	2.55 ± 0.67	1.31 ± 0.44	3.35 ± 0.8	2.19 ± 0.11	3.42 ± 0.03
a-Galacturonic acid	2.31 ± 0.34	2.42 ± 0.30	2.70 ± 0.61	0.15 ± 0.04	0.23 ± 0.02	0.14 ± 0.07
b-Galacturonic acid	9.89 ± 0.34	12.78 ± 0.31	11.87 ± 1.22	0.00	0.00	0.00
N-Acetyl-glucosamine	897.03 ± 33.29	1034.11 ± 145.45	952.12 ± 44.8	0.21 ± 0.04	0.34 ± 0.11	0.21 ± 0.10
a-Fucose	2.20 ± 0.42	1.01 ± 0.01	1.05 ± 0.30	0.00	0.00	0.00
b-Fucose	80.45 ± 3.02	75.56 ± 4.31	71.91 ± 12.83	0.12 ± 0.01	0.16 ± 0.03	0.33 ± 0.07
a-Xylose	0.00	0.00	0.00	1.62 ± 0.37	0.78 ± 0.14	0.98 ± 0.22
b-Xylose	0.00	0.00	0.00	1.12 ± 0.33	0.46 ± 0.01	0.90 ± 0.27

Table 1. The average content of specific sugars [ng/mg of sample] in cell-free *S. aureus* and *P. aeruginosa* matrix obtained from biofilms exposed and unexposed to RMF.

that one of the factors limiting the action of antimicrobial substances is the decreased metabolic activity of cells in the biofilm[39]. Thus, it can be assumed that bacteria with lower activity are also less sensitive not only to chemical agents (e.g. antibiotics and antiseptics) but also to physical factors (e.g. magnetic fields). It is also worth emphasizing that it is for this reason that in the conducted analyzes we chose the MTT test, which in addition to its standard purpose (analysis of cell viability) provided us also data on changes in cellular metabolic activity[43]. On the other hand, it should also be noted that in the current study, due to the relatively short experimental time selected for the analysis of the antimicrobial effect induced by antiseptics, exposure to the RMF was also relatively short as compared to our earlier research[19], as well as compared to the research by other authors[10,12].

In the further stages of the analysis, it was also shown, that the exposure of biofilm samples to the RMF (regardless of its frequency) when combined with the solution of the antimicrobial, significantly increased the antibacterial effect against *S. aureus* as well as *P. aeruginosa,* although in the case when both factors acted separately, no effect (measured by the MTT test) was observed. The effect was mainly dependent on the time of exposure to the RMF and to a lesser extent on the biofilm-forming bacterial species and the RMF frequency. Such observation stays in line with the previous reports of our research group[17,44] as well as reports of other authors[13,45] indicating that the time of magnetic exposure is also of key importance concerning the effect exerted on biological systems. Depending on the exposure time, magnetic fields may have a different effect on bacterial viability, i.e. it may increase it[32–34] or reduce it[28–31].

It was also found that the RMF influenced the degree of octenidine dihydrochloride penetration into specific agar discs. The greatest effect was observed during continuous, 3 h exposure to the RMF and stronger for frequency of 50 Hz than of 5 Hz (the difference exceeded 20%). When the experimental setting was exposed for a time shorter than 3 h, the concentration of octenidine dihydrochloride was also higher, compared to the RMF unexposed setting, however this time, the differences did not exceed 3%. As already mentioned, the strength of magnetic field impact (regardless of its type or the phenomenon analyzed in its presence), except for the exposure duration, depends on its intensity and/or frequency[17,28,44,46], because these two factors determine the physical characteristics of the magnetic signal[47,48]. In the case of the RMF setup used in the present study, the magnetic field is axially symmetric and magnetic field lines rotate in a horizontal direction, with the rotation frequency equal to the frequency of the electric current[49]. Therefore, depending on the applied electric current frequencies, also the synchronous speed of the magnetic flux rotation around the stator is different, as can be seen in the simulations: 5 Hz—https://www.youtube.com/watch?v=EwojY3mR11A; 50 Hz—https://www.youtube.com/watch?v=swCPxvRdZoc.

Moreover, the electric current frequency determines the magnetic field intensity and it is responsible for the magnetic wave's physical characteristics. At 5 Hz (the lowest current frequency that can be used in the setup), the amplitude of the RMF was characterized by a longer period of maximal/minimal magnetic induction (B) state with B_{max}/B_{min} 8.354/8.352 mT. In contrast, the RMF generated at 50 Hz (the highest current frequency that can be used in the setup) was characterized by a shorter period, with B_{max}/B_{min} 8.700/8.698 mT (Fig. 10, Supplementary Table S2). It was also estimated, that the observed effects resulted mainly from the influence of the magnetic field, whereas the energy flux density affecting the exposed samples caused by the generated electric field was negligible. The estimation of the energy flux density of the electric field is presented in Supplementary Information.

Nevertheless, although our studies showed that the RMF influence the rate of octenidine dihydrochloride penetration, it should be noted that these differences should not be treated as the fundamental reason for the changes observed in biological analyzes using bacterial biofilms (A.D.A.M. test). In these analyzes, as already mentioned, the applied antiseptic concentration, (6.25% for *S. aureus* and 25% for *P. aeruginosa*) did not reduce the viability of the bacterial cells (in case of the contact time of 3 h). Therefore, taking into account approx. 25% increase in the concentration of the octenidine dihydrochloride as a result of exposure to the RMF for 3 h, it could be also assumed that the results obtained in the A.D.A.M. could be bound to the higher concentration of the active substance in the agar discs. However, the analyzes carried out using the LC–MS/MS technique did not show any substantial differences in the octenidine dihydrochloride concentrations as a result of exposure to the RMF for 2 h as compared to the exposure lasting for1 h. In turn, the results obtained from the measurement of the antibiofilm activity using the A.D.A.M. test did not differ significantly between 3 and 2 h exposure variants. Thus, although the 2 h RMF-exposed agar discs contained approximately the same concentration of octenidine dihydrochloride as the discs exposed for 1 h, the antimicrobial effect recorded after the exposure lasting for 2 h was comparable to the one which was observed after 3 h. For this reason, it can be assumed that although the increased concentration of octenidine dihydrochloride may have a positive impact on the outcome observed, the interpretation of the results should explicitly take into account also the influence of the RMF on bacterial cells and/or the biofilm matrix. With regard to that, the previous studies have indicated the ability of different types of magnetic fields to disturb microbial structures, i.e. to permanently damage the bacterial cell walls, presumably by their irreversible electroporation[50,51]. Fojt et al. (2004) explained that a drop in bacterial viability after exposure to the magnetic field was caused by an increase in the permeability of ion channels in the cytoplasmic membranes or by the formation of free radicals in bacterial cells[28]. Similarly, also in our previous studies concerning the impact of combined use of the RMF with various classes of antibiotics against *S. aureus*, the most promising results involved two groups of antibiotics, β-lactams, and glycopeptides[20], the common feature of which is the site of their antimicrobial activity, i.e., the bacterial cell wall.

The in vitro biofilm, applied in our research consists of three components: biofilm-forming cells, biofilm matrix, and biofilm milieu understood here as the medium immersing biofilm and filling the empty spaces (the light of matrix pores) within biofilm structure. The analyses of the distribution of biofilm-forming cells and the integrity of their cell walls, performed using confocal microscopy indicated at least two noticeable phenomena. The first of them was that number of cells with altered/compromised cell walls in biofilms exposed to the RMF only (without the antiseptic) was higher compared to the unexposed controls; while the second of them was that

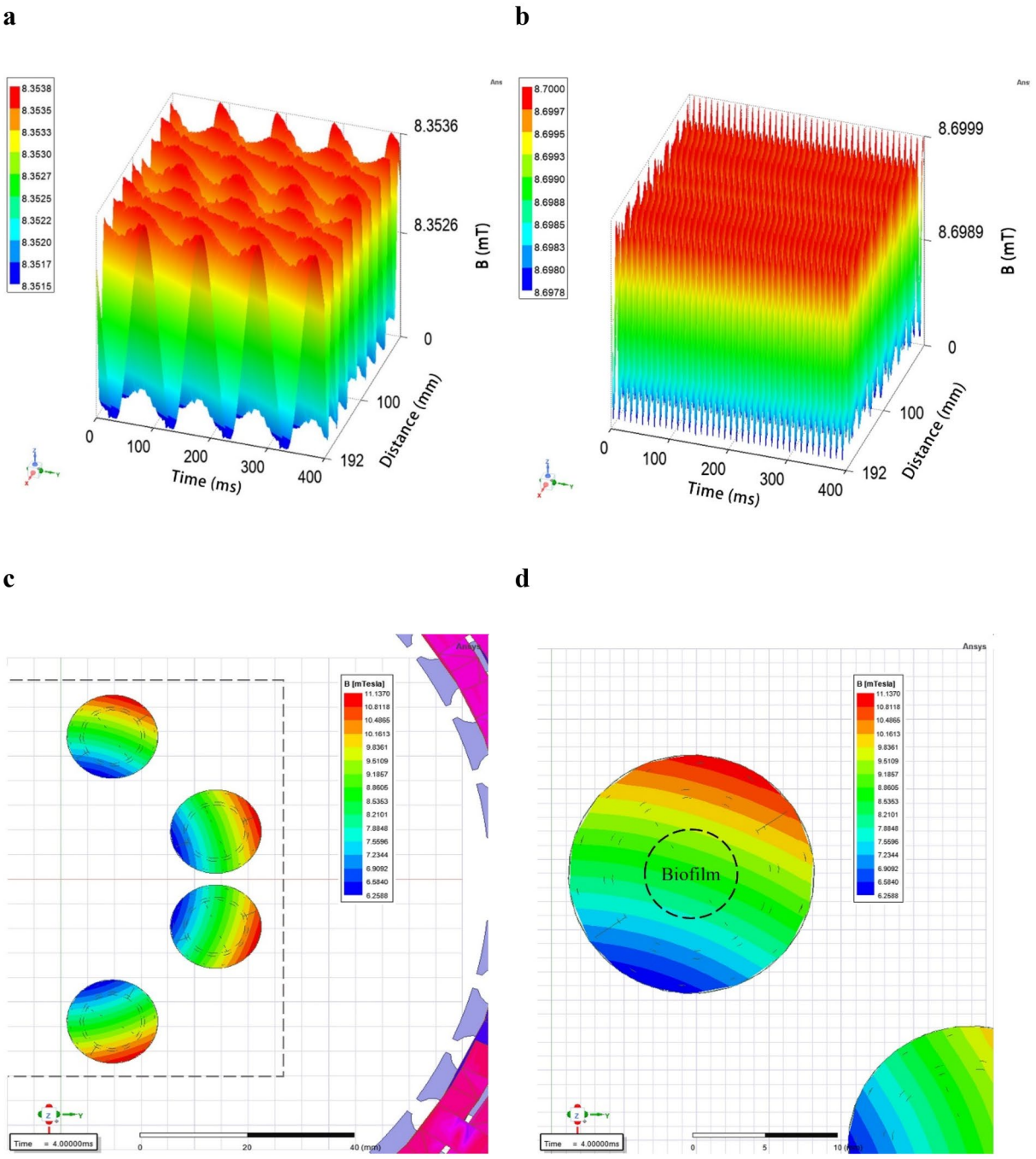

Figure 10. Periodical changes in magnetic induction in the center of the well of a test plate depending on the applied current frequency: (**a**) 5 Hz; (**b**) 50 Hz and distribution of the magnetic induction: (**c**) in the wells of a test plate; (**d**) at the location of the agar disc covered with biofilm.

these cell-wall altered cells were found in every analyzed (upper, middle and basal) biofilm cross-section. Bearing in mind the fact that metabolic analyses indicated no loss of cell viability, it has to be assumed that alterations of cell walls being the result of the RMF activity were of minor functional character (they did not lead to cell death, but at the same time they were strong enough to be detected by applied visualization technique). In turn, the occurrence of altered cells across the Z-axis of the whole biofilm structure suggests that this effect should be attributed to the RMF, and its wave-like properties, not compromised by such physical factors as biofilm thickness or matrix density. Noteworthy, the data obtained from confocal microscopy showed high compliance with the results of metabolic tests with this regard that combined application of the RMF and antiseptic led to the strong eradication of biofilm in all its parts, while the application of the antiseptic only (in a given 3 h contact time) did not correlate with a significant drop of viable cells and with the increase of dead cells.

The subsequent analysis performed using SEM revealed that the RMF-exposed cells forming pseudomonal or staphylococcal biofilm exhibit the whole spectrum of alterations, recognized as typical manifestations of

disturbances in cell walls/membranes[52]. Even weak magnetic fields, such as the RMF applied in the current work, are considered to be able to cause not only the already-mentioned mixing effect of electrically charged particles in liquids or colloids (such as bacterial cytoplasm containing large quantities of mobile ions) but also to excite the electrons in cytoplasmatic molecules. As shown by Hong et al. (1995), the effects of such magnetic induction concentrate on the cellular walls/membranes, due to the shielding effect mostly[53]. Such a statement is coherent not only with the data presented in the current work (showing disturbances in the bacterial cell walls as a result of the RMF exposure) but also with the results shown recently by Sharpe et al. (2021), who reported the damage of mitochondrial membranes in cancer cells exposed to the RMF[54]. It should be underlined that process of biofilm matrix formation is facilitated to a major extent by specialized protein systems localized throughout the bacterial cell walls and membranes[55]. Because the impact of the RMF on these particular cellular compartments was explicitly shown (and partially elucidated) in this work, it would be rational to assume that their alteration may have also an impact on the secreted biofilm matrix. Indeed, the average number of pores in the RMF-exposed biofilm matrices was significantly higher as compared to the RMF-unexposed controls (regardless of the species). We are aware of fact that such parametric analysis of SEM images, as performed, might be not completely representative, taking into consideration the fact that only a relatively small area of the whole biofilm structure could be analyzed by its means. Therefore, this part of the experiment should be treated as the pilotage and it requires the development with the use of more suitable, parametric analyses. To overcome the above-mentioned disadvantage, we performed GC–MS/MS analyses of the whole, cell-free biofilm matrices to investigate whether the application of the RMF translates into a change of one of their main components, i.e. saccharides. The results showed that the concentration of all detected saccharides changed in the RMF-exposed biofilms (regardless of the applied RMF frequency and biofilm-forming bacteria). In the case of the Gram-negative *P. aeruginosa*, the significant drop of saccharides' concentration (in the setting applying the RMF of 5 Hz, mostly) was visible, while such an effect was not detected so explicitly in the case of the Gram-positive *S. aureus* biofilm. Taking into consideration the data presented in the already mentioned work of Hong et al. (1995) concerning the shielding effect manifesting primarily in cellular boundaries, it may be assumed that the rigid, multi-layer cell wall of *S. aureus* was more resistant (than relatively thin cell wall of *P. aeruginosa*) to the RMF-induced electron excitation and resulting disturbances in the protein-mediated secretion of matrix components[53]. Such observation requires, undoubtedly, further investigation of the biofilm proteome (with special stress put on the membrane/cell walls proteins) to interconnect the already demonstrated changes in the biofilm matrix with possible alteration in these proteins' expression and concentration. Moreover, in our analyses, we focused on the saccharides only, while recent data show that also other components, such as extracellular DNA may constitute the majority of the biofilm matrix[56]. Nevertheless, even at the present stage, the presented data is another example of the complex nature of the interaction of RMF on biofilm structure.

When octenidine dihydrochloride-based antiseptic is applied against pathogenic biofilm, it needs to, in the first place, penetrate the biofilm milieu. In the case of the experimental model applied in this research, the milieu is microbiological medium and agar discs. As we already indicated in our earlier work[2], the plethora of organic compounds in applied TSB medium, derived from hydrolyzate of casein and soybean, may have an impact on cationic octenidine dihydrochloride. In fact, the normative methods of assessment of antiseptic activity imply the use of an "organic burden" to analyze the impact of this load on antiseptic molecules' activity, which is mostly negative (the effectiveness drops)[57]. The agar discs are another component of the biofilm milieu. The parametric processing of SEM images of agar surfaces revealed that the average Ferret's diameter of agar pores, through which octenidine dihydrochloride molecules had to penetrate was 70 nm (Supplementary Fig. S9), which is coherent with the data presented by Crowle et al. (1973)[58]. Such pore size, at the first glance, should not interfere with the penetration of a relatively small molecule (106 atoms) of octenidine dihydrochloride. Nevertheless, one-third of agar consists of agaropectin, which is negatively charged due to the presence of pyruvate and sulfate groups[59]. Therefore, one may assume that such negatively charged, medium-filled nano-pores of agar may interact with the cationic (i.e. net positive) charge of octenidine dihydrochloride and decrease its penetrability. The antiseptic needs also to penetrate through the biofilm matrix, which may consist of molecules trapping its molecules and decreasing its concentration. Next, the octenidine dihydrochloride binds to the cell walls and membranes and disrupts them, leading to the cells' death followed by leakage of cytoplasm to the external environment.

In turn, when RMF is applied as a self-reliant factor, it interacts with virtually all components (milieu, biofilm matrix, and the biofilm-forming cells) of the applied experimental model. The RMF increases also the penetration of cationic octenidine dihydrochloride molecule through the agar pores-filling medium, by increasing its mixing efficacy. The RMF-induced mixing effect occurs also in intracellular, colloidal cytoplasm which exerts elevated pressure on bacterial cell walls[15,60]. Another RMF-induced phenomenon is related to supra-molecular excitation of electrons[55], manifesting mostly in, indicated in this work, disturbances of cell walls/membranes. These alterations are also most likely the reason standing behind observed changes in the biofilm matrix porosity and composition because they affect the cell wall/membrane-localized protein systems facilitating synthesis and transportation of matrix components from the cell to the external environment. Although all these above-mentioned RMF-induced changes, seem to not disturb significantly the general viability of the staphylococcal and pseudomonal biofilms (as indicated in metabolic tests), they significantly facilitate the activity of antiseptic by weakening the cell wall/membrane structures (main target site of the octenidine dihydrochloride). From the clinical perspective and future potential application of the RMF as a therapeutic agent, it can be assumed that thanks to the RMF it is possible to destroy the biofilm, even in its basal layers, with the use of relatively low concentrations of antiseptic, in a much shorter contact time, comparing to the setting in which the same therapeutical effect would be achieved, but without the use of the magnetic field.

In conclusion, the current study showed, that 3 h exposure to the RMF without antiseptic did not destroy biofilm as compared to the unexposed controls. Similarly, the application of antiseptic without the RMF did not influence biofilm viability during 3 h contact time. However, in the simultaneous presence of the antiseptic

and RMF, the significant antibiofilm effect was revealed after already 1 h of the exposure, and it increased along with the exposure time. It was also demonstrated, that the RMF weakened the cell wall/membranes of biofilm-forming, increased the porosity of the biofilm matrix, and altered its chemical composition. Therefore, in the future perspective, the RMF may find an application as a therapeutic agent increasing antiseptics' effectiveness, especially in an environment where physical obstacles may hinder their activity.

Data availability

The original datasets generated during the current study have been deposited with link to Figshare database (https://figshare.com/articles/dataset/The_Multi-Directional_Effect_of_Rotating_Magnetic_Field_and_Antiseptic_on_In_Vitro_Pathogenic_Biofilm_and_Its_Milieu/19494143).

Received: 17 January 2022; Accepted: 16 May 2022
Published online: 25 May 2022

References

1. Moormeier, D. E. & Bayles, K. W. *Staphylococcus aureus* biofilm: A complex developmental organism. *Mol. Microbiol.* **104**, 365–376 (2017).
2. Paleczny, J. *et al.* The high impact of *Staphylococcus aureus* biofilm culture medium on in vitro outcomes of antimicrobial activity of wound antiseptics and antibiotic. *Pathogens* **10**, 1385 (2021).
3. Omar, A., Wright, J. B., Schultz, G., Burrell, R. & Nadworny, P. Microbial biofilms and chronic wounds. *Microorganisms* **5**, 9 (2017).
4. Norman, G., Dumville, J. C., Mohapatra, D. P., Owens, G. L. & Crosbie, E. J. Antibiotics and antiseptics for surgical wounds healing by secondary intention. *Cochrane Database Syst. Rev.* **3**, CD011712 (2016).
5. Zhao, G. *et al.* Biofilms and inflammation in chronic wounds. *Adv. Wound Care* **2**, 389–399 (2013).
6. Spear, M. Wound exudate—The good, the bad, and the ugly. *Plast. Surg. Nurs.* **32**, 77–79 (2012).
7. Bjarnsholt, T. *et al.* Why chronic wounds will not heal: A novel hypothesis. *Wound Repair Regen.* **16**, 2–10 (2008).
8. Sapotoczna, M., O'Neill, E. & O'Gara, J. P. Untangling the diverse and redundant mechanisms of *Staphylococcus aureus* biofilm formation. *PLoS Pathog.* **12**, e1005671 (2016).
9. Muller, G. & Kramer, A. Biocompatibility index of antiseptic agents by parallel assessment of antimicrobial activity and cellular cytotoxicity. *J. Antimicrob. Chemother.* **61**, 1281–1287 (2008).
10. Novickij, V. *et al.* Overcoming antimicrobial resistance in bacteria using bioactive magnetic nanoparticles and pulsed electromagnetic fields. *Front. Microbiol.* **8**, 2678 (2017).
11. Wang, X. *et al.* Microenvironment–responsive magnetic nanocomposites based on silver nanoparticles/gentamicin for enhanced biofilm disruption by magnetic field. *ACS Appl. Mater. Interfaces* **10**, 34905–34915 (2018).
12. Salmen, S. H., Alharbi, S. A., Faden, A. A. & Wainwright, M. Evaluation of effect of high frequency electromagnetic field on growth and antibiotic sensitivity of bacteria. *Saudi J. Biol. Sci.* **25**, 105–110 (2018).
13. Bajpai, I., Saha, N. & Basu, B. Moderate intensity static magnetic field has bactericidal effect on *E. coli* and *S. epidermidis* on sintered hydroxyapatite. *J. Biomed. Mater. Res. B Appl. Biomater.* **100**, 1206–1217 (2012).
14. Brkovic, S., Postic, S. & Ilic, D. Influence of the magnetic field on microorganisms in the oral cavity. *J. Appl. Oral Sci.* **23**, 179–186 (2015).
15. Rakoczy, R. *et al.* The study of influence of a rotating magnetic field on mixing efficiency. *Chem. Eng. Process. Process Intensif.* **112**, 1–8 (2017).
16. Fijałkowski, K., Nawrotek, P., Struk, M., Kordas, M. & Rakoczy, R. The effects of rotating magnetic field on growth rate, cell metabolic activity and biofilm formation by *Staphylococcus aureus* and *Escherichia coli*. *J. Magn.* **18**, 289–296 (2013).
17. Fijałkowski, K., Nawrotek, P., Struk, M., Kordas, M. & Rakoczy, R. Effects of rotating magnetic field exposure on the functional parameters of different species of bacteria. *Electromagn. Biol. Med.* **34**, 48–55 (2015).
18. Woroszyło, M. *et al.* The impact of intraspecies variability on growth rate and cellular metabolic activity of bacteria exposed to rotating magnetic field. *Pathogens* **10**, 1427 (2021).
19. Junka, A. F. *et al.* Application of rotating magnetic fields increase the activity of antimicrobials against wound biofilm pathogens. *Sci. Rep.* **8**, 167 (2018).
20. Woroszyło, M. *et al.* The effect of rotating magnetic field on susceptibility profile of methicillin-resistant *Staphylococcus aureus* strains exposed to activity of different groups of antibiotics. *Int. J. Mol. Sci.* **22**, 11551 (2021).
21. Woroszyło, M. *et al.* Rotating magnetic field increases β-lactam antibiotic susceptibility of methicilin-resistant *Staphylococcus aureus* strains. *Int. J. Mol. Sci.* **22**, 12397 (2021).
22. Junka, A. F. *et al.* A.D.A.M. test (antibiofilm dressing's activity measurement)-simple method for evaluating anti-biofilm activity of drug-saturated dressings against wound pathogens. *J. Microbiol. Methods* **143**, 6–12 (2017).
23. Junka, A. *et al.* Potential of biocellulose carrier impregnated with essential oils to fight against biofilms formed on hydroxyapatite. *Sci. Rep.* **9**, 1256 (2019).
24. Kramer, A. *et al. Octenidine, Chlorhexidine, Iodine and Iodophores* (Georg Thieme, 2008).
25. Malanovic, N., Ön, A., Pabst, G., Zellner, A. & Lohner, K. Octenidine: Novel insights into the detailed killing mechanism of Gram-negative bacteria at a cellular and molecular level. *Int. J. Antimicrob. Agents* **56**, 106146 (2020).
26. Karygianni, L., Ren, Z., Koo, H. & Thurnheer, T. Biofilm matrixome: Extracellular components in structured microbial communities. *Trends Microbiol.* **2020**, 668–681 (2020).
27. Jennings, L. K. *et al.* Pel is a cationic exopolysaccharide that cross-links extracellular DNA in the *Pseudomonas aeruginosa* biofilm matrix. *Proc. Natl. Acad. Sci. U. S. A.* **112**, 11353–11358 (2015).
28. Fojt, L., Strašák, L., Vetterl, V. & Šmarda, J. Comparison of the low-frequency magnetic field effects on bacteria *Escherichia coli*, *Leclercia adecarboxylata* and *Staphylococcus aureus*. *Bioelectrochemistry* **63**, 337–341 (2004).
29. Strašák, L., Vetterl, V. & Fojt, L. Effects of 50 Hz magnetic fields on the viability of different bacterial strains. *Electrom. Biol. Med.* **24**, 293–300 (2005).
30. Piatti, E. *et al.* Antibacterial effect of a magnetic field on *Serratia marcescens* and related virulence to *Hordeum vulgare* and *Rubus fruticosus* callus cells. *Comp. Biochem. Physiol. B Biochem. Mol. Biol.* **132**, 359–365 (2002).
31. Strašák, L., Vetterl, V. & Šmarda, J. Effects of low-frequency magnetic fields on bacteria *Escherichia coli*. *Bioelectrochemistry* **55**, 161–164 (2002).
32. Babushkina, I. V. *et al.* The influence of alternating magnetic field on *Escherichia coli* bacterial cells. *Pharm. Chem. J.* **39**, 398–400 (2005).
33. Justo, O. R., Pérez, V. H., Alvarez, D. C. & Alegre, R. M. Growth of *Escherichia coli* under extremely low-frequency electromagnetic fields. *Appl. Biochem. Biotechnol.* **134**, 155–164 (2006).
34. Cellini, L. *et al.* Bacterial response to the exposure of 50 Hz electromagnetic fields. *Bioelectromagnetics* **29**, 302–311 (2009).

35. László, J. & Kutasi, J. Static magnetic field exposure fails to affect the viability of different bacteria strains. *Bioelectromagnetics* **31**, 220–225 (2010).
36. Gao, W., Liu, Y., Zhou, J. & Pan, H. Effects of a strong static magnetic field on bacterium *Shewanella oneidensis*: An assessment by using whole genome microarray. *Bioelectromagnetics* **26**, 558–563 (2005).
37. Grosman, Z., Kolár, M. & Tesaríková, E. Effects of static magnetic field on some pathogenic microorganisms. *Acta Univ. Palacki. Olomuc. Fac. Med.* **134**, 7–9 (1992).
38. Poortinga, A. T., Bos, R. & Busscher, H. J. Lack of effect of an externally applied electric field on bacterial adhesion to glass. *Colloids Surf. B Biointerfaces* **20**, 189–194 (2001).
39. Gebreyohannes, G., Nyerere, A., Bii, C. & Sbhatu, D. B. Challenges of intervention, treatment, and antibiotic resistance of biofilm-forming microorganisms. *Heliyon* **5**, e02192 (2019).
40. Guzmán-Soto, I. *et al.* Mimicking biofilm formation and development: Recent progress in in vitro and in vivo biofilm models. *Iscience* **24**, 102443 (2021).
41. Luppens, S. B., Reij, M. W., van der Heijden, R. W., Rombouts, F. M. & Abee, T. Development of a standard test to assess the resistance of *Staphylococcus aureus* biofilm cells to disinfectants. *Appl. Environ. Microbiol.* **68**, 4194–4200 (2002).
42. Stanley, N. R. & Lazazzera, B. A. Environmental signals and regulatory pathways that influence biofilm formation. *Mol. Microbiol.* **52**, 917–924 (2004).
43. Kumar, P., Nagarajan, A. & Uchil, P. D. Analysis of cell viability by the MTT assay. *Cold Spring Harb. Protoc.* **2018**, pdb-prot095505 (2018).
44. Nawrotek, P., Fijałkowski, K., Struk, M., Kordas, M. & Rakoczy, R. Effects of 50 Hz rotating magnetic field on the viability of *Escherichia coli* and *Staphylococcus aureus*. *Electromagn. Biol. Med.* **33**, 29–34 (2014).
45. Segatore, B. *et al.* Evaluations of the effects of extremely low-frequency electromagnetic fields on growth and antibiotic susceptibility of *Escherichia coli* and *Pseudomonas aeruginosa*. *Int. J. Microbiol.* **2012**, 587293 (2012).
46. Dunca, S., Creanga, D.-E., Ailiesei, O. & Nimitan, E. Microorganisms growth with magnetic fluids. *J. Magn. Magn. Mater.* **289**, 445–447 (2005).
47. Del Re, B., Bersani, F., Agostini, C., Mesirca, P. & Giorgi, G. Various effects on transposition activity and survival of *Escherichia coli* cells due to different ELF-MF signals. *Radiat. Environ. Biophys.* **43**, 265–270 (2004).
48. Del Re, B. *et al.* Extremely low frequency magnetic fields affect transposition activity in *Escherichia coli*. *Radiat. Environ. Biophys.* **42**, 113–118 (2003).
49. Jabłońska, J. *et al.* Evaluation of ferrofluid-coated rotating magnetic field-assisted bioreactor for biomass production. *Chem. Eng. J.* **431**, 133913 (2022).
50. Golberg, A. *et al.* Eradication of multidrug-resistant *A. baumannii* in burn wounds by antiseptic pulsed electric field. *Technology* **2**, 153–160 (2014).
51. Tagourti, J. *et al.* Static magnetic field increases the sensitivity of *Salmonella* to gentamicin. *Ann. Microbiol.* **60**, 519–522 (2010).
52. Wong, F. *et al.* Cytoplasmic condensation induced by membrane damage is associated with antibiotic lethality. *Nat. Commun.* **12**, 2321 (2021).
53. Hong, F. T. Magnetic field effects on biomolecules, cells, and living organisms. *Biosystems* **36**, 187–229 (1995).
54. Sharpe, M. A., Baskin, D. S., Pichumani, K., Ijare, O. B. & Helekar, S. A. Rotating magnetic fields inhibit mitochondrial respiration, promote oxidative stress and produce loss of mitochondrial integrity in cancer cells. *Front. Oncol.* **11**, 768758 (2021).
55. Hobley, L., Harkins, C., MacPhee, C. E. & Stanley-Wall, N. R. Giving structure to the biofilm matrix: An overview of individual strategies and emerging common themes. *FEMS Microbiol. Rev.* **39**, 649–669 (2015).
56. Seviour, T. *et al.* The biofilm matrix scaffold of *Pseudomonas aeruginosa* contains G-quadruplex extracellular DNA structures. *NPJ Biofilms Microbiomes* **7**, 27 (2021).
57. EN 13727: Chemical disinfectants and antiseptics—Quantitative suspension test for the evaluation of bactericidal activity in the medical area. (Accessed 15 December 2021); https://www.situbiosciences.com/product/en-13727-chemical-disinfectants-and-antiseptics-quantitative-suspension-test-for-the-evaluation-of-bactericidal-activity-in-the-medical-area/.
58. Crowle, A. J. General information. In *Immunodiffusion* (ed. Crowle, A. J.) 65–206 (Elsevier, 1973).
59. Pawlicka, A. & Donoso, J. P. Polymer electrolytes based on natural polymers. In *Polymer Electrolytes* (eds Sequeira, C. & Santo, D.) 95–128 (Elsevier, 2010).
60. Fijałkowski, K. *et al.* Increased yield and selected properties of bacterial cellulose exposed to different modes of a rotating magnetic field. *Eng. Life Sci.* **16**, 483–493 (2016).

Acknowledgements

We would like to thank Daniel Styburski from the Laboratory of Chromatography and Mass Spectroscopy at the West Pomeranian University of Technology, Szczecin for his help in the analysis using LC–MS/MS. We would also like to express our gratitude to Professor Jerzy Detyna from Department of Mechanics, Materials and Biomedical Engineering, Wrocław University of Science and Technology for providing us the inestimable help in understanding the correlations between the magnetic and electrical phenomena occurring in microorganisms exposed to the rotating magnetic field.

Author contributions

D.C.-J., A.J., K.F. designed the study and contributed to the analysis of the results; D.C.-J., A.Ż., A.J., M.W. (Marta Woroszyło), M.W. (Marcin Wardach), G.C., P.S.-Z., P.M. performed the experiments and data calculations; D.C.-J., A.J. M.W. (Marcin Wardach) generated the figures; D.C.-J., A.J., K.F. wrote the manuscript.

Funding

This work was funded by National Science Centre in Poland (Grant No. 2017/27/B/NZ6/02103, Opus 14, granted to Karol Fijałkowski).

Competing interests

The authors declare no competing interests.

Additional information

Supplementary Information The online version contains supplementary material available at https://doi.org/10.1038/s41598-022-12840-y.

Correspondence and requests for materials should be addressed to A.J. or K.F.

Zachodniopomorski Uniwersytet Technologiczny w Szczecinie

Wydział Biotechnologii i Hodowli Zwierząt

Załącznik 2

Kopie suplementów publikacji naukowych wchodzących w skład cyklu stanowiącego rozprawę doktorską

Daria Ciecholewska-Juśko

Rozprawa doktorska

OPRACOWANIE I CHARAKTERYSTYKA MATERIAŁÓW BIONANOCELULOZOWYCH DO ZAPOBIEGANIA KOLONIZACJI PRZEZ DROBNOUSTROJE PATOGENNE ORAZ DO ERADYKACJI BIOFILMÓW BAKTERYJNYCH

Supplementary data

Superabsorbent crosslinked bacterial cellulose biomaterials for chronic wound dressings

Daria Ciecholewska-Juśko[a], Anna Żywicka[a], Adam Junka[b], Radosław Drozd[a], Peter Sobolewski[c], Paweł Migdał[d], Urszula Kowalska[e], Monika Toporkiewicz[f], Karol Fijałkowski[a*]

[a]Department of Microbiology and Biotechnology, Faculty of Biotechnology and Animal Husbandry, West Pomeranian University of Technology in Szczecin, Piastów 45, 70-311 Szczecin, Poland; daria.ciecholewska@zut.edu.pl; anna.zywicka@zut.edu.pl; radoslaw.drozd@zut.edu.pl; karol.fijalkowski@zut.edu.pl

[b]Department of Pharmaceutical Microbiology and Parasitology, Wrocław Medical University, Borowska 211A, 50-556 Wrocław, Poland; adam.junka@umed.wroc.pl

[c]Department of Polymer and Biomaterials Science, Faculty of Chemical Technology and Engineering, West Pomeranian University of Technology in Szczecin, Piastów 45, 70-311 Szczecin, Poland; psobolewski@zut.edu.pl

[d]Department of Environment, Hygiene and Animal Welfare, Faculty of Biology and Animal Science, Wrocław University of Environmental and Life Sciences, Chełmońskiego 38C, 51-630 Wrocław, Poland; pawel.migdal@upwr.edu.pl

[e]Centre of Bioimmobilization and Innovative Packaging Materials, West Pomeranian University of Technology in Szczecin, Janickiego 35, 71-270 Szczecin, Poland; urszula.kowalska@zut.edu.pl

[f]Laboratory of Confocal Microscopy, Łukasiewicz Research Network - PORT Polish Center for Technology Development, Stabłowicka 147, 54-066 Wrocław, Poland; monika.toporkiewicz@port.pl

***Corresponding author**

E-mail address: karol.fijalkowski@zut.edu.pl (K. Fijałkowski).

Abbreviations

BC, bacterial cellulose; CAT, catalyst; CA, citric acid; M1, modification with disodium phosphate as a catalyst (CAT); M2, modification with sodium bicarbonate as a CAT; M3, modification with mixture of disodium phosphate and sodium bicarbonate in the ratio 1:1 as a CAT; M4, modification with ammonium bicarbonate as a CAT; M5, modification with disodium phosphate and ammonium bicarbonate in the ratio 1:1 as a CAT; M6, modification with sodium bicarbonate and ammonium bicarbonate in the ratio 1:1 as a CAT; M7, modification with sodium hypophosphite as a CAT; SHP, sodium hypophosphite; SR, swelling ratio; WHC, water holding capacity; WPG , weight percent gain.

1. Optimization of BC crosslinking reaction

The SR (%) values for BC samples modified using different CATs under the same reaction conditions displayed a comparable trend. The SR (%) results for the most effective M3 modification are presented in **Fig. S1,** while the entire data set of the results from the optimization process are tabulated in **Tab. S1 – S9.**

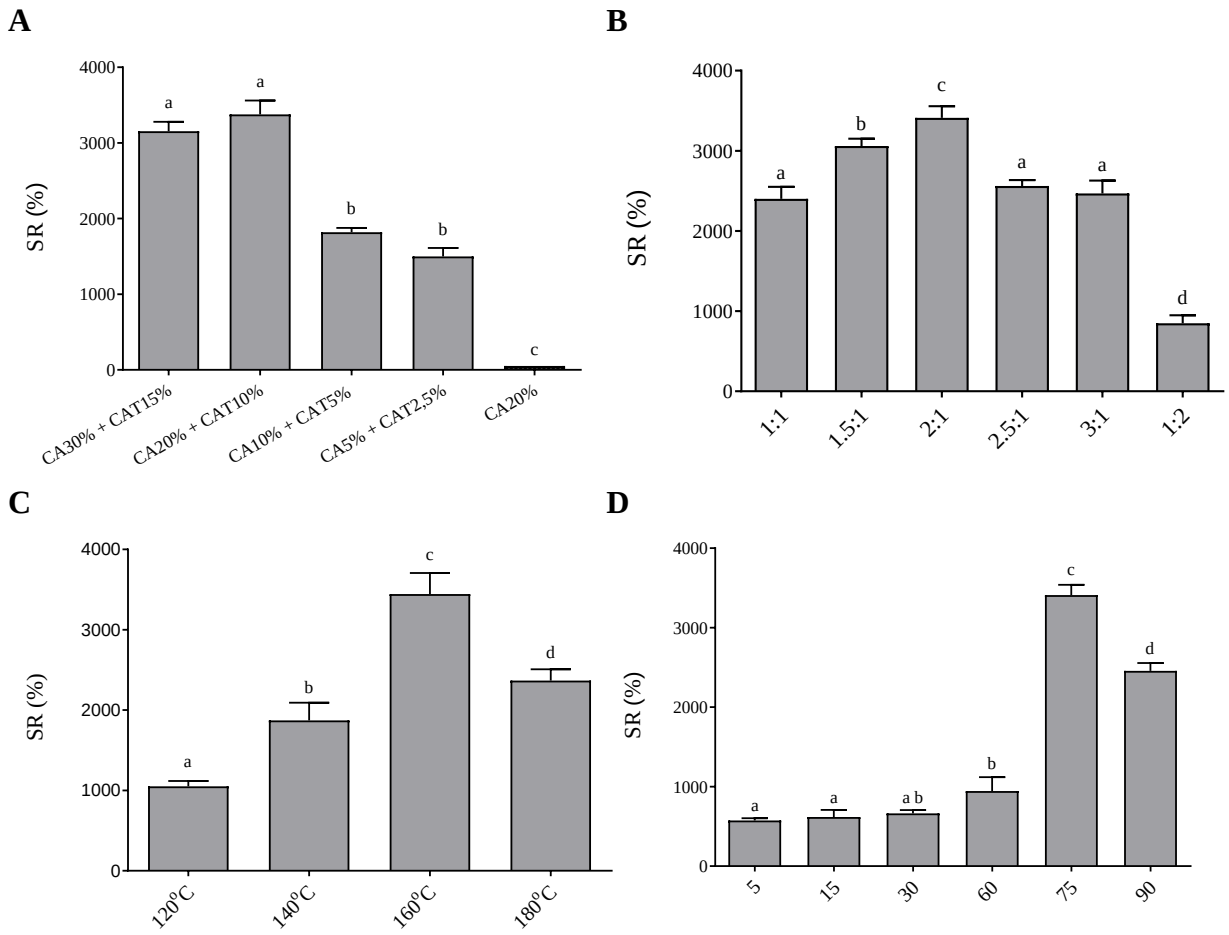

Fig. S1. Swelling ratio (SR (%)) measured after 24 h, depending on the parameters used during optimization of BC crosslinking with CAT3 (disodium phosphate and sodium bicarbonate 1:1); A – different percentage of CA and CAT; B – different CA:CAT mass ratio; C – different reaction temperature; D – different reaction time.

Data are presented as mean ± standard error of the mean (SEM); values with different letters are significantly different ($p<0.05$): a, b, c, d – statistically significant differences between the analyzed parameters.

1.1. Concentration of citric acid (CA) and catalysts (CAT) solutions

Solutions consisting of 20% CA and 10% CAT, as well as 30% CA and 15% CAT – regardless CAT used – yielded BC pellicles with significantly higher values of SR (%), as compared to lower concentrations of both compounds (**Fig. S1A**, **Tab. S1**, **Tab. S2**). Further, SR (%) did not differ significantly between 20% CA + 10% CAT and 30% CA + 15% CAT solutions. The highest SR (%) (3377.09 ± 184.43) was obtained for the M3. With decreasing CA and CAT concentration, below 20% CA and 10% CAT, a gradual decrease of SR (%) was observed. Thus, taking into account the economic aspect, for the further optimization stages the lower, but still highly effective, concentration of CA and CAT (CA20% + CAT10%) was chosen. These results are consistent with the results of Meftahi, Khajavi, Rashidi, Rahimi, & Bahador (2018), who reported the same concentration of CA and CAT (in their case, SHP) as the yielding the highest SR (%) values.

Tab. S1. Swelling ratio (SR (%)) of BC samples measured after 24 h of incubation in water depending on the percentage of citric acid (CA) and catalysts (CAT) solution.

Type of modification	CA30% + CAT15%	CA20% + CAT10%	CA10% + CAT5%	CA5% + CAT2,5%
M1	2449.16 ± 156.45	**2528.32 ± 192.08**	1826.14 ± 100.02	1517.57 ± 62.19
M2	**2232.43 ± 112.60**	**2201.56 ± 50.66**	1039.72 ± 46.89	933.58 ± 63.76
M3	3154.53 ± 124.08	**3377.09 ± 184.43**	1818.91 ± 57.98	1499.65 ± 112.31
M4	**1084.74 ± 80.41**	**1082.45 ± 131.98**	968.81 ± 68.64	966.31 ± 38.34
M5	2292.05 ± 141.70	**2324.66 ± 22.52**	1786.63 ± 60.10	1186.33 ± 50.10
M6	2247.87 ± 200.02	**2343.81 ± 43.81**	1556.29 ± 135.01	1176.79 ± 53.98
M7	2016.87 ± 152.37	**2033.25 ± 118.50**	1245.54 ± 162.51	1049.19 ± 84.81

C – control BC sample; M1-M7 – modified BC samples.

Tab. S2. Statistical differences between SR (%) values presented in Tab. S1.

	CA30% + CAT15%	CA20% + CAT10%	CA10% + CAT5%	CA5% + CAT2,5%	CA20%
CA30% + CAT15%	×	ns	****	****	****
CA20% + CAT10%	ns	×	****	****	****
CA10% + CAT5%	****	****	×	*	****
CA5% + CAT2,5%	****	****	*	×	****
CA20%	****	****	****	****	×

* p<0.05, ** p<0.01, *** p<0.001, **** p<0.0001.

1.2. Citric acid and catalyst solution mass ratio

BC samples modified using 20% CA + 10% CATs 1-5 and CAT7 reached the highest values of SR (%) at a CA:CAT mass ratio of 2:1 (**Fig. S1B**, **Tab. S3**, **Tab. S4**). The highest values of SR (%) were obtained for M3 (3410.72 ± 146.97) and the SR (%) values were significantly higher, as compared to the other ratio variants. When CAT6 (mixture of sodium bicarbonate and ammonium bicarbonate) was used, the values of SR (%) obtained did not significantly differ between mass ratios 2:1 and 1.5:1. For the case of the M7, although the SR (%) reached the highest values at mass ratio 2:1, the further increase did not result in statistically significant differences (likewise between 1.5:1, 2.5:1 and 3:1). As a result, the 2:1 (CA:CAT) ratio was chosen for the further steps of the optimization. Additionally, our results are consistent with the CA:SHP ratio previously reported by Reddy & Yang (2010).

Tab. S3. Swelling ratio (SR (%)) of BC samples measured after 24 h of incubation in water depending on the CA:CAT ratio.

Type of modification	CA:CAT					
	1:1	1.5:1	2:1	2.5:1	3:1	1:2
M1	2012.14 ± 109.11	2228.20 ± 62.50	**2468.47 ± 34.69**	2083.67 ± 62.41	2074.08 ± 69.13	743.71 ± 109.19
M2	1887.34 ± 87.49	2010.88 ± 79.14	**2178.67 ± 61.31**	2036.58 ± 57.11	2073.20 ± 146.58	685.82 ± 85.04
M3	2400.17 ± 147.02	3060.65 ± 89.58	**3410.72 ± 146.97**	2561.84 ± 73.33	2468.16 ± 160.54	849.62 ± 99.14
M4	1001.73 ± 114.37	1031.81 ± 40.40	**1110.47 ± 33.42**	1101.47 ± 119.91	1069.14 ± 68.07	776.02 ± 105.40
M5	2114.87 ± 102.96	2178.25 ± 22.70	**2500.39 ± 47.87**	2361.61 ± 201.80	2239.19 ± 10.88	839.18 ± 83.96
M6	1944.51 ± 39.75	**2403.25 ± 60.18**	**2399.71 ± 121.64**	2172.80 ± 164.02	2090.97 ± 173.99	770.12 ± 48.43
M7	1888.74 ± 88.38	1945.37 ± 179.11	**2028.26 ± 57.11**	2020.59 ± 50.41	1985.56 ± 86.06	866.32 ± 108.60

C – control BC sample; M1-M7 – modified BC samples.

Tab. S4. Statistical differences between SR (%) values presented in Tab. S3.

	1:1	1.5:1	2:1	2.5:1	3:1	1:2
1:1	×	***	****	ns	ns	****
1.5:1	***	×	*	**	***	****
2:1	****	*	×	****	****	****
2.5:1	ns	**	****	×	ns	****
3:1	ns	***	****	ns	×	****
1:2	****	****	****	****	****	×

* p<0.05, ** p<0.01, *** p<0.001, **** p<0.0001.

1.3. Reaction temperature

Regardless of the CAT used (**Fig. S1C**, **Tab. S5**, **Tab. S6**) the highest SR (%) was obtained at a temperature of 160 °C. Overall, increasing the temperature up to 160 °C correlated with increase of SR (%) in all BC samples, but when the temperature exceeded 160 °C, the SR (%) decreased.

Tab. S5. Swelling ratio (SR (%)) of BC samples measured after 24 h of incubation in water depending on the reaction temperature.

Type of modification	Reaction temperature (°C)			
	120	140	160	180
M1	844.87 ± 141.14	1605.45 ± 230.53	**2479.11 ± 97.01**	1834.64 ± 78.82
M2	911.85 ± 81.53	1235.85 ± 75.58	**2193.29 ± 371.01**	1832.06 ± 133.83
M3	1051.64 ± 65.72	1871.51 ± 221.02	**3444.81 ± 262.25**	2367.43 ± 139.72
M4	680.51 ± 102.15	857.58 ± 75.31	**1101.29 ± 46.17**	961.62 ± 35.76
M5	1087.18 ± 150.58	1491.20 ± 49.00	**2223.27 ± 117.86**	2009.50 ± 93.58
M6	918.38 ± 95.86	1722.73 ± 134.25	**2265.81 ± 363.48**	1883.16 ± 89.70
M7	707.86 ± 92.64	802.36 ± 88.81	**2019.84 ± 75.91**	1315.95 ± 187.29

C – control BC sample; M1-M7 – modified BC samples.

Tab. S6. Statistical differences between SR (%) values presented in Tab. S5.

	120	140	160	180
120	×	**	****	***
140	**	×	****	*
160	****	****	×	***
180	***	*	***	×

* p<0.05, ** p<0.01, *** p<0.001, **** p<0.0001.

1.4. Duration of crosslinking reaction

Once again, regardless of the CAT used, the highest SR (%) values were obtained after 75 min of crosslinking reaction (**Fig. S1D**, **Tab. S7**, **Tab. S8**). However, it is important to note that the duration of crosslinking must be adjusted to the weight of the sample – the heavier it is, the longer time of crosslinking is required (data not shown). Here, the BC samples had an average weight of 4.5 g. Compared to the work of Meftahi et al. (2018), where BC samples were crosslinked at 160 °C for just 5 min, the optimal crosslinking duration determined here was significantly longer, however the precise size and weight of BC samples used in that work were not clearly specified.

Tab. S7. Swelling ratio (SR (%)) of BC samples measured after 24 h of incubation in water depending on the time of reaction carried out at 160 °C.

Type of modification	Reaction time (min)					
	5	15	30	60	75	90
M1	529.57 ± 28.20	632.38 ± 51.50	668.04 ± 50.72	928.64 ± 88.97	**2417.22 ± 122.38**	1621.78 ± 35.97
M2	629.98 ± 42.83	751.51 ± 30.88	816.66 ± 36.72	937.05 ± 154.54	**2037.51 ± 74.38**	1146.15 ± 51.36
M3	573.89 v 28.77	618.04 ± 89.14	662.94 ± 42.53	944.21 ± 176.28	**3410.32 ± 130.04**	2456.54 ± 98.43
M4	523.39 ± 44.48	602.04 ± 17.57	659.34 ± 40.00	712.83 ± 62.14	**989.52 ± 58.44**	915.05 ± 71.75
M5	568.39 ± 24.09	633.18 ± 58.49	628.67 ± 14.74	918.83 ± 128.36	**2229.65 ± 106.17**	1711.16 ± 137.43
M6	603.73 ± 46.82	611.33 ± 21.59	562.30 ± 73.09	1095.10 ± 12.13	**2340.193 ± 196.60**	1974.74 ± 101.48
M7	542.68 ± 48.27	630.32 ± 53.38	632.16 ± 98.74	879.46 ± 57.53	**2018.44 ± 166.23**	1508.25 ± 173.19

C – control BC sample; M1-M7 – modified BC samples.

Tab. S8. Statistical differences between SR (%) values presented in Tab. S7.

	5	15	30	60	75	90
5	×	ns	**ns**	*	****	****
15	ns	×	**ns**	*	****	****
30	ns	ns	×	ns	****	****
60	*	*	**ns**	×	****	****
75	****	****	****	****	×	****
90	****	****	****	****	****	×

* p<0.05, ** p<0.01, *** p<0.001, **** p<0.0001.

Tab. S9. Adjusted p-values for each variant of optimization.

	*	**	***	****
Percentage of CA and CAT solutions	0.0412	-	-	< 0.0001
CA and CAT solutions mass ratio	0.0444	0.0039	0.0003 – 0.009	< 0.0001
Reaction temperature	0.0481	0.0031	0.0001 – 0.0005	< 0.0001
Reaction time	0.0111 – 0.0261	-	-	< 0.0001

1.5. BC samples treated with CA w/o CAT or CATs w/o CA

As controls, we tested BC samples treated with 20% CA without any CAT or treated with 10% of individual CATs without addition of CA (CA and CATs concentrations were selected based on the results presented in section *1.1.* Concentration of citric acid (CA) and catalysts (CAT) solutions). In all cases, the obtained modified BC samples were characterized by substantially lower SR (%) values as compared to the dry, unmodified BC (**Fig. S2A**). The low rehydration capacity of the samples treated with just a single reaction component (CA or CAT) was associated with reduced formation of layers and air cavities (**Fig. S2B**), which were observed in the case of samples modified with the use of the CA / CAT combination. The difference between SR (%) values of unmodified BC and BC treated with individual components was also related to the differences between their dry weights – weight of the unmodified samples was considerably lower as compared to the CA or CAT treated samples.

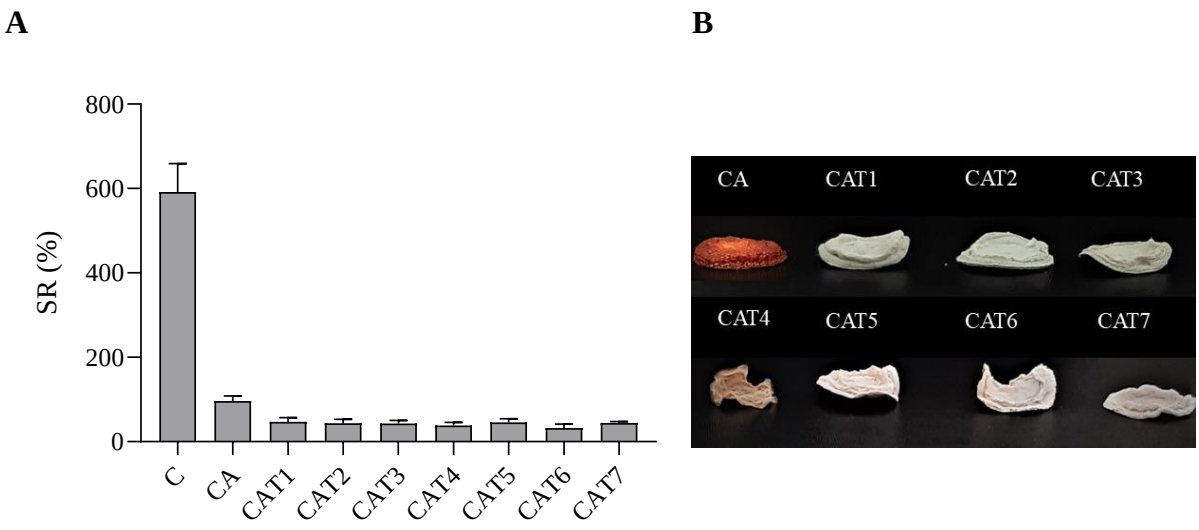

Fig. S2. Swelling ratio (SR (%)) measured after 24 h (A) and images (B) of BC samples treated with 20% solution of CA w/o CAT or with 10% solutions of CAT w/o CA. C – control BC sample; CA – BC treated with 20% CA w/o CAT; CAT1-CAT7 – BC treated with 10% of individual CATs w/o CA."

References

Meftahi, A., Khajavi, R., Rashidi, A., Rahimi, M. K., & Bahador, A. (2018). Preventing the collapse of 3D bacterial cellulose network via citric acid. *Journal of Nanostructure in Chemistry*, 8(3), 311-320.

Reddy, N., & Yang, Y. (2010). Citric acid cross-linking of starch films. *Food Chemistry*, 118(3), 702-711.

2. Macro and micromorphological characteristics of modified BC

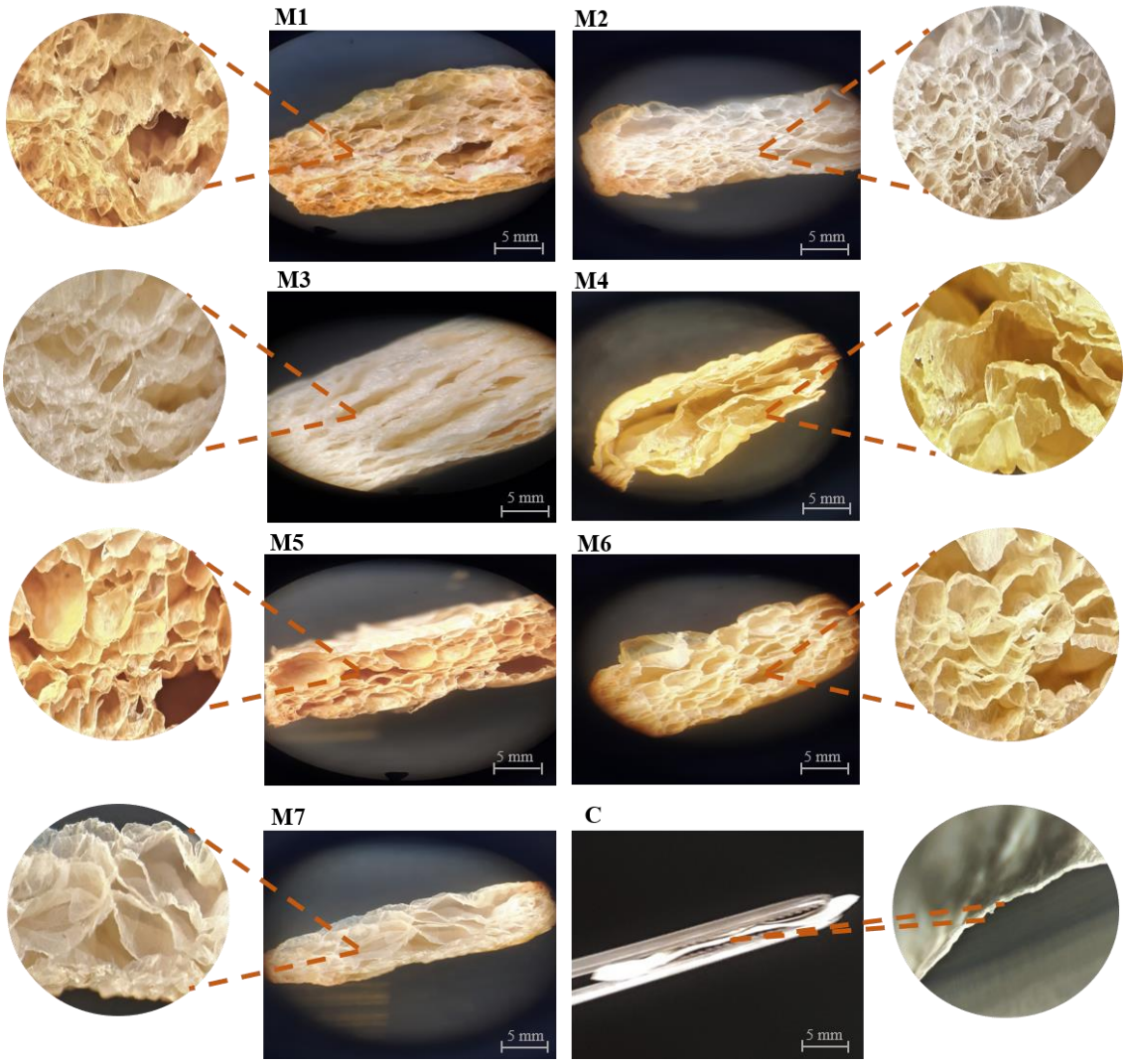

Fig. S3. Cross sections of modified BC samples (magnification 5x and 25x, pictures in the center and on the edges of the figure, respectively). Pictures were taken using stereoscopic microscope (MST, Zeiss, Oberkochen, Germany). C – control BC sample; M1-M7 – modified BC samples.

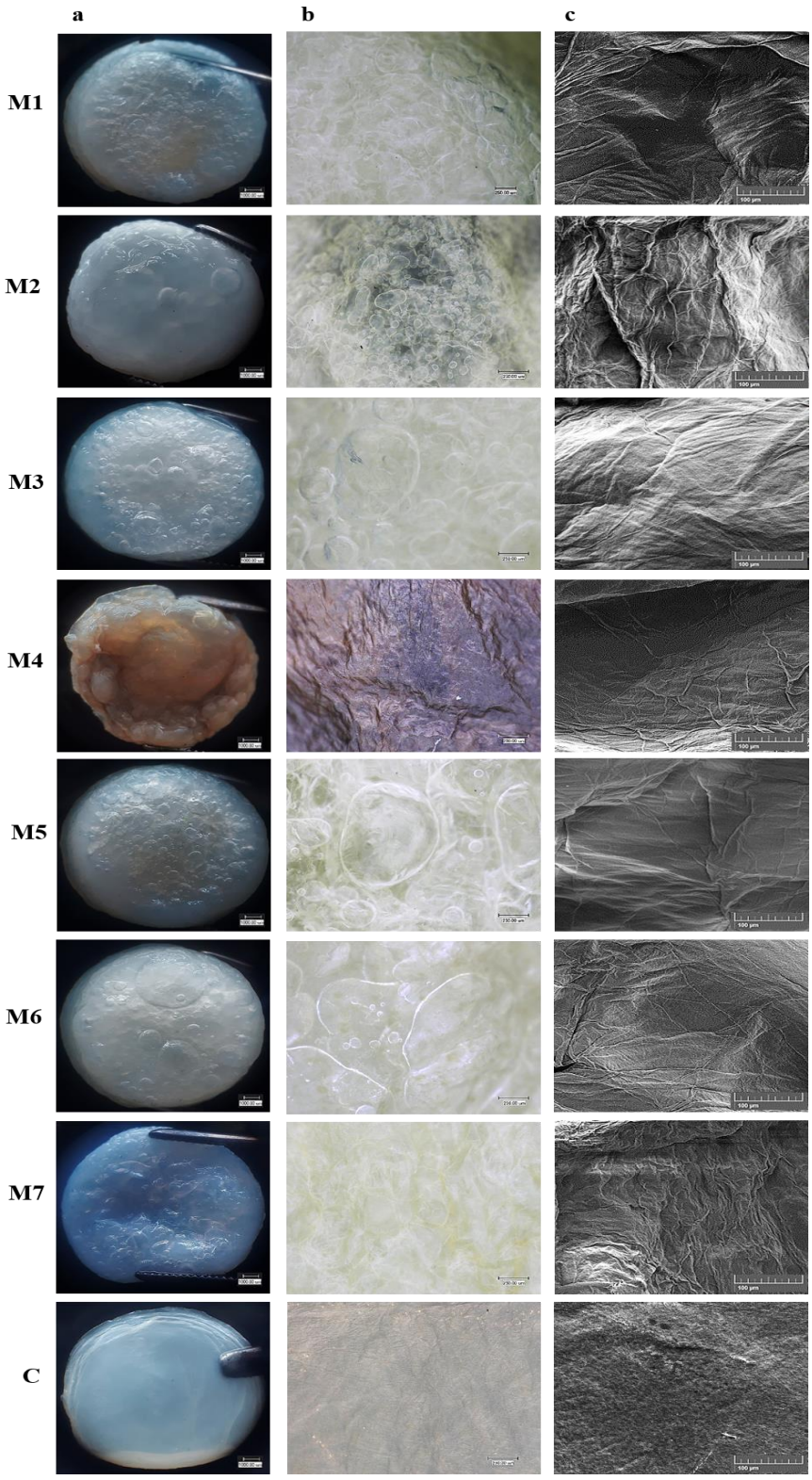

Fig. S4. The surface of modified and unmodified (control) BC samples. a, b – magnification 20x and 150x, respectively (stereoscopic microscope, MST, Zeiss, Oberkochen, Germany); c – magnification 300x (SEM, Auriga 60, Zeiss, Oberkochen, Germany). C – control BC sample; M1-M7 – modified BC samples.

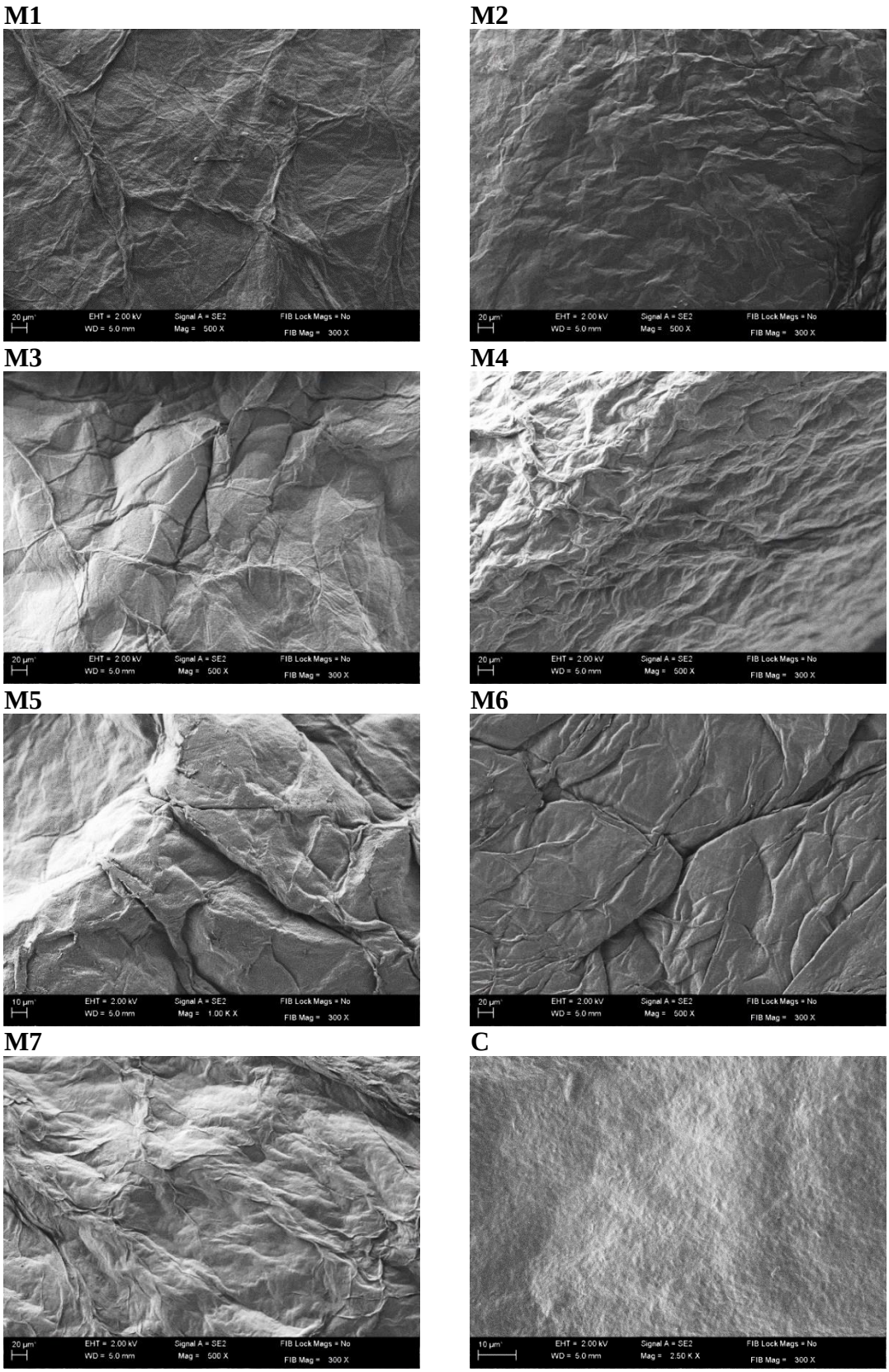

Fig. S5. The surface of modified and unmodified (control) BC samples (magnification 500x, SEM, Auriga 60, Zeiss, Oberkochen, Germany). C – control BC sample; M1-M7 – modified BC samples.

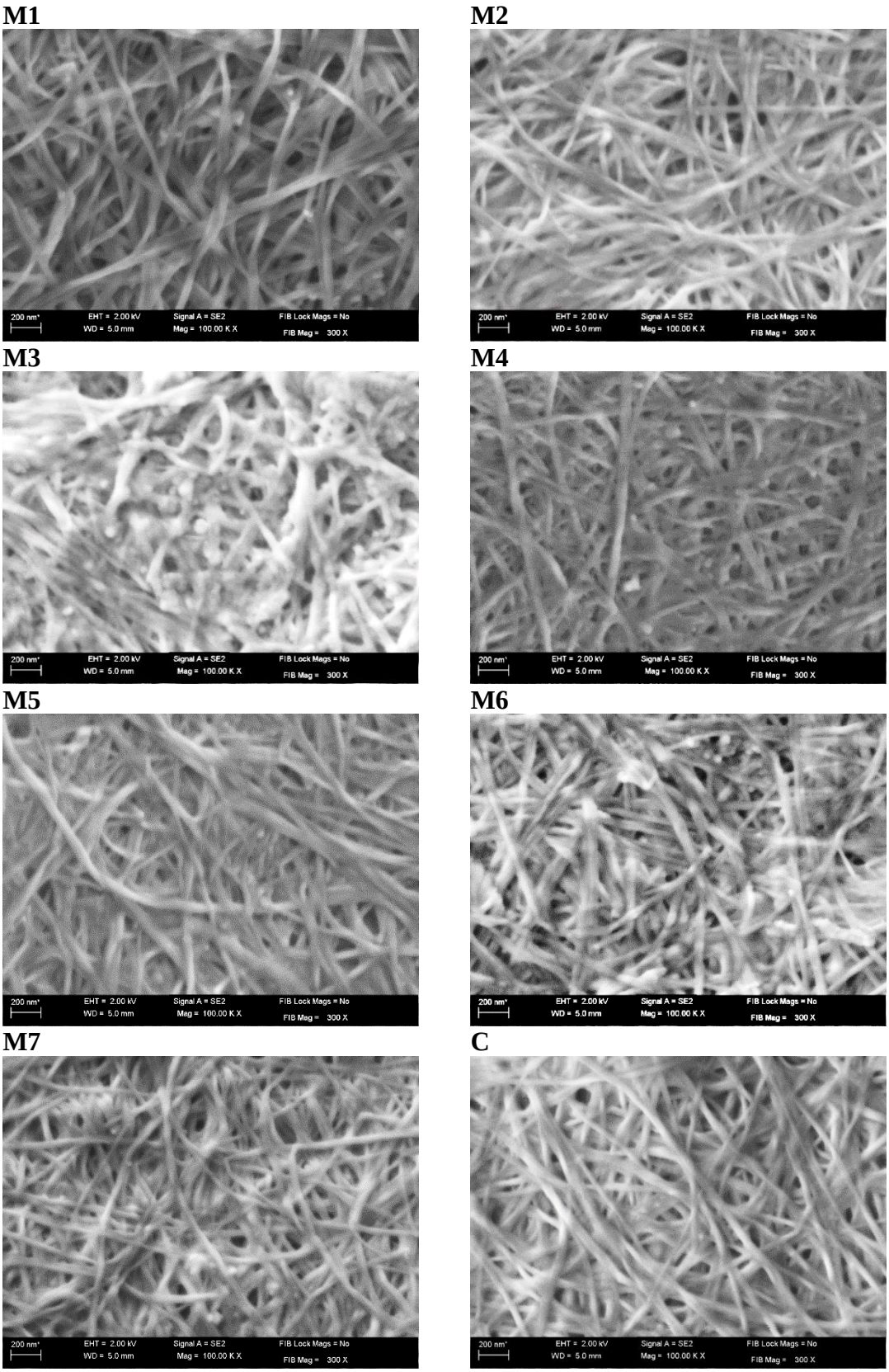

Fig. S6. The microstructure of the surface of modified and unmodified (control) BC samples (magnification 10 000x, SEM, Auriga 60, Zeiss, Oberkochen, Germany). C – control BC sample; M1-M7 – modified BC samples.

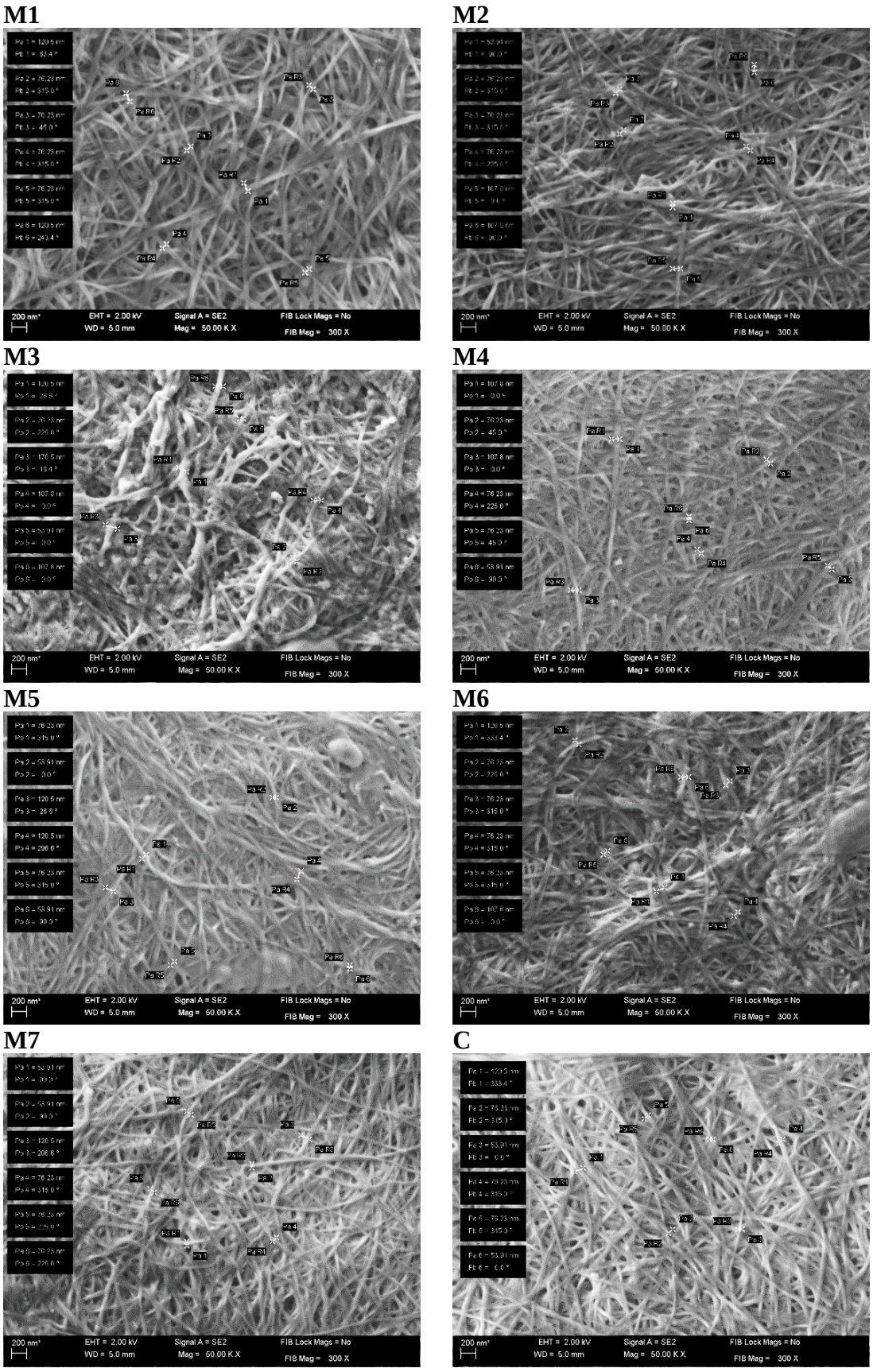

Fig. S7. SEM images of modified and unmodified (control) BC samples with microfibrils diameters marked (magnification 5 000x, SEM, Auriga 60, Zeiss, Oberkochen, Germany). C – control BC sample; M1-M7 – modified BC samples.

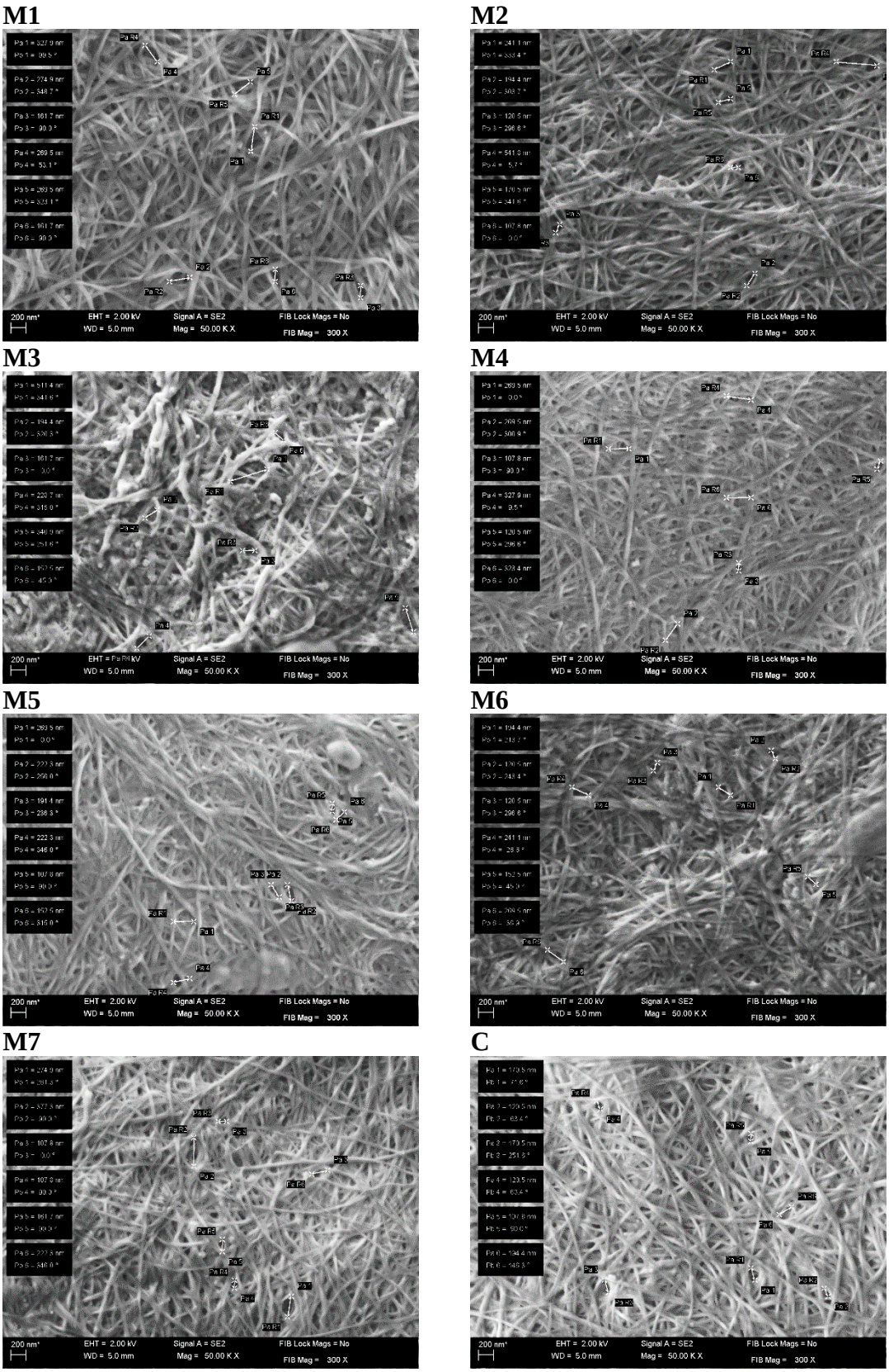

Fig. S8. SEM images of modified and unmodified (control) BC samples with pore diameters marked (magnification 5 000x, SEM, Auriga 60, Zeiss, Oberkochen, Germany). C – control BC sample; M1-M7 – modified BC samples.

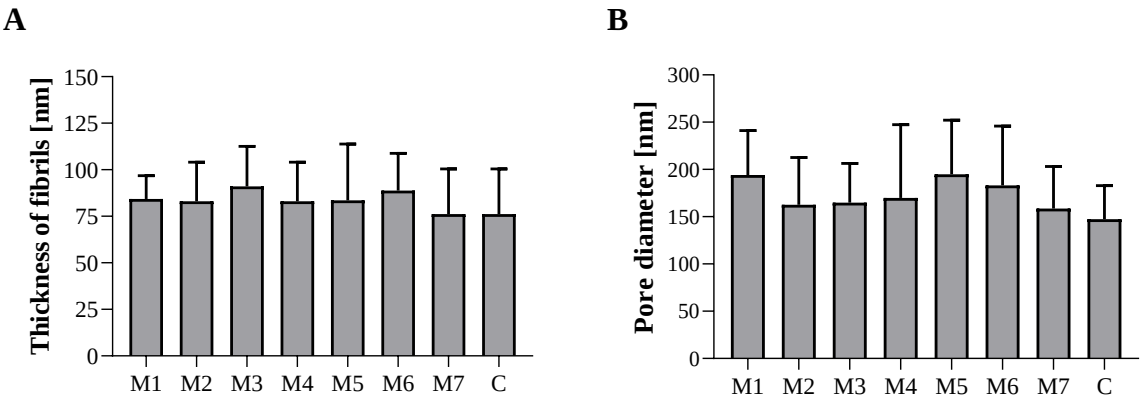

Fig. S9. The thickness (A) and pore diameter (B) measured on the surface of modified and unmodified (control) BC samples. The BC microfibril diameters were analyzed using software integrated with Auriga 60 SEM (Zeiss, Oberkochen, Germany), while pore size was analyzed using ImageJ software (NIH). Data are presented as mean ± standard error of the mean (SEM). There were no statistically significant differences between the samples. C – control BC sample; M1-M7 – modified BC samples.

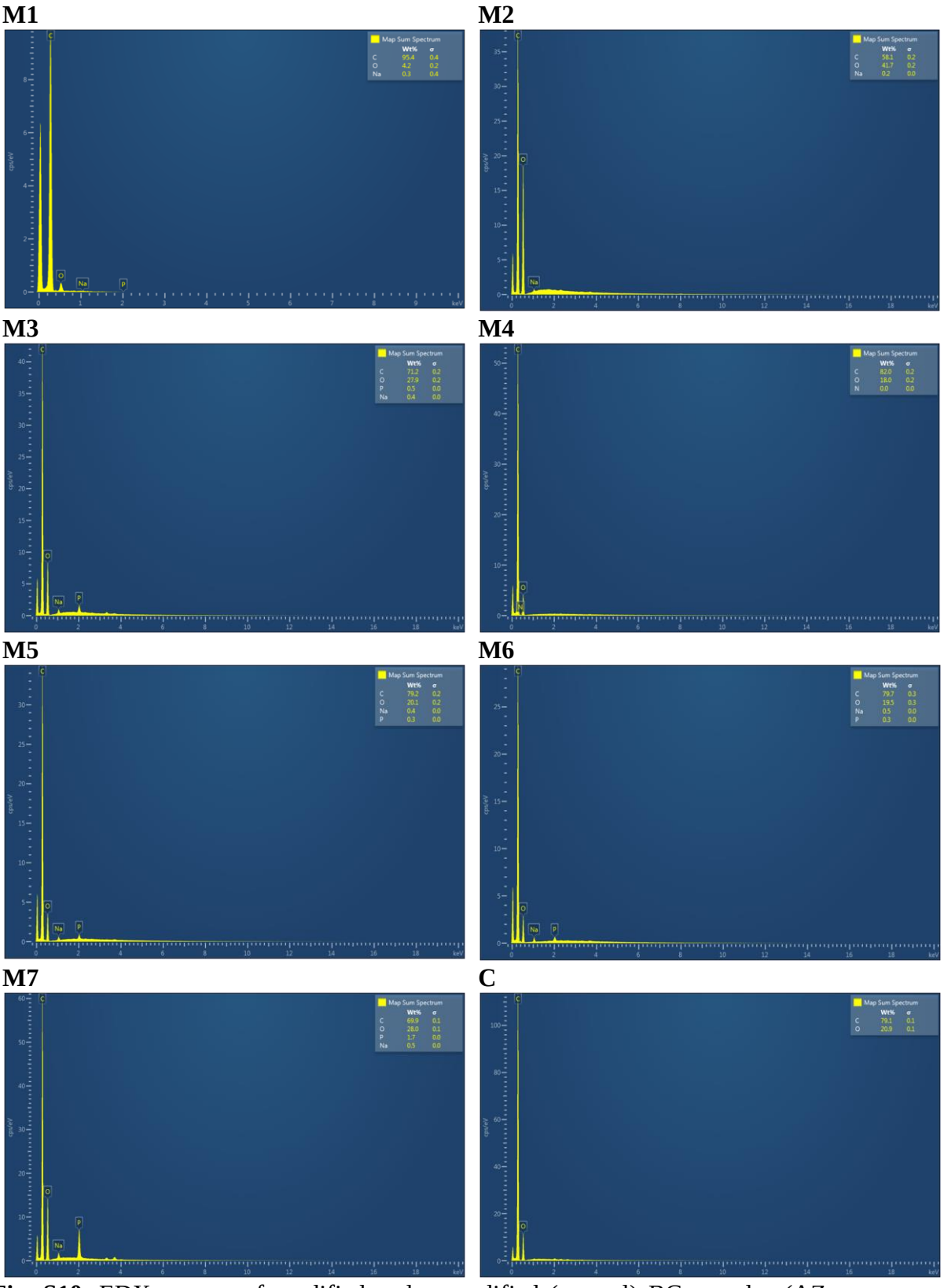

Fig. S10. EDX spectra of modified and unmodified (control) BC samples (AZtec system, Oxford Instruments, Abingdon, United Kingdom). C – control BC sample; M1-M7 – modified BC samples.

Tab. S10. Results of EDX analysis.

		M1	**M2**	**M3**	**M4**	**M5**	**M6**	**M7**	**C**
W_t%	C	73.7	58.1	71.2	82.0	79.2	79.7	69.9	79.1
	O	25.4	41.7	27.9	18.0	20.1	19.5	28.0	20.9
	Na	0.4	0.2	0.4	-	0.4	0.5	0.5	-
	P	0.5	-	0.5	-	0.3	0.3	1.7	-
	N	-	-	-	-	-	-	-	-

W_t% - Elemental composition (%); C – control BC sample; M1-M7 – modified BC samples.

3. Analysis of ATR-FTIR spectra

3.1. Principle Component Analysis of ATR-FTIR spectra

A

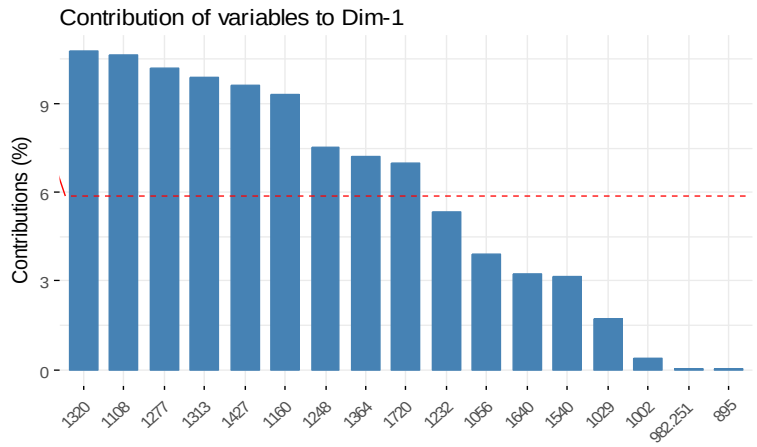

B

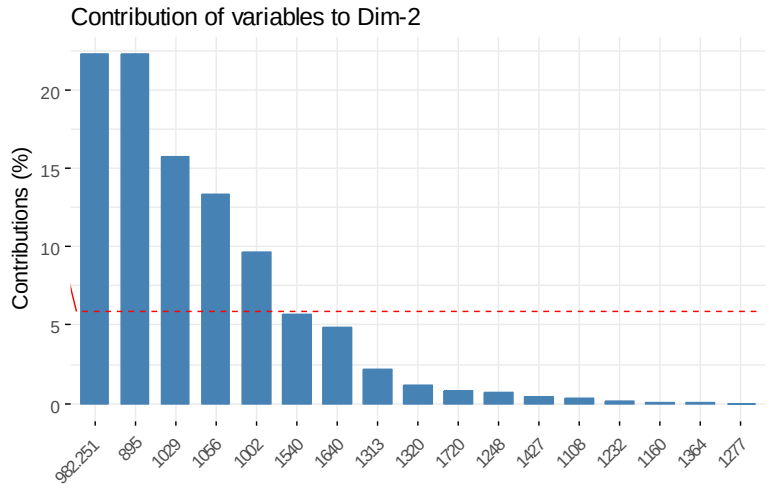

C

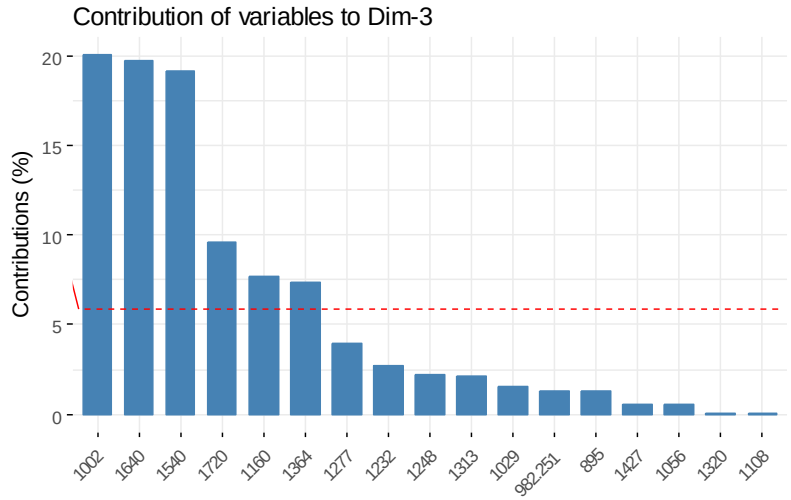

Fig. S11. Contribution of variables according to the results from ATR-FTIR analyses.

3.2. Analysis of ATR-FTIR spectra of BC modified with CA w/o CATs and with each CAT w/o CA

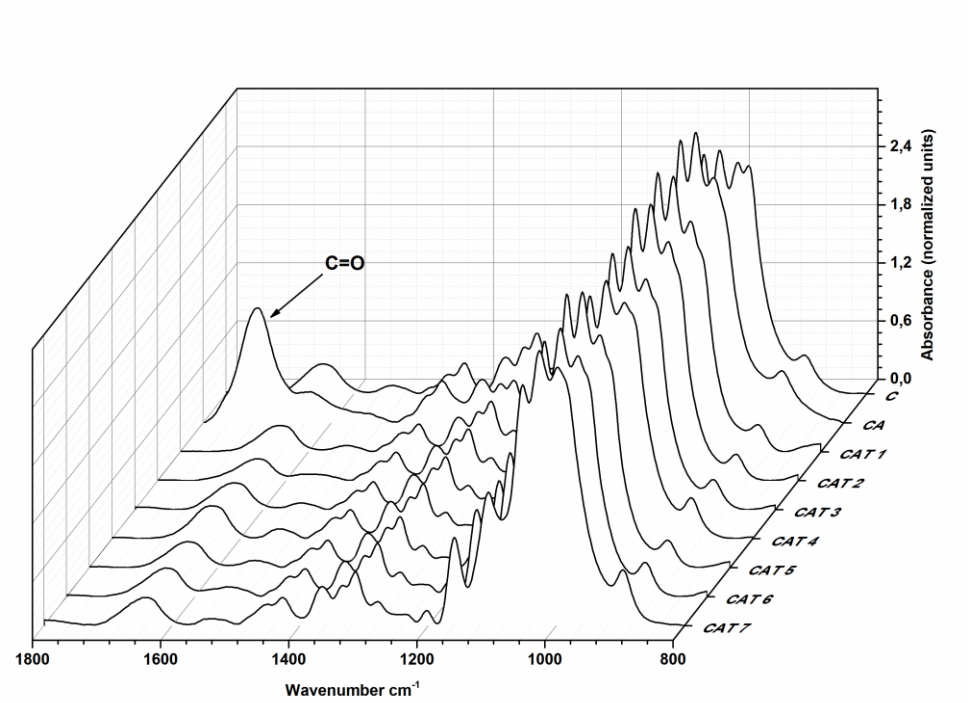

Fig. S12. The ATR-FTIR spectra of BC treated with 20% solution of CA w/o CAT or with 10% solutions of individual CATs w/o CA. C – control BC sample; CA – BC treated with 20% CA w/o CAT; CAT1-CAT7 – BC treated with 10% of individual CATs w/o CA.

4. Water-related properties and density of modified BC and efficiency of crosslinking reaction

Tab. S11. Statistical differences between SR (%) values obtained after 60 min of incubation of BC samples in water.

	M1	M2	M3	M4	M5	M6	M7	C
M1	×	ns	ns	***	****	****	ns	****
M2	ns	×	ns	ns	****	****	ns	*
M3	ns	ns	×	**	****	****	ns	***
M4	***	ns	**	×	****	****	ns	ns
M5	****	****	****	****	×	ns	***	****
M6	****	****	****	****	ns	×	ns	****
M7	ns	ns	ns	ns	****	****	×	**
C	****	*	***	ns	****	****	**	×

C – control BC sample; M1-M7 – modified BC samples; * $p<0.05$, ** $p<0.01$, *** $p<0.001$, **** $p<0.0001$.

Tab. S12. Statistical differences between SR (%) values obtained after 24 h of incubation of BC samples in water.

	M1	M2	M3	M4	M5	M6	M7	C
M1	×	*	ns	****	ns	ns	**	****
M2	*	×	***	**	ns	ns	ns	****
M3	ns	***	×	****	*	*	****	****
M4	****	**	****	×	****	****	**	ns
M5	ns	ns	*	****	×	ns	ns	****
M6	ns	ns	*	****	ns	×	ns	****
M7	**	ns	****	**	ns	ns	×	***
C	****	****	****	ns	****	****	***	×

C – control BC sample; M1-M7 – modified BC samples; * $p<0.05$, ** $p<0.01$, *** $p<0.001$, **** $p<0.0001$.

Tab. S13. Statistical differences between WHC (%) values obtained after 60 min of the incubation of BC samples at 37°C.

	M1	M2	M3	M4	M5	M6	M7	C
M1	×	ns	ns	ns	ns	ns	ns	****
M2	ns	×	ns	ns	ns	ns	ns	****
M3	ns	ns	×	ns	ns	ns	ns	****
M4	ns	ns	ns	×	ns	ns	ns	****
M5	ns	ns	ns	ns	×	ns	ns	****
M6	ns	ns	ns	ns	ns	×	ns	****
M7	ns	ns	ns	ns	ns	ns	×	****
C	****	****	****	****	****	****	****	×

C – control BC sample; M1-M7 – modified BC samples; * $p<0.05$, ** $p<0.01$, *** $p<0.001$, **** $p<0.0001$.

Tab. S14. Statistical differences between weight (g) values of BC samples after 30 min of centrifuging (200 *g*).

	M1	M2	M3	M4	M5	M6	M7	C
M1	×	ns	ns	ns	ns	ns	ns	****
M2	ns	×	ns	ns	ns	ns	ns	****
M3	ns	ns	×	ns	ns	ns	ns	****
M4	ns	ns	ns	×	ns	ns	ns	****
M5	ns	ns	ns	ns	×	ns	ns	****
M6	ns	ns	ns	ns	ns	×	ns	****
M7	ns	ns	ns	ns	ns	ns	×	****
C	****	****	****	****	****	****	****	×

C – control BC sample; M1-M7 – modified BC samples; * $p<0.05$, ** $p<0.01$, *** $p<0.001$, **** $p<0.0001$.

Tab. S15. Statistical differences between the values of the density of BC samples.

	M1	M2	M3	M4	M5	M6	M7	C
M1	×	ns	ns	**	ns	ns	ns	****
M2	ns	×	ns	*	ns	ns	ns	****
M3	ns	ns	×	***	ns	ns	ns	****
M4	**	*	***	×	**	*	*	****
M5	ns	ns	ns	**	×	ns	ns	****
M6	ns	ns	ns	*	ns	×	ns	****
M7	ns	ns	ns	*	ns	ns	×	****
C	****	****	****	****	****	****	****	×

C – control BC sample; M1-M7 – modified BC samples; * $p<0.05$, ** $p<0.01$, *** $p<0.001$, **** $p<0.0001$.

Tab. S16. Adjusted p-values for the results presented in Tab. S11 – S15.

	*	**	***	****
SR% after 60 min	0.0711 – 0.9997	0.0149	0.0032 – 0.0061	< 0.0001
SR% after 24 h	0.0107 – 0.0254	0.0018 – 0.0074	0.0002 – 0.0003	< 0.0001
WHC % after 60 min	-	-	-	< 0.0001
Weight (g) after 30 min of centrifuging	-	-	-	< 0.0001
Density	0.0176 – 0.0215	0.0028 – 0.0090	0.0006	< 0.0001

5. Assessment of cytotoxicity of modified BC

5.1. Extract assay

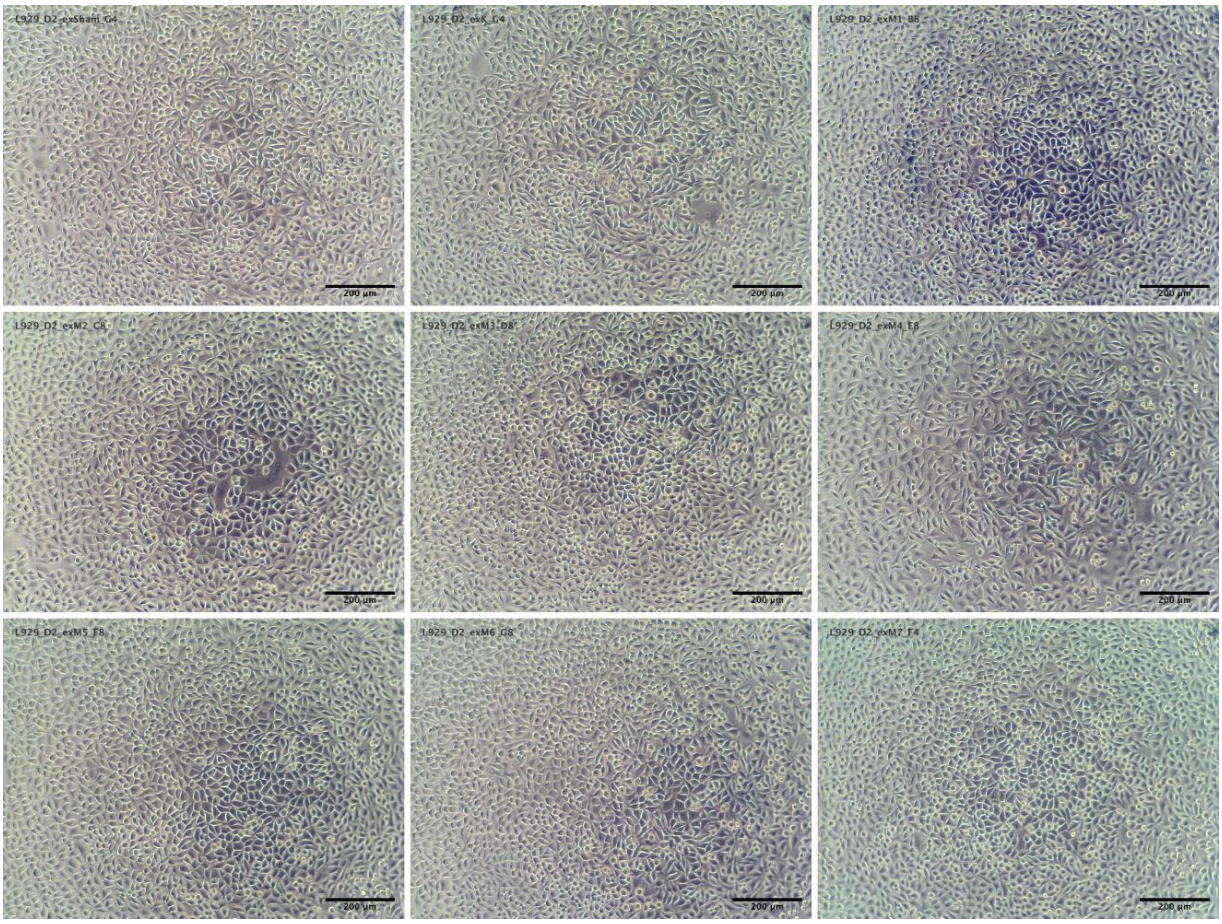

Fig. S13. Representative micrographs of L929 cells after 24 h of culture with BC extracts. Sequentially from top left to bottom right: sham, control BC sample, M1-M7 – modified BC samples. Scale bar represents 200 µm.

5.2. Direct contact assay

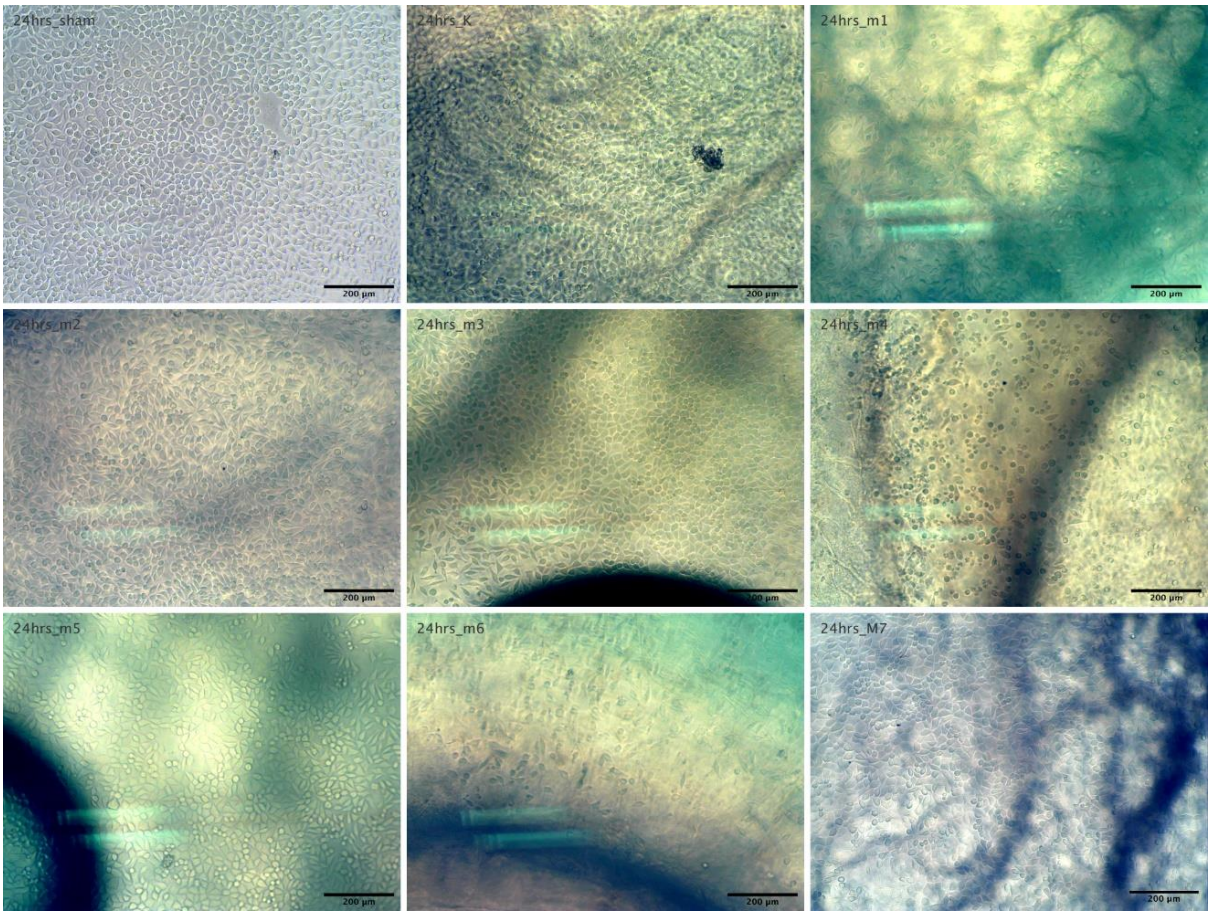

Fig. S14. Representative micrographs of L929 cells after 24 h of culture beneath sham (CellCrown insert alone, top left panel) and cellulose discs; sequentially from top left to bottom right: control BC sample, M1-M7 – modified BC samples. Scale bar represents 200 µm. Overall, the CellCrown insert made visualization at the edges of the well difficult, thus only the center was imaged. To avoid any disruption to the monolayer, discs were not removed, thus image quality is reduced due to the effect of the sample on the transmitted light.

Tab. S17. Statistical differences between normalized cell viability (% of Sham) in extract assay.

	M1	M2	M3	M4	M5	M6	M7	C
M1	×	ns	ns	*	ns	ns	**	****
M2	ns	×	**	****	ns	*	ns	****
M3	ns	**	×	ns	ns	ns	****	****
M4	*	****	ns	×	*	ns	****	****
M5	ns	ns	ns	*	×	ns	**	****
M6	ns	*	ns	ns	ns	×	***	****
M7	**	ns	****	****	**	***	×	****
C	****	****	****	****	****	****	****	×

C – control BC sample; M1-M7 – modified BC samples; * $p<0.05$, ** $p<0.01$, *** $p<0.001$, **** $p<0.0001$.

Tab. S18. Statistical differences between normalized cell viability (% of Sham) in direct contact assay.

	M1	M2	M3	M4	M5	M6	M7	C
M1	×	ns	ns	*	ns	ns	ns	ns
M2	ns	×	ns	*	ns	ns	ns	ns
M3	ns	ns	×	ns	ns	ns	**	ns
M4	*	*	ns	×	ns	**	****	***
M5	ns	ns	ns	ns	×	ns	**	ns
M6	ns	ns	ns	**	ns	×	ns	ns
M7	ns	ns	**	****	**	ns	×	ns
C	ns	ns	ns	***	ns	ns	ns	×

C – control BC sample; M1-M7 – modified BC samples; * $p<0.05$, ** $p<0.01$, *** $p<0.001$, **** $p<0.0001$.

Tab. S19. Adjusted p-values for the results presented in Tab. S17 – S18.

	*	**	***	****
Contact assay	0.0140 – 0.0198	0.0045 – 0.0070	0.0005	< 0.0001
Extract assay	0.0173 – 0.0231	0.0017 – 0.0074	0.0002	< 0.0001

6. Comparison of swelling ability of modified BC with commercial superabsorbent dressings

Tab. S20. Comparison of SR (%) values after 24 h for commercial dressings and M3 sample.

	SR(%) after 24 h	
Polyacrylate fiber superabsorbent commercial dressing	1432.23 ± 37.25	
Hydrofiber superabsorbent commercial dressing	2590.53 ± 235.33	
Modified BC (M3)	3334.21 ± 353.54	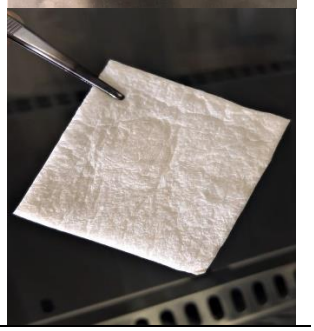

Tab. S21. Statistical differences between SR (%) of commercial dressings and M3 sample.

	Fiber dressing	Hydrofiber dressing	M3
Fiber dressing	×	**	***
Hydrofiber dressing	**	×	*
M3	***	*	×

* p<0.05, ** p<0.01, *** p<0.001.

Tab. S22. Adjusted p-values for SR (%) values for the results presented in Tab. S21.

	*	**	***	****
SR (%)	0.0319	0.0041	0.0001	-

Supplementary material

Potato juice, a starch industry waste, as a cost-effective medium for the biosynthesis of bacterial cellulose

Daria Ciecholewska-Juśko [1], Michał Broda [1,2], Anna Żywicka [1], Daniel Styburski [3], Peter Sobolewski [4], Krzysztof Gorący [4], Paweł Migdał [5], Adam Junka [6], and Karol Fijałkowski [1,*]

[1] Department of Microbiology and Biotechnology, Faculty of Biotechnology and Animal Husbandry,
West Pomeranian University of Technology, Szczecin, Piastów 45, 70-311 Szczecin, Poland; daria.ciecholewska@zut.edu.pl (D.C.-J.); michal.broda@zut.edu.pl (M.B.); anna.zywicka@zut.edu.pl (A.Ż.)
[2] Pomeranian-Masurian Potato Breeding Company, 76-024 Strzekęcino, Poland
[3] Laboratory of Chromatography and Mass Spectroscopy, Faculty of Biotechnology and Animal Husbandry, West Pomeranian University of Technology, Szczecin, Klemensa Janickiego 29, 71-270 Szczecin, Poland; daniel.styburski@zut.edu.pl (D.S.)
[4] Department of Polymer and Biomaterials Science, Faculty of Chemical Technology and Engineering,
West Pomeranian University of Technology, Szczecin, Piastów 45, 70-311 Szczecin, Poland;
psobolewski@zut.edu.pl (P.S.); krzysztof.goracy@zut.edu.pl (K.G.)
[5] Department of Environment, Hygiene and Animal Welfare, Faculty of Biology and Animal Science, Wroclaw University of Environmental and Life Sciences, Chełmońskiego 38C, 51-630 Wrocław, Poland;
pawel.migdal@upwr.edu.pl (P.M.)
[6] Department of Pharmaceutical Microbiology and Parasitology, Faculty of Pharmacy, Medical University of Wroclaw, Borowska 211a, 50-534 Wrocław, Poland;
adam.junka@umed.wroc.pl (A.J.)
* Correspondence: karol.fijalkowski@zut.edu.pl; Tel.: +48 91-449-6714

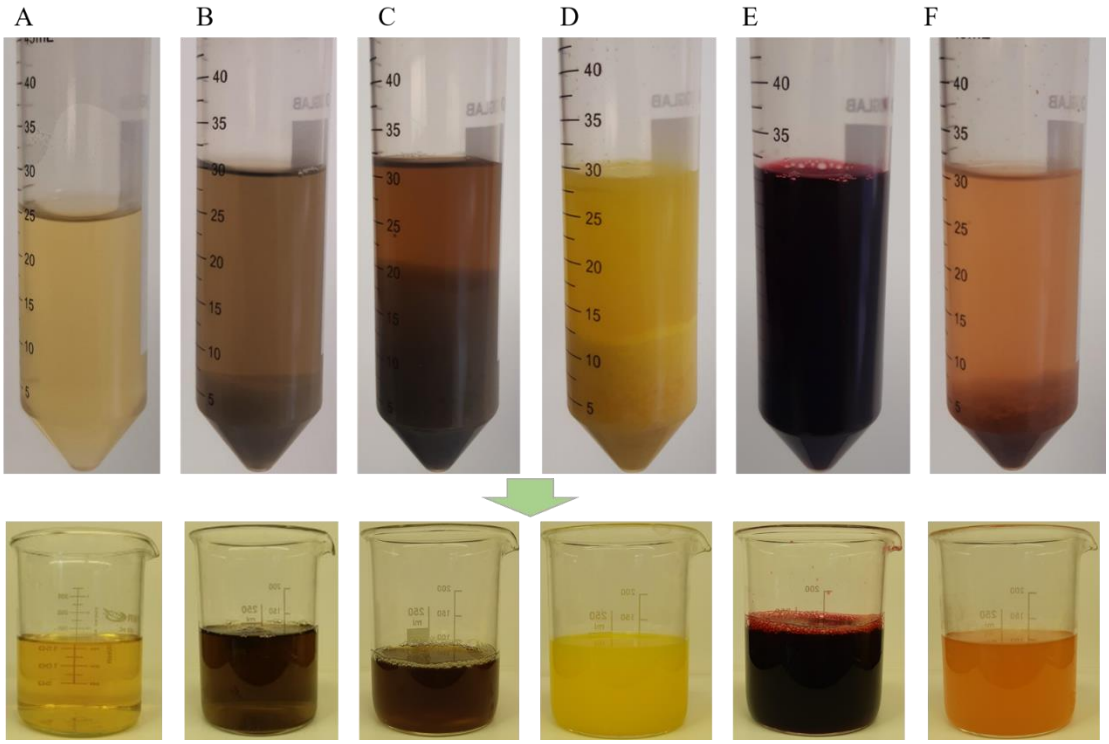

Figure S1. HS and natural ingredients-based media before (in 50 mL plastic tubes) and after decantation (in glass beakers); (**A**) HS; (**B**) potato juice; (**C**) potato peels; (**D**) orange peels; (**E**) beetroot; (**F**) apple.

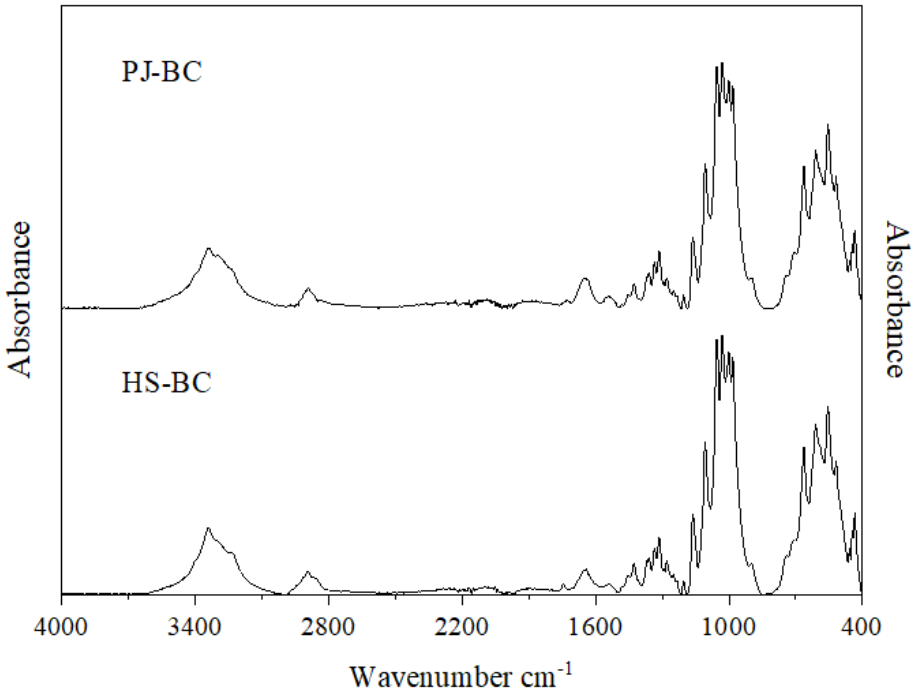

Figure S2. ATR-FTIR spectra of HS-BC and PJ-BC obtained from *K. xylinus* ATCC 53524 cultures.

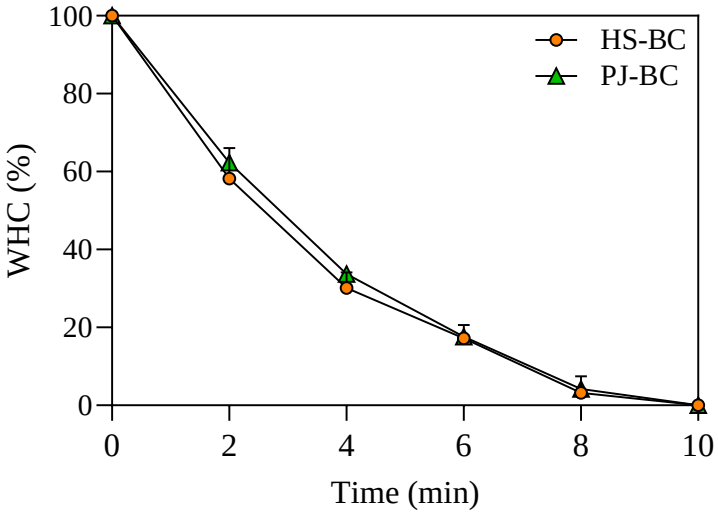

Figure S3. Water holding capacity (%) of HS-BC and PJ-BC obtained from *K. xylinus* ATCC 53524 during drying process at 60°C. Data are presented as a mean ± standard error of the mean (SEM).

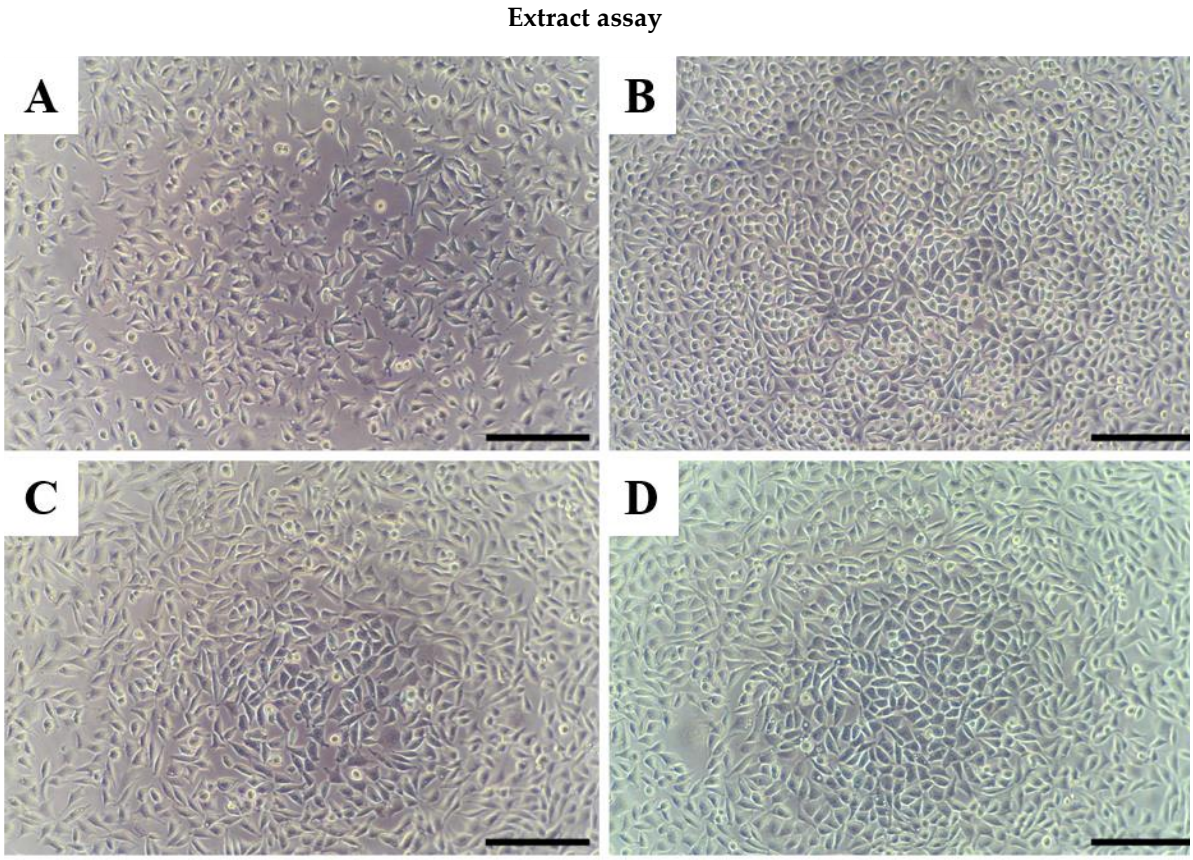

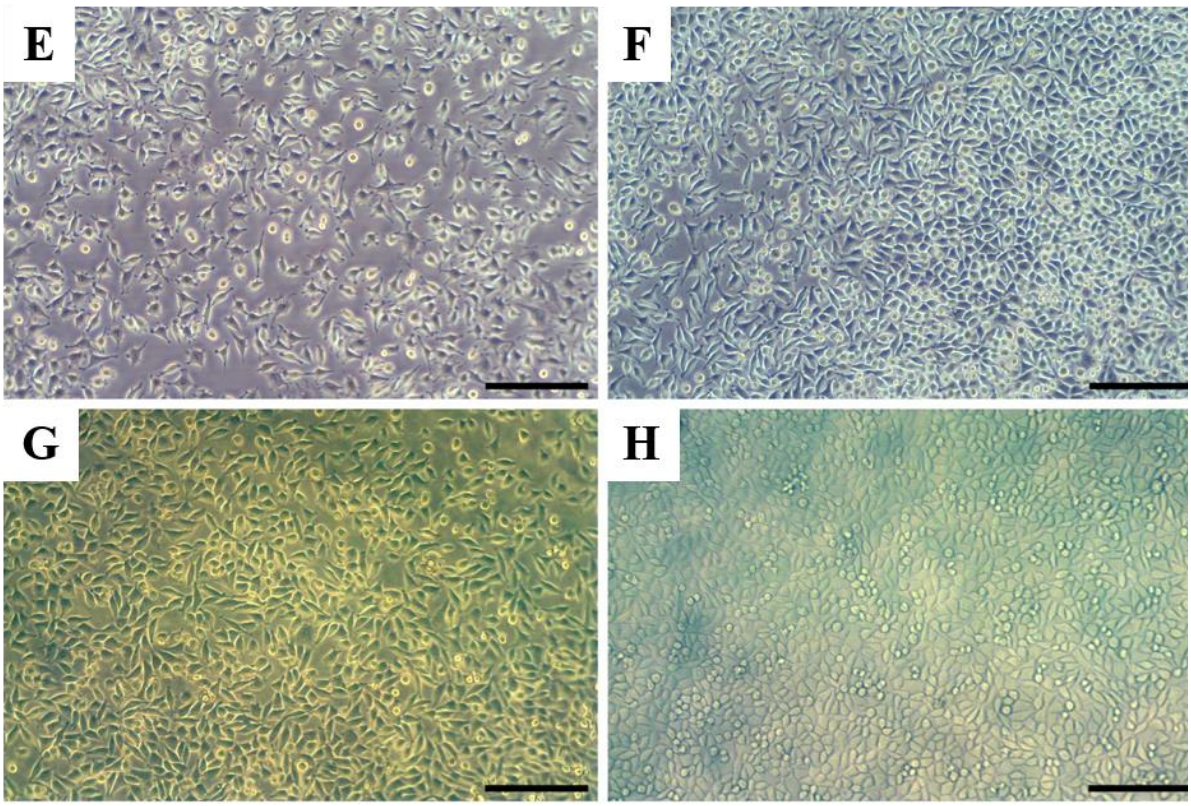

Figure S4. Representative micrographs of L929 cells. (**A**) 24 h after seeding (10000 cells per well); (**B**) After 24 h of incubation with sham extract; (**C**),(**D**) After 24 h incubation with extracts of HS-BC and PJ-BC obtained from *K. xylinus* ATCC 53524, respectively; (**E**) 24 h after seeding, prior to disc placement; (**F**) After incubation for 24 h without disc (sham); (**G**),(**H**) After 24 h incubation beneath discs of HS-BC and PJ-BC obtained from *K. xylinus* ATCC 53524, respectively. Images taken with discs in place - prior to removal. Scale bar indicates 200 μm.

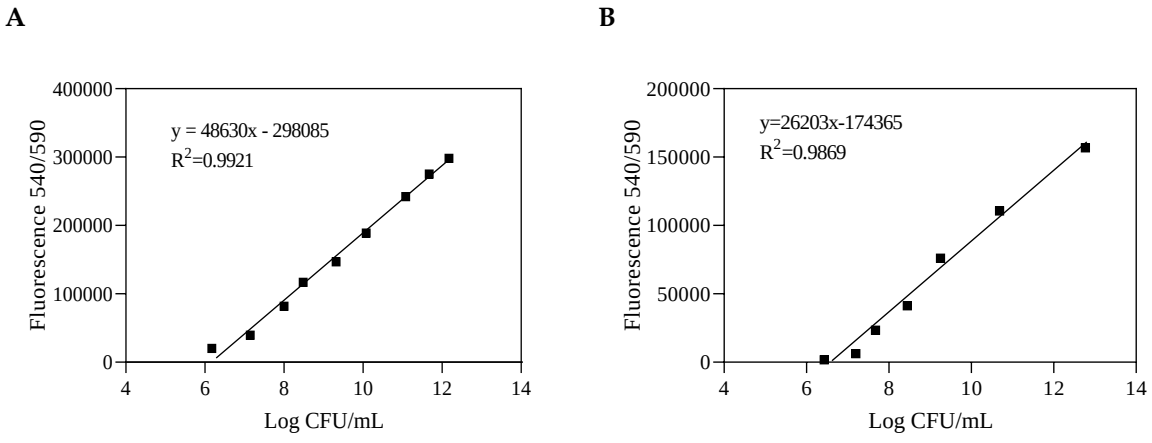

Figure S5. Standard curve of alamarBlue fluorescence intensity versus logarithm of *K. xylinus* ATCC 53524 cell concentration in the culture medium (**A**) and in the BC membranes (**B**).

Supplementary material

The cross-linked bacterial cellulose impregnated with octenidine dihydrochloride-based antiseptic as an antibacterial dressing material for highly-exuding, infected wounds

Daria Ciecholewska-Juśko[a], Adam Junka[b], Karol Fijałkowski[a,*]

[a]Department of Microbiology and Biotechnology, Faculty of Biotechnology and Animal Husbandry, West Pomeranian University of Technology, Szczecin, Piastów 45, 70-311 Szczecin, Poland, daria.ciecholewska@zut.edu.pl; karol.fijalkowski@zut.edu.pl;

[b]Department of Pharmaceutical Microbiology and Parasitology, Faculty of Pharmacy, Medical University of Wroclaw, Borowska 211a, 50-534 Wrocław, Poland, adam.junka@umed.wroc.pl;

*Corresponding author: karol.fijalkowski@zut.edu.pl

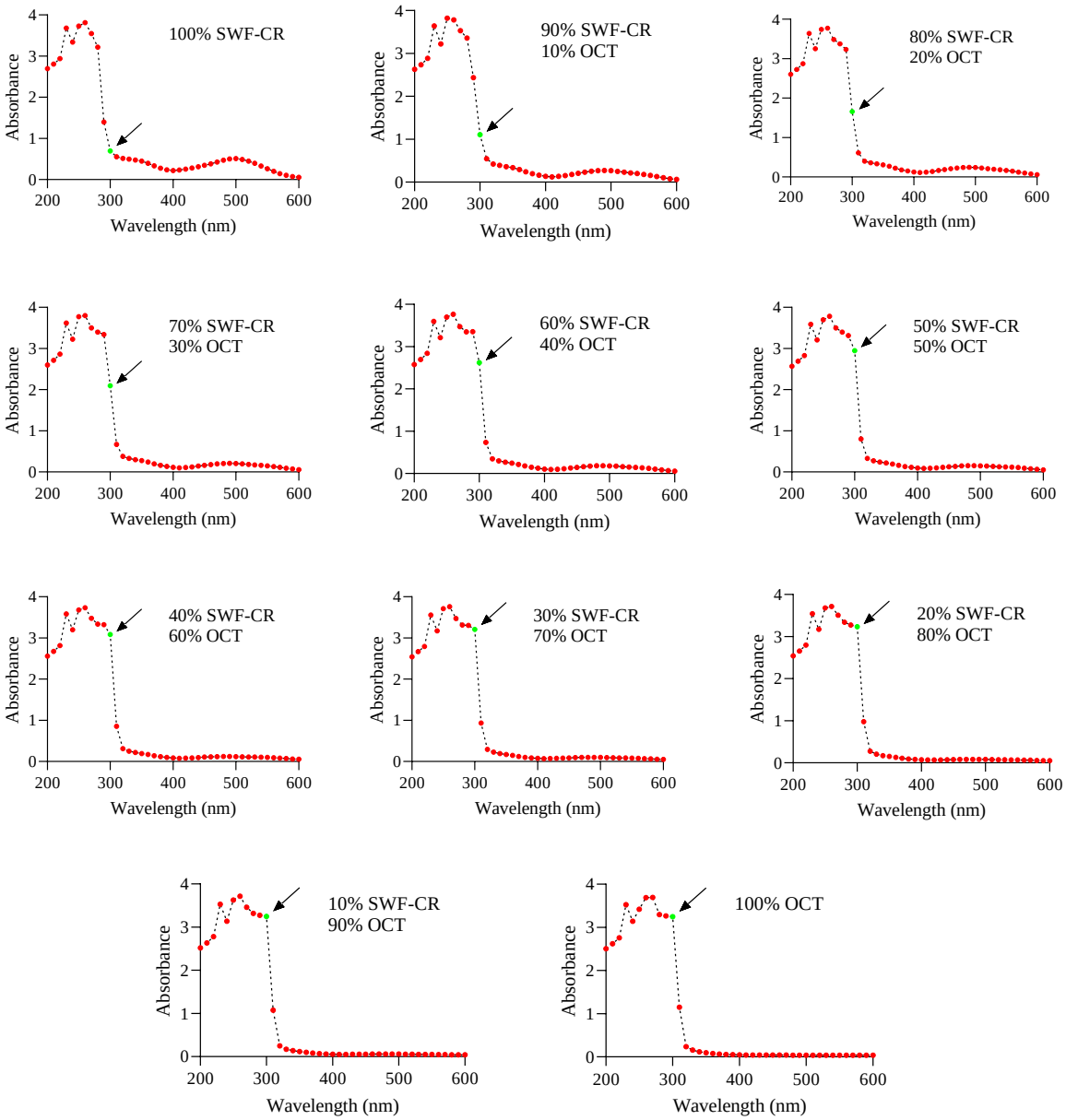

Fig. S1. Spectral scanning of SWF-CR/OCT standard solutions. The black arrows indicate the changes in absorbance at 300 nm.

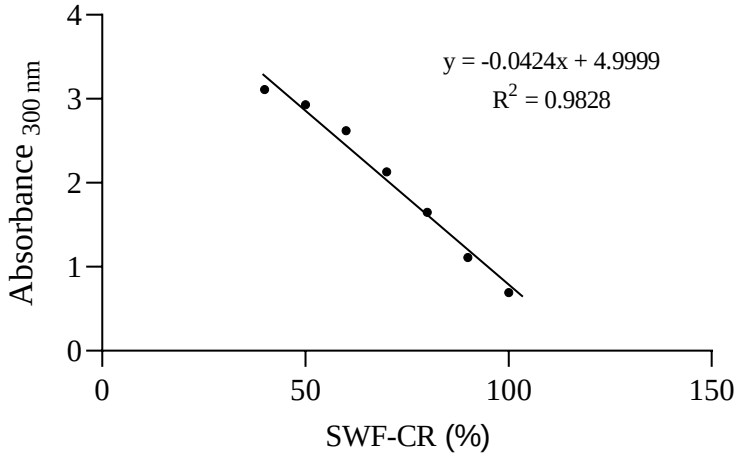

Fig. S2. Standard curve of absorbance at 300 nm versus concentration of SWF-CR (%).

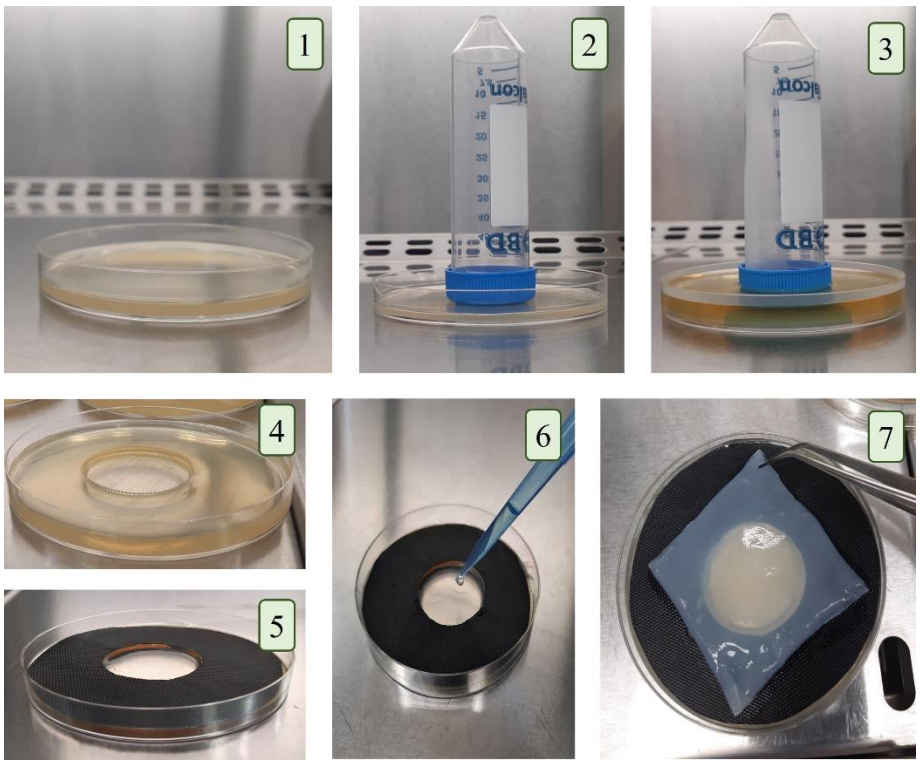

Fig.S3. Scheme of the preparation of experimental setup for OCT releasing study.

1 – Pouring the first layer of TSA medium (15 mL) on Petri dishes with a diameter of 9 cm; 2 – Placing a sterile 50 mL falcon with a stopper pointing downwards in the center of the plate after the medium has solidified; 3 – Pouring the second layer of TSA medium (20 mL) to form a round-shaped artificial wound bed with a diameter of 2.8 cm; 4 – Removal of the falcon after the medium has solidified; 5 – Placing a Teflon mat with round cut in the middle on the surface of TSA medium; 6 – Filling the artificial wound beds with 3 mL of simulated wound fluid (SWF); 7 – Placing the OCT-BC and OCT-MBC materials on the top.

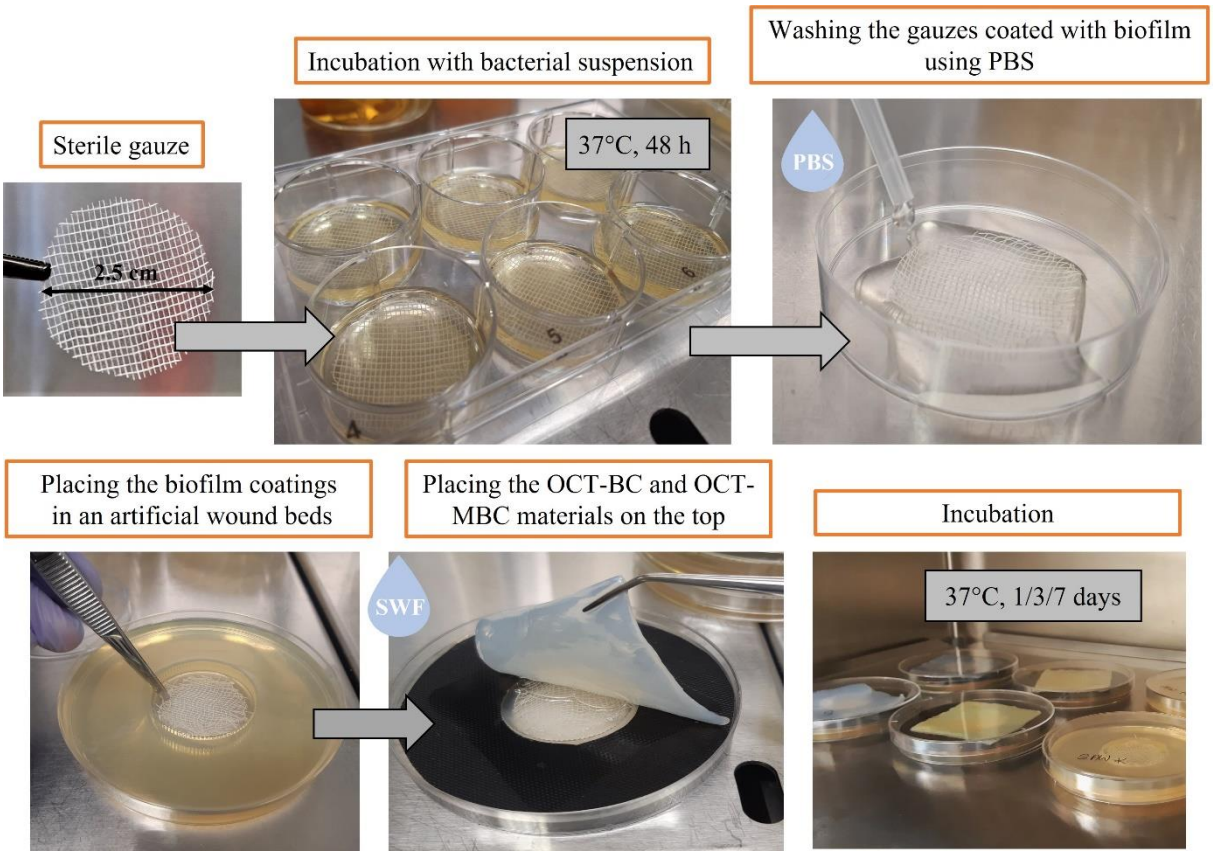

Fig. S4. The scheme of the experimental setup for testing the antibiofilm activity of OCT-MBC and OCT-BC materials.

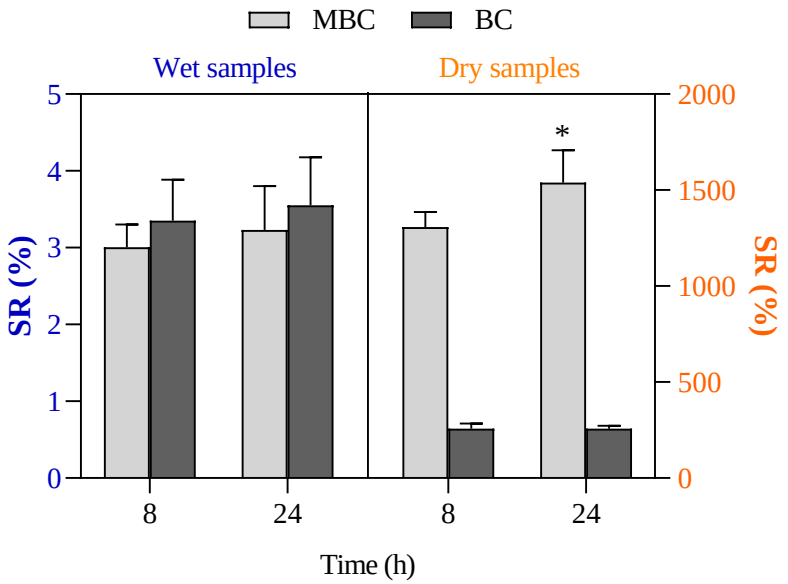

Fig. S5. Comparison of swelling ratio (%) of MBC and BC materials after 8 h and 24 h.

Tab. S1. OCT content in OCT-MBC and OCT-BC materials.

Time (min)	OCT content (mL)			
	OCT-MBC_w	OCT-MBC_d	OCT-BC_w	OCT-BC_d
0	7.405 ± 0.177	4.595 ± 0.304	9.987 ± 0.162	0.255 ± 0.012
10	7.23 ± 0.127	4.43 ± 0.311	9.472 ± 0.31	0.028 ± 0.008
20	7.06 ± 0.127	4.28 ± 0.297	9,078 ± 0.261	0.009 ± 0.003
30	6.755 ± 0.12	4.035 ± 0.318	8.747 ± 0.346	0
60	6.525 ± 0.106	3.74 ± 0.424	8.237 ± 0.332	0
120	6.11 ± 0.085	3.375 ± 0.445	7.702 ± 0.155	0
180	5.665 ± 0.134	3.01 ± 0.481	7.122 ± 0.0007	0
240	5.225 ± 0.163	2.69 ± 0.467	6.487 ± 0.008	0
300	4.785 ± 0.219	2.49 ± 0.537	5.958 ± 0.206	0
360	4.42 ± 0.339	2.17 ± 0.523	5.357 ± 0.319	0
420	4.065 ± 0.346	1.86 ± 0.467	4.947 ± 0.375	0
480	3.77 ± 0.325	1.6 ± 0.509	4.337 ± 0.63	0
1440	2.565 ± 0.346	0.915 ± 0.601	3.397 ± 0.432	0
2880	1.905 ± 0.12	0.595 ± 0.459	2.682 ± 0.552	0
4320	1.345 ± 0.148	0.37 ± 0.368	1.847 ± 0. 503	0
5760	0.855 ± 0.092	0.2 ± 0269	1.137 ± 0.135	0
7200	0.435 ± 0.163	0	0.649 ± 0.264	0
8640	0	0	0.289 ± 0.409	0
10080	0	0	0	0
*11520	0	0	0	0

*- additional measurement after 8th day for OCT-BC_w dry weight confirmation

Tab. S2. Average values of growth inhibition zones (mm) around OCT-MBC and OCT-BC materials.

	S. aureus	*P. aeruginosa*
OCT-MBC_w	42 ± 2	33 ± 2
OCT-MBC_d	38 ± 3	31 ± 1
OCT-BC_w	45 ± 2	31 ± 3
OCT-BC_d	29 ± 2	18 ± 1

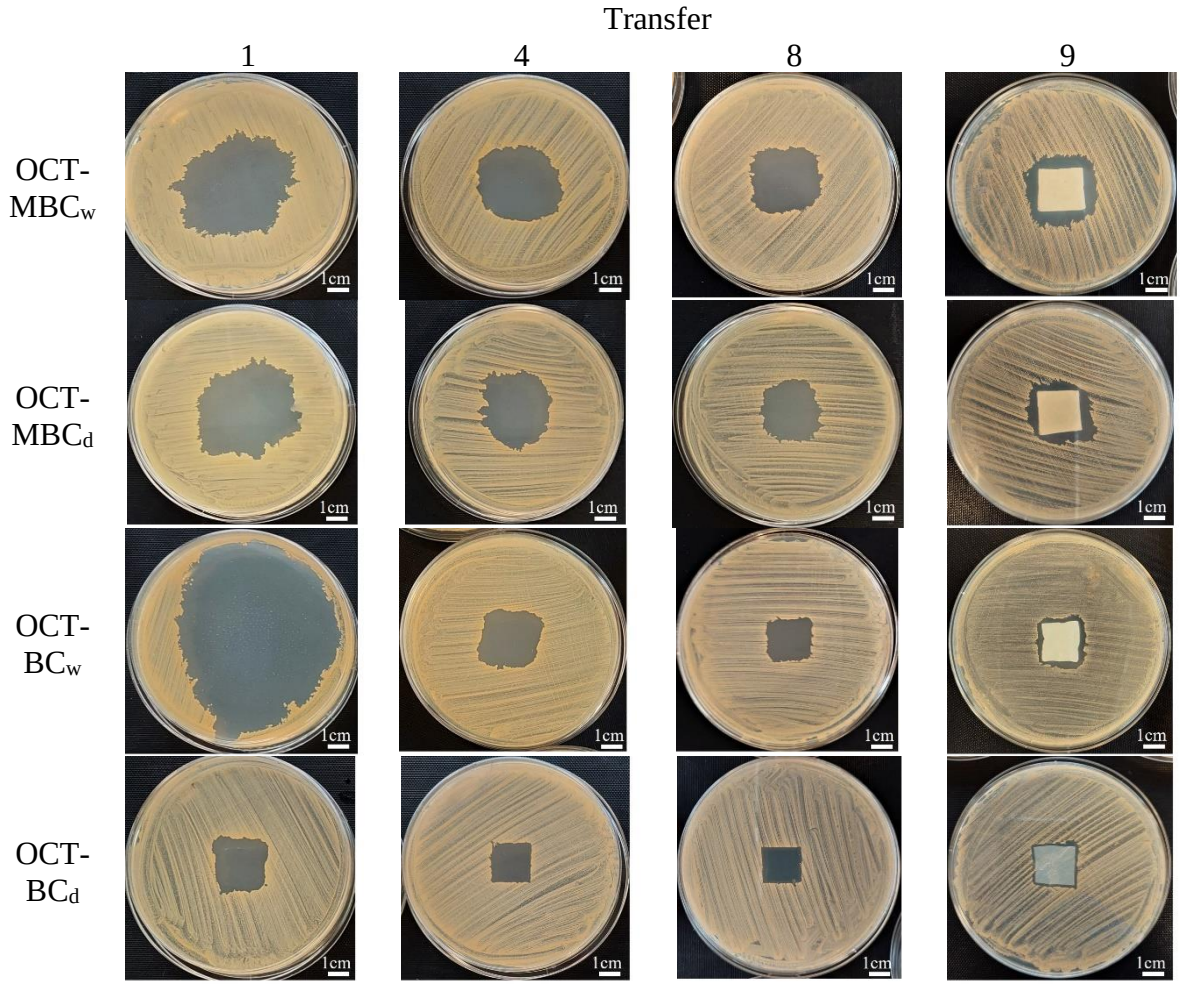

Fig. S6. Growth inhibition zones around OCT-MBC and OCT-BC materials for *S. aureus* reference strain (ATCC 6538).

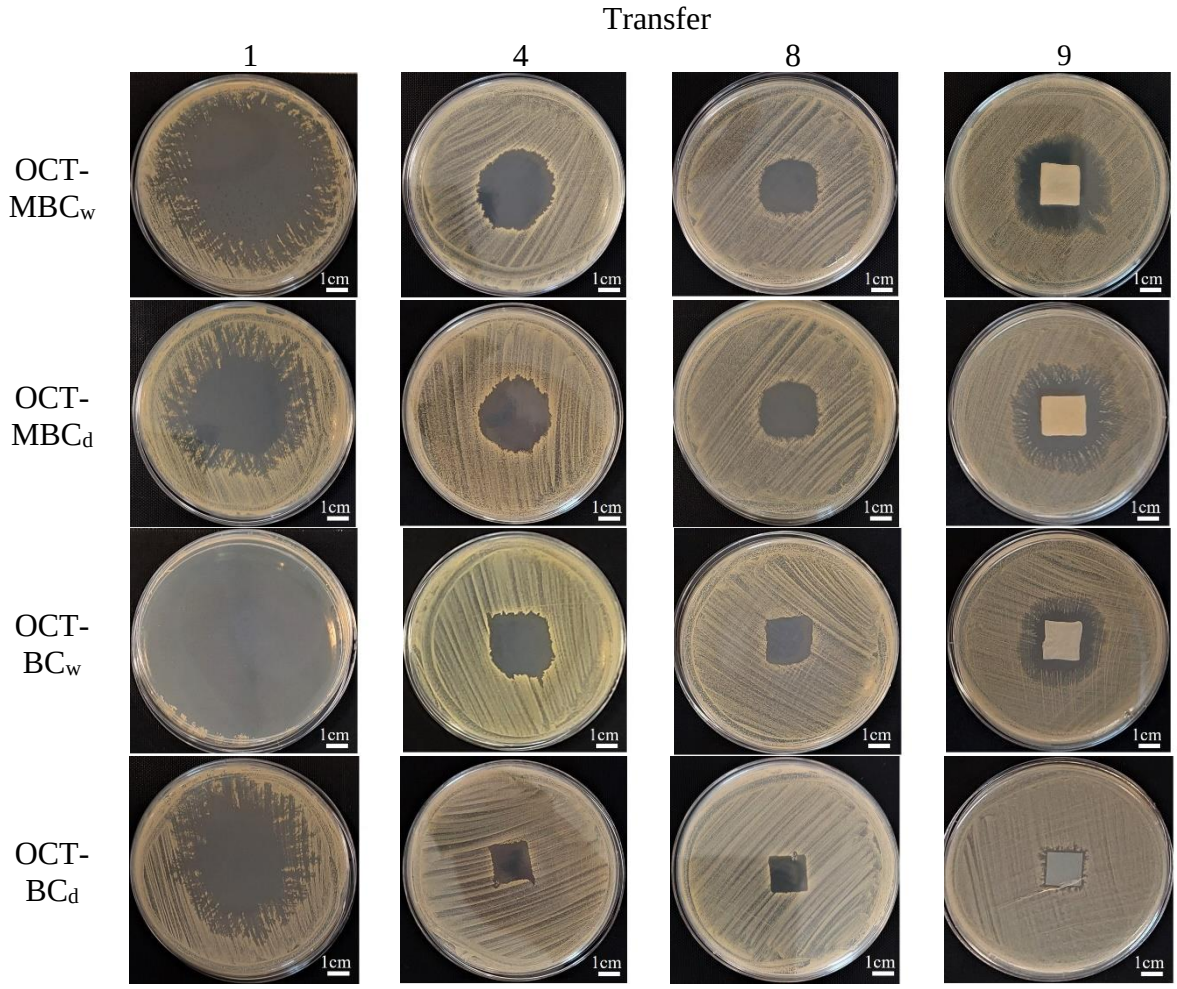

Fig. S7. Growth inhibition zones around OCT-MBC and OCT-BC materials for *S. aureus* clinical isolate.

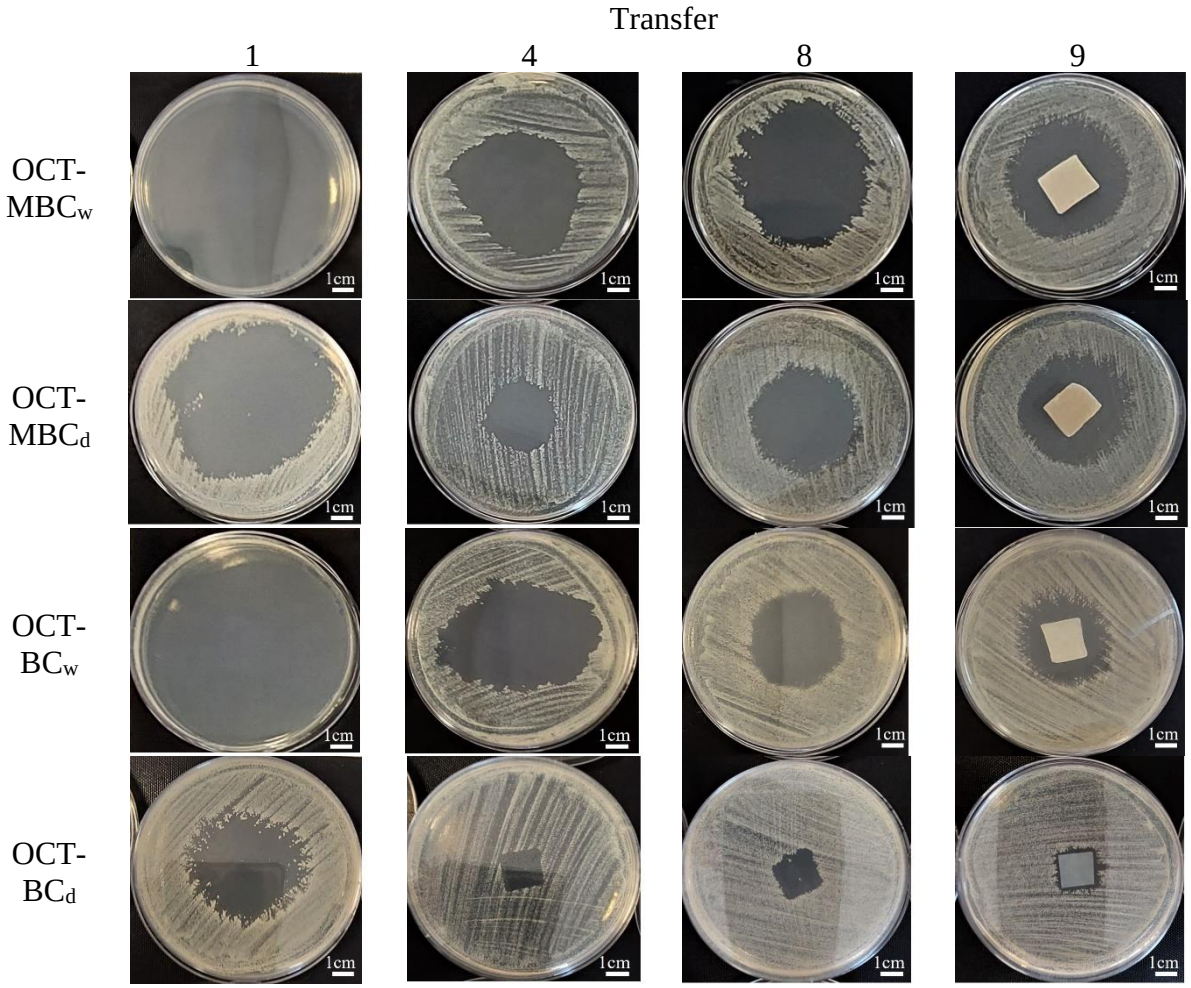

Fig. S8. Growth inhibition zones around OCT-MBC and OCT-BC materials for *S. equorum* clinical isolate.

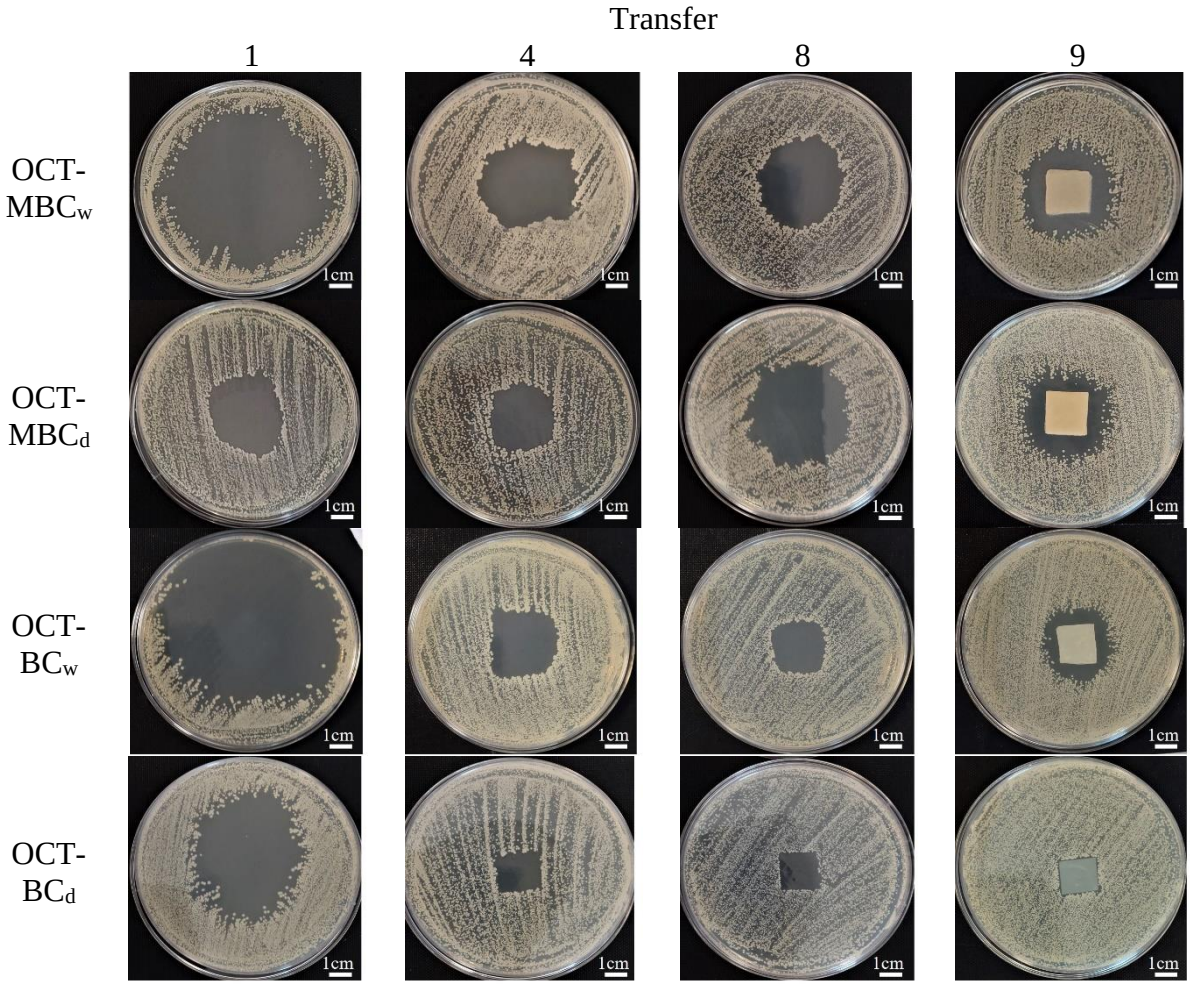

Fig. S9. Growth inhibition zones around OCT-MBC and OCT-BC materials for *S. warneri* clinical isolate.

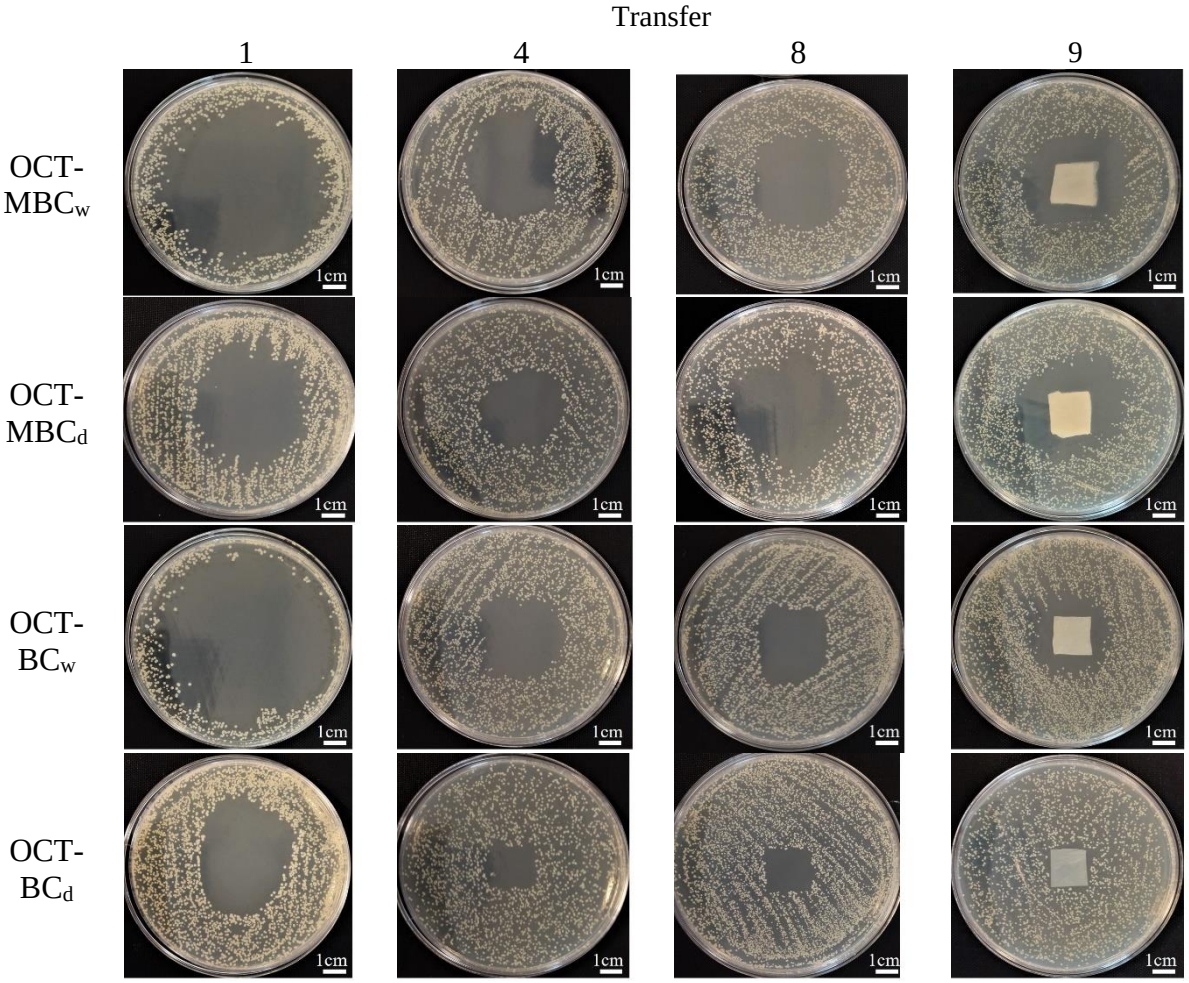

Fig. S10. Growth inhibition zones around OCT-MBC and OCT-BC materials for *S. xylosus* clinical isolate.

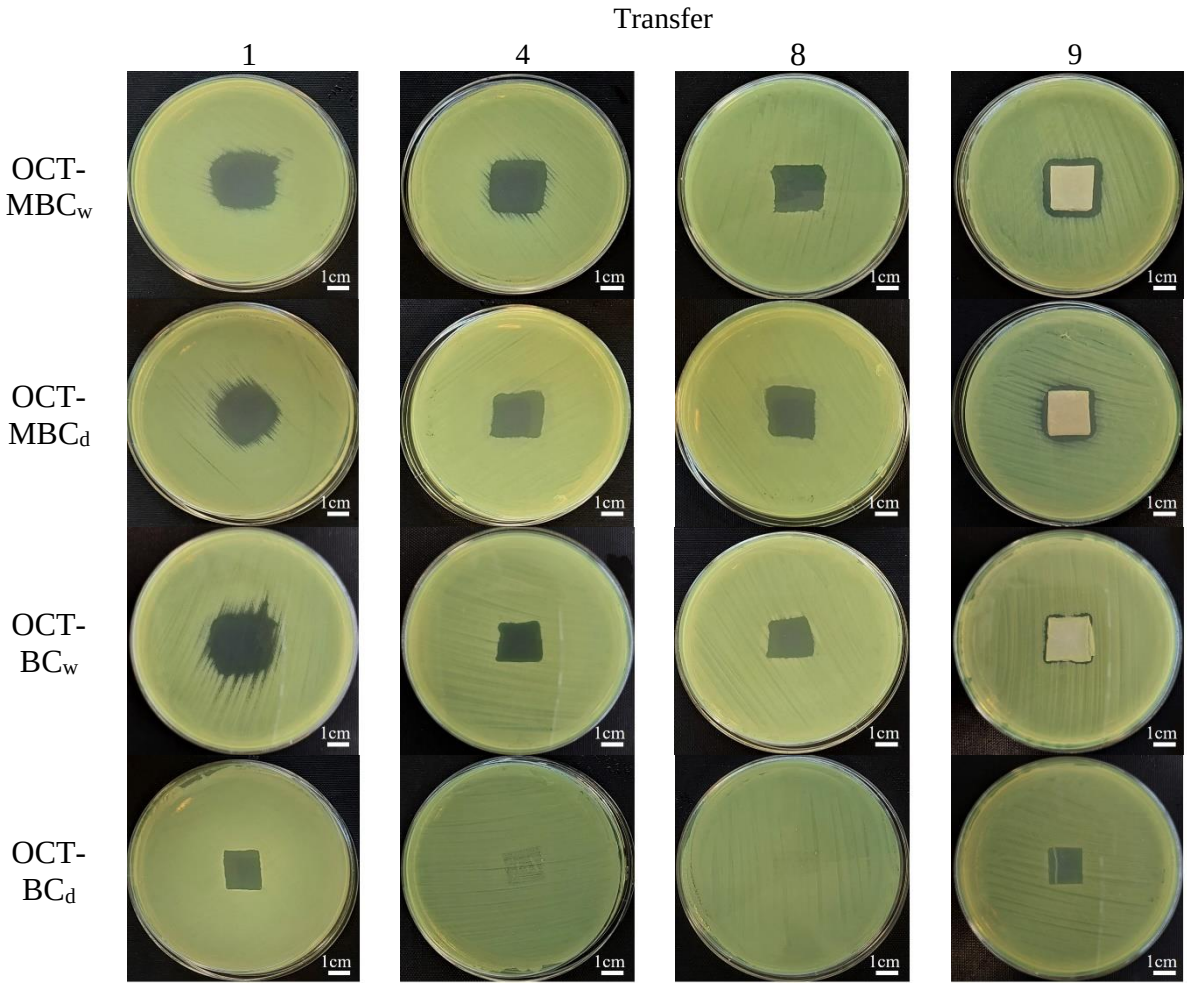

Fig. S11. Growth inhibition zones around OCT-MBC and OCT-BC materials for *P. aeruginosa* reference strain (ATCC 15442).

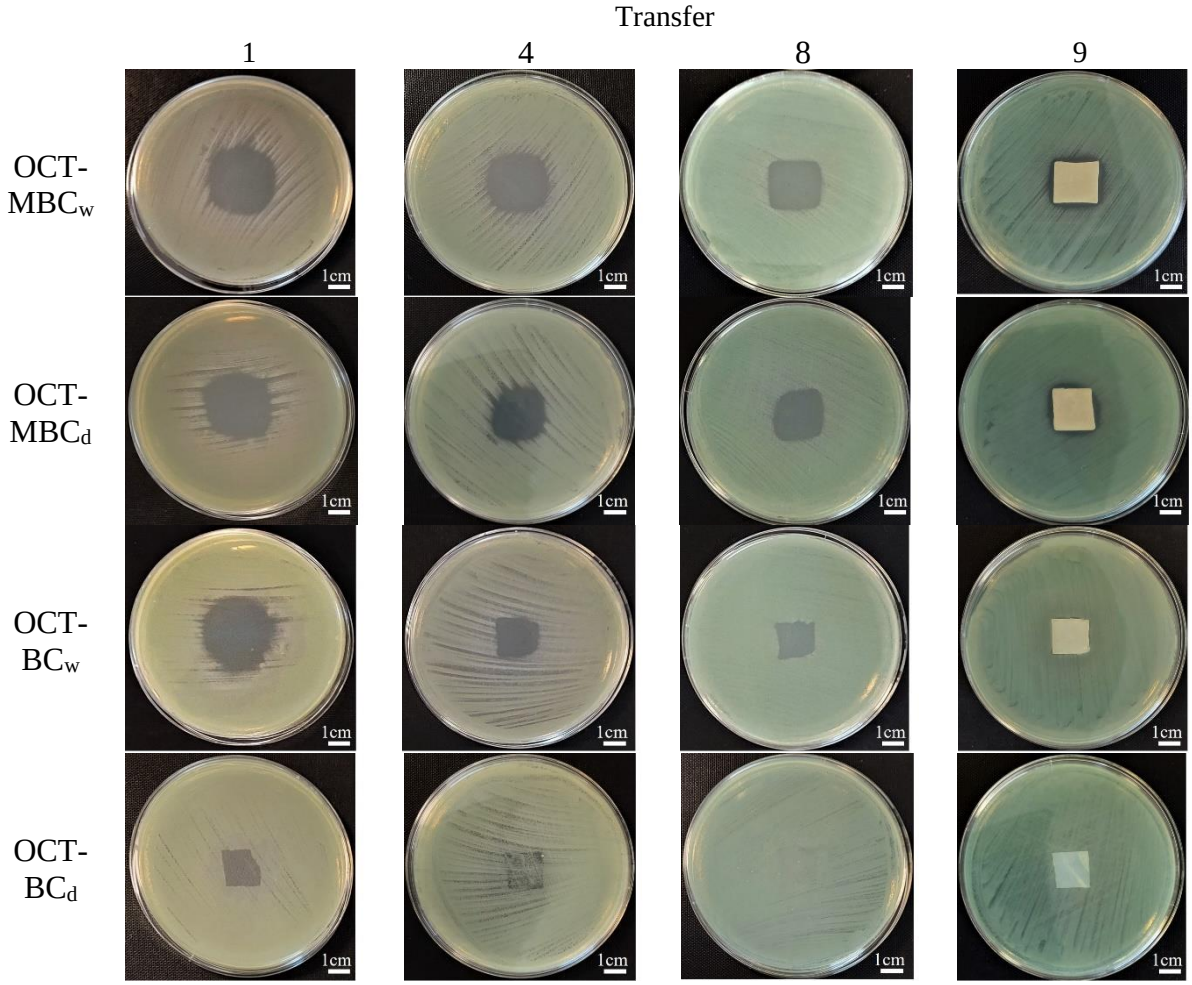

Fig. S12. Growth inhibition zones around OCT-MBC and OCT-BC materials for *P. aeruginosa* clinical isolate no.1.

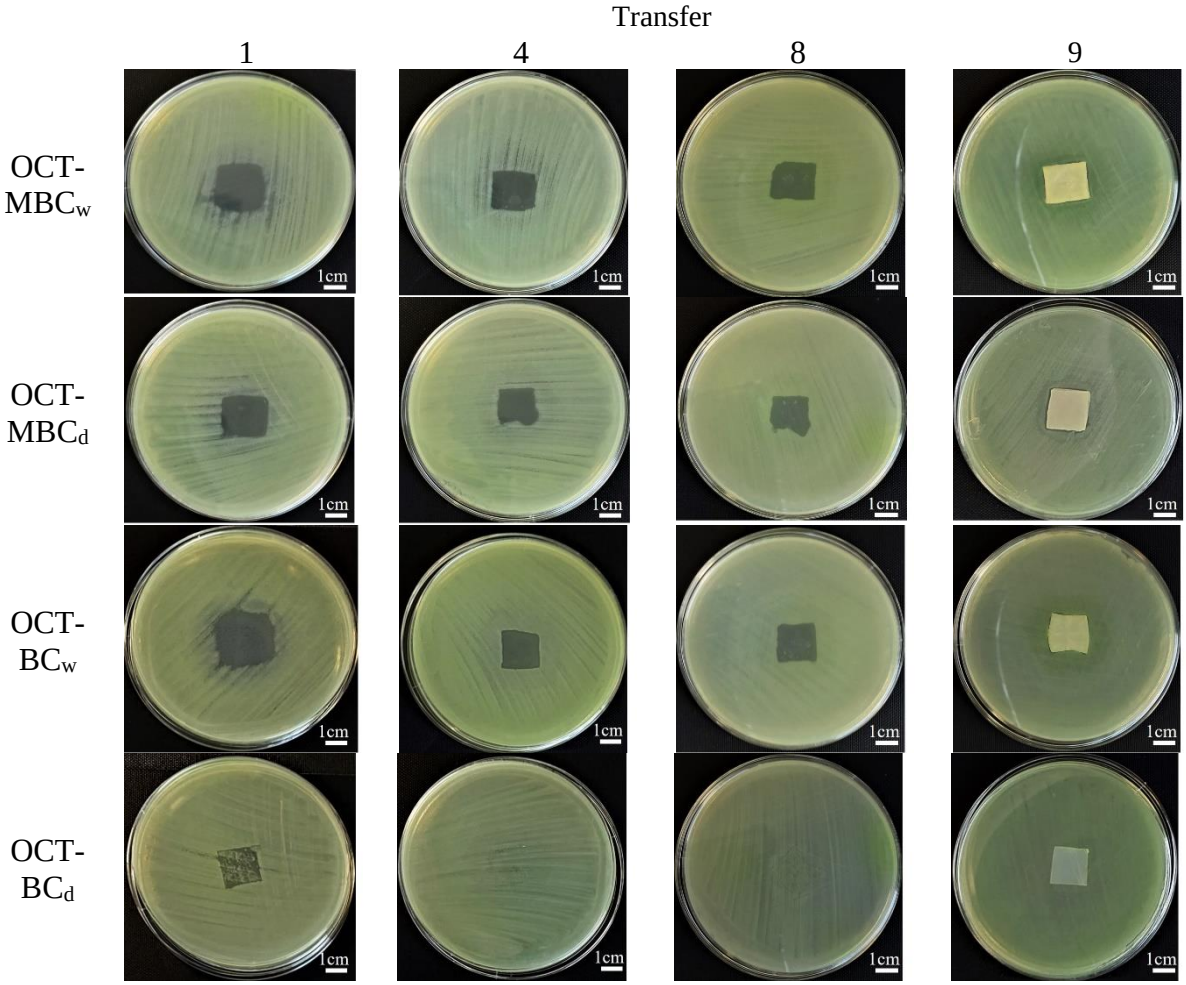

Fig. S13. Growth inhibition zones around OCT-MBC and OCT-BC materials for *P. aeruginosa* clinical isolate no.2.

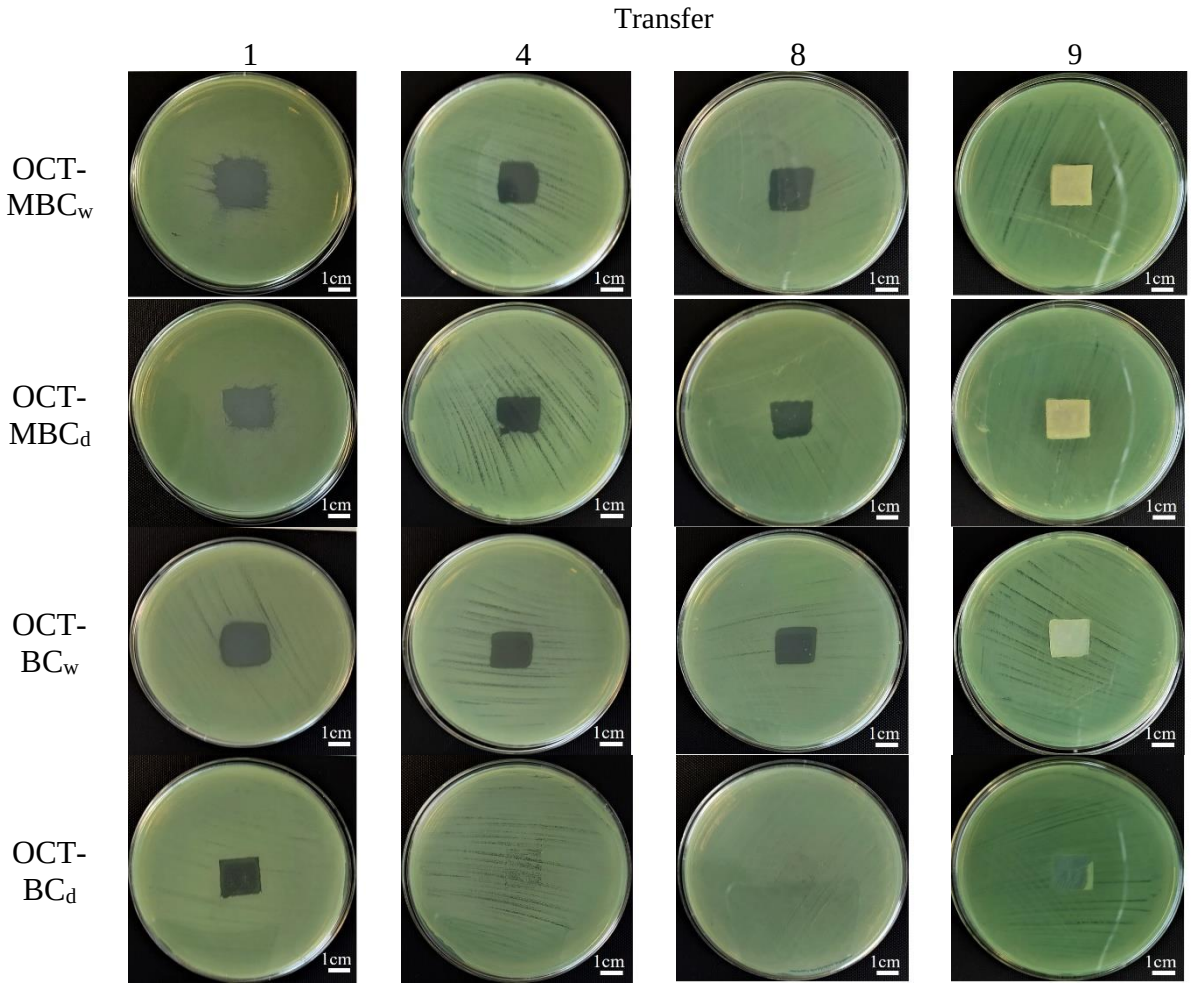

Fig. S14. Growth inhibition zones around OCT-MBC and OCT-BC materials for *P. aeruginosa* clinical isolate no.3.

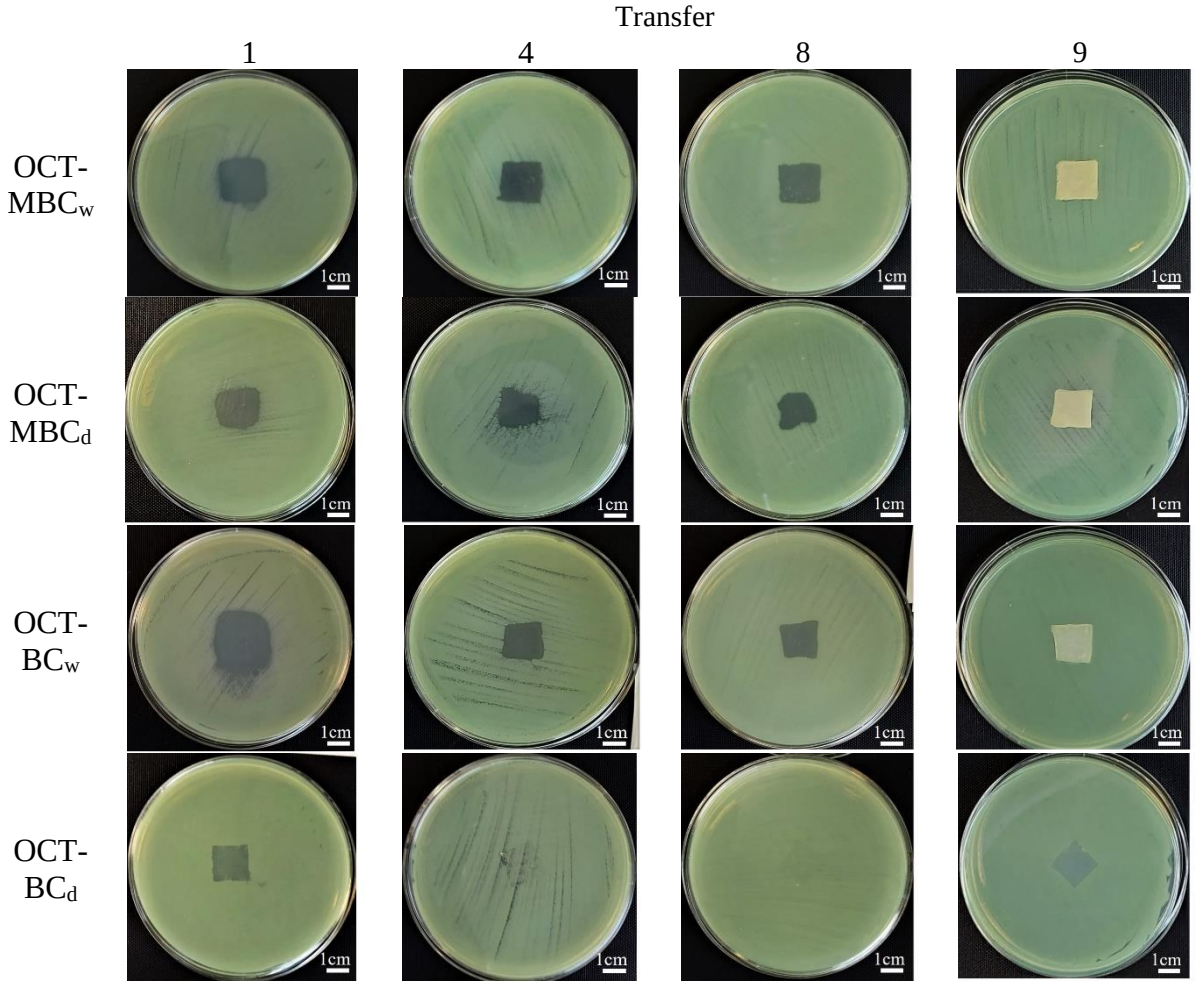

Fig. S15. Growth inhibition zones around OCT-MBC and OCT-BC materials for *P. aeruginosa* clinical isolate no.4.

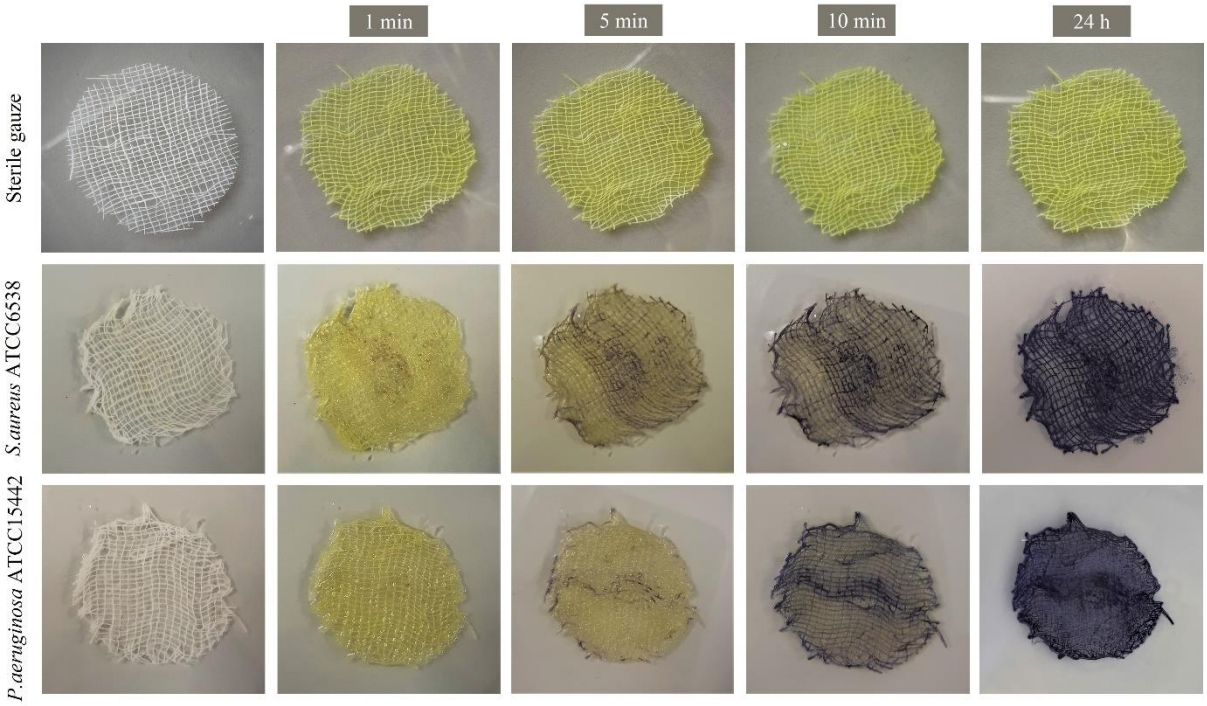

Fig. S16. Color changes occurred due to the reduction of MTT to formazan crystals on gauzes with staphylococcal and pseudomonal biofilms.

Tab. S3. Absorbance values during the study of OCT release on the consecutive days of the experiment.

	OCT-MBC_w	OCT-MBC_d	OCT-BC_w	OCT-BC_d
1 day	2.76 ± 0.18	2.48 ± 0.17	2.94 ± 0.03	0.80 ± 0.04
3 days	2.23 ± 0.01	1.63 ± 0.24	2.57 ± 0.17	0.31 ± 0.04
7 days	1.43 ± 0.07	1.09 ± 0.08	1.60 ± 0.14	0.05 ± 0.01

SUPPLEMENTARY INFORMATION

The Effects of Rotating Magnetic Field and Antiseptic on In Vitro Pathogenic Biofilm and Its Milieu

Daria Ciecholewska-Juśko[1], Anna Żywicka[1], Adam Junka[2,*], Marta Woroszyło[1], Marcin Wardach[3], Grzegorz Chodaczek[4], Patrycja Szymczyk-Ziółkowska[5], Paweł Migdał[6], Karol Fijałkowski[1,*]

[1] Department of Microbiology and Biotechnology, Faculty of Biotechnology and Animal Husbandry, West Pomeranian University of Technology, Szczecin, Piastów 45, 70-311 Szczecin, Poland

[2] Department of Pharmaceutical Microbiology and Parasitology, Faculty of Pharmacy, Medical University of Wroclaw, Borowska 211a, 50-534 Wrocław, Poland

[3] Faculty of Electrical Engineering, West Pomeranian University of Technology, Szczecin, Sikorskiego 37, 70-313 Szczecin, Poland

[4] Laboratory of Confocal Microscopy, Łukasiewicz Research Network-PORT Polish Center for Technology Development, Stabłowicka 147, 54-066 Wrocław, Poland

[5] Centre for Advanced Manufacturing Technologies (CAMT/FPC), Faculty of Mechanical Engineering, Wroclaw University of Science and Technology, Łukasiewicza 5, 50-371 Wrocław, Poland

[6] Department of Environment, Hygiene and Animal Welfare, Faculty of Biology and Animal Science, Wroclaw University of Environmental and Life Sciences, Chełmońskiego 38C, 51-630 Wrocław, Poland

* karol.fijalkowski@zut.edu.pl; adam.junka@umed.wroc.pl

Table S1. The main data of the RMF generator.

No.	Parameter	Description	Value
1.	R_{so}	Stator's outer radius	110.0 mm
2.	R_{si}	Stator's inner radius	80.0 mm
3.	l	RMF generator's length	199.0 mm
4.	p	Number of pole pairs	2
5.	k_s	Number of stator windings in slot	50
6.	s	Number of slots	36
7.	U_n	Nominal phase voltage	230 V
8.	I_n	Nominal phase current	17.1 A
9.	p_b	Number of winding parallel branches	2
10.	R_{ph}	Phase resistance	1.94 Ω
11.	L_{ph}	Phase inductance	8.04 mH

RMF generator is powered by an inverter with the use of U/f = const control. The stator used was from a mass-produced 15 kW four-pole induction motor (INDUKTA S.A., 2SIE160L4, Poland). Since the stator worked without a rotor (there were test samples in place of the rotor), the nature of its operation, from the point of view of power supply, was similar to that of a three-phase choke. As a result, the induced voltage (back-EMF) reached a relatively small value, therefore it was necessary to limit the supply voltage to a value of 100 V. The stator used is a three-phase wound and star-connected. After applying power to the stator phase bands, magnetic poles were formed inside the stator, which shifted in time according to the frequency of the supply current. Thus, a system configured in this way generated a rotating magnetic field (RMF) inside the stator.

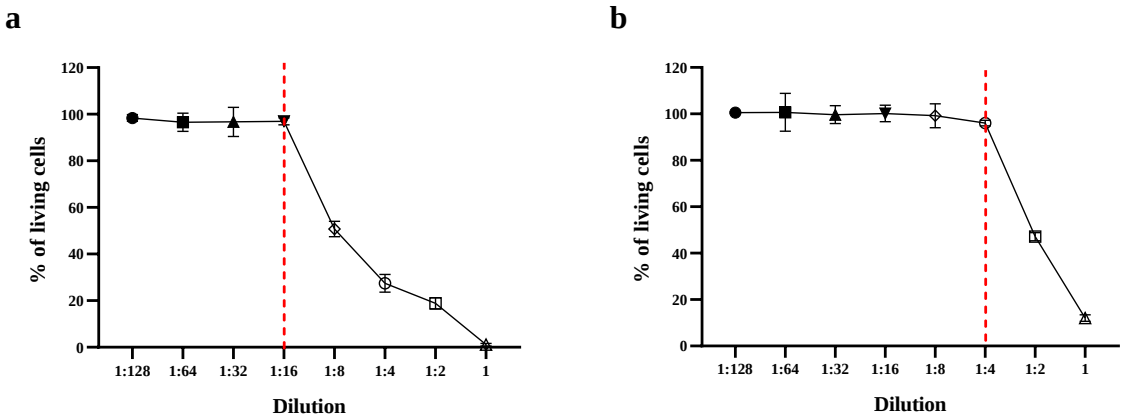

Figure S1. The antibiofilm effect of OCT solution after 3 h contact time, depending on the dilution, (**a**) *S. aureus* and (**b**) *P. aeruginosa.*

a

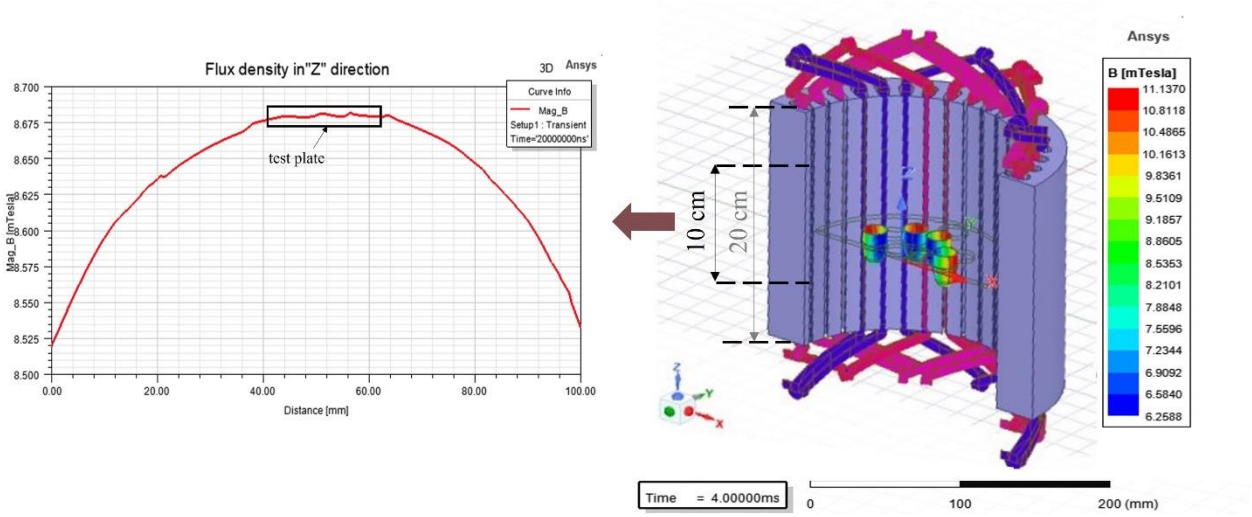

b

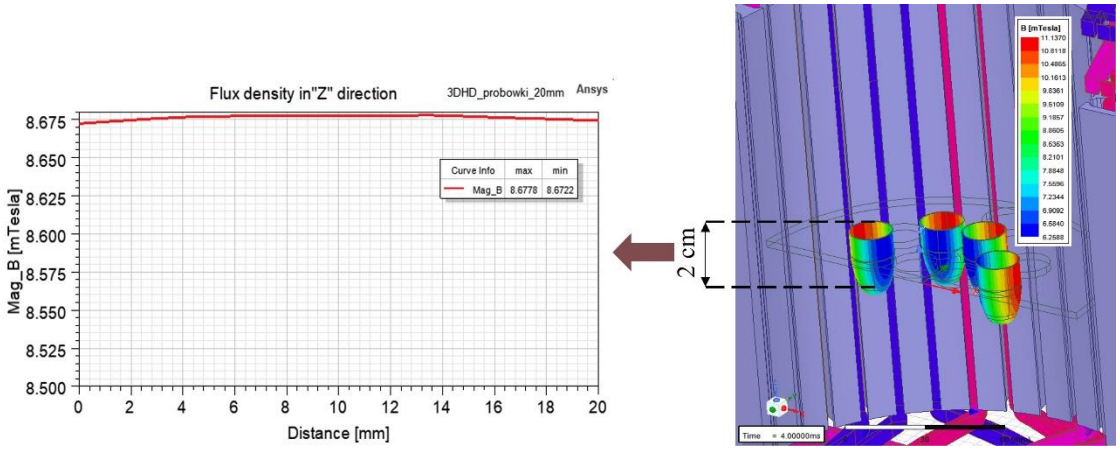

Figure S2. Spatial distribution of magnetic field a) in cross-section (h = 10 cm) of RMF-bioreactor in center of representative well of a test plate, b) in cross-section of center of representative well of a test plate (h = 2 cm) placed inside RMF-bioreactor.

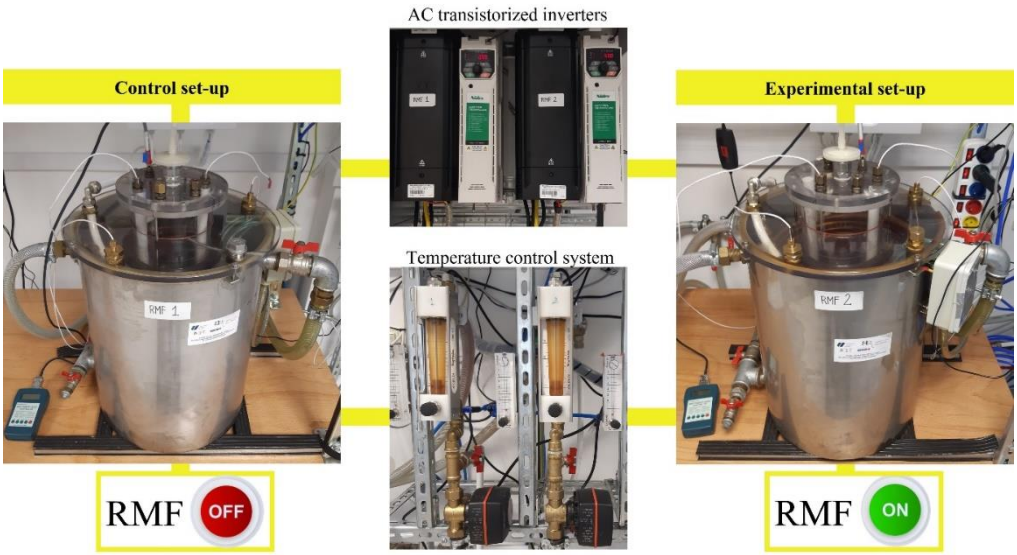

Figure S3. RMF generator and control settings with monitoring and control equipment.

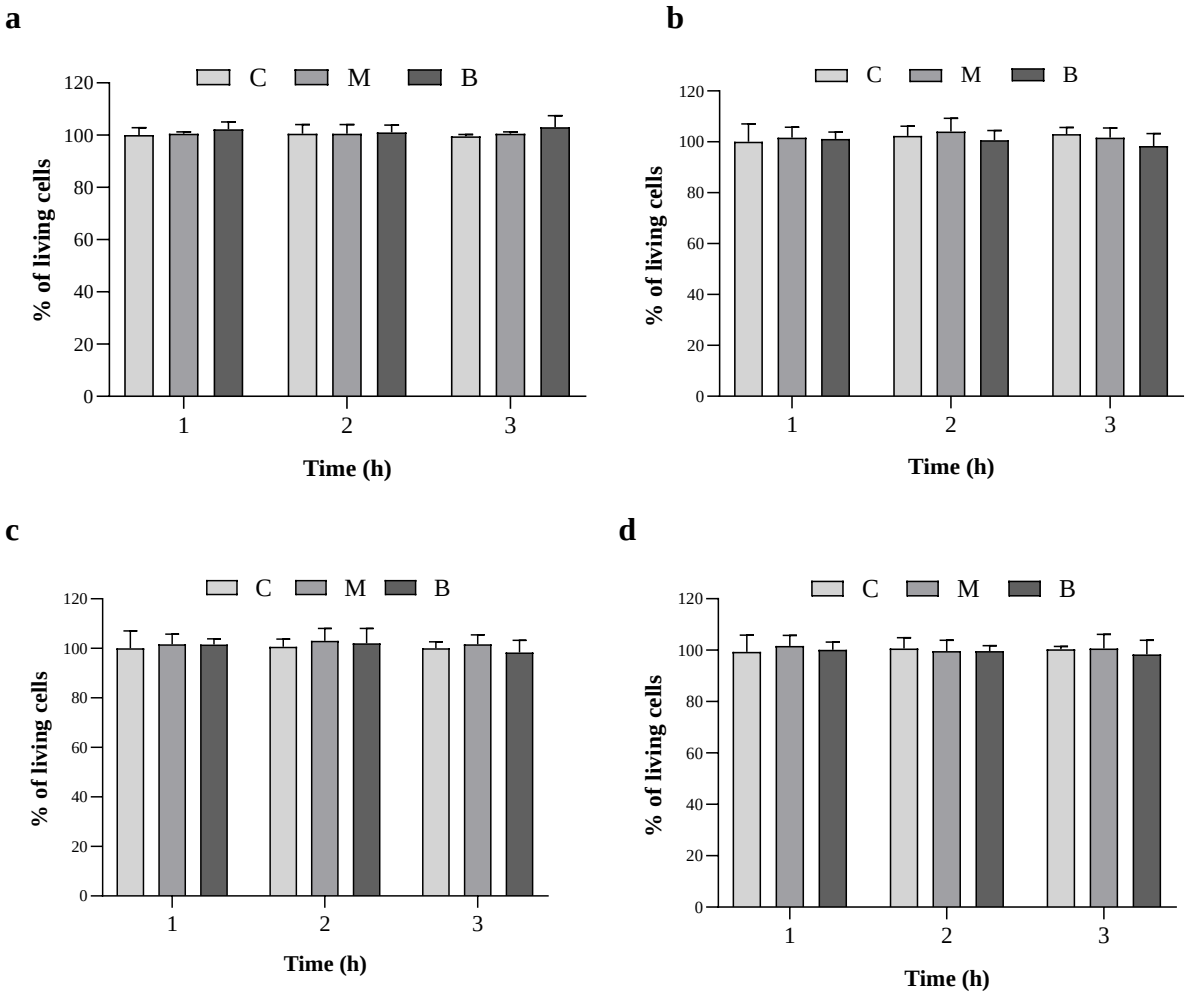

Figure S4. Percent of living biofilm-forming cells on successive agar discs exposed to RMF of (**a**) *S. aureus* RMF of 5 Hz, (**b**) *S. aureus* RMF of 50 Hz, (**c**) *P. aeruginosa* RMF of 5 Hz and (**d**) *P. aeruginosa* RMF of 50 Hz in comparison to RMF-unexposed settings.
The results are presented as mean ± SEM. There were no statistically significant differences in cells viability between individual discs (C, M, B) and in comparison to RMF-unexposed control ($p < 0.05$, Tukey's HSD test).

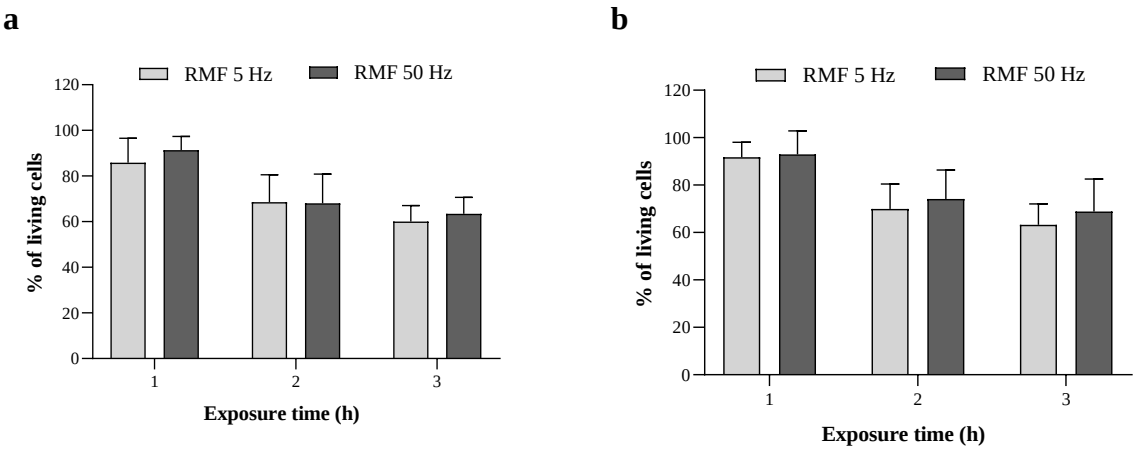

Figure S5. Percent of living (**a**) *S. aureus* and (**b**) *P. aeruginosa* biofilm-forming cells treated with OCT-saturated carriers and exposed to RMF at different frequencies in comparison to RMF-unexposed settings.
The results are presented as mean ± SEM calculated from the results obtained for all agar discs (C, M, B).

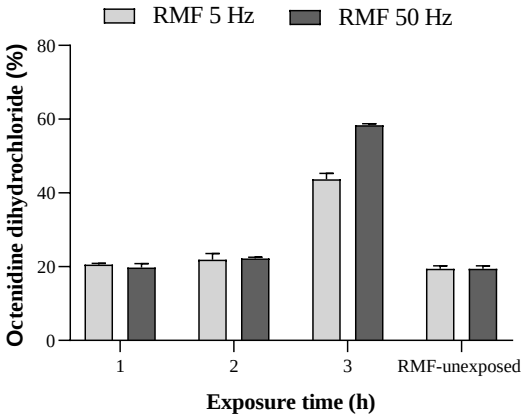

Figure S6. Percent of octenidine dihydrochloride extracted from all agar discs (C, M, B) exposed to RMF of 5 Hz and 50 Hz, in comparison to its initial concentration in the paper disc.
The results are presented as mean ± SEM calculated from the results obtained for all agar discs (C, M, B).

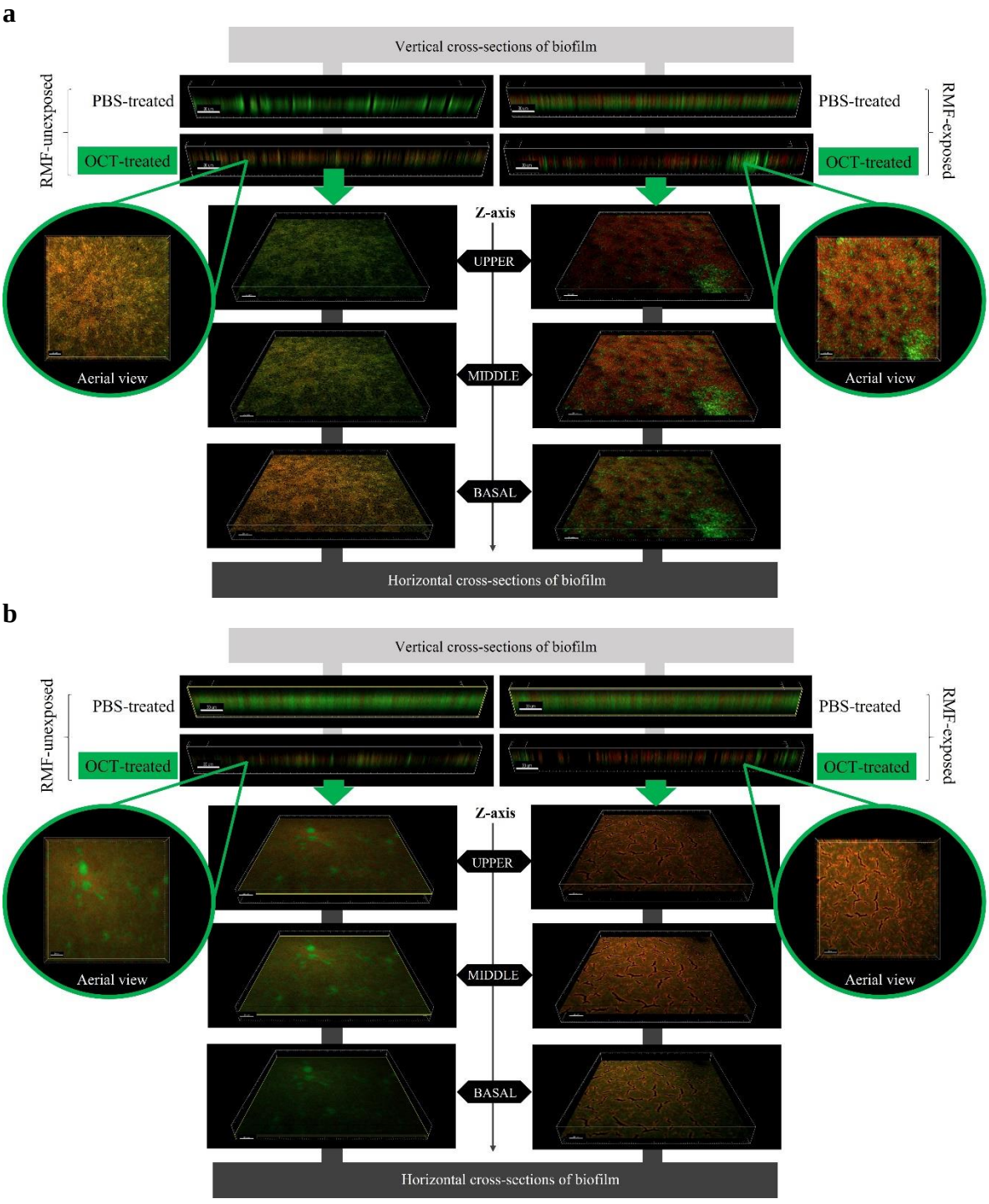

Figure S7. The spatial location of (**a**) staphylococcal and (**b**) pseudomonal cells within biofilm treated with OCT-saturated carriers and/or exposed to RMF (50 Hz).
The cells with non-altered cell walls dye green (as a result of SYTO-9), while the cells with compromised cell walls dye red/orange (as a result of propidium-iodide incorporation).

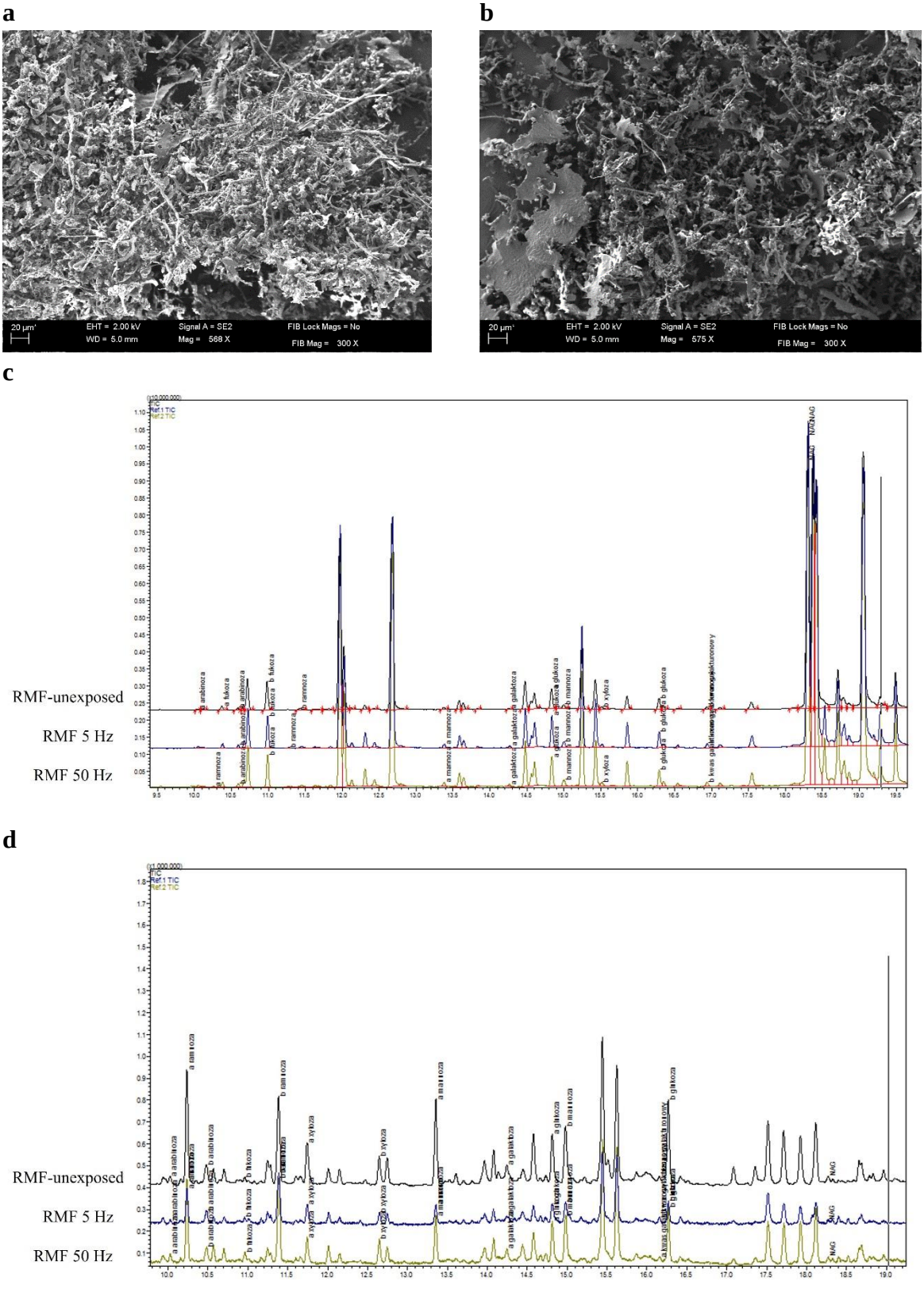

Figure S8. The cell-free (**a**) pseudomonal and (**b**) staphylococcal biofilm matrix subjected to GC-MS/MS analysis (**c**, **d**, respectively). Unexposed - matrix obtained from RMF-unexposed biofilm; 5 Hz - matrix obtained from biofilm exposed to RMF of 5 Hz; 50 Hz - matrix obtained from biofilm exposed to RMF of 50 Hz.

Table S2. The values of magnetic induction inside the RMF generator, at the location of the biofilm samples depending on the applied AC frequency.

Magnetic induction [mT]	**5 Hz**	**50 Hz**
MIN	8.352	8.698
MAX	8.354	8.700
Average	8.353	8.699

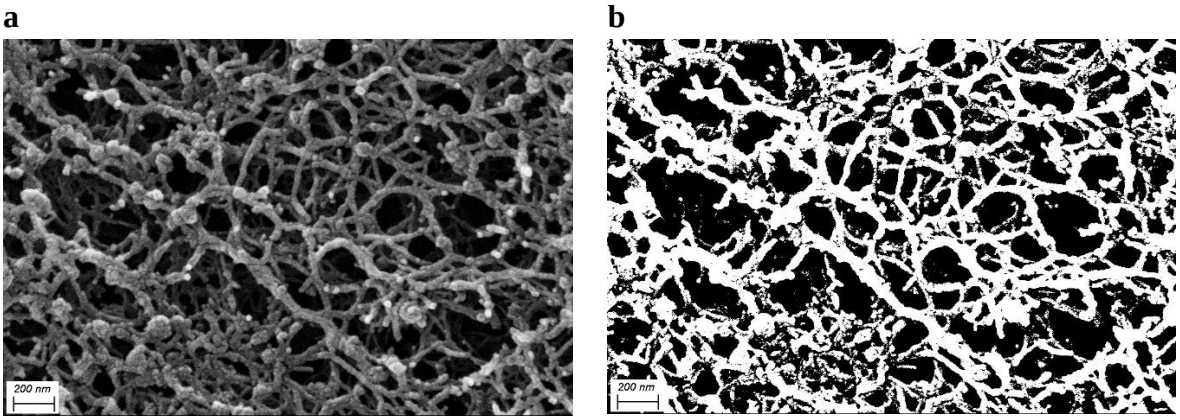

Figure S9. SEM-visualized structure of agar disk (**a**) and parametric processing of the image to assess agar porosity (**b**).

The estimation of energy flux density of the electric field

The relationship between the electric and magnetic field of an electromagnetic wave is presented by the system of Maxwell equations:

$$\begin{aligned} \varepsilon\varepsilon_0 div\vec{E} &= \rho \\ rot\vec{E} &= -\mu\mu_0 \frac{\partial \vec{H}}{\partial_t} \\ div\vec{B} &= 0 \\ rot\vec{H} &= \varepsilon\varepsilon_0 \frac{\partial \vec{E}}{\partial_t} + \vec{j} \end{aligned} \quad (1)$$

where: $\vec{E}$ - vector of electric field intensity, $\vec{H}, \vec{B}$ - vectors of magnetic field intensity and induction, respectively, $\varepsilon, \varepsilon_0$ - electric permeability of the medium and vacuum, μ, μ_0 - magnetic permeability of the medium and vacuum, ρ - electric charge density, $\vec{j}$- electric current density.

Equation (1) shows, that the alternating magnetic field ($\frac{\partial \vec{H}}{\partial_t}$) creates a rotating electric field ($rot\vec{E}$). This equation expresses the content of Faraday's law of induction.

Maxwell's equations describing the propagation of an electromagnetic wave along the Z-axis have the following form:

$$\begin{aligned} \frac{\partial \vec{H}}{\partial_z} &= -\varepsilon\varepsilon_0 \frac{\partial E}{\partial_t} \\ \frac{\partial E}{\partial_z} &= -\mu\mu_0 \frac{\partial H}{\partial_t} \end{aligned} \quad (2)$$

The above equations show that a change in one of the electromagnetic field vectors with time causes a change in the second vector in space.

The disturbance of the electromagnetic field propagating in space is related to energy, the density of which (energy contained in a unit of volume) is equal to the sum of the electric and magnetic field densities.

$$u = \frac{1}{2}(\varepsilon\varepsilon_0 E^2 + \mu\mu_0 H^2) \quad (3)$$

After determining the partial derivatives in the Maxwell equations describing the electromagnetic wave (2), we get:

$$\frac{1}{v} H = \varepsilon\varepsilon_0 E \quad (4)$$

where: $v = \frac{1}{\varepsilon\varepsilon_0\mu\mu_0}$ - speed of propagation of an electromagnetic wave in a given medium.

So, substituting the velocity formula, we get:

$$\sqrt{\mu\mu_0}H = \sqrt{\varepsilon\varepsilon_0}E \tag{5}$$

Using the above dependence, the energy density of the electromagnetic field (3) can be represented as follows:

$$u = \frac{1}{2}\left(\varepsilon\varepsilon_0 E^2 + \mu\mu_0 H^2\right) = \varepsilon\varepsilon_0 E^2 = \mu\mu_0 H^2 = \frac{1}{2\mu\mu_0}B^2 \tag{6}$$

Formula (6) directly shows that the energy density of the electric field is equal to the magnetic field density, and thus, given the magnetic induction values and the magnetic and electric permeability coefficients of the medium and the vacuum, the value of the electric field can be calculated. In view of the above, an important quantity characterizing the interaction of the electric field on the surface perpendicular to the direction of propagation of the disturbance is the energy flux density, which can be expressed by the following relationship:

$$J_p = E^2\frac{\sqrt{\varepsilon\varepsilon_0}}{\sqrt{\mu\mu_0}} \tag{7}$$

The change in energy density in a charge-free region is related to the influence or outflow of the energy density flux equivalent to this change. When the disturbances spread in a medium containing free charges, the part of the energy that converts into Joule's heat should also be taken into account in the energy balance. In the RMF-generating system used in our study, the magnetic field lines are arranged orthonormally with respect to the biofilm-containing plates. In this case, the energy flux density affecting the sample caused by the generated electric field is negligible (the magnetic field was so large that only the observed and described effects related to magnetic fields were dominant).

Zachodniopomorski Uniwersytet Technologiczny w Szczecinie

Wydział Biotechnologii i Hodowli Zwierząt

Załącznik 3

Oświadczenia współautorów publikacji naukowych wchodzących w skład cyklu stanowiącego rozprawę doktorską wraz z określeniem ich indywidualnego udziału

Daria Ciecholewska-Juśko

Rozprawa doktorska

OPRACOWANIE I CHARAKTERYSTYKA MATERIAŁÓW BIONANOCELULOZOWYCH DO ZAPOBIEGANIA KOLONIZACJI PRZEZ DROBNOUSTROJE PATOGENNE ORAZ DO ERADYKACJI BIOFILMÓW BAKTERYJNYCH

Szczecin, 07.09.2022

dr hab. inż. Karol Fijałkowski, prof. ZUT

Katedra Mikrobiologii i Biotechnologii

Wydział Biotechnologii i Hodowli Zwierząt

Zachodniopomorski Uniwersytet Technologiczny w Szczecinie

al. Piastów 45

70-311 Szczecin

Oświadczenie

Oświadczam, że jestem współautorem prac wchodzących w skład rozprawy doktorskiej mgr inż. Darii Ciecholewskiej-Juśko:

1. Ciecholewska-Juśko, D., Żywicka, A., Junka, A., Drozd, R., Sobolewski, P., Migdał, P., Kowalska, U., Toporkiewicz, M., Fijałkowski, K. (2021). Superabsorbent crosslinked bacterial cellulose biomaterials for chronic wound dressings. *Carbohydrate Polymers*, *253*, 117247. https://doi.org/10.1016/j.carbpol.2020.117247

   Mój wkład w powstanie tej pracy polegał na udziale w opracowaniu koncepcji i metodologii badań, konsultacji uzyskanych wyników, pomocy przy napisaniu oraz przygotowaniu manuskryptu (jako autor do korespondencji).

2. Ciecholewska-Juśko, D., Broda, M., Żywicka, A., Styburski, D., Sobolewski, P., Gorący, K., Migdał, P., Junka, A., Fijałkowski, K. (2021). Potato juice, a starch industry waste, as a cost-effective medium for the biosynthesis of bacterial cellulose. *International Journal of Molecular Sciences*, *22*(19), 10807. https://doi.org/10.3390/ijms221910807

   Mój wkład w powstanie tej pracy polegał na udziale w opracowaniu koncepcji i metodologii badań, konsultacji uzyskanych wyników, pomocy przy napisaniu oraz przygotowaniu manuskryptu (jako autor do korespondencji).

3. Ciecholewska-Juśko, D., Junka, A., Fijałkowski, K. (2022). The cross-linked bacterial cellulose impregnated with octenidine dihydrochloride-based antiseptic as an antibacterial dressing material for highly-exuding, infected wounds. *Microbiological Research, 263,* 127125.
https://doi.org/10.1038/s41598-022-12840-y

   Mój wkład w powstanie tej pracy polegał na udziale w opracowaniu koncepcji i metodologii badań, konsultacji uzyskanych wyników, pomocy przy napisaniu oraz przygotowaniu manuskryptu (jako autor do korespondencji).

4. Ciecholewska-Juśko, D., Żywicka, A., Junka, A., Woroszyło, M., Wardach, M., Chodaczek, G., Szymczyk-Ziółkowska, P., Migdał, P., Fijałkowski, K. (2022). The effects of rotating magnetic field and antiseptic on in vitro pathogenic biofilm and its milieu. *Scientific reports*, *12*(1), 1-19.
https://doi.org/10.1016/j.micres.2022.127125

   Mój wkład w powstanie tej pracy polegał na udziale w opracowaniu koncepcji i metodologii badań, konsultacji uzyskanych wyników, pomocy przy napisaniu oraz przygotowaniu manuskryptu (jako autor do korespondencji).

Podpis współautora

Karol Fijałkowski

.....

dr hab. inż. Karol Fijałkowski, prof. ZUT

Wrocław, 07.09.2022

dr hab.n.med Adam Junka, prof. Uczelni

Katedra i Zakład Mikrobiologii Farmaceutycznej i Parazytologii

Wydział Farmaceutyczny

Uniwersytet Medyczny im. Piastów Śląskich we Wrocławiu

ul. Borowska 211a

50-534 Wrocław

Oświadczenie

Oświadczam, że jestem współautorem prac wchodzących w skład rozprawy doktorskiej mgr inż. Darii Ciecholewskiej-Juśko:

1. Ciecholewska-Juśko, D., Żywicka, A., Junka, A., Drozd, R., Sobolewski, P., Migdał, P., Kowalska, U., Toporkiewicz, M., Fijałkowski, K. (2021). Superabsorbent crosslinked bacterial cellulose biomaterials for chronic wound dressings. *Carbohydrate Polymers*, *253*, 117247. https://doi.org/10.1016/j.carbpol.2020.117247

   Mój wkład w powstanie tej pracy polegał na udziale w interpretacji uzyskanych wyników oraz napisaniu manuskryptu.

2. Ciecholewska-Juśko, D., Broda, M., Żywicka, A., Styburski, D., Sobolewski, P., Gorący, K., Migdał, P., Junka, A., Fijałkowski, K. (2021). Potato juice, a starch industry waste, as a cost-effective medium for the biosynthesis of bacterial cellulose. *International Journal of Molecular Sciences*, *22*(19), 10807. https://doi.org/10.3390/ijms221910807

   Mój wkład w powstanie tej pracy polegał na udziale w interpretacji uzyskanych wyników oraz napisaniu manuskryptu.

3. Ciecholewska-Juśko, D., Junka, A., Fijałkowski, K. (2022). The cross-linked bacterial cellulose impregnated with octenidine dihydrochloride-based antiseptic as an antibacterial dressing material for highly-exuding, infected wounds. *Microbiological Research, 263,* 127125. https://doi.org/10.1038/s41598-022-12840-y

Uniwersytet Medyczny we Wrocławiu
KATEDRA I ZAKŁAD MIKROBIOLOGII FARMACEUTYCZNEJ I PARAZYTOLOGII
dr hab. Adam Junka, prof. uczelni

Mój wkład w powstanie tej pracy polegał na wykonaniu testów cytotoksyczności, udziale w interpretacji uzyskanych wyników oraz napisaniu manuskryptu.

4. Ciecholewska-Juśko, D., Żywicka, A., Junka, A., Woroszyło, M., Wardach, M., Chodaczek, G., Szymczyk-Ziółkowska, P., Migdał, P., Fijałkowski, K. (2022). The effects of rotating magnetic field and antiseptic on in vitro pathogenic biofilm and its milieu. *Scientific reports*, *12*(1), 1-19. https://doi.org/10.1016/j.micres.2022.127125

   Mój wkład w powstanie tej pracy polegał na udziale w interpretacji uzyskanych wyników oraz napisaniu manuskryptu.

Podpis współautora

Uniwersytet Medyczny we Wrocławiu
KATEDRA I ZAKŁAD MIKROBIOLOGII FARMACEUTYCZNEJ I PARAZYTOLOGII
dr hab. Adam Junka, prof. Uczelni

.....Adam Junka.....

dr hab.n.med. Adam Junka, prof. Uczelni

Wrocław, 07.09.2022

dr inż. Paweł Migdał

Katedra Higieny Środowiska i Dobrostanu Zwierząt

Wydział Biologii i Hodowli Zwierząt

Uniwersytet Przyrodniczy we Wrocławiu

ul. Norwida 25

50-375 Wrocław

Oświadczenie

Oświadczam, że jestem współautorem prac wchodzących w skład rozprawy doktorskiej mgr inż. Darii Ciecholewskiej-Juśko:

1. Ciecholewska-Juśko, D., Żywicka, A., Junka, A., Drozd, R., Sobolewski, P., Migdał, P., Kowalska, U., Toporkiewicz, M., Fijałkowski, K. (2021). Superabsorbent crosslinked bacterial cellulose biomaterials for chronic wound dressings. *Carbohydrate Polymers*, *253*, 117247. https://doi.org/10.1016/j.carbpol.2020.117247

   Mój wkład w powstanie tej pracy polegał na wykonaniu analiz przy użyciu skaningowego mikroskopu elektronowego ze spektrometrem rentgenowskim z dyspersją energii (SEM-EDX).

2. Ciecholewska-Juśko, D., Broda, M., Żywicka, A., Styburski, D., Sobolewski, P., Gorący, K., Migdał, P., Junka, A., Fijałkowski, K. (2021). Potato juice, a starch industry waste, as a cost-effective medium for the biosynthesis of bacterial cellulose. *International Journal of Molecular Sciences*, *22*(19), 10807. https://doi.org/10.3390/ijms221910807

   Mój wkład w powstanie tej pracy polegał na wykonaniu analiz z użyciem skaningowego mikroskopu elektronowego.

3. Ciecholewska-Juśko, D., Żywicka, A., Junka, A., Woroszyło, M., Wardach, M., Chodaczek, G., Szymczyk-Ziółkowska, P., Migdał, P., Fijałkowski, K. (2022). The effects of rotating magnetic field and antiseptic on in vitro pathogenic biofilm and its milieu. *Scientific reports*, *12*(1), 1-19. https://doi.org/10.1016/j.micres.2022.127125

Mój wkład w powstanie tej pracy polegał na wykonaniu analiz z użyciem skaningowego mikroskopu elektronowego.

Podpis współautora

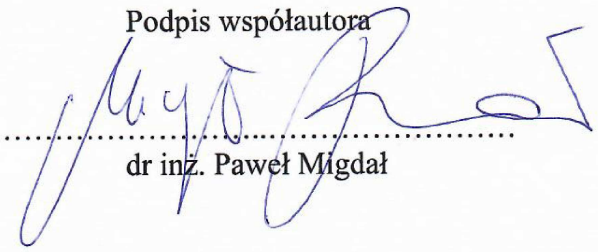

.....

dr inż. Paweł Migdał

Szczecin, 07.09.2022

dr inż. Anna Żywicka

Katedra Mikrobiologii i Biotechnologii

Wydział Biotechnologii i Hodowli Zwierząt

Zachodniopomorski Uniwersytet Technologiczny w Szczecinie

al. Piastów 45

70-311 Szczecin

Oświadczenie

Oświadczam, że jestem współautorem prac wchodzących w skład rozprawy doktorskiej mgr inż. Darii Ciecholewskiej-Juśko:

1. Ciecholewska-Juśko, D., Żywicka, A., Junka, A., Drozd, R., Sobolewski, P., Migdał, P., Kowalska, U., Toporkiewicz, M., Fijałkowski, K. (2021). Superabsorbent crosslinked bacterial cellulose biomaterials for chronic wound dressings. *Carbohydrate Polymers*, *253*, 117247. https://doi.org/10.1016/j.carbpol.2020.117247

   Mój wkład w powstanie tej pracy polegał na konsultacji uzyskanych wyników oraz pomocy przy napisaniu manuskryptu.

2. Ciecholewska-Juśko, D., Broda, M., Żywicka, A., Styburski, D., Sobolewski, P., Gorący, K., Migdał, P., Junka, A., Fijałkowski, K. (2021). Potato juice, a starch industry waste, as a cost-effective medium for the biosynthesis of bacterial cellulose. *International Journal of Molecular Sciences*, *22*(19), 10807. https://doi.org/10.3390/ijms221910807

   Mój wkład w powstanie tej pracy polegał na konsultacji uzyskanych wyników oraz pomocy przy napisaniu oraz przygotowaniu manuskryptu.

3. Ciecholewska-Juśko, D., Żywicka, A., Junka, A., Woroszyło, M., Wardach, M., Chodaczek, G., Szymczyk-Ziółkowska, P., Migdał, P., Fijałkowski, K. (2022). The effects of rotating magnetic field and antiseptic on in vitro pathogenic biofilm and its milieu. *Scientific reports*, *12*(1), 1-19. https://doi.org/10.1016/j.micres.2022.127125

   Mój wkład w powstanie tej pracy polegał na pomocy w wykonaniu analiz z użyciem wirującego pola magnetycznego, konsultacji uzyskanych wyników oraz pomocy przy napisaniu manuskryptu.

Podpis współautora

Anna Żywicka

dr inż. Anna Żywicka

Szczecin, 07.09.2022

dr inż. Piotr Sobolewski

Katedra Inżynierii Polimerów i Biomateriałów

Wydział Technologii i Inżynierii Chemicznej

Zachodniopomorski Uniwersytet Technologiczny w Szczecinie

al. Piastów 45

70-311 Szczecin

Oświadczenie

Oświadczam, że jestem współautorem prac wchodzących w skład rozprawy doktorskiej mgr inż. Darii Ciecholewskiej-Juśko:

1. Ciecholewska-Juśko, D., Żywicka, A., Junka, A., Drozd, R., Sobolewski, P., Migdał, P., Kowalska, U., Toporkiewicz, M., Fijałkowski, K. (2021). Superabsorbent crosslinked bacterial cellulose biomaterials for chronic wound dressings. *Carbohydrate Polymers*, *253*, 117247. https://doi.org/10.1016/j.carbpol.2020.117247

   Mój wkład w powstanie tej pracy polegał na wykonaniu testów cytotoksyczności oraz pomocy w napisaniu manuskryptu.

2. Ciecholewska-Juśko, D., Broda, M., Żywicka, A., Styburski, D., Sobolewski, P., Gorący, K., Migdał, P., Junka, A., Fijałkowski, K. (2021). Potato juice, a starch industry waste, as a cost-effective medium for the biosynthesis of bacterial cellulose. *International Journal of Molecular Sciences*, *22*(19), 10807. https://doi.org/10.3390/ijms221910807

   Mój wkład w powstanie tej pracy polegał na wykonaniu testów cytotoksyczności oraz pomocy w napisaniu manuskryptu.

Podpis współautora

.....

dr inż. Piotr Sobolewski

Wrocław, 07.09.2022

dr Monika Toporkiewicz

Laboratorium Mikroskopii Konfokalnej

Sieć Badawcza ŁUKASIEWICZ - PORT Polski Ośrodek Rozwoju Technologii

ul. Stabłowicka 147

54-066 Wrocław

Oświadczenie

Oświadczam, że jestem współautorem pracy wchodzącej w skład rozprawy doktorskiej mgr inż. Darii Ciecholewskiej-Juśko:

1. Ciecholewska-Juśko, D., Żywicka, A., Junka, A., Drozd, R., Sobolewski, P., Migdał, P., Kowalska, U., Toporkiewicz, M., Fijałkowski, K. (2021). Superabsorbent crosslinked bacterial cellulose biomaterials for chronic wound dressings. *Carbohydrate Polymers*, *253*, 117247. https://doi.org/10.1016/j.carbpol.2020.117247

   Mój wkład w powstanie tej pracy polegał na wykonaniu analiz z użyciem mikroskopu konfokalnego.

Podpis współautora

Monika Toporkiewicz

dr Monika Toporkiewicz

Szczecin, 07.09.2022

dr inż. Urszula Kowalska

Centrum Bioimmobilizacji i Innowacyjnych Materiałów Opakowaniowych

Wydział Nauk o Żywności i Rybactwa

Zachodniopomorski Uniwersytet Technologiczny w Szczecinie

ul. Klemensa Janickiego 35

71-270 Szczecin

Oświadczenie

Oświadczam, że jestem współautorem pracy wchodzącej w skład rozprawy doktorskiej mgr inż. Darii Ciecholewskiej-Juśko:

1. Ciecholewska-Juśko, D., Żywicka, A., Junka, A., Drozd, R., Sobolewski, P., Migdał, P., Kowalska, U., Toporkiewicz, M., Fijałkowski, K. (2021). Superabsorbent crosslinked bacterial cellulose biomaterials for chronic wound dressings. *Carbohydrate Polymers*, *253*, 117247. https://doi.org/10.1016/j.carbpol.2020.117247

   Mój wkład w powstanie tej pracy polegał na wykonaniu zdjęć powierzchni celulozy bakteryjnej z użyciem skaningowego mikroskopu elektronowego.

Podpis współautora

.....

dr inż. Urszula Kowalska

Szczecin, 07.09.2022

dr inż. Radosław Drozd

Katedra Mikrobiologii i Biotechnologii

Wydział Biotechnologii i Hodowli Zwierząt

Zachodniopomorski Uniwersytet Technologiczny w Szczecinie

al. Piastów 45

70-311 Szczecin

Oświadczenie

Oświadczam, że jestem współautorem pracy wchodzącej w skład rozprawy doktorskiej mgr inż. Darii Ciecholewskiej-Juśko:

1. Ciecholewska-Juśko, D., Żywicka, A., Junka, A., Drozd, R., Sobolewski, P., Migdał, P., Kowalska, U., Toporkiewicz, M., Fijałkowski, K. (2021). Superabsorbent crosslinked bacterial cellulose biomaterials for chronic wound dressings. *Carbohydrate Polymers*, *253*, 117247. https://doi.org/10.1016/j.carbpol.2020.117247

   Mój wkład w powstanie tej pracy polegał na pomocy w interpretacji wyników uzyskanych techniką spektroskopii fourierowskiej.

Podpis współautora

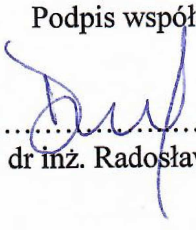

.....

dr inż. Radosław Drozd

Szczecin, 26.09.2022

dr Daniel Styburski

Laboratorium Chromatografii i Spektroskopii Mas

Wydział Biotechnologii i Hodowli Zwierząt

Zachodniopomorski Uniwersytet Technologiczny w Szczecinie

ul. Klemensa Janickiego 29

71-270 Szczecin

Oświadczenie

Oświadczam, że jestem współautorem pracy wchodzącej w skład rozprawy doktorskiej mgr inż. Darii Ciecholewskiej-Juśko:

1. Ciecholewska-Juśko, D., Broda, M., Żywicka, A., Styburski, D., Sobolewski, P., Gorący, K., Migdał, P., Junka, A., Fijałkowski, K. (2021). Potato juice, a starch industry waste, as a cost-effective medium for the biosynthesis of bacterial cellulose. *International Journal of Molecular Sciences*, *22*(19), 10807. https://doi.org/10.3390/ijms221910807

   Mój wkład w powstanie tej pracy polegał na wykonaniu analiz chromatograficznych (chromatografia cieczowa z tandemową spektrometrią mas).

Podpis współautora

.....Daniel Styburski.....

dr Daniel Styburski

Szczecin, 07.09.2022

mgr inż. Michał Broda

Katedra Mikrobiologii i Biotechnologii

Wydział Biotechnologii i Hodowli Zwierząt

Zachodniopomorski Uniwersytet Technologiczny w Szczecinie

al. Piastów 45

70-311 Szczecin

Pomorsko Mazurska Hodowla Ziemniaka Sp. z o.o. z siedzibą w Strzekęcinie

Strzekęcino 11

76-024 Świeszyno

Oświadczenie

Oświadczam, że jestem współautorem pracy wchodzącej w skład rozprawy doktorskiej mgr inż. Darii Ciecholewskiej-Juśko:

1. Ciecholewska-Juśko, D., Broda, M., Żywicka, A., Styburski, D., Sobolewski, P., Gorący, K., Migdał, P., Junka, A., Fijałkowski, K. (2021). Potato juice, a starch industry waste, as a cost-effective medium for the biosynthesis of bacterial cellulose. *International Journal of Molecular Sciences*, *22*(19), 10807. https://doi.org/10.3390/ijms221910807

   Mój wkład w powstanie tej pracy polegał na udziale w opracowaniu koncepcji i metodologii badań, pomocy w przygotowaniu materiału do badań, konsultacji uzyskanych wyników oraz pomocy przy napisaniu oraz przygotowaniu manuskryptu.

Podpis współautora

.....Michał Broda.....

mgr inż. Michał Broda

Szczecin, 07.09.2022

dr inż. Krzysztof Gorący

Katedra Inżynierii Polimerów i Biomateriałów

Wydział Technologii i Inżynierii Chemicznej

Zachodniopomorski Uniwersytet Technologiczny w Szczecinie

al. Piastów 45

70-311 Szczecin

Oświadczenie

Oświadczam, że jestem współautorem pracy wchodzącej w skład rozprawy doktorskiej mgr inż. Darii Ciecholewskiej-Juśko:

1. Ciecholewska-Juśko, D., Broda, M., Żywicka, A., Styburski, D., Sobolewski, P., Gorący, K., Migdał, P., Junka, A., Fijałkowski, K. (2021). Potato juice, a starch industry waste, as a cost-effective medium for the biosynthesis of bacterial cellulose. *International Journal of Molecular Sciences*, *22*(19), 10807. https://doi.org/10.3390/ijms221910807

   Mój wkład w powstanie tej pracy polegał na wykonaniu analiz właściwości mechanicznych celulozy bakteryjnej.

Podpis współautora

.....

dr inż. Krzysztof Gorący

Wrocław, 07.09.2022

dr hab. Grzegorz Chodaczek

Laboratorium Bioobrazowania

Sieć Badawcza ŁUKASIEWICZ - PORT Polski Ośrodek Rozwoju Technologii

ul. Stabłowicka 147

54-066 Wrocław

Oświadczenie

Oświadczam, że jestem współautorem pracy wchodzącej w skład rozprawy doktorskiej mgr inż. Darii Ciecholewskiej-Juśko:

1. Ciecholewska-Juśko, D., Żywicka, A., Junka, A., Woroszyło, M., Wardach, M., Chodaczek, G., Szymczyk-Ziółkowska, P., Migdał, P., Fijałkowski, K. (2022). The effects of rotating magnetic field and antiseptic on in vitro pathogenic biofilm and its milieu. *Scientific reports*, *12*(1), 1-19. https://doi.org/10.1016/j.micres.2022.127125

   Mój wkład w powstanie tej pracy polegał na wykonaniu analiz z użyciem mikroskopu konfokalnego.

Podpis współautora

.....

dr hab. Grzegorz Chodaczek

Wrocław, 07.09.2022

dr inż. Patrycja Szymczyk-Ziółkowska

Katedra Technologii Laserowych, Automatyzacji i Organizacji Produkcji

Wydział Mechaniczny

Politechnika Wrocławska

ul. Łukasiewicza 5

50-371 Wrocław

Oświadczenie

Oświadczam, że jestem współautorem pracy wchodzącej w skład rozprawy doktorskiej mgr inż. Darii Ciecholewskiej-Juśko:

1. Ciecholewska-Juśko, D., Żywicka, A., Junka, A., Woroszyło, M., Wardach, M., Chodaczek, G., Szymczyk-Ziółkowska, P., Migdał, P., Fijałkowski, K. (2022). The effects of rotating magnetic field and antiseptic on in vitro pathogenic biofilm and its milieu. *Scientific reports*, *12*(1), 1-19. https://doi.org/10.1016/j.micres.2022.127125

   Mój wkład w powstanie tej pracy polegał na wykonaniu analiz z użyciem skaningowego mikroskopu elektronowego.

Podpis współautora

.....

dr inż. Patrycja Szymczyk-Ziółkowska

Szczecin, 07.09.2022

dr hab. inż. Marcin Wardach, prof. ZUT

Katedra Maszyn i Napędów Elektrycznych

Wydział Elektryczny

Zachodniopomorski Uniwersytet Technologiczny w Szczecinie

ul. Sikorskiego 37

70-313 Szczecin

Oświadczenie

Oświadczam, że jestem współautorem pracy wchodzącej w skład rozprawy doktorskiej mgr inż. Darii Ciecholewskiej-Juśko:

1. Ciecholewska-Juśko, D., Żywicka, A., Junka, A., Woroszyło, M., Wardach, M., Chodaczek, G., Szymczyk-Ziółkowska, P., Migdał, P., Fijałkowski, K. (2022). The effects of rotating magnetic field and antiseptic on in vitro pathogenic biofilm and its milieu. *Scientific reports*, *12*(1), 1-19. https://doi.org/10.1016/j.micres.2022.127125

   Mój wkład w powstanie tej pracy polegał na wykonaniu analiz i wizualizacji związanych z charakterystyką wirującego pola magnetycznego.

Podpis współautora

.....

dr hab. inż. Marcin Wardach, prof. ZUT

Szczecin, 07.09.2022

mgr inż. Marta Woroszyło

Katedra Mikrobiologii i Biotechnologii

Wydział Biotechnologii i Hodowli Zwierząt

Zachodniopomorski Uniwersytet Technologiczny w Szczecinie

al. Piastów 45

70-311 Szczecin

Oświadczenie

Oświadczam, że jestem współautorem pracy wchodzącej w skład rozprawy doktorskiej mgr inż. Darii Ciecholewskiej-Juśko:

1. Ciecholewska-Juśko, D., Żywicka, A., Junka, A., Woroszyło, M., Wardach, M., Chodaczek, G., Szymczyk-Ziółkowska, P., Migdał, P., Fijałkowski, K. (2022). The effects of rotating magnetic field and antiseptic on in vitro pathogenic biofilm and its milieu. *Scientific reports*, *12*(1), 1-19. https://doi.org/10.1016/j.micres.2022.127125

   Mój wkład w powstanie tej pracy polegał na udziale w analizach związanych z wykorzystaniem wirującego pola magnetycznego oraz wykonaniu testów żywotności komórek bakteryjnych.

Podpis współautora

M. Woroszyło

.....

mgr inż. Marta Woroszyło

Zachodniopomorski Uniwersytet Technologiczny w Szczecinie

Wydział Biotechnologii i Hodowli Zwierząt

Załącznik 4

Sumaryczne zestawienie dorobku naukowego

Daria Ciecholewska-Juśko

Rozprawa doktorska

OPRACOWANIE I CHARAKTERYSTYKA MATERIAŁÓW BIONANOCELULOZOWYCH DO ZAPOBIEGANIA KOLONIZACJI PRZEZ DROBNOUSTROJE PATOGENNE ORAZ DO ERADYKACJI BIOFILMÓW BAKTERYJNYCH

Mgr inż. Daria Ciecholewska-Juśko – dorobek naukowy

Prace dyplomowe

1. **01.10.2011 – 07.07.2016 - Studia inżynierskie**

   Kierunek: Biotechnologia

   Miejsce realizacji pracy: Katedra Biotechnologii Molekularnej i Mikrobiologii, Wydział Chemiczny, Politechnika Gdańska

   Temat pracy: Komórki macierzyste w gojeniu ran – możliwości farmakologicznej stymulacji

   Praca realizowana pod kierownictwem: prof. dr hab. inż. Pawła Sachadyna

2. **01.03.2017 – 05.07.2018 - Studia magisterskie**

   Kierunek: Mikrobiologia stosowana

   Miejsce realizacji pracy: Katedra Toksykologii, Technologii Mleczarskiej i Przechowalnictwa Żywności, Wydział Nauk o Żywności i Rybactwa, Zachodniopomorski Uniwersytet Technologiczny w Szczecinie

   Temat pracy: Wpływ różnych metod grillowania na zawartość wybranych metali ciężkich w mięśniach pstrąga tęczowego

   Praca realizowana pod kierownictwem: dr inż. Moniki Rajkowskiej-Myśliwiec

3. **01.10.2018 – obecnie - Studia doktorskie**

   Kierunek: Biotechnologia

   Miejsce realizacji pracy: Katedra Mikrobiologii i Biotechnologii, Wydział Biotechnologii i Hodowli Zwierząt, Zachodniopomorski Uniwersytet Technologiczny w Szczecinie

   Temat pracy: Opracowanie i charakterystyka materiałów bionanocelulozowych do zapobiegania kolonizacji przez drobnoustroje patogenne oraz do eradykacji biofilmów bakteryjnych

   Praca realizowana pod kierownictwem: dr hab. inż. Karola Fijałkowskiego, prof. ZUT

Publikacje naukowe

a) Publikacje naukowe wchodzące w skład cyklu stanowiącego rozprawę doktorską:

1. **Ciecholewska-Juśko, D**., Żywicka, A., Junka, A., Drozd, R., Sobolewski, P., Migdał, P., Kowalska, U., Toporkiewicz, M., Fijałkowski, K. (2021). Superabsorbent crosslinked bacterial cellulose biomaterials for chronic wound dressings. *Carbohydrate Polymers, 253,* 117247.

   IF_{2022} – 9.381, 140 pkt. MEiN

2. **Ciecholewska-Juśko, D**., Broda, M., Żywicka, A., Styburski, D., Sobolewski, P., Gorący, K., Migdał, P., Junka, A., Fijałkowski, K. (2021). Potato juice, a starch industry waste, as a cost-effective medium for the biosynthesis of bacterial cellulose. *International Journal of Molecular Sciences*, *22*(19), 10807.

   IF_{2022} – 5.923, 140 pkt. MEiN

3. **Ciecholewska-Juśko, D**., Żywicka, A., Junka, A., Woroszyło, M., Wardach, M., Chodaczek, G., Szymczyk-Ziółkowska, P., Migdał, P., Fijałkowski, K. (2022). The effects of rotating magnetic field and antiseptic on in vitro pathogenic biofilm and its milieu. *Scientific reports*, *12*(1), 1-19.

   IF_{2022} – 4.380, 140 pkt. MEiN

4. **Ciecholewska-Juśko, D**., Junka, A., Fijałkowski, K. (2022). The cross-linked bacterial cellulose impregnated with octenidine dihydrochloride-based antiseptic as an antibacterial dressing material for highly-exuding, infected wounds. *Microbiological Research, 263,* 127125.

   IF_{2022} – 5.07, 100 pkt. MEiN

b) Pozostałe:

5. Woroszyło, M., Pendrak, K., **Ciecholewska, D.**, Padzik, N., Szewczuk, M., & Karakulska, J. (2019). Investigation of biofilm formation ability of coagulase-negative staphylococci isolated from ready-to-eat meat. *Acta Scientiarum Polonorum Zootechnica*, *17*(4), 27-34.

   40 kt. MEiN

6. Żywicka, A., Junka, A., **Ciecholewska-Juśko, D**., Migdał, P., Czajkowska, J., Fijałkowski, K. (2020). Significant enhancement of citric acid production by Yarrowia lipolytica immobilized in bacterial cellulose-based carrier. *Journal of Biotechnology, 321,* 13-22.

   IF_{2022} – 3.503, 70 pkt. MEiN

7. Rajkowska-Myśliwiec, M., Pokorska-Niewiada, K., Witczak, A., Balcerzak, M., **Ciecholewska-Juśko, D**. (2021). Health benefits and risks associated with element

uptake from grilled fish and fish products. *Journal of the Science of Food and Agriculture, 102*(3), 957-964.

IF_{2022} – 3.638, 100 pkt. MEiN

8. Woroszyło, M., **Ciecholewska-Juśko, D**., Junka, A., Wardach, M., Chodaczek, G., Dudek, B., Fijałkowski, K. (2021). The effect of rotating magnetic field on susceptibility profile of methicillin-resistant *Staphylococcus aureus* strains exposed to activity of different groups of antibiotics. *International Journal of Molecular Sciences, 22*(21), 11551.

IF_{2022} – 5.923, 140 pkt. MEiN

9. Paleczny, J., Junka, A., Brożyna, M., Dydak, K., Oleksy-Wawrzyniak, M., **Ciecholewska-Juśko, D**., Dziedzic, E., Bartoszewicz, M. (2021). The high impact of *Staphylococcus aureus* biofilm culture medium on in vitro outcomes of antimicrobial activity of wound antiseptics and antibiotic. *Pathogens, 10*(11), 1385.

IF_{2022} – 3.492, 100 pkt. MEiN

10. Woroszyło, M., **Ciecholewska-Juśko, D**., Junka, A., Pruss, A., Kwiatkowski, P., Wardach, M., Fijałkowski, K. (2021). The impact of intraspecies variability on growth rate and cellular metabolic activity of bacteria exposed to rotating magnetic field. *Pathogens, 10*(11), 1427.

IF_{2022} – 3.492, 100 pkt. MEiN

11. Żywicka, A., **Ciecholewska-Juśko, D**., Drozd, R., Rakoczy, R., Konopacki, M., Kordas, M., Junka, A., Migdał, B., Fijałkowski, K. (2021). Preparation of *Komagataeibacter xylinus* inoculum for bacterial cellulose biosynthesis using magnetically assisted external-loop airlift bioreactor. *Polymers, 13*.

IF_{2022} – 4.329, 100 pkt. MEiN

12. Woroszyło, M., **Ciecholewska-Juśko, D**., Junka, A., Drozd, R., Wardach, M., Migdał, P., Szymczyk-Ziółkowska, P., Styburski, D., Fijałkowski, K. (2021). Rotating Magnetic Field increases β-lactam antibiotic susceptibility of methicillin-resistant Staphylococcus aureus strains. *International Journal of Molecular Sciences, 22*(22), 12397.

IF_{2022} – 5.923, 140 pkt. MEiN

13. Zielińska, S., Matkowski, A., Dydak, K., Czerwińska, M. E., Dziągwa-Becker, M., Kucharski, M., Wójciak, M., Sowa, I., Plińska, S., Fijałkowski, K., **Ciecholewska-Juśko, D**., Broda, M., Gorczyca, D., Junka, A. (2021). Bacterial nanocellulose fortified with antimicrobial and anti-inflammatory natural products from Chelidonium majus plant cell cultures. *Materials, 15*(1), 16.

IF_{2022} – 3.623, 140 pkt. MEiN

14. Brożyna, M., Paleczny, J., Kozłowska W., **Ciecholewska-Juśko, D**., Parfieńczyk, A., Chodaczek, G., Junka, A. (2022). Chemical composition and antibacterial activity of liquid and volatile phase of essential oils against planktonic and biofilm-forming cells of Pseudomonas aeruginosa. *Molecules, 27*(13), 4096.

IF_{2022} – 4.412, 100 pkt. MEiN

15. Żywicka, A., **Ciecholewska-Juśko, D.**, Szymańska, M., Drozd, R., Sobolewski, P., Junka, A., Gorgieva, S., El Fray, M., Fijałkowski, K. (2022). Argon plasma-modified bacterial cellulose filters for protection against respiratory pathogens.
(Praca dostępna obecnie jako preprint pod adresem: https://www.biorxiv.org/content/10.1101/2022.04.28.489859v1)
DOI: 10.1101/2022.04.28.489859

- obecnie w recenzji

Łącznie: **63.089 IF**, **1550 pkt. MEiN**

***h*-index**: **3** (wg bazy Scopus oraz Web of Science)

liczba cytowań (wyłączając autocytowania): **43**

Patenty i zgłoszenia patentowe

1. Patent: Fijałkowski, K., **Ciecholewska, D**. Sposób wytwarzania modyfikowanej celulozy bakteryjnej o znacznych właściwościach sorpcyjnych, nr zgłoszenia: P. 430888, nr prawa wyłącznego: Pat.240308, 2019.

2. Zgłoszenie patentowe: Fijałkowski, K., **Ciecholewska-Juśko, D**., Broda, M. Sposób otrzymywania inokulum do wytwarzania celulozy bakteryjnej oraz sposób wytwarzania celulozy bakteryjnej z wykorzystaniem pożywki pochodzenia roślinnego, nr zgłoszenia: P.433327, 2020.

3. Zgłoszenie patentowe: Fijałkowski, K., El Fray, M., Drozd, R., Żywicka, A., Sobolewski, P., **Ciecholewska-Juśko, D.**, Szymańska, M. Sposób wytwarzania modyfikowanej celulozy bakteryjnej o właściwościach przeciwdrobnoustrojowych, nr zgłoszenia: P.430149, 2021.

4. Zgłoszenie patentowe: Fijałkowski, K., El Fray, M., Drozd, R., Żywicka, A., Sobolewski, P., **Ciecholewska-Juśko, D.**, Szymańska, M. Sposób wytwarzania biodegradowalnych materiałów filtracyjnych na bazie bionanocelulozy, nr zgłoszenia: P.430150, 2021.

Udział w projektach

1. *Biodegradowalne, przeciwbakteryjne i przeciwwirusowe filtry na bazie bionanocelulozy do zastosowania w maseczkach ochronnych*; okres realizacji: 07.2020-09.2020; projekt badawczo-rozwojowy „Odpowiedzialny społecznie „Proto_lab”

realizowany w ramach **Regionalnego Programu Operacyjnego Województwa Zachodniopomorskiego** 2014-2020; Proto_lab/K1/2020/U/11; **wykonawca**.

2. *Analiza mechanizmów zwiększonej efektywności substancji przeciwdrobnoustrojowych względem biofilmów w obecności wirującego pola magnetycznego*; okres realizacji: 12.2020-12.2021; **Opus 14, Narodowe Centrum Nauki**, OPUS 2017/27/B/NZ6/02103; projekt realizowany w ramach konsorcjum z instytutem naukowo-badawczym Sieć Badawcza Łukasiewicz – PORT (Polski Ośrodek Rozwoju Technologii); **wykonawca**.

3. *Testowanie w warunkach rzeczywistych innowacyjnych maseczek ochronnych (NanoBioCell) z bionanocelulozy*; okres realizacji: 04.2021-09.2021; projekt badawczo-rozwojowy „Odpowiedzialny społecznie „Proto_lab" realizowany w ramach **Regionalnego Programu Operacyjnego Województwa Zachodniopomorskiego** 2014-2020; Proto_lab/K2/2021/U/7; **wykonawca**.

Udział w konferencjach

1. 11-12.04.2019, International Seminar on Sustainability, Economics and Safety, Szczecin Ostoja, "Structural modifications of bacterial cellulose allowing to obtain material with increased water absorption capacity" (referat).

2. 14.05.2019, IV Szczecińskie Sympozjum Młodych Chemików, Szczecin, Zachodniopomorski Uniwersytet Technologiczny w Szczecinie, „Wysokochłonny bionanomateriał na bazie celulozy bakteryjnej" (referat).

3. 17-19.05.2019, 8 Międzyuczelniane Sympozjum Biotechnologiczne "Symbioza", Warszawa, Politechnika Warszawska, "Nanomaterials based on bacterial cellulose with increased water absorption" (referat).

4. 06-07.06.2019, IV Interdyscyplinarna Konferencja Nano & Biomateriały, Toruń, Uniwersytet Mikołaja Kopernika w Toruniu, „Bionanomateriały celulozowe przeznaczone do aplikacji biomedycznych" (referat).

5. 07.12.2019, III Ogólnopolskie Sympozjum Chemii Bioorganicznej, Organicznej i Biomateriałów, Poznań, Politechnika Poznańska, „Bionanomateriały na bazie celulozy bakteryjnej jako opatrunki skierowane przeciwko biofilmom bakteryjnym" (referat).

6. 28-31.10.2020, FEMS Online Conference on Microbiology, "Influence of the rotating magnetic field on the mixing/diffusion process of antimicrobials in bacterial cellulose as an example of microbial biofilm matrix" (referat).

7. 21-23.05.2021, 9 Międzyuczelniane Sympozjum Biotechnologiczne "Symbioza", Konferencja Online, „Influence of the rotating magnetic field on the diffusion process of antibiotics" (poster).

8. 20-24.06.2021, World Microbe Forum Online Conference, "Controlled release of antimicrobials from wound dressings using rotating magnetic field" (poster).

9. 20-22.09.2021, XIV Kopernikańskie Seminarium Doktoranckie, Toruń, Uniwersytet Mikołaja Kopernika w Toruniu, „Wpływ wirującego pola magnetycznego na proces dyfuzji antybiotyków” (referat).

10. 22-23.09.2022, Baltic BioMat, Szczecin, Zachodniopomorski Uniwersytet Technologiczny w Szczecinie, „Superabsorbent crosslinked bacterial cellulose as an antibiofilm dressing material for highly exuding wounds” (poster).

Doniesienia konferencyjne

1. 19-21.09.2019, 5 Polska Konferencja „Grafen i inne materiały 2D”, Szczecin, Zachodniopomorski Uniwersytet Technologiczny w Szczecinie, M. Gliźniewicz, **D. Ciecholewska-Juśko**, M. Jędrzejczak-Silicka, „Application of bacterial cellulose produced by Komagataeibacter xylinus as a cell growth substrate for bovine mammary epithelial cells (MAC-T)”.

2. 03-04.10.2019, 4th International Symposium on Bacterial Nanocellulose, Porto, Portugalia, K. Fijałkowski, **D. Ciecholewska-Juśko**, A. Junka, “Development and characterization of native and citric acid-modified cellulose’s drug-delivery system for bacterial biofilm eradication”.

3. 21-23.05.2021, 9 Międzyuczelniane Sympozjum Biotechnologiczne “Symbioza”, Konferencja Online, Michał Broda, **Daria Ciecholewska-Juśko**, Karol Fijałkowski, „The potato juice as a cost-effective medium for biosynthesis of bacterial cellulose”.

4. 20-22.09.2021, XIV Kopernikańskie Seminarium Doktoranckie, Toruń, Uniwersytet Mikołaja Kopernika w Toruniu, Michał Broda, **Daria Ciecholewska-Juśko**, Karol Fijałkowski, „Sok komórkowy z bulw ziemniaków – odpad przemysłu skrobiowego, jako podłoże do biosyntezy celulozy bakteryjnej”.

Szkolenia i warsztaty

1. 02.2019 – ukończenie szkolenia „Audytor wewnętrzny systemu zarządzania jakością wg normy ISO 9001:2015” potwierdzone certyfikatem.

2. 12.2019 – uczestnictwo w warsztatach „Mikroskop FTIR” organizowanych przez firmę MEDSON w ramach III Ogólnopolskiego Sympozjum Chemii Bioorganicznej, Organicznej i Biomateriałów na Politechnice Poznańskiej (potwierdzone certyfikatem).

3. 12.2019 – uczestnictwo w warsztatach „Mikroskop ramanowski” organizowanych przez firmę MEDSON w ramach III Ogólnopolskiego Sympozjum Chemii Bioorganicznej, Organicznej i Biomateriałów na Politechnice Poznańskiej (potwierdzone certyfikatem).

4. 12.2019 – uczestnictwo w warsztatach „Najnowsze rozwiązania w dziedzinie badań topografii powierzchni metodami optycznymi” zorganizowanych przez Politechnikę Poznańską, Instytut Technologii i Inżynierii Chemicznej (potwierdzone certyfikatem).

5. 06.2020 – ukończenie szkolenia „Dobra Praktyka Kliniczna standard ICH GCP E6” potwierdzone certyfikatem.

6. 01.2021 – ukończenie szkolenia w zakresie obsługi cytometru przepływowego wraz z oprzyrządowaniem i oprogramowaniem (BC Accuri™ C6 Plus, BD CSampler™ Plus, BD Accuri C6 Plus Software, BD CSampler Plus Software) potwierdzone certyfikatem.

Praktyki i Staże

1. 07.2015 – 08.2015
   Praktyka w Krajowym Laboratorium Pasz, Pracownia w Szczecinie

2. 07.2017 – 07.2018
   Praktyka w laboratorium mikrobiologicznym PPC GRYF S.A., Szczecin

3. 07.2020-08.2020
   Staż w Pomorsko-Mazurskiej Hodowli Ziemniaka w Strzekęcinie

4. 08.2021 – 09.2021
   Staż w Instytucie Hodowli i Aklimatyzacji Roślin – Państwowy Instytut Badawczy, Oddział w Boninie

Inne

1. 03.2021 – obecnie
   Członek Koła Naukowego „BioReaktor” w Katedrze Mikrobiologii i Biotechnologii ZUT w Szczecinie

2. 05.2021 – obecnie
   Członek Polskiego Towarzystwa Mikrobiologów